

7-2021

Mitigating Calcium Oxychloride Damage in Cementitious Paste and Concrete Utilizing Supplementary Cementitious Materials

Casey Jones
University of Arkansas, Fayetteville

Follow this and additional works at: <https://scholarworks.uark.edu/etd>



Part of the [Civil Engineering Commons](#), [Construction Engineering and Management Commons](#), [Structural Engineering Commons](#), and the [Transportation Engineering Commons](#)

Citation

Jones, C. (2021). Mitigating Calcium Oxychloride Damage in Cementitious Paste and Concrete Utilizing Supplementary Cementitious Materials. *Graduate Theses and Dissertations* Retrieved from <https://scholarworks.uark.edu/etd/4164>

This Dissertation is brought to you for free and open access by ScholarWorks@UARK. It has been accepted for inclusion in Graduate Theses and Dissertations by an authorized administrator of ScholarWorks@UARK. For more information, please contact scholar@uark.edu.

Mitigating Calcium Oxychloride Damage in Cementitious Paste and Concrete Utilizing
Supplementary Cementitious Materials

A dissertation submitted in partial fulfillment
of the requirements for the degree of
Doctor of Philosophy in Engineering with a concentration in Civil Engineering

by

Casey Jones
University of Arkansas
Bachelor of Science in Civil Engineering, 2011
University of Arkansas
Masters of Science in Civil Engineering, 2013

July 2021
University of Arkansas

This dissertation is approved for recommendation to the Graduate Council.

W. Micah Hale, Ph.D.
Dissertation Director

Mark Arnold, Ph.D.
Committee Member

Cameron Murray, Ph.D.
Committee Member

Prannoy Suraneni, Ph.D.
Ex-Officio Member

Abstract

It is understood among engineers in the United States (U.S.) that improvement is needed throughout the transportation infrastructure. In the 2021 Infrastructure Report Card produced by the American Society of Civil Engineers, the roadways of this nation merit a D. This leaves room for improvement in order to provide durable pavements throughout this nation. Areas with significant winter weather may have exacerbated effects in decreased roadway longevity due to freezing/thawing cycles and the use of chemical deicers to mitigate gelid roadway conditions. Much research focuses on surface scaling and reinforcement corrosion using these materials; however, joint deterioration, due to chemical interactions between the deicers/anti-icers and hydration products from the cementitious paste, may also lead to significant pavement distress. One significant interaction can lead to the formation of calcium oxychloride (CAOXY). CAOXY is a product of the interaction between calcium hydroxide, found in cementitious paste, and calcium and magnesium chloride deicing salts. While conducting a significant review of the literature surrounding CAOXY, it is observed that the use of supplementary cementitious materials (SCMs) is shown effective to mitigate CAOXY formation in cementitious systems. However, the availability of quality SCMs, such as fly ash, is in question due to a reduction of active coal fired power plants. Therefore, a portion of this research investigates alternative SCMs for use to mitigate CAOXY in cementitious paste. The other portion of this research focuses on CAOXY mitigation in concrete using SCMs and establishing a link between cementitious paste testing and concrete testing.

Cementitious paste and concrete mixtures are developed for this investigation using the Arkansas Department of Transportation's Standard Specifications for Highway Construction. Alternative SCMs include rice husk ash (RHA), bottom ash (BA), limestone filler (LS), granite filler (GR),

sandstone filler (SS) and silica flour (SFL). Also, a traditional SCM (fly ash (FA)) is used for comparison. From this research it is shown that the RHA is the best alternative SCM of those tested to mitigate CAOXY, while mineral fillers are shown to be less effective. In concrete, specimens are cast using fly ash as a partial cement replacement given the prolific use of fly ash in the U.S. Concrete specimens are exposed to a 30% calcium chloride solution for 202 days at 5 °C. It is shown that the compressive and flexural strength of non-air entrained (NAE) and air entrained (AE) concrete specimens is significantly reduced in cement only specimens; however, those cast with 30% or more fly ash and 5% entrained air did not experience deterioration. For the paste and concrete specimens, low-temperature differential scanning calorimetry and thermogravimetric analysis are used to quantify calcium hydroxide and CAOXY levels. Using this data, a correlation is established to predict stoichiometric CAOXY levels in concrete based on cementitious paste samples. A maximum theoretical upper CAOXY level for AE concrete of 3.5 g/100 g powder is proposed. This new CAOXY limit for concrete could be used to supplement the AASHTO PP 84 specification which currently only provides a CAOXY limit for cementitious paste.

Acknowledgements

To begin, many individuals must be recognized for their pivotal role in completing the work for this degree; however, first and foremost, I would like to recognize my Lord and Savior Jesus Christ. It was his call that led me back to graduate school to pursue a PhD and his provision that helped me complete it. Next, I have to thank my wife, Courtney, for encouraging me to pursue this degree and for her support throughout the entire process. I could not have done it without you babe!

Outside of my Lord and my wife, no other individual has been more influential in this entire process than my advisor/mentor/friend Dr. Micah Hale. He supported me through the master's program and has continued to support me throughout this degree as well. Sincerely, thank you Dr. Hale! I would also like to thank my parents for their support as well and encouragement along the way. Both of you have always been there for me and I am forever grateful. Next, I would like to thank Dr. Prannoy Suraneni for his tireless effort and continued patience as I worked toward the completion of this degree. No other person has critiqued this work more than Dr. Suraneni and it is all the better for it!

A special thanks are in order to Dr. Cameron Murray for his help and the equipment along the way. Not only these, but I am also grateful for his friendship as well. A special thanks are in order to the numerous graduate students that have pushed me to become a better student as well and especially to Fatoumata Traore and Dr. Sivakumar Ramanathan for their hard work on this project. While there are too many graduate students to list everyone, the likes of Remington Reed, Caleb LeBow, Gabe Cook, Dr. Ahmed Al-Mohammed, Dr. Rahman Kareem, Bryan and Dr. Sadie Casillas, Dr. Elvis Castillo, and Yancy Schrader are thanked. Further, without David Peachee, Mark Kuss, Frances Griffith, and Roselie Conley this work would not be possible.

Thank you to everyone at the University of Arkansas for your continued support!

Dedication

This work is dedicated to my Lord and Savior Jesus Christ. It was His calling that led me back to pursue this degree and His provision that made it possible. Further, I would like to dedicate this work to my wife for her tireless support throughout this entire process. I love you Courtney!

Table of Contents

1. Introduction and Research Objectives	1
1.1. Introduction	1
1.2. Scope of Work.....	5
1.2.1. Review of the Literature	5
1.2.2. Cementitious Paste Investigation.....	6
1.2.3. Concrete Investigation	7
1.3. Dissertation Outline.....	8
2. Calcium Oxychloride: A Critical Review of the Literature Surrounding the Formation, Deterioration, Testing Procedures, and Recommended Mitigation Techniques	13
2.1. Introduction	14
2.2. Calcium Oxychloride Formation.....	16
2.2.1. Historical Background	16
2.2.2. Chemical Interaction Between Deicing Salts and Cementitious Phases	18
2.2.2.1. Formation of CAOXY in CaCl ₂ Solutions	22
2.2.2.2. Formation of CAOXY in MgCl ₂ Solutions	26
2.2.2.3. Formation of CAOXY in NaCl Solutions	27
2.2.3. Phase Diagrams.....	28
2.2.4. Impact on Structural Integrity and Microstructure	31
2.2.5. Impact on Mechanical Properties of Cementitious Systems.....	33
2.2.6. Deterioration Mechanisms.....	37
2.2.7. CAOXY Deterioration in Field-Placed Concrete	38

2.2.7.1.	Concrete Sleeper/ Tie Deterioration	38
2.2.7.2.	Concrete Wall Deterioration Exposed to Seawater	38
2.2.7.3.	Concrete Pavement Joint Deterioration.....	39
2.3.	Testing Strategies for Assessment of CAOXY Formation	40
2.3.1.	Novel Test Methods for Assessing CAOXY Formation and Deterioration	40
2.3.1.1.	X-Ray Diffraction (XRD).....	40
2.3.1.2.	Energy-Dispersive X-Ray Spectroscopy (EDXS).....	41
2.3.1.3.	Environmental Scanning Electron Microscopy (ESEM).....	41
2.3.1.4.	Thermogravimetric Analysis (TGA)	42
2.3.1.5.	Low-Temperature Differential Scanning Calorimetry (LT-DSC).....	42
2.3.1.6.	Volume Change Measurement (VCM).....	43
2.4.	Prevention and Mitigation Strategies	44
2.4.1.	Utilizing Mixture Design Parameters	44
2.4.1.1.	Utilizing Supplementary Cementitious Materials	45
2.4.1.1.1.	Impact of SCMs on Calcium Oxychloride Formation.....	45
2.4.1.1.2.	Impact of SCMs on Mechanical Properties of Cementitious Materials Exposed to CaCl ₂	48
2.4.1.2.	Proper Air-Entrainment	51
2.4.1.3.	Lower w/cm.....	52
2.4.1.4.	Lower Cement Content Due to Optimized Aggregate Gradation	53
2.4.2.	Utilizing Various Deicing Salts	53
2.4.3.	Utilizing Sealants	54
2.4.4.	Utilizing Preferential Carbonation.....	55

2.4.5.	Utilizing Bacteria (<i>Sporosarcina pasteurii</i>).....	55
2.5.	Prescriptive Guidelines and Future Research Recommendations.....	56
2.5.1.	Prescriptive Guideline Recommendations.....	56
2.5.2.	Future Research Recommendations.....	58
3.	Mitigating Calcium Oxychloride Formation in Cementitious Paste Using Alternative Supplementary Cementitious Materials	73
3.1.	Introduction	74
3.1.1.	Calcium Oxychloride Background	74
3.1.2.	Need for Research.....	75
3.2.	Materials and Methods	76
3.2.1.	Material Characterization.....	76
3.2.2.	Batching and Curing	81
3.2.3.	Test Methodology	82
3.2.3.1.	Compressive Strength Testing.....	82
3.2.3.2.	Thermogravimetric Analysis	82
3.2.3.3.	Low-Temperature Differential Scanning Calorimetry	83
3.3.	Results and Discussion.....	83
3.3.1.	Compressive Strength Results	83
3.3.2.	Thermogravimetric Analysis Results.....	88
3.3.3.	Low-Temperature Differential Scanning Calorimetry Results.....	91
3.3.4.	Discussion.....	94

3.3.4.1.	A Comparison of CAOXY and Ca(OH) ₂	94
3.3.4.2.	A Comparison of Ca(OH) ₂ Reduction and Compressive Strength Reduction	95
3.3.4.3.	A Comparison of CAOXY Reduction and Compressive Strength Reduction	97
3.3.4.4.	A Comparison of Ca(OH) ₂ Consumption: Reactivity Testing vs. Paste	98
3.3.4.5.	A Comparison of Predicted CAOXY Mitigation for Each Testing	
	Methodology	100
3.4.	Conclusion.....	103
4.	Investigating Concrete Deterioration Due to Calcium Oxychloride Formation	111
4.1.	Introduction	112
4.1.1.	Background.....	112
4.1.2.	Need for Research.....	114
4.2.	Materials and Methods	114
4.2.1.	Materials and Mixture Design Development.....	114
4.2.2.	Mixing and Casting Specimens	117
4.2.3.	Specimen Storage and Testing.....	119
4.3.	Results and Discussion.....	121
4.3.1.	Visual Observations	121
4.3.2.	Concrete Strength.....	123
4.3.2.1.	Compressive Strength.....	123
4.3.2.2.	Flexural Strength	127
4.3.2.3.	Correlation of Compressive and Flexural Strength	130
4.3.3.	Mass Change.....	132

4.3.4.	Silver Nitrate.....	135
4.3.5.	Length Change.....	137
4.4.	Conclusions.....	139
5.	Correlating Calcium Hydroxide and Calcium Oxchloride Formation with Resulting Deterioration in Cementitious Paste and Concrete Mixtures.....	146
5.1.	Introduction.....	147
5.2.	Materials and Methods.....	149
5.2.1.	Materials.....	149
5.2.2.	Previous Work.....	151
5.2.2.1.	Summary of Cementitious Paste Investigation.....	151
5.2.2.2.	Summary of Concrete Deterioration Investigation.....	152
5.2.3.	Thermogravimetric Analysis.....	154
5.2.4.	Low-Temperature Differential Scanning Calorimetry.....	155
5.3.	Results and Discussion.....	157
5.3.1.	Thermogravimetric Test Data.....	157
5.3.1.1.	Paste and Concrete TGA Data.....	157
5.3.1.2.	Correlating Paste-Concrete TGA Results.....	160
5.3.2.	Low-Temperature Differential Scanning Calorimetry Test Data.....	163
5.3.2.1.	Paste and Concrete LT-DSC Data.....	163
5.3.2.2.	Correlating Paste-Concrete LT-DSC Results.....	166
5.3.3.	Correlated Ca(OH) ₂ Levels and Damage in Concrete.....	170
5.3.3.1.	Non-Air Entrained Concrete.....	170

5.3.3.2. Air Entrained Concrete	174
5.4. Conclusions	177
6. Conclusions and Additions to the Field of Knowledge.....	183
6.1. Summary of Each Publication.....	183
6.1.1. Paper 1: Review of the Literature	183
6.1.2. Paper 2: Alternative SCM Investigation.....	184
6.1.3. Paper 3: Calcium Oxychloride Deterioration in Concrete.....	185
6.1.4. Paper 4: Correlated Calcium Oxychloride Levels in Paste and Concrete	186
6.2. Additions to the Field of Knowledge	187
7. Complete Reference List.....	189

List of Tables

Table 2.1. Typical chemical reaction products and deterioration mechanisms associated with various chloride-based deicing salts in paste, mortar, and concrete specimens (adapted in part from [20]).....	20
Table 2.2. CAOXY phases corresponding to Eq. 2.1 as reported in cement paste/mortar/concrete specimens in the literature with molecular weights and referenced citations (adapted in part from [102]).....	21
Table 2.3. Crystal systems of the 3:1:12 phase with reported densities (adapted in part from [101]).....	22
Table 2.4. Influence of CAOXY formation on mechanical properties of pure cement systems as reported in the literature for paste, mortar and concrete specimens	34
Table 2.5. Main parameters controlling CAOXY damage in cement paste, mortar, and concrete	36
Table 2.6. Influence of mitigation techniques to reduce mechanical property deterioration associated with CAOXY damage as reported in the literature for paste, mortar and concrete specimens	48
Table 2.7. Impact of various CAOXY mitigation techniques on mechanical properties and deterioration of cement paste, mortar, and concrete	50
Table 3.1. Cement and alternative SCM chemical compositions (%) and specific gravities.	78
Table 3.2. Pozzolanic reactivity classification of alternative SCM (developed from [41]).....	79
Table 3.3. Cementitious paste mixture design proportions.....	82
Table 3.4. Linear trend line equations for percentage strength loss based for each alternative SCM.....	88
Table 3.5. Linear trend line equations for Ca(OH)_2 reduction from Fig. 3.6	91
Table 3.6. Linear trend line equations for CAOXY mitigation in Fig. 3.7 based on cement replacement with alternative SCM and predicted CAOXY mitigation based on [19].	92
Table 3.7. Predicted effectiveness of each SCM for CAOXY mitigation for each test.....	102
Table 4.1. PCCP prescriptive requirements developed from [28].	115
Table 4.2. Chemical analysis of the cement and each fly ash (Bulk oxides given as % mass). .	116
Table 4.3. Concrete mixture designs (Materials given in kg/m^3).....	117

Table 4.4. Plastic property data for each concrete mixture. Air contents are corrected for aggregate effects.	118
Table 5.1. Cement, fly ash and aggregate properties. Developed from Jones et al. [23]. (Bulk oxide given in percent mass.).....	151
Table 5.2. Cementitious paste data summarized from Traore et al. [22].	152
Table 5.3. Concrete data summarized from Jones et al. [23].	154

List of Figures

Figure 1.1. Concrete pavement staining from a brine application of deicing solution on Highway 67/167 near Searcy, AR (by Casey Jones).....	2
Figure 1.2. Deteriorated concrete bridge deck crossing Interstate 40 near Alma, AR (by Casey Jones).	4
Figure 1.3. Heavy surface scaling, delamination and corroded reinforcement due to the use of chemical deicers such as $MgCl_2$ (by Casey Jones).	4
Figure 2.1. Potential formation location of CAOXY inside a deicing solution saturated concrete joint (unpublished data from authors).....	23
Figure 2.2. Illustrated representation of CAOXY formation in a saturated joint region of concrete pavement. Formation of CAOXY leads to deterioration by in-filling of available air voids and instigating microcracking in the pore space (unpublished data from authors).....	24
Figure 2.3. CAOXY crystals located on the exterior surface of specimens exposed to $CaCl_2$ solutions. (A) Deteriorated 50 mm cement paste cube specimen (0.45 water-to-cementitious materials ratio (w/cm), 10% fly ash replacement of cement) exposed to 23.1% $CaCl_2$ solution at 5 °C. (B) Deteriorated 100 mm x 200 mm concrete cylinder (0.40 water-to-cementitious materials ratio (w/cm), 20% fly ash replacement of cement) exposed to 25% $CaCl_2$ solution and repeated temperature cycles ranging from -10 °C to 23 °C. (Unpublished data from authors).....	25
Figure 2.4. $Ca(OH)_2 - CaCl_2 - H_2O$ ternary phase diagram plotting various known formations of CAOXY. It should be noted that not all phases can be present in similar temperature and solution concentrations.	29
Figure 2.5. Binary phase diagram showing the interaction of $Ca(OH)_2$ and $CaCl_2$ based on temperature. A – $Ca(OH)_2:CaCl_2 \leq 3$, B – $Ca(OH)_2:CaCl_2 > 3$ (adapted from [23,24,58]).	31
Figure 2.6. Deteriorated 50 mm cement paste cube specimen (0.45 water-to-cementitious materials ratio (w/cm), 10% fly ash replacement of cement) exposed to 23.1% $CaCl_2$ solution at 5 °C (A) Flaking observed throughout the entire specimen (B) Delamination observed along specimen edges (Unpublished data from authors).	32
Figure 2.7. Best fit lines for CAOXY reduction utilizing various SCM types with a w/cm 0.36. Similar data observed for w/cm 0.50 (adapted from [108]).	47
Figure 2.8. Influence of air entrainment for relief of CAOXY damage in cementitious systems (unpublished data from authors).	52
Figure 3.1. SEM images of cement and each alternative SCM: A) PC B) RHA C) BA D) LS E) NS F) SS G) SFL and H) FA.	80
Figure 3.2. Compressive strength data for alternative SCM pastes (15% mass replacement).	84

Figure 3.3. Compressive strength data for alternative SCM pastes (30% mass replacement).	85
Figure 3.4. Compressive strength data for alternative SCM pastes (45% mass replacement).	85
Figure 3.5. Strength loss percentage as a function of SCM replacement for each SCM.	88
Figure 3.6. Calcium hydroxide mitigation at each cement replacement level with alternative SCM.	90
Figure 3.7. CAOXY mitigation with each alternative SCM and cement replacement level.	92
Figure 3.8. Comparison of calcium hydroxide and CAOXY contents with alternative SCMs and linear trend line.	95
Figure 3.9. A comparison of the compressive strength reduction and $\text{Ca}(\text{OH})_2$ reduction for each SCM replacement type and level. Hollow markers denote a cement replacement level of 15%, half-filled markers denote a cement replacement level of 30%, and filled markers denote a cement replacement level of 45%.	96
Figure 3.10. A comparison of the compressive strength reduction and CAOXY reduction for each SCM type and replacement level. Hollow markers denote a cement replacement level of 15%, half-filled markers denote a cement replacement level of 30%, and filled markers denote a cement replacement level of 45%.	98
Figure 3.11. A comparison of $\text{Ca}(\text{OH})_2$ consumption from the reactivity testing vs. $\text{Ca}(\text{OH})_2$ consumption in the paste.	99
Figure 3.12. Reactivity testing of each alternative SCM type.	100
Figure 4.1. Exterior CAOXY crystal formation in concrete cast with 45% Class C fly ash: A) flexural strength beam (100 mm x 100 mm x 405 mm), B) cylindrical specimen (100 mm x 200 mm).	122
Figure 4.2. Compressive strength data for each concrete mixture following 90 days of curing in a limewater bath. Hollow markers represent NAE specimens while filled markers represent AE specimens.	124
Figure 4.3. Compressive strength difference based on fly ash level in NAE (hollow markers) and AE (filled markers) concrete specimens.	125
Figure 4.4. Deteriorated cylindrical compressive strength specimen following storage in a 30% mass CaCl_2 solution at 5 °C: A) cement only NAE concrete, B) cement only 4.9% AE concrete.	125

Figure 4.5. Flexural strength data for each concrete mixture following 90 days of curing in a limewater bath. Hollow markers represent NAE specimens while filled markers represent AE specimens.	128
Figure 4.6. Flexural strength difference based on fly ash level in NAE (hollow markers) and AE (filled markers) concrete specimens.	129
Figure 4.7. Correlation of compressive and flexural strength in CAOXY deteriorated samples.	132
Figure 4.8. Mass change data based on fly ash level for NAE (filled markers) and AE (hollow markers) concrete specimens.	133
Figure 4.9. Comparison of mass change percentage and strength difference in CAOXY deteriorated concrete specimens with hollow markers indicating NAE specimens while filled markers are AE specimens: A) all specimens, B) specimens near 0% mass change.....	135
Figure 4.10. Chloride penetration depth based on fly ash level for concrete specimens exposed to a 30% CaCl ₂ solution. Hollow markers represent NAE concrete while filled markers represent AE concrete.....	136
Figure 4.11. Chloride penetration depth in NAE concrete specimens when sprayed with a 0.1 N AgNO ₃ solution: A) cement only, B) 15% mass Class C fly ash, C) 30% mass Class C fly ash, and D) 45% mass Class C fly ash.	137
Figure 4.12. Ultimate strain measurements in CAOXY deteriorated concrete specimens. Hollow markers represent NAE concrete while filled markers represent AE concrete.	139
Figure 5.1. Diaphanous CAOXY crystals on the surface of specimens exposed to a 30% (mass) CaCl ₂ solution stored at 5 °C; A) cementitious paste and B) concrete.	148
Figure 5.2. Calcium hydroxide levels in cementitious paste specimens.....	158
Figure 5.3. Calcium hydroxide levels in concrete specimens.....	159
Figure 5.4. Correlated average Ca(OH) ₂ concrete and paste data.	161
Figure 5.5. Percentage of Ca(OH) ₂ measured in concrete (c) compared to Ca(OH) ₂ measured in paste (p) at each cement replacement level with fly ash (0, 15, 30, and 45%).	162
Figure 5.6. Calcium oxychloride levels in the cementitious paste samples cast with varying levels of fly ash.	163
Figure 5.7. Calcium oxychloride levels in concrete specimens cast with varying levels of fly ash.	166

Figure 5.8. Correlated calcium oxychloride levels in cementitious paste and concrete.	168
Figure 5.9. Percentage of CAOXY measured in concrete (c) compared to CAOXY measured in paste (p) at each cement replacement level with fly ash (0, 15, 30, and 45%).	169
Figure 5.10. Correlated compressive strength difference and Ca(OH) ₂ levels in NAE concrete specimens. Data are grouped at similar fly ash levels.	171
Figure 5.11. Comparison of paste and concrete compressive strength difference based on Ca(OH) ₂ in NAE concrete specimens. Concrete data are plotted on the primary X-Y axis while paste data are plotted on the secondary X-Y axis.	172
Figure 5.12. Stoichiometric CAOXY levels correlated with compressive strength loss in NAE concrete.	173
Figure 5.13. Correlated Ca(OH) ₂ levels and compressive strength difference in AE concrete specimens. Data are grouped at similar fly ash levels.	174
Figure 5.14. Comparison of paste and concrete compressive strength difference based on Ca(OH) ₂ in AE concrete specimens. Concrete data are plotted on the primary X-Y axis while paste data are plotted on the secondary X-Y axis.	175
Figure 5.15. Stoichiometric CAOXY levels correlated with compressive strength loss in AE concrete.	176

List of Published and Submitted Journal Articles

Published

1. **C. Jones**, S. Ramanathan, P. Suraneni, W.M. Hale, Calcium oxychloride: A critical review of the literature surrounding the formation, deterioration, testing procedures, and recommended mitigation techniques, *Cem. Concr. Comp.* 113 (2020) 103663.
<https://doi.org/10.1016/j.cemconcomp.2020.103663>. Chapter – 2.

Submitted

2. **C. Jones**, S. Ramanathan, P. Suraneni, W.M. Hale, Mitigating calcium oxychloride formation in cementitious paste using alternative supplementary cementitious materials, *Cem. Concr. Comp.* 2021 (**Submitted**). Chapter – 3.
3. **C. Jones**, P. Suraneni, W.M. Hale, Investigating concrete deterioration due to calcium oxychloride formation, *Cem. Concr. Comp.* 2021 (**Submitted**). Chapter – 4.
4. **C. Jones**, S. Ramanathan, P. Suraneni, W.M. Hale, Correlating calcium oxychloride formation and resulting deterioration cementitious paste and concrete mixtures, *Cem. Concr. Comp.* 2021 (**Submitted**). Chapter – 5.

1. Introduction and Research Objectives

1.1. Introduction

The transportation system in the United States (U.S.) is vital to the continued success of our nation. Numerous jobs and commerce are vitally connected to this system. While the transportation infrastructure is comprised of many parts, such as rail, air and vehicular traffic, the nation's interstates and roadways carry more than 63.3% of freight traffic [1]. Further, numerous noncommercial trips are also made in conjunction with the freight, totaling more than 4 trillion miles per year [2]. Given the unique reliance upon this system of interconnected roadways, it is vitally important as engineers to understand best practices when it comes to designing and maintaining this system.

Best practices may vary based on the region in which a particular section of roadway is located. Parts of the U.S. have extreme cold and snow while others are covered with mostly year-round warmth and sunlight. These significant changes in environmental conditions can impact the performance and long-term durability of roadways. However, a large portion of the U.S. experiences a portion of both hot and cold climatic conditions throughout each year. According to the Federal Highway Administration (FHWA), more than 70% of the nation's roadways are located in climatic regions receiving 13 cm of snow or more per year [3]. This means that many of the state department of transportation (DOT) agencies must work to keep roadways open to the public during times of significant winter weather. While a number of mitigation methods exist such as snowplows and placement of aggregate/grit on the roadways, one of the most effective methods at preventing gelid conditions is the use of chemical deicers/anti-icers [4]. Chemical deicers/anti-icers (referred to throughout the text as deicers) suppress the freezing point of water below 0 °C [4]. The most widely used deicer is sodium chloride (NaCl),

commonly referred to as rock salt. This material is cheap, widely available and can be placed on roadways in either a solid or brine form [5]. When used as a brine, prior to winter weather, concrete pavements can absorb this deicing solution causing staining and durability concerns as shown in **Fig. 1.1**. The eutectic temperature of a NaCl solution is $-21\text{ }^{\circ}\text{C}$; however, it has been shown that at temperatures below $-12\text{ }^{\circ}\text{C}$, NaCl may no longer be effective to mitigate snow and ice [5]. While NaCl is still very useful to DOT agencies, part of the nation may experience significant portions of winter weather at environmental temperatures lower than $-12\text{ }^{\circ}\text{C}$. When the prevention of snow and ice is required at these lower temperatures in order to ensure public safety, other deicing materials such as calcium chloride (CaCl_2) and magnesium chloride (MgCl_2) may be required [5].

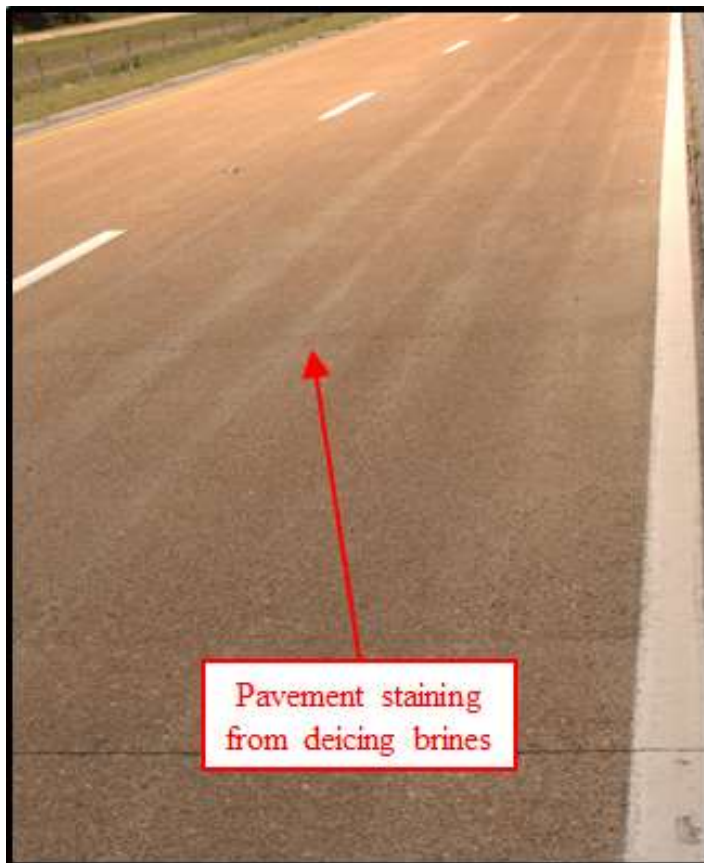


Figure 1.1. Concrete pavement staining from a brine application of deicing solution on Highway 67/167 near Searcy, AR (by Casey Jones).

The eutectic temperature of CaCl_2 solution is $-51\text{ }^\circ\text{C}$ while the eutectic temperature of a MgCl_2 solution is able to suppress water's freezing point to $-33\text{ }^\circ\text{C}$ [5]. In comparison to rock salt, these materials give the opportunity for DOT officials to keep roadways safe and navigable at lower temperature ranges; however, these materials do come with some drawbacks. The primary disadvantage is the cost associated with using these deicers [5]. Another, potentially more serious disadvantage is the increased deterioration associated with their use. Concrete roadways and bridge decks continuously exposed to chemical deicers are at higher risk for durability related concerns than those that do not receive these treatments [5]. However, the use of CaCl_2 and MgCl_2 exacerbate this deterioration when compared to NaCl . Located in **Fig. 1.2** is a picture of a heavily deteriorated concrete bridge deck in Arkansas. **Fig. 1.3** shows heavy surface scaling and top layer reinforcement corrosion of the same bridge deck. Discussions with officials from the Arkansas Department of Transportation (ARDOT) indicate that this bridge deck was continuously treated with MgCl_2 during winter weather [6]. It is clear from the near complete surface scaling of the entire bridge deck and the upper layer reinforcement corrosion that the use of MgCl_2 significantly deteriorated this bridge deck. While other factors such as freezing/thawing and the use of NaCl may also have caused damage to this structure, the use of MgCl_2 and often CaCl_2 can lead to significant deterioration concerns.



Figure 1.2. Deteriorated concrete bridge deck crossing Interstate 40 near Alma, AR (by Casey Jones).

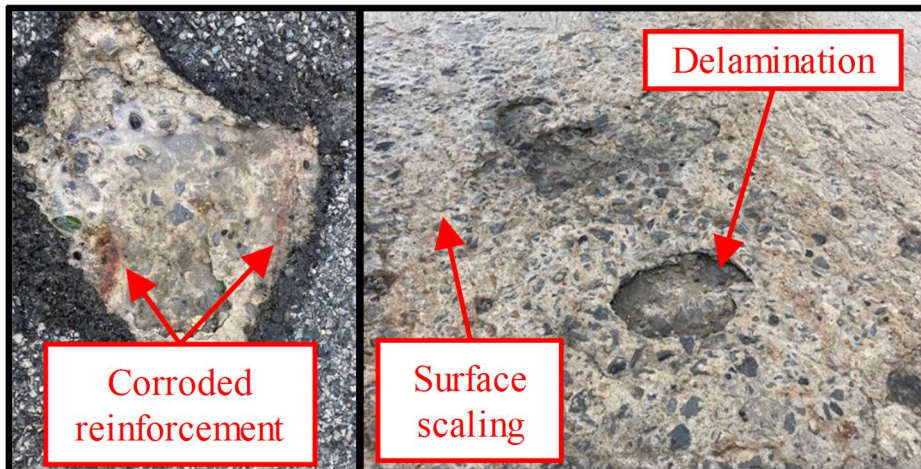


Figure 1.3. Heavy surface scaling, delamination and corroded reinforcement due to the use of chemical deicers such as $MgCl_2$ (by Casey Jones).

A quick review of the literature reveals that $CaCl_2$ and $MgCl_2$ deicing salts can significantly impact concrete pavements through numerous deterioration mechanisms [8,9,10,11]. While surface scaling [12,13,14] and reinforcement corrosion [15,16,17] have been heavily investigated, less research has focused on the potential of these materials to chemically interact with hydration products in the concrete. Some of the phases present following chemical interaction with these deicing materials are Kuzel's salt, Friedel's salt, calcium oxychloride

(CAOXY), magnesium oxychloride (MAOXY), magnesium hydroxide ($\text{Mg}(\text{OH})_2$ or brucite), and magnesium-silicate-hydrate (M-S-H) [7]. While the latter three (MAOXY, $\text{Mg}(\text{OH})_2$, and M-S-H) are only associated with MgCl_2 , the others can be associated with both CaCl_2 and MgCl_2 [7,10,11]. It is believed that in concrete pavements, CAOXY and MAOXY can be significant deterioration mechanisms, especially in the joints [7]. Recently, research has focused on investigating CAOXY for deterioration in concrete pavements given that both deicing materials may cause this type of deterioration [9,10,18,19]. Therefore, for this research program, an investigation into CAOXY deterioration in concrete pavements is proposed.

1.2. Scope of Work

The scope of work for this research will focus on 3 main topics:

1. A significant review of the literature
2. Cementitious paste testing
3. Concrete testing

By utilizing testing procedures from the literature, a correlation is sought in order to use cementitious paste testing to predict CAOXY levels in concrete. This could provide a level of “predicted/expected” CAOXY development/damage in concrete pavements which would aid design professionals in developing concrete pavement mixtures to mitigate CAOXY formation/deterioration.

1.2.1. Review of the Literature

In order to elucidate deterioration in concrete pavements due to CAOXY, an understanding of previous research conducted on this topic is required. While numerous pieces of literature are available which have investigated concrete deterioration in the presence of CaCl_2 and MgCl_2 deicing solution, it is clear that significant variations occur between testing procedures in these

works [9,10,18,19]. Further, there is little agreement upon standardized testing procedures in order to compare CAOXY deterioration in inter-laboratory testing of concrete specimens. Similarly, there is even less standardized testing for correlating field concrete deterioration to laboratory testing concrete deterioration. It is therefore proposed that a significant review of the literature be conducted in order to understand the scope of previous research. This is to include all specimen types (i.e. cement paste, mortar, and concrete) and testing procedures. This work is to be summarized into a significant of the review of the literature and to be submitted as a journal article for publication.

1.2.2. Cementitious Paste Investigation

As mentioned in **Section 1.2.1**, a portion of previous research has focused on cementitious paste investigations. While further detail from these investigations will be discussed in **Chapter 3**, a summary of the highlights shows that supplementary cementitious materials (SCMs) are an effective method to mitigate CAOXY formation in cementitious paste. A number of recent investigations have focused on the use of traditional SCMs such as fly ash, slag, and silica fume [18,19]. While these tests are needed given the current reliance upon fly ash and slag, alternative SCMs may play a significant role in future concrete applications. There is a movement across the U.S. to mitigate greenhouse gas emissions associated with coal energy production. In recent years, there has been a significant reduction in the number of coal fired power plants [20] and even here in Arkansas the White Bluff Generating Station is no longer online. Though currently viable, the long-term use of fly ash may be questionable as coal fired power plants are continued to be taken offline. Therefore, a need exists to investigate use of alternative SCMs for CAOXY mitigation in cementitious systems.

For this investigation the following materials are proposed for use as alternative SCMs in cementitious paste specimens: rice husk ash (RHA), bottom ash (BA), limestone filler (LS), sandstone filler (SS), granite filler (GR), and silica flour (SFL). Fly ash (FA) is also investigated for comparison as a traditional SCM. It should be noted that some of these alternative materials classify as inert mineral fillers (See **Chapter 3**); however, the designation of SCM will be utilized collectively for the alternative materials list throughout this work. Given that some of the alternative SCMs are not consistently used in concrete mixtures, a portion of this research investigates the physical and chemical attributes of these materials. The impact on the mechanical properties of the cementitious pastes is investigated by compressive strength testing and mitigation in CAOXY is investigated through the use of low-temperature differential scanning calorimetry (LT-DSC) and thermogravimetric analysis (TGA). Further details for this investigation can be found in **Chapter 3**.

1.2.3. Concrete Investigation

While cementitious paste testing is useful, ultimately the goal is to understand CAOXY deterioration in concrete. It has been shown that as aggregates and entrained air are added to paste, forming concrete, the influence of deicing solutions can vary. Transport properties and paste content are significantly altered when comparing cementitious paste and concrete. This difference complicates comparing CAOXY deterioration/formation in cementitious paste and concrete samples. For this investigation, equivalent paste and concrete samples are proposed for investigation. Following the ARDOT Standard Specifications for Highway Construction [21], paste and concrete mixture designs are developed. Samples with cement only and samples with fly ash are proposed for investigation. Though the long-term availability of fly ash could be in question as stated in **Section 1.2.2**, it is the only material investigated that is currently allowed as

a cement replacement based on the Qualified Products List in Arkansas. In order to quantify CAOXY in the paste and concrete samples, TGA and LT-DSC is utilized to test each sample. As shown in Suraneni and Weiss [22], CAOXY levels in paste specimens are greater than in concrete specimens. Aggregate from the concrete dilutes powder samples leading to reduced CAOXY levels and larger standard deviations in testing. Therefore, for testing purposes, it could be beneficial to find a correlation between paste and concrete specimens [23,24]. This would allow industry professionals or state DOTs to conduct testing on the paste portion of concrete samples in order to determine the potential CAOXY formation. A mixture design recommendation could be made using a minimum potential for CAOXY formation. Future investigations based on this research could provide recommendations for acceptance of concrete mixture designs prior to approval for placement. This could prevent premature deterioration of newly constructed highways due to CAOXY.

1.3. Dissertation Outline

As detailed in **Section 1.2**, this dissertation will cover CAOXY mitigation in cementitious paste and concrete specimens. This dissertation consists of seven chapters. **Chapter 1** is an introduction which includes the scope of work and relevant background information to understand the purpose of this research. **Chapters 2-5** are journal manuscripts which have either been accepted or submitted for review to their respective journals. **Chapter 2** is a review of the literature. This work has been accepted for publication in Cement and Concrete Composites. The literature review details former investigations into CAOXY deterioration while highlighting significant future research that is required to continue to elucidate this complex deterioration mechanism.

In **Chapter 3**, an investigation is described which examines the use of alternative SCMs as a partial cement replacement in cementitious paste in order to prevent CAOXY formation. This work builds upon previous research which shows that the use of traditional SCMs such as fly ash, slag, and silica fume can significantly mitigate the formation and damage associated with CAOXY [18,19]. (It should be noted that another portion of paste research using fly ash as a SCM was also conducted under the overview of the paste research. Traore et al. [25] investigated the proposed CAOXY threshold value of 15 g/100 g paste using fly ash as a cement replacement to mitigate CAOXY).

Chapter 4 provides an investigation into deteriorated portland cement concrete specimens exposed to a 30% CaCl₂ solution. Fly ash is used to mitigate CAOXY formation at cement replacement levels of 0, 15, 30 and 45% by mass. Both non-air entrained (NAE) and air entrained (AE) specimens were investigated. This work builds upon the research of Traore et al. [25] by conducting an investigation into concrete with similar cementitious paste. Compressive and flexural strength change along with mass change, length change and chloride penetration are investigated. To the author's knowledge, this is the first investigation into flexural strength loss in concrete specimens due to CAOXY deterioration. This work was submitted to Cement and Concrete Composites for publication.

The work conducted in **Chapter 5** seeks to correlate damage due to CAOXY in cementitious paste and concrete. In order to accomplish this paste-concrete correlation, CAOXY levels in concrete are needed. **Chapter 5** presents methods to accomplish TGA and LT-DSC testing on concrete specimens. Data from these analyses are compared with paste data found in Traore et al. [25]. Further, concrete deterioration presented in **Chapter 4** is used to specify theoretical Ca(OH)₂ and CAOXY limits in concrete specimens. To the author's knowledge, this is the first

work to specify maximum Ca(OH)_2 and CAOXY levels in concrete in order to mitigate damage caused by CAOXY. This could be used by designers to help ensure protection against CAOXY prior to placement of a large section of field concrete.

Chapter 6 contains the conclusions from this research investigating CAOXY. The conclusions are referenced to their respective journal article/location in this dissertation. Further, the contributions made to this field are provided in **Chapter 6**. Presented in **Chapter 7** is a full reference list for this dissertation. Some references are used in multiple chapters/submitted journal articles; therefore, **Chapter 7** consolidates all references into a single list.

References

1. Bureau of Transportation Statistics, 2017 North American Freight Numbers. <https://www.bts.gov/newsroom/2017-north-american-freight-numbers>, 2017, (accessed 23 March 2020).
2. Bureau of Transportation Statistics, National Household Travel Survey Daily Travel Quick Facts. <https://www.bts.gov/statistical-products/surveys/national-household-travel-survey-daily-travel-quick-facts>, 2017, (accessed 23 March 2020).
3. U.S. Department of Transportation Federal Highway Administration, Road Weather Management Program, Snow and Ice. https://ops.fhwa.dot.gov/weather/weather_events/snow_ice.htm, (accessed November 18, 2019).
4. National Academies of Sciences, Engineering, and Medicine 2004. Snow and Ice Control: Guidelines for Materials and Methods, Washington, DC: The National Academies Press. <https://doi.org/10.17226/13776>.
5. X. Shi, L. Fay, C. Gallaway, K. Volkening, M.M. Peterson, T. Pan, A. Creighton, C. Lawlor, S. Mumma, Y. Liu, T.A. Nguyen, Evaluation of alternative anti-icing and deicing compounds using sodium chloride and magnesium chloride as baseline deicers – Phase I, Final Report for the Colorado Department of Transportation, CDOT-2009-1.
6. Personal Communication with Chad Davis and Alan Meadors. 8 August 2018.
7. X. Wang, S. Sadati, P. Taylor, C. Li, X. Wang, A. Sha, Material characterization to assess effectiveness of surface treatment to prevent joint deterioration from oxychloride formation mechanism, *Cem. Concr. Comp.* 104 (2019) 103394. <https://doi.org/10.1016/j.cemconcomp.2019.103394>.

8. H.G. Smolczyk, Chemical reactions of strong chloride-solutions with concrete, Proceedings of the 5th International Symposium on the Chemistry of Cement, 1968, Tokyo, Japan, pp. 274-280.
9. G.A. Julio-Betancourt, Effect of de-icer and anti-icer chemicals on the durability, microstructure, and properties of cement based materials, University of Toronto, 2009, Ph.D. Thesis.
10. C. Qiao, P. Suraneni, M.T. Chang, J. Weiss, Damage in cement pastes exposed to MgCl₂ solutions, *Mater. Struct.* 51 (2018) 74. <https://doi.org/10.1617/s11527-018-1191-2>.
11. C. Qiao, P. Suraneni, T.N.W. Ying, A. Choudhary, J. Weiss, Chloride binding of cement pastes with fly ash exposed to CaCl₂ solutions at 5 and 23 °C, *Cem. Concr. Comp.* 97 (2019) 43-53. <https://doi.org/10.1016/j.cemconcomp.2018.12.011>.
12. G.J. Verbeck, P. Klieger, Studies of "salt" scaling of concrete, *Highw. Res. Board Bull.* 150 (1957) 1-17.
13. J.J. Valenza II, G.W. Scherer, A review of salt scaling: I. Phenomenology, *Cem. Concr. Res.* 37 (7) (2007) 1007-1021. <https://doi.org/10.1016/j.cemconres.2007.03.005>.
14. J.J. Valenza II, G.W. Scherer, A review of salt scaling: II. Mechanisms, *Cem. Concr. Res.* 37 (7) (2007) 1022-1034. <https://doi.org/10.1016/j.cemconres.2007.03.003>.
15. S. Ahmad, Reinforcement corrosion in concrete structures, its monitoring and service life prediction – a review, *Cem. Concr. Comp.* 25 (4-5) (2003) 459-471. [https://doi.org/10.1016/S0958-9465\(02\)00086-0](https://doi.org/10.1016/S0958-9465(02)00086-0).
16. U. Angst, B. Elsener, C.K. Larsen, Ø. Vennesland, Critical chloride content in reinforced concrete – a review, *Cem. Concr. Res.* 39 (12) (2009) 1122-1138. <https://doi.org/10.1016/j.cemconres.2009.08.006>.
17. K. Hornbostel, C.K. Larsen, M.R. Geiker, Relationship between concrete resistivity and corrosion rate – a literature review, *Cem. Concr. Comp.* 39 (2013) 60-72. <https://doi.org/10.1016/j.cemconcomp.2013.03.019>.
18. P. Suraneni, V.J. Azad, O.B. Isgor, W.J. Weiss, Use of fly ash to minimize deicing salt damage in concrete pavements, *Transp. Res. Rec.* 2629 (2017) 24-32. <https://doi.org/10.3141/2629-05>.
19. P. Suraneni, V.J. Azad, O.B. Isgor, J. Weiss, Role of supplementary cementitious material type in the mitigation of calcium oxychloride formation in cementitious pastes, *J. Mater. Civ. Eng.* 30 (10) (2018) 04018248. [https://doi.org/10.1061/\(ASCE\)MT.1943-5533.0002425](https://doi.org/10.1061/(ASCE)MT.1943-5533.0002425).
20. Phys.Org, 50 US coal power plants shut under Trump. <https://phys.org/news/2019-05-coal-power-trump.html> (accessed 27 June 2019).

21. Arkansas Department of Transportation. Standard specifications for highway construction. 2014. http://www.arkansashighways.com/standard_spec/2014/2014SpecBook.pdf.
22. P. Suraneni, J. Weiss, Extending low-temperature differential scanning calorimetry from paste to mortar and concrete to quantify the potential for calcium oxychloride formation, *Adv. Civ. Eng. Mater.* 7 (1) (2018) 1-16. <https://doi.org/10.1520/ACEM20170113>.
23. X. Wang, S. Sadati, P. Taylor, C. Li, X. Wang, A. Sha, Material characterization to assess effectiveness of surface treatment to prevent joint deterioration from oxychloride formation mechanism, *Cem. Concr. Comp.* 104 (2019) 103394. <https://doi.org/10.1016/j.cemconcomp.2019.103394>.
24. C. Jones, S. Ramanathan, P. Suraneni, W.M. Hale, Calcium oxychloride: a critical review of the literature surrounding the formation, deterioration, testing procedures, and recommended mitigation techniques, *Cem. Concr. Comp.* (Submitted).
25. F. Traore, C. Jones, S. Ramanathan, P. Suraneni, W.M. Hale, Using compressive strength and mass change to verify the calcium oxychloride threshold in cementitious pastes with fly ash, *Constr. Build. Mater.* 296 (2021) 123640. <https://doi.org/10.1016/j.conbuildmat.2021.123640>.

2. Calcium Oxychloride: A Critical Review of the Literature Surrounding the Formation, Deterioration, Testing Procedures, and Recommended Mitigation Techniques

Casey Jones^a, Sivakumar Ramanathan^b, Prannoy Suraneni^c, W. Micah Hale^d

^a Graduate Research Assistant, Department of Civil Engineering, University of Arkansas, 4190 Bell Engineering Center, Fayetteville, AR 72701, United States of America.

^b Graduate Research Assistant, Civil, Architectural, Environmental Engineering Department, University of Miami, 1251 Memorial Drive, Coral Gables, FL 33146, United States of America.

^c Assistant Professor, Civil, Architectural, Environmental Engineering Department, University of Miami, 1251 Memorial Drive, Coral Gables, FL 33146, United States of America.

^d Professor and Chair, Department of Civil Engineering, University of Arkansas, 4190 Bell Engineering Center, Fayetteville, AR 72701, United States of America.

Corresponding author: Casey Jones

Abstract

Deicing salts have long been known to cause deterioration in concrete pavements. Freeze/thaw, surface scaling, and reinforcement corrosion are well documented deterioration mechanisms. However, another mechanism exists causing severe concrete damage that is much less understood. This deterioration is due to the formation of calcium oxychloride, from chemical interactions between the cementitious paste and certain chloride-based deicing salts. The basic chemical structure of calcium oxychloride, with slight variations, has been reported in

deteriorated samples. Ideas have been postulated about failure mechanisms associated with the formation of calcium oxychloride. Further, testing techniques such as thermogravimetric analysis, low-temperature differential scanning calorimetry, and volume change measurements have been successfully utilized to better understand/quantify calcium oxychloride. Mitigation techniques to minimize the impact of calcium oxychloride include reducing cement content through the use of supplementary cementitious materials or other means, the use of adequate air entrainment, preferential carbonation, and the use of concrete sealants. This review of the literature highlights the current understanding of calcium oxychloride, provides best practice guidance and postulates new areas of research needed in order to effectively mitigate calcium oxychloride damage in concrete pavements.

Keywords: Calcium Oxychloride, Deicing Salts, Supplementary Cementitious Materials, Low-Temperature Differential Scanning Calorimetry, Literature Review

2.1. Introduction

The 2017 American Society for Civil Engineers (ASCE) rates the roadways of the United States a D, indicating that the system as a whole has serious deterioration concerns, and is susceptible to failure [1]. Given the current deteriorated state of the United States highways, research is needed to aid pavement longevity in both new construction and rehabilitation of older roadways. One step needed for this research to instigate the turnabout for drastic improvement in the transportation infrastructure is a critical understanding of various concrete deterioration mechanisms.

Damage due to deicing salt is one major cause of deterioration in concrete pavements. Deicing salts are placed on roadways as a means to depress the freezing point of water in winter. The use of deicing salts is highly effective in preventing hazardous driving conditions and their use is

required until a more effective winter weather mitigation technique is developed. Therefore, the knowledge of all deterioration mechanisms associated with deicing salts is critical for agencies responsible for concrete pavement construction and maintenance. Much research has focused on surface scaling [2-8], reinforcement corrosion [9-14], and freeze/thaw damage [15-20].

However, another very serious deterioration mechanism exists, namely, damage due to the formation of calcium oxychloride (CAOXY) (sometimes denoted as calcium-hydroxide-chlorides, calcium hydroxychloride hydrates, chlorohydroxy hydrates, hydroxychloro hydrates, or calcium chloride hydrate). This mode of damage occurs typically with chloride-based deicing salts such as magnesium chloride ($MgCl_2$) and calcium chloride ($CaCl_2$) and results in significant concrete spalling and scaling, especially around the joints.

In the past, CAOXY deterioration was observed, but the transient nature of the crystals proved difficult to accurately study. However, advances in testing techniques [21-24], coupled with prominent pavement failures possibly linked to chemical deterioration associated with deicing salts [25-29] have promoted a renewed interest in understanding this deterioration mechanism. A recent article [20] investigated CAOXY and its role in deterioration of critically saturated joints. One section of that article reviews recent advances in the knowledge of CAOXY; however, the work was aimed at developing long-term prediction performance of concrete pavements for freeze/thaw and CAOXY. While such work is required for pavement designers and the future implementation of performance-based specifications, the current practice of many local United States department of transportation (DOT) agencies follows a prescriptive approach. Two conference papers exist that have examined the impact of CAOXY in concrete [30,31]; while they are review works, they are not comprehensive, and the extent of each work does not thoroughly cover this topic. Further, ACI 201.3T-19 [32] provides a brief introduction and

background to concrete joint deterioration and CAOXY formation, but does not extensively review the current state of CAOXY knowledge. Therefore, a significant review of the literature is required to compile known information regarding CAOXY with the intent to aid prescriptive measures until performance-based specifications are available and widely implementable. Apart from a review of CAOXY, further, this work provides recommendations for future research endeavors.

2.2. Calcium Oxychloride Formation

2.2.1. Historical Background

Oxychlorides in construction can be traced back to 1855 when Sorel first introduced zinc oxychloride cements as an alternative to portland cement systems [33]. However, this product was never widely accepted but his subsequent material, magnesium oxychloride (MAOXY) cements, remain in use today. In traditional portland cement, the main reaction product is calcium-silica-hydrate (C-S-H); however, in MAOXY systems, the main strength-giving components are the 3-phase ($3\text{MgO}\cdot\text{MgCl}_2\cdot 8\text{H}_2\text{O}$) and the 5-phase ($5\text{MgO}\cdot\text{MgCl}_2\cdot 8\text{H}_2\text{O}$) forms of MAOXY [34]. A number of early research investigations were performed to understand the formation process of MAOXY and subsequently uncovered the formation of a secondary reaction product namely CAOXY [35-38]. However, early research did not consider MAOXY or CAOXY as potential deterioration mechanisms in portland cement systems. Future investigations would uncover the significant deterioration concerns caused by these precipitates. MAOXY and CAOXY cement systems are not covered in this paper. More detailed information regarding oxychloride use in magnesium cements is provided elsewhere [34].

Prior to deicing salt applications, CaCl_2 and CaOCl_2 , a possible variation of the CAOXY phase known to cause deterioration in concrete, were utilized as accelerators in early portland cement

concrete mixture designs [39,40]. Today, specifications often prohibit the use of CaCl_2 added into reinforced concrete due to concerns regarding corrosion of reinforcing steel; however, significant amounts are utilized annually in maintaining safe driving conditions during winter weather. Though CaCl_2 effectively mitigates gelid conditions by depressing the freezing point of water, significant chemical deterioration of cement paste [41-50], mortar [41,51-59] and concrete [43,49,56,60-78] exposed to concentrated CaCl_2 solutions have been reported.

In 1960, Lawrence and Vivian [41] described significant deterioration in portland cement paste and mortar specimens exposed to a 30% CaCl_2 solution, which was attributed to the formation of calcium chloroaluminate, commonly known as Friedel's salt [41]. The authors acknowledged that the damage was in contradiction with Bogue [79], who stated chlorides were benign to concrete unless accompanied with wet/dry cycles. The authors expressed concerns that concrete exposed to refrigerant coolants or housing chloride-based deicing salts could be at risk for chloride damage [41].

In 1968, Smolczyk [51] observed similar deterioration to [41] following placement of mortar specimens in MgCl_2 (24.5%) and CaCl_2 (28%) solutions. A NaCl (26%) environment was also investigated; however much less deterioration was observed in this exposure condition [51]. Smolczyk [51] utilized X-ray analysis (see **Section 2.3.1.1**) to identify crystalline compounds present in deteriorated samples. Specimens exposed to MgCl_2 solutions showed the formation of 5-phase MAOXY crystals while CAOXY (1:1:1 see **Section 2.2.2**) crystals were present in specimens exposed to CaCl_2 . This provided the first evidence for the formation of CAOXY in portland cement systems. No MAOXY or CAOXY were observed in the specimens exposed to NaCl ; however, a recent investigation, covered in **Section 2.2.2.3**, suggests CAOXY may occur in carbonated (10% CO_2) specimens exposed to NaCl . Friedel's salt was also noted in specimens

from all three environments. Smolczyk [51] determined that the formation of oxychloride crystals caused significant deterioration in mortars.

Chatterji and Jensen [60] were in agreement with Smolczyk [51] and refuted the ideas that Friedel's salt formation and leaching of $\text{Ca}(\text{OH})_2$ were the primary deterioration mechanisms in specimens exposed to 30% CaCl_2 solutions. It has been postulated that the damage was most likely due to the precipitation of a more complex salt due to the chemical reaction between the cement paste and CaCl_2 possibly coupled with freeze/thaw [60,61]. During this time frame, significant data was compiled by numerous research groups investigating this deterioration mechanism [41,51,60-63,80]. The general findings indicated a reaction between the cement paste and CaCl_2 caused an unknown expansive product [61]. However, the exact CAOXY compound remained a mystery until 1989 when Monosi et al. [42] compared known X-ray diffraction patterns to those observed in the deteriorated cement paste specimens. This led to the identification of the 3:1:12 phase (see **Section 2.2.2**), widely believed to be responsible for significant deterioration in portland cement systems. Following this identification, research continued to develop an understanding of this deterioration process, providing evidence of reduced mechanical properties, and the ability of MgCl_2 to cause CAOXY deterioration [46,47,49-52,64,72,77,81].

2.2.2. Chemical Interaction Between Deicing Salts and Cementitious Phases

While CAOXY is a deleterious product formed due to chemical interactions between cement paste and some chloride-based deicing salts, a number of other products/reactions may also occur. Kuzel's salt and Friedel's salt are reported as reaction products due to aluminate phases in the cementitious paste interacting with chloride-based deicing solutions [41,49,51,52,56,58,62,67,72-74,80,82-89]. Further, the leaching of $\text{Ca}(\text{OH})_2$, due to changes in

its solubility and hydrolysis with the deicing solution, from cement paste has also been reported [49,56,57,62,80,81,86,87]. In MgCl_2 solutions, the formation of brucite ($\text{Mg}(\text{OH})_2$) [49,66,72,81,83-85,88,90-95], MAOXY [49,51,55,56,66,72,81,83,85], and magnesium silicate hydrate (M-S-H) [49,66,83,85,86,88,91-96] have been reported. **Table 2.1** provides typical reaction products and deterioration mechanisms associated with each deicing salt type. This paper focuses mainly on CAOXY and its role in concrete deterioration; however, it must be noted that often its formation coincides simultaneously with other reaction products/deterioration mechanisms.

The transitory nature of CAOXY provides a unique hurdle to elucidate its behavior in portland cement systems as changes in environmental conditions, such as temperature and relative humidity, modify/destroy CAOXY phases prior to testing [49,50,55-57,98-102]. Testing methodologies designed to study CAOXY must account for these differences in order to protect the phase prior to an investigation. Further complicating the comprehension of this system is the variation in chemical reactions leading to CAOXY formation in CaCl_2 [42,44-50,54,55,57,58,65,72,76,77,103-108] and MgCl_2 [38,49,55,56,66,67,72,77,81,82,109] brines. These characteristics have made it difficult for researchers to accurately document CAOXY in lab and especially field experiments.

Table 2.1. Typical chemical reaction products and deterioration mechanisms associated with various chloride-based deicing salts in paste, mortar, and concrete specimens (adapted in part from [20]).

	Type	NaCl			CaCl ₂			MgCl ₂		
		P	M	C	P	M	C	P	M	C
Typical Chemical Reaction Products	Friedel's/ Kuzel's Salts	X	X	X	X	X	X	X	X	X
	Leaching of Ca(OH) ₂	I	I	I	X	X	X	X	X	X
	CAOXY			*	X	X	X	X	X	X
	MAOXY							X	X	X
	Mg(OH) ₂							X	X	X
	M-S-H							X	X	X
Typical Physical Deterioration	Surface Scaling	X	X	X	X	X	X	X	X	X
	Visible Crumbling				X	X	X	X	X	X
	Compressive Strength Loss				X	X	X	X	X	X
	Flexural Strength Loss				X	X		X	X	
	Increased Permeability				X	X	X	X	X	X
	Reduced Elastic Modulus						X			X
	Expansion				X	X	X	X	X	X
	Mass Change				X	X	X	X	X	X

P (Paste); M (Mortar); C (Concrete).

I (Inconclusive) There appears to be disagreement in the literature regarding the dissolution of Ca(OH)₂ in NaCl solutions as two studies [56,66] state that dissolution occurs while two others [51,62] did not observe dissolution. Variations in observations could be due to different solution concentrations and testing conditions.

* CAOXY was found in carbonated samples in one study [97]; however, CAOXY is not typically observed in specimens exposed to NaCl.

Eq. 2.1 is the generalized chemical equation showing the formation of CAOXY [23,24,28,46,47,49,51,65,72,74,89,106-116]. A shorthand denotation x:y:z, where x is the amount of Ca(OH)₂ present, y is the amount of CaCl₂, and z is the amount of H₂O, may be used to describe a specific phase [44,74,76,97-99,101,115]. **Table 2.2** provides various phase structures that have been reported in the literature. It should be noted that some researchers have used **Eq. 2.2** as an alternative description for CAOXY [42,44,49-52,64,66,67,77,81,82,97]; however, the x:y:z notation shown in the rest of the text follows **Eq. 2.1**. The most widely reported phase responsible for deterioration in concrete for **Eq. 2.1** is 3:1:12 (reported as 3:1:15 when using **Eq. 2.2**). Various crystal systems have been suggested for the 3:1:12 phase and are presented in **Table 2.3** along with densities for each system.

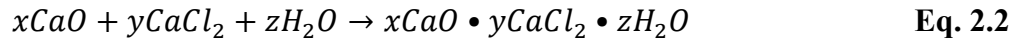
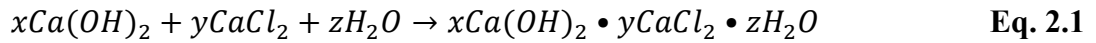


Table 2.2. CAOXY phases corresponding to **Eq. 2.1** as reported in cement paste/mortar/concrete specimens in the literature with molecular weights and referenced citations (adapted in part from [102]).

	x:y:z	Molecular Weight (g/mol)	References
Anhydrous/ Dehydrated Phases	1:1:0	185.07	[73,74,87,102]
	1:1:1	203.09	[43,51,56,59,62,65,73,82,87,89,98-102,117,118]*
	1:1:2	221.10	[57,73,74,102]
	1:1:3	239.12	[102]
	1:1:4	257.13	[102]
	3:1:0	333.26	[56]
Hydrated Phases	3:1:7	459.37	[85]
	3:1:8	477.38	[38,74,102]
	3:1:9	495.40	[38,43,74,102,118]
	3:1:10	513.41	[38,74,102,118]
	3:1:11	531.43	[38,56,74,102,118]
	3:1:12	549.44	[20,21,23,24,28,32,38,42,44-50,52-59,64-67,69,70,72-77,81,82,86,89,94-109,111-125]**
	3:1:13	567.46	[38,56,74,102,118]
	4:1:10	587.50	[74,102,118]
	3:1:15	603.49	[73,74]

*Common phase present in portland cement/concrete specimens following significant drying/preparation procedures after immersion in CaCl₂ solution.

Table 2.2. (Cont.)

**Common phase present in portland cement/concrete specimens when no drying/preparation procedures are utilized after immersion in CaCl₂ solution.

Table 2.3. Crystal systems of the 3:1:12 phase with reported densities (adapted in part from [101]).

Phase	Density (g/cm ³)	Phase Assemblage/Symmetry	Reference
	1.650	Pseudocubic	[124]
	1.805	Orthorhombic	[87]
3:1:12	1.613	Tetragonal	[56]
	1.620	Cubic (P23, Pm3, P432, P-43 m, Pm3m)	[101]
	1.820	Orthorhombic	[102]

2.2.2.1. Formation of CAOXY in CaCl₂ Solutions

CaCl₂ may be placed on roadways in either solid or brine form [32]. In a brine solution, the ionic forms of Ca²⁺ and Cl⁻ are present in solution; however, when solid CaCl₂ is utilized, the salt dissolves into its cations and anions as it absorbs moisture from the surrounding environment becoming a brine. Traffic and precipitation runoff remove much of the residual deicing material; however, salts can become lodged in joints or large cracks in the pavement [32,49,77]. Over time, the concentration of salts increases up to the point where the salts and the concrete start reacting, initiating the deterioration of the material. Glasser et al. [126] noted that CaCl₂ used in concrete pavements most likely would not reach sufficient solution strengths to cause damage due to CAOXY, unless the evaporation of moisture significantly increased solution concentration. Others have also suggested evaporation as a potential mechanism that could lead to significant chloride concentrations in concrete [49,98]. Over time, CaCl₂ ingresses into the concrete, and reacts with Ca(OH)₂ to form CAOXY through **Eq. 2.1**. The accumulation of

deicing salts in concrete modifies drying behavior; therefore, saturated areas tend to occur near deicing material deposition [72]. As the deicing salts absorb moisture for prolonged periods causing localized saturation, $\text{Ca}(\text{OH})_2$ is also leached from the hardened cement paste causing strength loss and increased porosity [66,67], which can lead to further CaCl_2 ingress and further damage. CAOXY formation is strongly affected by solution concentration and temperature (covered in **Section 2.2.3**). **Fig. 2.1** highlights a potential interaction location of $\text{Ca}(\text{OH})_2$ with Ca^{2+} and Cl^- ions inside a saturated concrete joint, while **Fig. 2.2** provides a pictorial illustration of potential deterioration mechanisms following the formation of CAOXY.

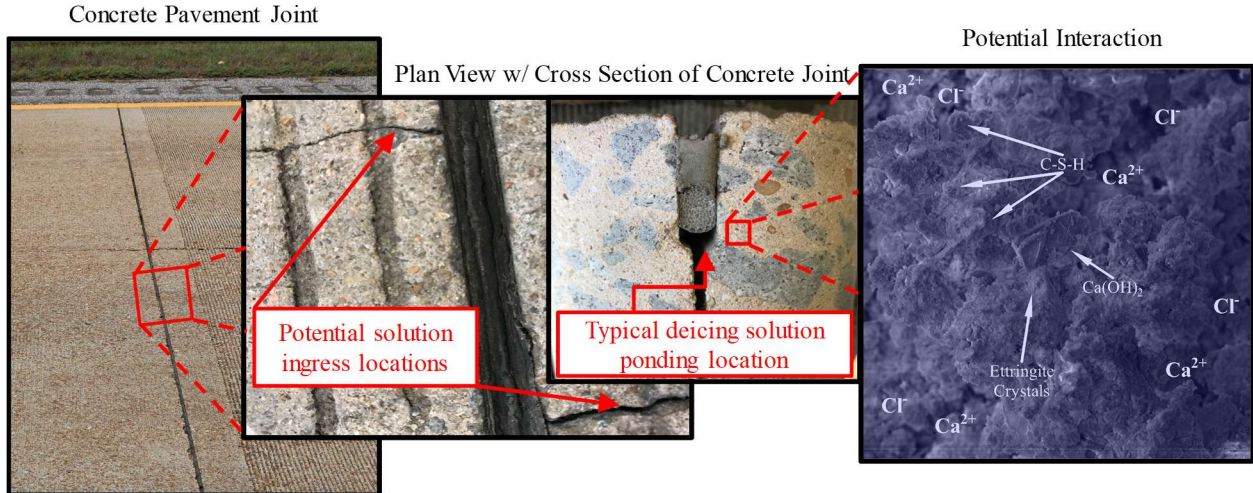


Figure 2.1. Potential formation location of CAOXY inside a deicing solution saturated concrete joint (unpublished data from authors).

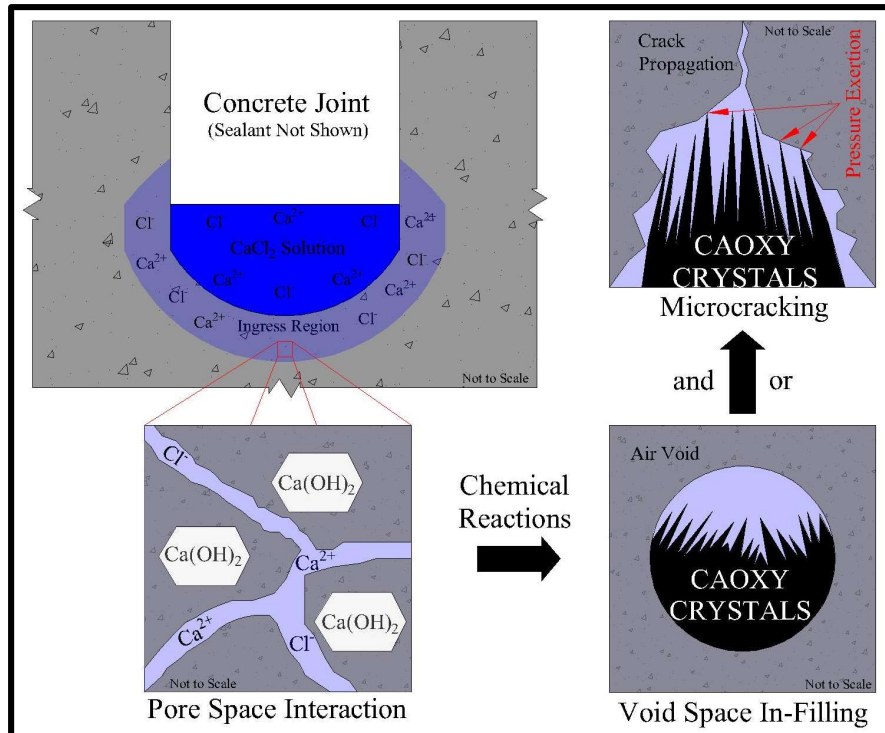


Figure 2.2. Illustrated representation of CAOXY formation in a saturated joint region of concrete pavement. Formation of CAOXY leads to deterioration by in-filling of available air voids and instigating microcracking in the pore space (unpublished data from authors).

Laboratory investigations have revealed two major and one minor CAOXY formations inside concrete specimens. Diaphanous shaped crystals of the 3:1:12 phase located on the surface of specimens were reported to be over 1 mm in length [56,66,74,82,120]. Similar product formations may be observed in **Fig. 2.3A** and **2.3B**. The second observed shape is a flat crystal described as a subhedral pseudo-hexagonal plate and is similar to $\text{Ca}(\text{OH})_2$ in appearance [56,66,74,82,120]. These platy structures have been measured up to 5 μm in diameter, less than 1 μm thick and located inside the specimen [74]. These structures have also been confirmed to be the 3:1:12 phase. Sutter et al. [66] reported similar CAOXY formations but suggested the material to be the 3:1:9 phase; however, this conclusion was based on recalculations rather than direct measurements. Ghazy and Bassuoni [74] further reported a third CAOXY crystal that was extremely small, fibrous and also located internally. These crystals corresponded to a 3:1:15

phase based on Energy-Dispersive X-Ray Spectroscopy (EDXS) analysis (covered in **Section 2.3.1.2**) [74].

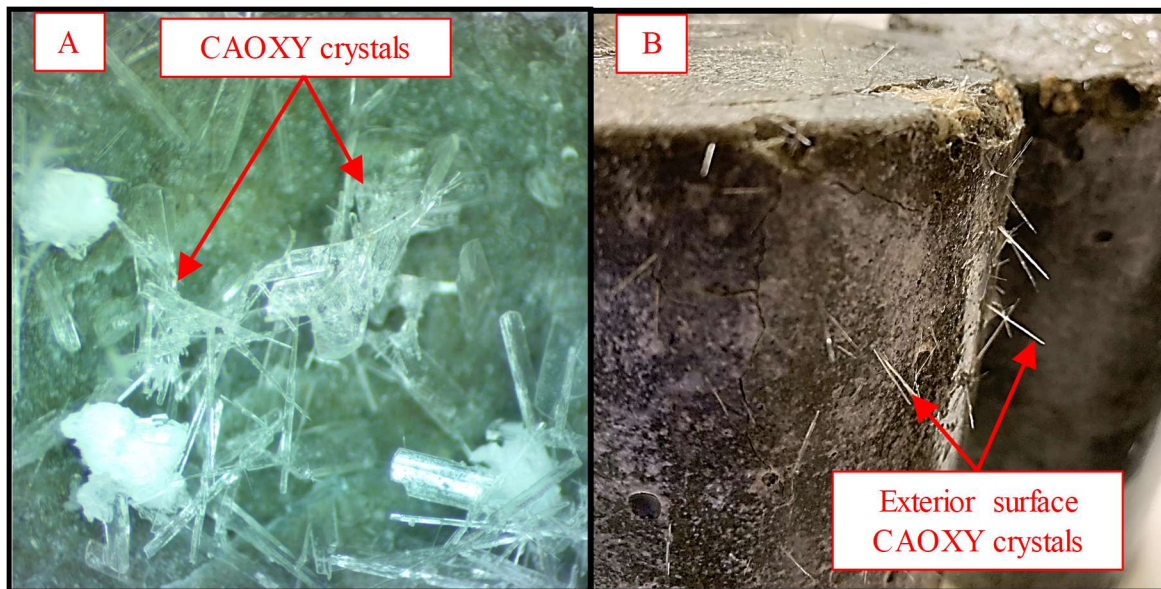


Figure 2.3. CAOXY crystals located on the exterior surface of specimens exposed to CaCl_2 solutions. (A) Deteriorated 50 mm cement paste cube specimen (0.45 water-to-cementitious materials ratio (w/cm), 10% fly ash replacement of cement) exposed to 23.1% CaCl_2 solution at 5 °C. (B) Deteriorated 100 mm x 200 mm concrete cylinder (0.40 water-to-cementitious materials ratio (w/cm), 20% fly ash replacement of cement) exposed to 25% CaCl_2 solution and repeated temperature cycles ranging from -10 °C to 23 °C. (Unpublished data from authors).

As previously shown, many researchers have attempted to comprehend the transitory nature of CAOXY. Birnin-Yauri and Glasser [98] developed a phase diagram showing that the 3:1:12 phase was the only stable version of CAOXY in an aqueous solution with $\text{Ca}(\text{OH})_2$ present. Although this study was performed on a pure $\text{Ca}(\text{OH})_2$ - CaCl_2 - H_2O system (i.e. not on a cementitious specimen), numerous researchers have reported damage in cement paste, mortar and concrete due to the 3:1:12 phase [20,28,42,44-50,52,54,56,59,64,66,69,73-77,81,82,106-109,112,113,115,120,123]. Shi [99] expanded upon this work [98], further revealing the transitory nature of the salt by detailing its decomposition at 20 °C and 20% relative humidity and suggested that careful sample preparation was critical to study deterioration caused by the

3:1:12 CAOXY phase. Julio-Betancourt [56] developed a list of general guidelines in order to aid in the determination of the presence of CAOXY precipitates in field concrete specimens:

1. Obtain samples during winter or the cold season when excessive rain and temperature change will not interfere with the crystal formation [56].
2. Do not use solvent or water to obtain and store samples; rather, wrap and place in sealed bags [56].
3. Test the samples immediately avoiding the use of heat or any contaminating material [56].
4. If the specimen cannot be tested immediately, store specimens in sealed containers in a frozen condition (-18 ± 2 °C) [56].

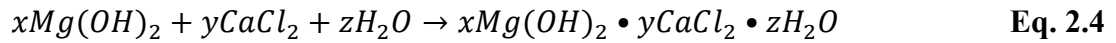
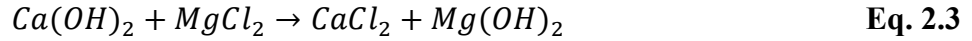
Similar suggestions have been reported by [57]. It should be noted that these guidelines do not provide full details in order to obtain, store and test specimens. Research is needed to fill these gaps and provide complete procedures for determining the presence of CAOXY in field samples.

2.2.2.2. Formation of CAOXY in MgCl₂ Solutions

Traditionally, CAOXY has been reported in CaCl₂ solutions; however, MgCl₂ may also instigate the formation of CAOXY as shown in **Table 2.1** [49,56,66,72,77,81-83,109,123]. Numerous studies have investigated the effects of placing paste, mortar and concrete specimens in MgCl₂ brines [49,56,57,66,74,77,81-84,88,90-93,109,120,123,127]. The results from these investigations vary based on solution concentrations and exposure conditions. General deterioration mechanisms and reaction products associated with cementitious paste exposed to MgCl₂ are covered in **Table 2.1**. These reaction products may lead to deterioration mechanisms different than CAOXY. These mechanisms are not covered in this work unless their formation aids the process of CAOXY formation, such as MAOXY and Mg(OH)₂.

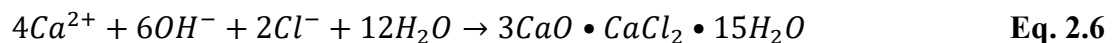
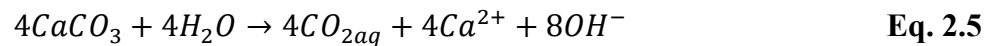
MgCl₂ can react with Ca(OH)₂ as shown in **Eq. 2.3** producing Mg(OH)₂, and further deteriorates concrete by forming expansive MAOXY according to **Eq. 2.4**

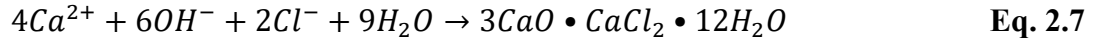
[49,51,55,56,66,72,81,83,85,88,120,123]. In systems with a Ca(OH)₂/MgCl₂ ratio greater than 1, Ca(OH)₂ is not fully converted to Mg(OH)₂; rather, a portion remains available in the system and can form CAOXY according to **Eq. 2.1** (x:y:z = 3:1:12) as detailed in **Section 2.2.2** [83].



2.2.2.3. Formation of CAOXY in NaCl Solutions

Studies have concluded NaCl does not lead to the formation of CAOXY in cementitious systems and NaCl causes the least damage when compared to CaCl₂ and MgCl₂ [51,56,66,68,71-74,77,101,128]. However, recently, oxychloride phases have been observed in carbonated concrete specimens exposed to NaCl solution [97]. In that study, specimens were prepared using ordinary portland cement (OPC), a high sulfate resistant cement, 50% slag, and 70% slag. After 28-days of curing, specimens were covered exposing only one end and placed in a 10% CO₂ environment until testing with freeze/thaw cycles in a NaCl solution. Following completion of freeze/thaw testing, paste scales were microscopically inspected and birefringent oxychloride crystals were observed [97]. In order to explain the presence of these crystals in a NaCl solution the authors developed **Eq. 2.5 - 2.7**. These equations provide the basis for the generation of CAOXY in NaCl solution in carbonated samples. Both 3:1:12 and 3:1:9 phases can precipitate according to these reactions. To the best knowledge of the authors, no CAOXY has been reported in specimens exposed to NaCl solution that were not intentionally carbonated.





2.2.3. Phase Diagrams

Phase diagrams provide chemical characterization information and conditions needed for the formation of different compounds. Stoichiometric data for the 3:1:12 compound can be traced back to Zahorsky from 1893 (according to [102]). Birnin-Yauri and Glasser [98] developed a ternary phase diagram with transition zones for the 1:1:1 and the 3:1:12 phases. A ternary phase diagram of known CAOXY variations is plotted in **Fig. 2.4**. It should be noted that not all formations can be present simultaneously as environmental factors significantly affect crystal structure and stability. Farnam et al. [58] utilized known binary phase diagrams $CaCl_2 - H_2O$ [129] and $Ca(OH)_2 - CaCl_2 - H_2O$ [130] to develop updated versions including CAOXY formation based on temperature, $CaCl_2$ concentration, and the molar ratio of $Ca(OH)_2$ and $CaCl_2$ ($Ca(OH)_2/CaCl_2$). Utilizing novel testing techniques such as low-temperature differential scanning calorimetry (LT-DSC) (described in more detail in **Section 2.3.1.5.**), Farnam et al. [58] developed **Eq. 2.8** capturing the relationship between $CaCl_2$ solution concentration and the temperature at which CAOXY precipitates. This isopleth characterizes the precipitation of CAOXY at temperatures above freezing (shown as a red-spaced line and labeled as $CAOXY_{(aq)}$ in **Fig. 2.5**). Qiao et al. [23,24] verified and extended these results. **Fig. 2.5** is adapted from [23,24,58].

$$T = 27.88 \ln \frac{C_0}{C^*} \quad \text{Eq. 2.8}$$

T = Temperature of CAOXY formation (°C)

C₀ = CaCl₂ solution concentration (%mass)

C* = Minimum CaCl₂ solution concentration for CAOXY formation (4.97%)

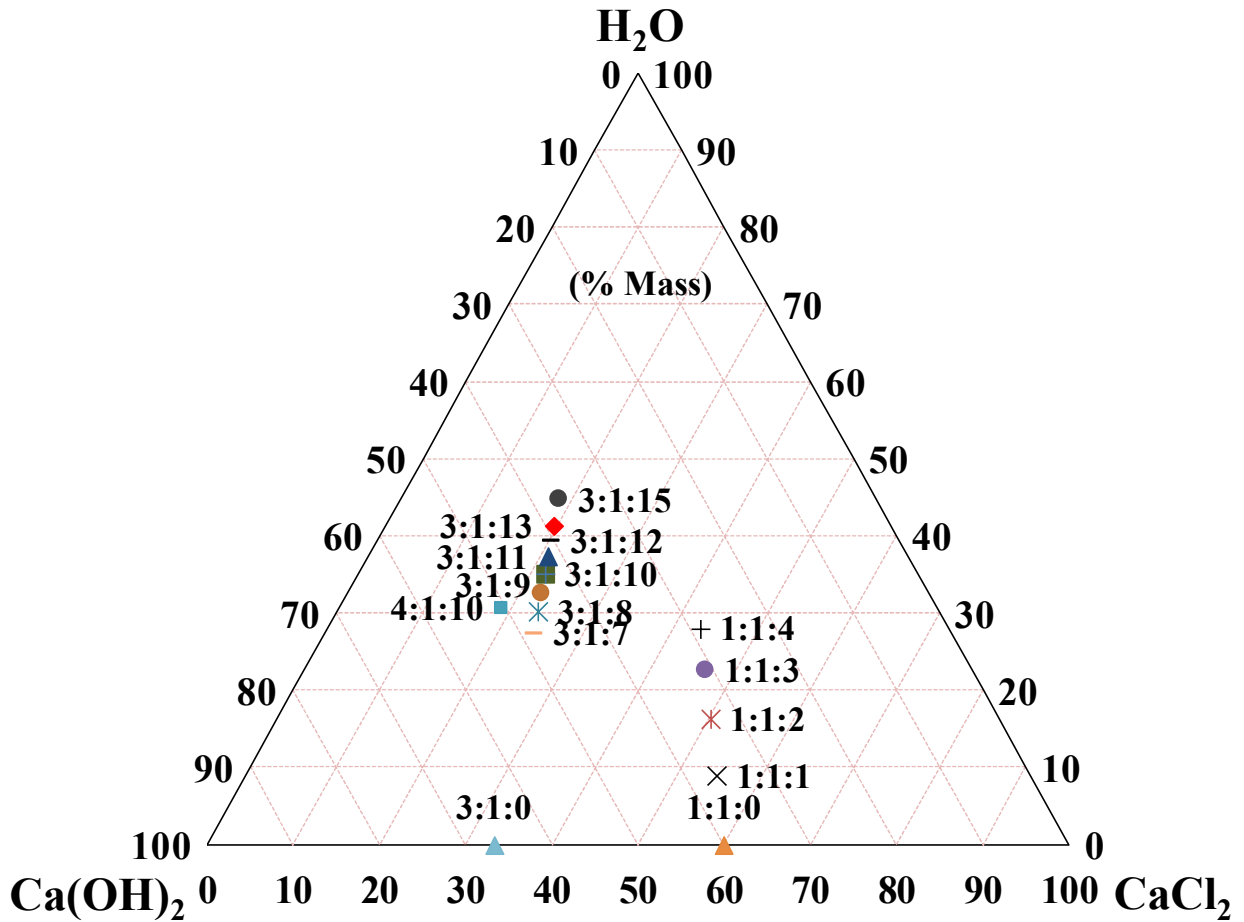


Figure 2.4. Ca(OH)₂ – CaCl₂ – H₂O ternary phase diagram plotting various known formations of CAOXY. It should be noted that not all phases can be present in similar temperature and solution concentrations.

The ratio of Ca(OH)₂ to CaCl₂ greatly effects the ability of deicing salts to properly mitigate gelid conditions [23,24,58]. This is simply explained by examining the amount of

consumed/available $\text{Ca}(\text{OH})_2$ in the system. If $\text{Ca}(\text{OH})_2/\text{CaCl}_2$ is greater than 3, all CaCl_2 (for solution concentrations $< 30\%$) will be consumed [23,24]. When $\text{Ca}(\text{OH})_2/\text{CaCl}_2$ is less than or equal to 3, not all CaCl_2 is consumed. Therefore, after all available $\text{Ca}(\text{OH})_2$ has reacted with CaCl_2 forming CAOXY, a portion of CaCl_2 remains in solution to depress the solution freezing point below $0\text{ }^\circ\text{C}$. This is clearly depicted in **Fig. 2.5A** where $\text{Ca}(\text{OH})_2/\text{CaCl}_2$ is less than or equal to 3 showing the depressed freezing point of the solution. **Fig. 2.5B** graphically represents $\text{Ca}(\text{OH})_2/\text{CaCl}_2$ greater than 3 indicating solution (i.e. water) solidification at $0\text{ }^\circ\text{C}$ due to the lack of CaCl_2 . From the literature, two of the most important factors for CAOXY formation are the deicing salt solution concentration and temperature [23,24,42,44,48,50,52,56,58,64,80,82,97,101,106-108,113,115]. Early observations of CAOXY reported that deterioration did not occur above $40\text{ }^\circ\text{C}$ or at lower solution concentrations ($\text{CaCl}_2 < 15\%$) [64,80]. However, research by [23,24,58] provides evidence that in high solution concentrations (30%), CAOXY precipitation can occur at temperatures near $50\text{ }^\circ\text{C}$ (shown in **Fig. 2.5**). The formation of CAOXY at $23\text{ }^\circ\text{C}$ is suggested to occur at a solution concentration of 11.3% [58]. While pure phase results may not always be directly transferrable to concrete pavement systems, these findings suggest that CAOXY could be a constant year-round threat to concrete pavements, rather than only in cold weather conditions [101].

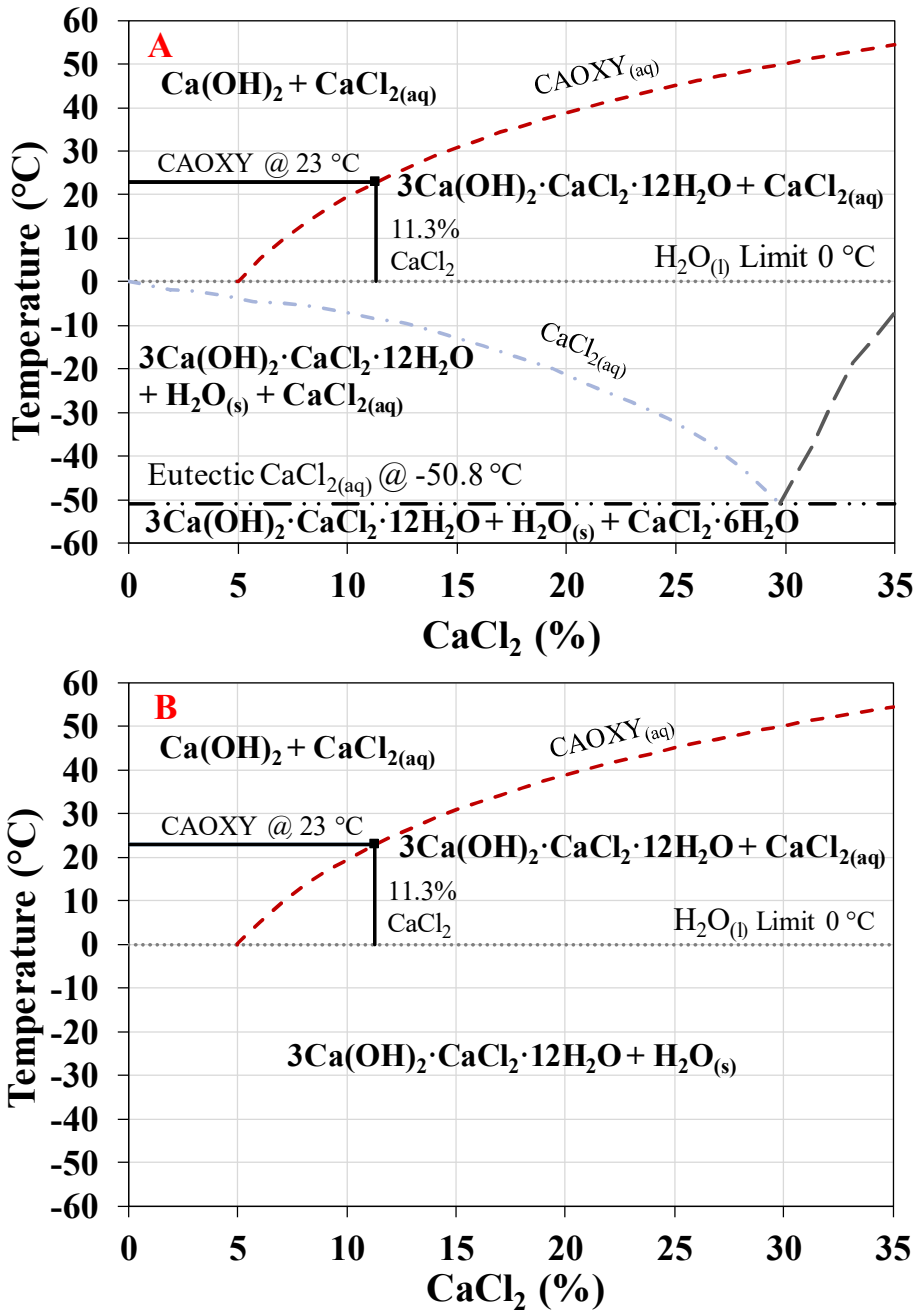


Figure 2.5. Binary phase diagram showing the interaction of Ca(OH)_2 and CaCl_2 based on temperature. A – $\text{Ca(OH)}_2:\text{CaCl}_2 \leq 3$, B – $\text{Ca(OH)}_2:\text{CaCl}_2 > 3$ (adapted from [23,24,58]).

2.2.4. Impact on Structural Integrity and Microstructure

Lawrence and Vivian [41] reported expansion and subsequent cracking/disintegration of paste and mortar specimens (w/c - 0.25 and 0.5) exposed to 30% CaCl_2 for 112-days. Smolyck [51]

developed a graph based on visual classifications of deterioration in mortar samples stored in CaCl_2 (28%) brine for 16-weeks. Numerous other investigations have noted significant/complete failure in specimens exposed to CaCl_2 solutions without additional stress [42,44,54-57,63,66-68,80,81]. Visual observations indicate excessive cracking and flaking/loss of external material, as shown in **Fig. 2.6A** and **2.6B**. Sutter et al. [66] provided images of CAOXY remnants filling void spaces inside concrete specimens. EDXS analysis (covered in **Section 2.3.1.2**) revealed a slightly modified CAOXY version (with some CaCO_3 present) [66], possibly due to damaged/morphed 3:1:12 phases during sample preparation as the specimens were air dried prior to testing. Ghazy and Bassuoni [74] confirmed the infilling of air voids with the 3:1:12 phase through environmental scanning electron microscopy (ESEM) (covered in **Section 2.3.1.3**) of undisturbed samples as described in **Section 2.2.2.1**. The precipitation of these phases may increase paste tortuosity (prior to cracking) mitigating the ingress of solutions containing Ca^{2+} and Cl^- ion penetration [58,59,86,109,131]. However, the combination of large diaphanous surface crystals, subhedral pseudo-hexagonal platy forms and tiny fibrous crystals combine to cause significant expansion, and deterioration, in paste, mortar, and concrete specimens.

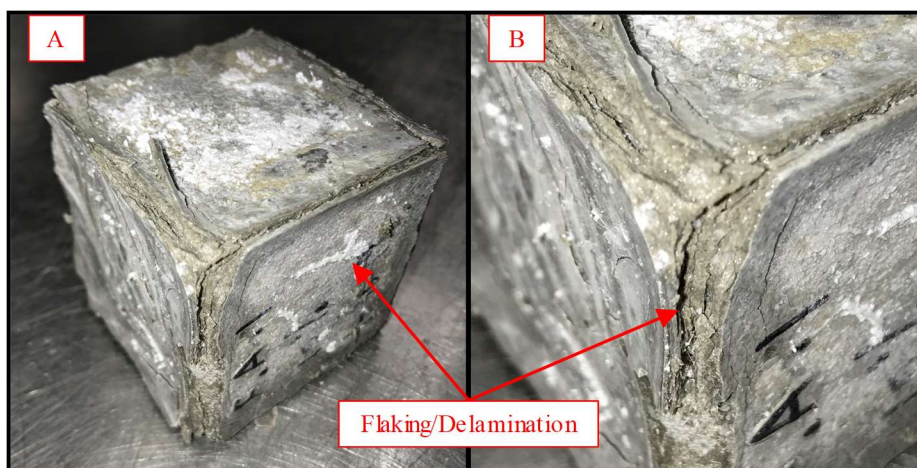


Figure 2.6. Deteriorated 50 mm cement paste cube specimen (0.45 water-to-cementitious materials ratio (w/cm), 10% fly ash replacement of cement) exposed to 23.1% CaCl_2 solution at 5 °C (A) Flaking observed throughout the entire specimen (B) Delamination observed along specimen edges (Unpublished data from authors).

2.2.5. Impact on Mechanical Properties of Cementitious Systems

It is known that CAOXY significantly impacts the structural integrity of cementitious systems; however, due to variations in testing methodologies, it is difficult to compare results in different cementitious systems to effectively elucidate the impact of CAOXY. The influence of aggregates, entrained air, and transport properties could impact deterioration observed in various sample types. Therefore, deterioration observation has been separated based on paste, mortar, and concrete specimens. Further, in an effort not to redundantly report the physical effects and mechanical impacts of CAOXY in cementitious systems, this section only focuses on the impact of CAOXY formation in pure cement systems. The effects of CAOXY formation in blended systems containing one or more supplementary cementitious materials (SCMs) or utilizing other mitigation techniques are covered in **Section 2.4**. **Table 2.4** has been developed to summarize deterioration observed in cement paste, mortar, and concrete specimens based on the literature; however, it must be noted that due to different testing methodologies and different mixture designs, a direct comparison of paste, mortar, and concrete samples is complicated. From **Table 2.4**, a number of observations are made for CAOXY deterioration in paste, mortar, and concrete samples which are summarized in **Table 2.5**.

Table 2.4. Influence of CAOXY formation on mechanical properties of pure cement systems as reported in the literature for paste, mortar and concrete specimens.

Material	Test Program		Ref.	w/cm Air	Exposure Solution	Exposure Temp.	*Property Reduction (%)			
Paste	Age of exposure	7-days	[42]	0.32 -	30%	5 °C	64% strength loss			
	Exposure protocol	90-days submerged in CaCl ₂		0.32 -	30%	20 °C	67% strength loss			
	Property measured	Compressive strength		0.32 -	30%	30 °C	63% strength loss			
	Age of exposure	91-days		[47]	0.36 -	10%	5 °C	11% strength loss		
					0.36 -	20%	5 °C	22% strength loss		
					0.36 -	30%	5 °C	58% strength loss		
					0.42 -	10%	5 °C	13% strength loss		
					0.42 -	20%	5 °C	34% strength loss		
					0.42 -	30%	5 °C	100% strength loss		
					0.50 -	10%	5 °C	18% strength loss		
					0.50 -	20%	5 °C	41% strength loss		
					0.50 -	30%	5 °C	100% strength loss		
	Property measured	Flexural strength								
	Mortar	Age of exposure	28-days	[56]	0.485 -	5%	5 °C	5% strength loss		
		Exposure protocol	30-days submerged in CaCl ₂		0.485 -	11%	5 °C	3% strength loss		
0.485 -					15%	5 °C	27% strength loss			
Property measured		Compressive strength	0.485 -	22%	5 °C	58% strength loss				
			0.485 -	28%	5 °C	59% strength loss				
Age of exposure		28-days		[54]	0.30 -	30%	5 °C	22% strength loss		
					0.30 -	30%	20 °C	16% strength loss		
					0.30 -	30%	40 °C	24% strength gain		
					0.50 -	30%	5 °C	34% strength loss		
					Property measured	Compressive strength	0.50 -	30%	20 °C	66% strength loss
							0.50 -	30%	40 °C	10% strength gain

Table 2.4. (Cont.)

Material	Test Program		Ref.	w/cm Air	Exposure Solution	Exposure Temp.	*Property Reduction (%)
Mortar	Age of exposure	60-days	[52]	0.35	30%	5 °C	67% strength loss
	Exposure protocol	176-days submerged in CaCl ₂		-			
	Property measured	Compressive strength		0.65			
Concrete	Age of exposure	28-days	[64]	0.40	30%	5 °C	79% strength loss
				2.2%			
				0.50			
	Exposure protocol	300-days submerged in CaCl ₂		2.1%	30%	5 °C	79% strength loss
				0.60			
				2.7%			
	Property measured	Compressive strength		4.9%	30%	5 °C	9% strength loss
				0.40			
				4.9%			
	Age of exposure	28-days		0.50	30%	5 °C	66% strength loss
				4.8%			
				0.60			
	Exposure protocol	300-days submerged in CaCl ₂		6.3%	30%	5 °C	91% strength loss
				0.60			
				-			
Property measured	Compressive strength	6.3%	30%	5 °C	No data provided		
		0.40					
		6.6%					
Age of exposure	28-days	0.50	30%	5 °C	20% strength loss		
		6.3%					
		0.60					
Exposure protocol	450-days submerged in CaCl ₂	6.3%	30%	5 °C	28% strength loss		
		0.45					
		8%					
Property measured	Compressive strength/Modulus of elasticity	8%	32%	23 °C	43% strength loss		
		0.45					
		8%					
Age of exposure	28-days	8%	32%	23 °C	25% strength loss		
		0.45					
		8%					
Exposure protocol	540-days submerged in CaCl ₂	8%	32%	23 °C	16% loss in MOE		
		0.45					
		8%					
Property measured	MOE	8%	32%	23 °C	100% loss in MOE		
		0.45					
		8%					
Age of exposure	28-days	8%	32%	23 °C	100% loss in MOE		
		0.45					
		8%					
Exposure protocol	108 W/D cycles in CaCl ₂	8%	32%	23 °C	100% loss in MOE		
		0.45					
		8%					
Property measured	MOE	8%	32%	23 °C	100% loss in MOE		
		0.45					
		8%					

^aIn order to calculate Property Reduction (%), each mechanical property was measured at the age of exposure and compared to an equivalent specimen following the length of exposure in CaCl₂

Table 2.4. (Cont.)

solution. It should be noted that continued cement hydration may occur in samples submerged in CaCl₂ for extended soaking durations.

^bSpecimens were heat cured to accelerate curing to an equivalent 91-day age specimen.

^cCommercially available product with slightly varying solution concentrations, and utilized as received from the manufacturer.

Table 2.5. Main parameters controlling CAOXY damage in cement paste, mortar, and concrete.

Parameter	Cement Paste	Mortar	Concrete
Solution Concentration	Deterioration increases as CaCl ₂ solution concentration increases.	Deterioration is insignificant in solution concentrations below 11%. Over 11% CaCl ₂ , an increase in solution concentration increases deterioration up to 22% CaCl ₂ , after which damage does not increase (“pessimism” effect).	Significant deterioration in solution concentrations from 22 – 32%. Possible “pessimism” concentration at 22%, similar to mortar.
Value of w/cm	Deterioration increases as w/cm increases.	Deterioration increases as w/cm increases.	Deterioration decreases as w/cm increases.
Temperature	Temperatures up to 30 °C provided equivalent deterioration as 5 °C, though deterioration at 5 °C was more rapid.	No deterioration occurred in specimens stored at 40 °C.	Significant deterioration occurred in specimens stored in 32% solution at 23 °C.
Air Content			An increase in air content reduced deterioration. Significantly less deterioration was observed in samples with air contents 6.5% compared to those with air contents 5.0%.

The conclusions in **Table 2.5** are for each material type only (i.e. paste, mortar, and concrete).

The variations in testing methodologies (i.e. curing and exposure conditions) and materials utilized for these programs differed significantly not allowing comparisons to be made between material types. Results may vary significantly based on individual testing regimes and environmental factors; however, it is interesting to note that in paste specimens an increased w/cm increased deterioration, while the opposite was observed in concrete specimens. This finding supports the theory that aggregates, air content and transport properties may influence the effects of CAOXY formation. Continued research is needed to connect equivalent paste, mortar,

and concrete specimen deterioration from CAOXY formation. Control of air content in paste and mortar specimens will be essential in being able to compare the damage with that observed in concrete specimens.

2.2.6. Deterioration Mechanisms

Specific deterioration mechanisms associated with CAOXY are still under investigation. Although total volume decreases during the formation of CAOXY, the volume of solids increases [47]. Qiao et al. [47] calculated CAOXY to be 303% larger in volume than Ca(OH)_2 . This increase in size, denoted as expansive pressure [44], is undoubtedly responsible for part of the deterioration associated with CAOXY; however, there is still work to be completed in understanding the exact deterioration mechanism. Chatterji [80] claimed crystallization pressure was responsible for the deterioration while Collepardi et al. [64] speculated hydraulic pressure may be the cause of failure. Other research suggested that pore wall pressures may increase significantly in cementitious systems when pore solutions became supersaturated with salts due to environmental conditions such as evaporation of fluid [132-134]. These deposited salts can have a crystallization stress of 200 – 350 MPa [134] exceeding the tensile strength of the cementitious pore wall. Though these mechanisms have been researched, further investigations are needed in order to determine the exact failure mechanism due to CAOXY formation. The determination may include several failure mechanisms such as crystallization pressure in conjunction with the leaching of Ca(OH)_2 . Determining the correct failure mechanism will aid in developing predictive life-cycle models for concrete exposed to deicing salt deterioration.

2.2.7. CAOXY Deterioration in Field-Placed Concrete

2.2.7.1. Concrete Sleeper/ Tie Deterioration

Significant deterioration due to CaCl_2 based deicing salts was observed by Berntsson and Chandra [61] in high strength concrete sleepers (known as concrete ties in the US). The members were designed with compressive strengths over 50 MPa and were used as crane tracks [61]. The region of placement required significant dosages of deicing materials during winter conditions [61]. Within a few years, the concrete sleepers/ties showed significant deterioration and it was noted the intended design life would not be met [61]. This was the first observation of field conditions with sufficient CaCl_2 solution concentrations to cause deterioration in concrete structures. Though the sleepers/ties were subjected to freeze/thaw deterioration in conjunction with deicers, the authors noted a chemical mechanism was likely the culprit for the observed deterioration [61].

2.2.7.2. Concrete Wall Deterioration Exposed to Seawater

In 2013, Justnes et al. [125] reported increased chloride binding in a concrete wall exposed to seawater for 10-years. Chloride contents were measured to be more than four times larger than expected (0.96% Cl^- by concrete mass) [125]. It was determined that the increased chloride content was due to the formation of CAOXY as magnesium from the seawater exchanged with calcium from the cement paste [125]. This resulted in deterioration from the 3:1:12 phase formation according to **Eq. 2.1** and 5-phase MAOXY according to **Eq. 2.4**. This is one of the first confirmed cases of CAOXY deterioration in field placed concrete. Deterioration in underground concrete tunnels exposed to chloride-based solutions due to MAOXY has also been suggested [121].

2.2.7.3. Concrete Pavement Joint Deterioration

In general, deicing salts do not reach levels required to deteriorate full sections of concrete pavement; however, localized sections, such as joints (as covered in **Section 2.2.2.1**), may buildup necessary levels to deteriorate concrete [32]. Taylor et al. [27] investigated a number of concrete pavement sites experiencing various levels of distress throughout Iowa, Michigan, Minnesota, and Wisconsin. Based on petrographic analysis of field cores taken from each site, a number of different deterioration mechanisms were suggested. These included poor air void systems, in-filling of air voids with reaction products such as ettringite, D-cracking, deicing salt damage, freeze/thaw damage, and failed sealants [27]. It was noted in some cores that significant chemical attack had occurred in the cementitious paste portion of the core as a result of the use of deicing salts other than NaCl. Similar joint damage is shown in [28] and is identified as 3:1:12 CAOXY.

Another recent failure that has been associated in part with deicing salt deterioration is the M-6 highway, also known as the Paul B. Henry Freeway, which provides a connection between I-196 and I-96 in Michigan. M-6 began failing much earlier than expected due to significant problems in the concrete durability, which has required repair as early as 8-years after placement [29]. Further, deterioration significantly varies throughout the site. The exact cause of the failure is still unclear; however, it has been indicated there may have been issues with the air void system in conjunction with the use of deicing salts [29]. Concrete mixture design reports indicate slag was used as a partial cement replacement in varying amounts; however, a portion of the project was paved with a pure cement system [29]. This is a major example of the rapidity at which concrete can deteriorate when deterioration mechanisms such as CAOXY may be present in a pavement with a poor air void system.

2.3. Testing Strategies for Assessment of CAOXY Formation

2.3.1. Novel Test Methods for Assessing CAOXY Formation and Deterioration

In the past, research used traditional methods for quantifying deterioration associated with CAOXY formation. Procedures typically included soaking specimens in high CaCl_2 solution concentrations (i.e. 15 – 30%) at cold (5 °C), mild (20 °C) or warm (40 °C) temperatures [41,42,51,60,63,64,78,80]. Visual observations of the specimen quality and compressive strength variations due to the deicing salt solution are generally reported. These tests are helpful in determining deterioration due to CAOXY formation; however, for this text no in-depth description is provided for testing techniques associated with general mechanical properties (i.e. compressive strength, flexural strength, modulus of elasticity, etc.). These tests are widely available, with slight variations, but with similar, reproducible results. However, novel techniques have been developed to better identify/quantify CAOXY formation in cementitious systems. Therefore, a brief description of each novel test method is provided along with references for a more detailed description.

2.3.1.1. X-Ray Diffraction (XRD)

The authors believe this test method, though older, still warrants a brief mention as a highly useful technique to determine the presence of CAOXY. In XRD, X-rays are directed through a crystal and the refracted wave patterns are collected. Monosi et al. [42] utilized this technique to identify the first 3:1:12 phase in deteriorated samples exposed to 30% CaCl_2 by comparing the refracted wave patterns to known crystal formations. Today crystal identification can be made utilizing known patterns in the JCPDS/ICDD XRD database [135] with unknown patterns representing a gap in the knowledge. It should be noted that some [101] have suggested that the current 3:1:12 (Eq. 2.1) file (card 02-0280) [135] does not match other known XRD patterns and

states that CAOXY identification by XRD should be accomplished utilizing XRD patterns from other literature [42]. A more in-depth overview of XRD is provided elsewhere [136] and this technique is still used today to verify the formation of CAOXY in samples.

2.3.1.2. Energy-Dispersive X-Ray Spectroscopy (EDXS)

Another highly useful technique to determine the presence of CAOXY is EDXS (often referred to as EDX). An X-ray or electron beam excites electrons inside the atomic structure of each element causing their release. EDXS provides the amount and type of each individual element inside a material. The individual elements can be summed up and a determination made of the parent material. Sutter et al. [66,82] utilized this technique in determining CAOXY deterioration in concrete specimens exposed to CaCl_2 solutions. However, the 3:1:9 phase determined in this research varies slightly from the 3:1:12 typically reported. This can possibly be attributed to dehydration of the samples prior to testing. Ghazy and Bassuoni [74] utilized this technique in conjunction with ESEM (covered in **Section 2.3.1.3**) to determine a new 3:1:15 phase in cementitious samples.

2.3.1.3. Environmental Scanning Electron Microscopy (ESEM)

A more modern testing technique is the use of scanning electron microscopy (SEM). This technique utilizes electron scattering under vacuum to provide an image of the microstructure of materials. Therefore, physical shapes of $\text{Ca}(\text{OH})_2$, C-S-H, ettringite or other hydration phases may be studied more in depth. However, CAOXY crystals are more sensitive to environmental conditions. Traditional SEM does not allow for the presence of moisture during testing; however, environmental scanning electron microscopy (ESEM) overcomes this limitation. Ghazy and Bassuoni [74] utilized ESEM to capture unaltered CAOXY in deteriorated concrete specimens allowing for measurements and accurate descriptions of each 3:1:12 phase variation.

2.3.1.4. Thermogravimetric Analysis (TGA)

Recently, thermogravimetric analysis (TGA) has been established as a very useful tool to quantify potential CAOXY formation in cement pastes [28,46-48,89,106-109,111-116]. This is due to the linear relationship between Ca(OH)_2 and CAOXY in ground cementitious pastes. TGA utilizes a small (20-50 mg) sample of ground (< 200 sieve) cement paste [48,115]. Samples are heated to a minimum of 500 °C [106,115] for Ca(OH)_2 ; however, some tests methodologies will heat to 1000 °C [28,46-48,89] in order to determine other phases present in the cementitious paste. Mass loss in the sample between 380 °C to 460 °C is used to calculate the Ca(OH)_2 content which can be used to estimate CAOXY that can form [137]. Suraneni et al. [115] established the relationship between Ca(OH)_2 and CAOXY formation at 2.47 g CAOXY formed per 1 g of Ca(OH)_2 in cementitious pastes. It should be noted that some Ca(OH)_2 is bound in C-S-H or other phases and may not be available for CAOXY formation [115]. The use of SCM reduces the amount of Ca(OH)_2 and CAOXY as Ca(OH)_2 is consumed through the pozzolanic reaction [115].

2.3.1.5. Low-Temperature Differential Scanning Calorimetry (LT-DSC)

Recently adopted as a test method by the American Association of State Highway and Transportation Officials as AASHTO T 365 [22], LT-DSC directly quantifies CAOXY formation in ground cement pastes by measuring heat released during the formation of the salt crystal [21]. Cured specimens are ground to a fine powder (< 200 sieve) and a small (10 mg) sample is mixed with a CaCl_2 solution of equal mass. The standard method specifies a 20% solution concentration; however, testing can be conducted to show CAOXY formation at different solution concentrations. Combined paste/solution mixtures sit in the container for 1-hour to allow any unhydrated cement grains to react prior to recording heat signatures. The

temperature of the calorimeter is then reduced to $-90\text{ }^{\circ}\text{C}$ at a rate of $3\text{ }^{\circ}\text{C}/\text{min}$. It is cycled from $-90\text{ }^{\circ}\text{C}$ to $-70\text{ }^{\circ}\text{C}$ and back to $-90\text{ }^{\circ}\text{C}$ to ensure the specimen is fully frozen removing any CAOXY precipitates that may have formed during cooling. The sample is then heated to $50\text{ }^{\circ}\text{C}$ at a rate of $0.25\text{ }^{\circ}\text{C}/\text{min}$ and heat associated with the formation of CAOXY is captured. The peak heat signature associated with CAOXY formation is dependent upon the solution concentration used for testing and the type of cement paste tested (i.e. a pure cement sample or a sample containing cement and SCM); however, peak heat signatures may be observed between $5\text{ }^{\circ}\text{C}$ and $50\text{ }^{\circ}\text{C}$, though they are usually between $30\text{ }^{\circ}\text{C}$ to $40\text{ }^{\circ}\text{C}$. Measurements determined by this test procedure are only applicable for a specific cementitious system and deicing solution concentration. A number of investigations have utilized this technique to determine CAOXY formation [21,28,46-49,58,59,89,106-109,111-116]. However, this is still a relatively new test and further research is ongoing including work to correlate CAOXY amounts determined from LT-DSC to damage in concrete specimens.

2.3.1.6. Volume Change Measurement (VCM)

Qiao et al. [23] developed a methodology to quantify CAOXY formation based on volume change measurements using a $\text{Ca}(\text{OH})_2\text{-CaCl}_2\text{-H}_2\text{O}$ mixture. By substituting $\text{Ca}(\text{OH})_2$ with ground cement paste, CAOXY could be determined in pure cement paste or cement paste containing SCMs prior to use in a concrete mixture design. In order to conduct this test, the solution is placed inside a glass vial with a rubber stopper ensuring no air bubbles remain in the system, and then a water-insoluble dye is added to the top portion of the mixture prior to sealing the system. Sample preparation is conducted at $50\text{ }^{\circ}\text{C}$ to ensure no CAOXY forms prior to testing. Once the $\text{Ca}(\text{OH})_2\text{-CaCl}_2\text{-H}_2\text{O}$ solution is in the vial, it is placed in a programmable water bath to rotate through a cooling and heating cycle starting at $50\text{ }^{\circ}\text{C}$ and going to $0\text{ }^{\circ}\text{C}$ and

then back to 50 °C. Each temperature step is held constant for 8-hours with a total test time of 11-days. VCM quantifies the system volume change, which may be linked to the physical growth of CAOXY as indicated by the movement of the dye on top of the solution. A recording device can be used to capture the movement of the dye for each time step if constant monitoring is not possible. However, the biggest limitation for this test method is the singularity of each system, which makes it somewhat laborious and time consuming. Only one deicing salt solution concentration can be measured with one cementitious system. To the authors knowledge, only a few studies have been conducted utilizing this test method [23,24,47], and further research programs are needed to verify these results.

2.4. Prevention and Mitigation Strategies

A number of techniques exist to prevent/mitigate the formation of CAOXY in cementitious systems. Two of the most effective strategies currently available are the use of SCMs [45-48,54,72,106,108,112-115] and providing a quality air void system [64,72,138]. Other methods include controlling mixture design parameters such as reducing cement content and optimizing aggregate gradations [72], the use of techniques such as preferential carbonation [52,111] and sealants [49,72,96,110,112], or through using non-chloride based deicing solutions [56,66-69,72,82,92,123]. Fortunately, a number of preventative/mitigation techniques can be applied simultaneously on projects maximizing potential CAOXY reduction.

2.4.1. Utilizing Mixture Design Parameters

Simple mixture design parameters can drastically affect the durability of concrete pavements. Lowering w/cm decreases permeability while increasing air content reduces initial degree of saturation and provides space for the formation of CAOXY [72]. Aggregates may also affect durability and it is stated that the largest nominal maximum aggregate size should be utilized to

reduce cement paste content [72]. Further, optimized aggregate gradations can lead to even lower paste contents possibly mitigating potential deleterious chemical interactions, such as CAOXY [72]. These parameters could potentially be utilized to aid in mitigating deterioration concerns associated with CAOXY formation.

2.4.1.1. Utilizing Supplementary Cementitious Materials

In general, SCMs do mitigate CAOXY formation/deterioration; however, their impact varies throughout the literature. Part of this variation may be related to SCM type and replacement level, test methodology (i.e. curing conditions, storage temperature, solution concentration, etc.) or whether cement paste, mortar or concrete was tested. In an effort to elucidate the role of SCM addition in CAOXY mitigation, a short review of the impact of SCMs on CAOXY formation of cementitious materials exposed to CaCl_2 is presented.

2.4.1.1.1. Impact of SCMs on Calcium Oxychloride Formation

SCMs impact cement hydrate formation through a dual action. The first action is dilution in which a portion of cement is directly replaced with an equivalent portion of SCM [45-48,72,106,108]. Given that SCMs do not react as cement, a reduction in the amount of hydration products is observed when comparing pure cement samples to equivalent samples containing a portion of SCM, especially at early ages. The second action of SCMs is due to the pozzolanic nature of some SCMs [45-48,72,106,108]. These materials are able to react with and subsequently reduce $\text{Ca}(\text{OH})_2$ (from cement hydration) forming C-S-H which decreases permeability. The combination of these two actions make SCMs an effective technique to mitigate CAOXY damage [45-48,72,106,108]. SCMs can have other significant effects on cement hydration including hydraulic reactions and filler effects [108], which are outside the scope of this work.

It is known that CAOXY that can form in ground cement pastes is linearly correlated to the quantity of $\text{Ca}(\text{OH})_2$ in ground cement paste [20,45-48,106,108,113,115] as shown in **Eq. 2.9** [108]. Similar correlations for mortar and concrete specimens are presented in [116]. In cement paste, a direct quantification of CAOXY reduction based on SCM addition can be measured utilizing testing techniques, such as LT-DSC and VCM (as described in **Sections 2.3.1.5** and **2.3.1.6**). Suraneni et al. [108] conducted LT-DSC testing of pure cement samples along with cement pastes containing SCMs such as fly ash, slag, silica fume, limestone dust, and calcined clay. Fly ash (both Class C and Class F), slag, and limestone dust were added at 20, 40, and 60% replacements by volume. Silica fume was utilized at 2, 6, and 10% volume replacements while calcined clay replacements were 5, 10, and 15% by volume. Presented in **Fig. 2.7** are best fit lines from this data along with their slopes. The slope is an indication of the efficiency of each material in reducing CAOXY [108]. For these materials, the order of most efficient to least is calcined clay, silica fume, slag, fly ash, and limestone [108]. Slag and fly ash, on average, show very similar performance in reducing CAOXY in ground cement pastes. In general, an increase in SCM replacement reduces CAOXY formation (although silica fume data indicated a slight increase in CAOXY between replacement rates of 2 and 6% [108,114]) due to a combination of dilution and pozzolanic reaction. This decrease in CAOXY was tentatively linked to the pozzolanic reactivity of each SCM [108]. Confirmation of decreasing CAOXY levels based on increasing SCM replacement was done by Qiao et al. [47] utilizing VCM testing on cement pastes with fly ash replacements of 0, 20, 40, and 60%. Suraneni et al. [48] determined CAOXY levels above 15 g/100 g paste may not be sufficient to protect paste samples from strength loss due to CAOXY deterioration. This threshold level is plotted in **Fig. 2.7** as a grey dashed line. It was concluded that fly ash and slag were the most viable options for CAOXY mitigation;

however more than 35% fly ash or slag (greater than replacement levels allowed by most DOTs) was required to meet the threshold guidelines [108]. The replacement levels of silica fume, calcined clay and limestone (25, 19, and 73%) required to mitigate CAOXY below the threshold level are most likely not realistic for concrete pavement applications [108]. Therefore, additional mitigation techniques may be required to effectively realistically mitigate CAOXY in concrete pavements.

$$M_{CAOXY} = 2.82 M_{Ca(OH)_2} - 8.32 \quad \text{Eq. 2.9}$$

$M_{Ca(OH)_2}$ = Amount of $Ca(OH)_2$ (g/100 g paste)

M_{CAOXY} = Amount of CAOXY (g/100 g paste)

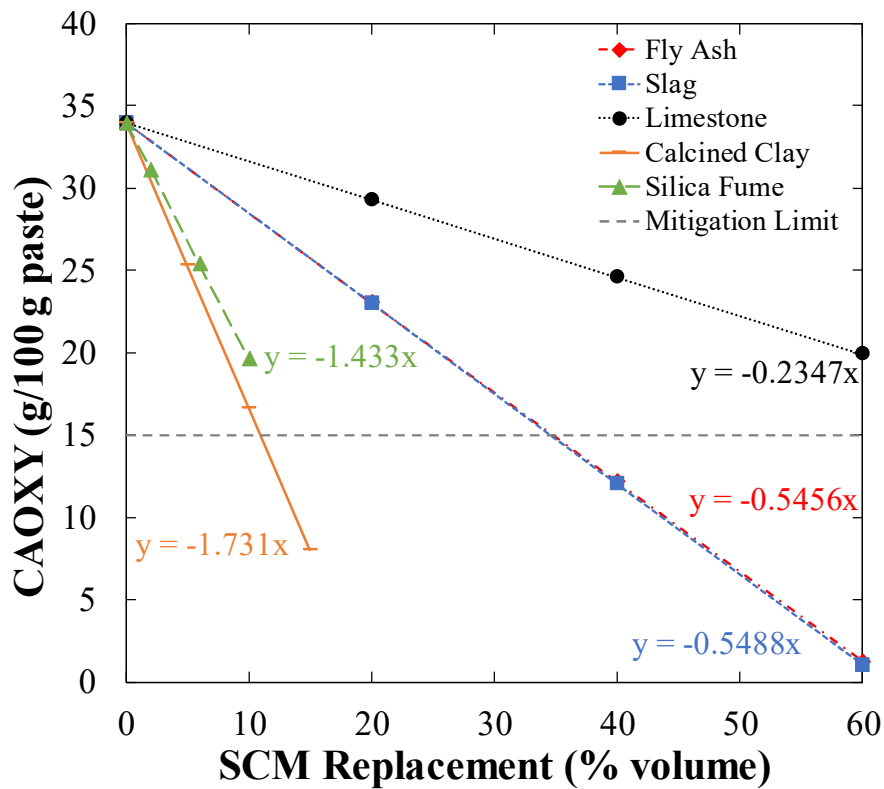


Figure 2.7. Best fit lines for CAOXY reduction utilizing various SCM types with a w/cm 0.36. Similar data observed for w/cm 0.50 (adapted from [108]).

2.4.1.1.2. Impact of SCMs on Mechanical Properties of Cementitious Materials Exposed to CaCl₂

As shown in **Section 2.4.1.1.1**, the addition of SCMs reduces the formation of CAOXY. As such, less deterioration, often observed as a less severe reduction in mechanical properties compared to an equivalent specimen containing no or less SCM, is observed. **Table 2.6** was developed to highlight research utilizing cementitious systems containing SCM and is divided into paste, mortar, and concrete specimens. Due to variations in curing conditions, test methodologies, and specimen types, it is difficult to connect deterioration between the paste, mortar, and concrete samples as also discussed in **Section 2.2.5**. General observations for paste, mortar, and concrete from **Table 2.6** are reported in **Table 2.7**.

Table 2.6. Influence of mitigation techniques to reduce mechanical property deterioration associated with CAOXY damage as reported in the literature for paste, mortar and concrete specimens.

Material	Test Program		Ref. ^a SCM	w/cm Air	Exposure Solution/ Temp.	Mitigation	^b Property Reduction (%)
Paste	Age of exposure	91-days	[47] Volume	0.42	30%	0%	100%
				-	5 °C	fly ash (C)	strength loss
	Exposure protocol	Thermal cycle 50°C–5°C–50°C		0.42	30%	20%	100%
				-	5 °C	fly ash (C)	strength loss
	Property measured	Flexural strength		0.42	30%	40%	33%
				-	5 °C	fly ash (C)	strength loss
-	-	0.42	30%	60%	10%		
-	-	-	5 °C	fly ash (C)	strength loss		
Mortar	Age of exposure	60-days	[52]	0.35	30%	Water cured	63%
				-	5 °C		strength loss
	Exposure protocol	176-days submerged in CaCl ₂		0.35	30%	Air cured	100%
				-	5 °C		strength loss
	Property measured	Compressive strength		0.35	30%	^d Carbonated 30% CO ₂	1%
				-	5 °C		strength gain
	-	-		0.65	30%	Water cured	100%
	-	-		-	5 °C		strength loss
-	-	0.65	30%	Air cured	100%		
-	-	-	5 °C		strength loss		
-	-	0.65	30%	^d Carbonated 30% CO ₂	6%		
-	-	-	5 °C		strength loss		

Table 2.6. (Cont.)

Material	Test Program		Ref. ^a SCM	w/cm Air	Exposure Solution/ Temp.	Mitigation	^b Property Reduction (%)		
Mortar	Age of exposure	28-days	[54] Not specified	0.50 -	30% 5 °C	0% SCM	34% strength loss		
	Exposure protocol	91-days submerged in CaCl ₂		0.50 -	30% 5 °C	30% fly ash (F)	14% strength loss		
				0.50 -	30% 5 °C	50% slag	6% strength gain		
	Property measured	Compressive strength		0.50 -	30% 5 °C	10% silica fume	13% strength gain		
Concrete	Age of exposure	28-days	[64] Mass	0.40 2.2%	30% 5 °C	0% SCM	79% strength loss		
				0.40 4.9%	30% 5 °C	0% SCM	66% strength loss		
				0.40 6.6%	30% 5 °C	0% SCM	20% strength loss		
				0.40 1.9%	30% 5 °C	50% slag	7% strength gain		
	Exposure protocol	300-days submerged in CaCl ₂		0.40 6.0%	30% 5 °C	50% slag	10% strength gain		
				0.40 2.0%	30% 5 °C	15% silica fume	7% strength gain		
				0.40 6.1%	30% 5 °C	15% silica fume	15% strength gain		
				Property measured	Compressive strength	0.40 1.8%	30% 5 °C	30% fly ash (F)	28% strength loss
	0.40 5.9%	30% 5 °C				30% fly ash (F)	22% strength loss		
	0.40 6±1%	21.9% 5 °C				0% SCM	100% loss in MOE		
	Age of exposure	28-days				0.40 6±1%	21.9% 5 °C	20% fly ash (F)	100% loss in MOE
				0.40 6±1%	21.9% 5 °C	30% fly ash (F)	100% loss in MOE		
				Exposure protocol	450-days submerged in CaCl ₂	0.40 6±1%	21.9% 5 °C	6% nanosilica	3% increased MOE
						0.40 6±1%	21.9% 5 °C	20% fly Ash (F)	2% increased MOE
	0.40 6±1%	21.9% 5 °C				6% nanosilica	2% increased MOE		
	Property measured	Modulus of elasticity				0.40 6±1%	21.9% 5 °C	30% fly ash (F)	2% increased MOE
0.40 6±1%			21.9% 5 °C	6% nanosilica	2% increased MOE				

^aThe inclusion of SCM as a replacement material for cement varied by mass or volume depending upon each specific reference. Cement replacement type used for each research program is provided below the reference.

Table 2.6. (Cont.)

^bIn order to calculate Property Reduction (%), each mechanical property was measured at the age of exposure and compared to an equivalent specimen following the length of exposure in CaCl₂ solution. It should be noted that continued cementitious hydration may occur in samples submerged in CaCl₂ for extended soaking durations.

^cSpecimens were heated to accelerate curing to an equivalent 91-day age specimen.

^dFollowing the initial 1-day cure in the molds, specimens were demolded and stored in a 30% CO₂ (by volume) 60% relative humidity chamber.

Table 2.7. Impact of various CAOXY mitigation techniques on mechanical properties and deterioration of cement paste, mortar, and concrete.

Parameter	Cement Paste	Mortar	Concrete
SCM Addition	Up to 20% fly ash, no observable deterioration mitigation; fly ash additions of 20-60% reduced deterioration; however, deterioration was observed for all replacement levels.	Additions of 50% slag and 10% silica fume eliminated deterioration and prompted strength gain, while 30% fly ash had minor strength reductions.	The addition of 50% slag or 15% silica fume effectively mitigated deterioration. Replacement of 30% fly ash was not effective at mitigating deterioration; however, the addition of nanosilica effectively mitigated deterioration.
Carbonation		Carbonation significantly mitigated deterioration in all specimens	

The conclusions in **Table 2.7** are for each material type only (i.e. paste, mortar, and concrete). Similar to data for the pure cement specimens, variations in testing methodologies (i.e. curing and exposure conditions) and materials utilized for these programs differed significantly not allowing direct comparisons to be made between material types. Results may vary significantly based on individual testing regimes and environmental factors; however, it appears that smaller cement replacements with SCM determine greater benefits for mortar and concrete specimens than paste specimens. This may possibly be explained by the influence of aggregates, air content, and transport properties. Research is needed to connect equivalent paste, mortar, and concrete specimen deterioration from CAOXY formation.

2.4.1.2. Proper Air-Entrainment

While an adequately entrained air system is required on all major concrete pavement projects, at this time air content is considered one of the two most effective means to mitigate damage from CAOXY. The use of entrained air does not preclude CAOXY formation; however, it may provide a binary benefit for CAOXY deterioration mitigation. First, air is known to reduce the initial degree of saturation and the time needed for critical saturation in concrete [72,138]. As water is a significant part of CAOXY formation, this aids in reducing the opportunity for CAOXY formation. Secondly, once saturation occurs, air voids may act as relief zones by providing space for the deposition of the expanding phase [64]. Collepardi et al. [64] reported OPC concrete specimens with air contents near 6.5% and w/cms of 0.40 and 0.50 had significantly less damage from CAOXY deterioration when immersed in 30% CaCl₂ solution at 5 °C for 300-days than specimens with air contents of 5.0% and non-air entrained specimens. When the w/cm increased to 0.60, similar damage was observed in both air entrained and non-air entrained specimens indicating the porosity of the paste at high w/cms may also provide some relief [64]. Nearly equivalent deterioration was reported in non-air entrained concrete with 30% fly ash and concrete with 6.5% air content but no cement replacement with SCM [64]. This indicates air content may be as important as replacing cement with SCM for mitigating deterioration by CAOXY formation. The use of SCM in conjunction with air contents near 6.0% were most effective in mitigating damage [64]. **Fig. 2.8** was developed to highlight potential benefits of an adequate air void system in cementitious systems. Some damage may still occur in air entrained systems, but much more damage potential exists in specimens without adequate air entrainment.

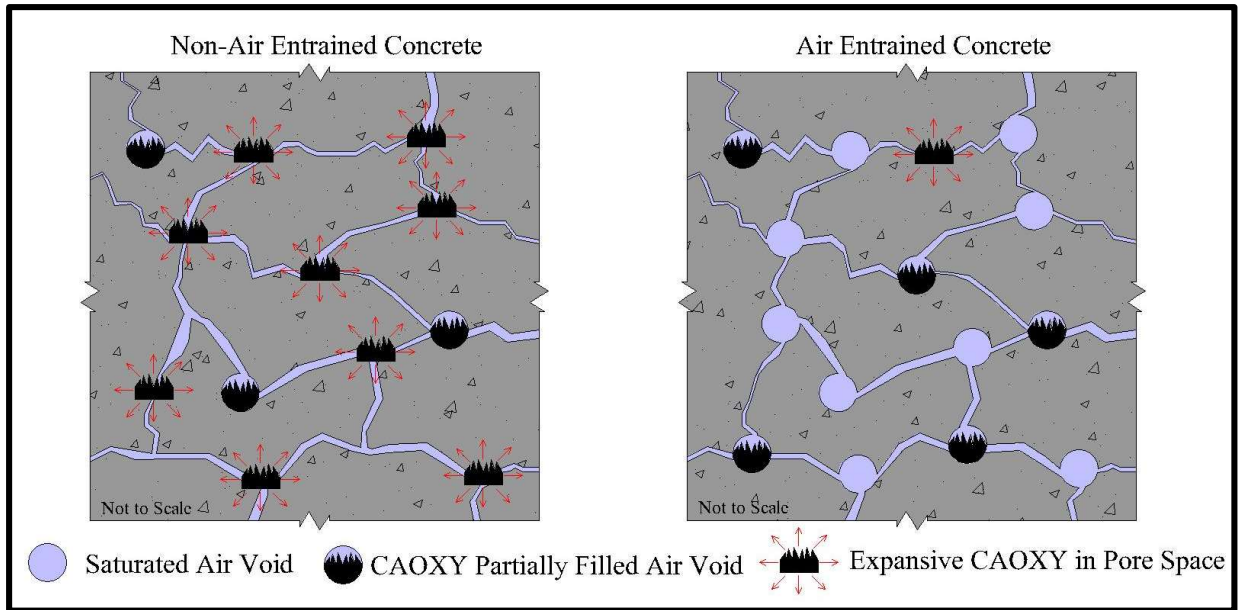


Figure 2.8. Influence of air entrainment for relief of CAOXY damage in cementitious systems (unpublished data from authors).

2.4.1.3. Lower w/cm

The exact role of w/cm on CAOXY mitigation is still unclear as shown in the cement paste, mortar, and concrete data from **Table 2.5**; however, lowering the w/cm of concrete reduces permeability which slows the transport of water and Ca^{2+} and Cl^- ions [72]. Further, w/cm influences the degree of saturation of the concrete with a lower w/cm reducing the level of saturation for both air entrained and non-air entrained specimens [72]. While inhibiting solution from entering the specimen is important, significant damage has been observed in specimens utilizing a wide range of w/cm values (0.30 – 0.70) [49,51,52,54,64,66,77]; however, the addition of SCMs may significantly reduce this damage associated with CAOXY [64].

Therefore, given that a lower w/cm may slow the initial ingress of Ca^{2+} and Cl^- ions, it cannot completely stop the formation of CAOXY. However, it is generally regarded as good practice to reduce the w/cm to the lowest practical value while still meeting workability requirements.

2.4.1.4. Lower Cement Content Due to Optimized Aggregate Gradation

Cement is not only the most expensive product in concrete, but higher than optimal cement contents can also lead to a number of durability concerns [72]. Higher cement content in concrete leads to increased shrinkage, as well as potential deleterious chemical interactions [72]. Therefore, a potential step to developing high-quality long-lasting concrete pavements is by providing only the cement required to ensure mechanical compliance. One way to ensure this is through the use of optimized aggregate gradations which reduce necessary paste requirements [72] and increase packing density reducing the transport of deicing salt solutions. To the authors' knowledge, no research has been conducted to study the effects of optimized aggregate gradations for CAOXY mitigation. It is unlikely CAOXY can be completely mitigated using this technique alone as $\text{Ca}(\text{OH})_2$ would still be present in the cement paste; however, in conjunction with other mitigation procedures, it could help by reducing deterioration due to CAOXY. More research is needed to further determine the effect of optimized aggregate gradations on CAOXY formation.

2.4.2. Utilizing Various Deicing Salts

As shown in **Section 2.2.2.3**, the use of NaCl does not produce CAOXY deterioration associated with CaCl_2 and MgCl_2 (unless the concrete is carbonated [97]). NaCl is known to cause surface scaling [2-8] and can have negative drawbacks, but in general is less harsh than other deicing salts. Therefore, under adequate conditions the use of NaCl is desired to mitigate gelid conditions. Often the lower depression points of CaCl_2 and MgCl_2 are required to ensure public safety in winter weather [32,77,113]. However, the use of binary or even ternary blends of deicing salts could provide a method to abate CaCl_2 and MgCl_2 deposits in pavement joints [113]. Similar to the dilution effect of mineral fillers in cement paste, the use of NaCl can reduce

the relative CaCl_2 content in deicing salt solutions while still providing adequate protection against winter weather precipitation [71,72,113].

Further, it has been noted a number of non-chloride-based chemicals can be utilized for deicing mitigation [56,66-69,72,82,92,123]. While some of these materials may be benign to CAOXY deterioration, cost or other durability concerns may preclude their use on concrete pavements. Concerns associated with the use of these materials are not covered in this paper.

2.4.3. Utilizing Sealants

Another strategy for mitigating CAOXY is to provide a moisture barrier for the concrete to prevent water from saturating localized sections of the concrete pavement [30,32,49,96,110,112,128]. Such a barrier would inhibit the deicing salt from reacting with the concrete hydration products. This has been successfully accomplished in the laboratory [49,72,96,110,112]. One research program stated soy methyl ester polystyrene sealers worked better than conventional sealant materials [110] for protecting paste samples; however, others have emphasized an epoxy-based sealant [96]. Recently, [49] determined sealants with hydrophobic properties demonstrated the best protection against deicing materials. Further, [49] is the first work to correlate LT-DSC paste results with equivalent concrete specimen expansion results. As stated in **Section 2.4.1.1.1**, when using LT-DSC, CAOXY results below 15 g/100 g paste may be adequate to protect cementitious paste from CAOXY deterioration. Wang et al. [49] determined that concrete expansions of 0.20 mm or less correlate with the LT-DSC predictions for mitigating CAOXY deterioration using sealants. The use of sealants may only be a short-term solution in CAOXY mitigation as deterioration of the sealant due to environmental conditions could leave the pavement exposed to CAOXY [32,49]. Therefore, a continual maintenance program is likely required to successfully utilize sealants to mitigate CAOXY in

concrete pavements. Further, existing concretes may already have the necessary salt deposits to cause deterioration [96].

2.4.4. Utilizing Preferential Carbonation

Preferential carbonation has also been utilized to reduce the negative effects associated with CAOXY [52,111]. Mortar specimens cured in a 30% CO₂ environment for 60-days and exposed to a 30% CaCl₂ environment did not show major deterioration [52] as shown in **Table 2.6**.

Researchers have intentionally exposed paste specimens to atmospheric carbonation and noted reduced CAOXY formation based on LT-DSC testing [111]. The removal of Ca(OH)₂ and subsequent replacement with CaCO₃ near the surface of each specimen provides a barrier surrounding the paste sample [111]. Subsequently, when the specimens were exposed to a CaCl₂ based deicing salt, no Ca(OH)₂ existed on the outside of the specimens to form CAOXY and the specimens were protected due to the carbonation coating. This method, though largely unrealistic for concrete pavements, could be applied at pre-stressing plants under tightly controlled curing conditions. This would be beneficial in areas where serious deicing salt deterioration is known to occur. However, preferentially carbonated concrete may be damaged by NaCl, which can cause CAOXY deterioration [97]. Further investigation is needed on the use of preferential carbonation to reduce CAOXY damage.

2.4.5. Utilizing Bacteria (*Sporosarcina pasteurii*)

A novel technique was recently reported as having potential to mitigate CAOXY by utilizing bacteria known as *Sporosarcina pasteurii* (SP) [139]. SP metabolize nutrients by consuming CaCl₂ solution and replacing it with CaCO₃ [139]. Therefore, the solution concentration of the CaCl₂ solution reduces and simultaneously, a CAOXY reactive product (CaCl₂) is replaced with a nonreactive product (CaCO₃) similar to carbonation. In a preliminary study, concrete

specimens were cast with SP and without SP and exposed to a CaCl_2 solution at varying temperatures [139]. Results [unpublished] indicate utilizing these bacteria does reduce the negative effects of CAOXY; however, their effectiveness is still unknown at this time. Further, these results should be compared to literature [97] to determine if the carbonated precipitant reacts in the presence of NaCl solution to form CAOXY.

2.5. Prescriptive Guidelines and Future Research Recommendations

2.5.1. Prescriptive Guideline Recommendations

There is a trend in the concrete industry in the United States to develop performance-based guidelines for acceptance requirements rather than continue with a prescriptive approach. However, in light of significant pavement failures and recent research, current prescriptive guidelines must be updated, in the interim, to account for potential CAOXY deterioration. As referenced in **Section 2.4**, a number of methods exist to mitigate CAOXY; fortunately, many of these methods may be utilized simultaneously to deter CAOXY damage in concrete pavements. The most implementable methods to significantly mitigate damage caused by CAOXY are utilizing SCMs in conjunction with adequate air entrainment in concrete pavements. Further benefits may be obtained by utilizing optimized aggregate gradations, lowering w/cm and eliminating/reducing the use of CaCl_2 and MgCl_2 based deicing salts when practical.

For cement replacements with SCMs, the following values have been suggested: 20-25% Class F fly ash replacement, 30-35% Class C fly ash replacement, or a 20% slag and 20% Class C fly ash combination replacement of the cement content for concrete pavement joint protection [72].

Others [67,95] do not provide replacement rates but stress that SCMs should be used in order to develop concrete pavements able to withstand deicing salt deterioration. Many state DOT agencies do not require cement replacement by SCMs but instead limit the maximum allowable

usage of SCMs in concrete pavement designs (typically around 20% by mass). For CAOXY mitigation, it may be advantageous to suggest a minimum cement replacement level with SCM for all concrete pavements; however, this may result in other issues (such as lower early-age strength). Even without utilizing high-volume cement replacement with SCMs, there is clearly much advantage with utilizing some SCM as a cement replacement to mitigate deicing salt deterioration [67,72,95].

While typical DOT air requirements are between 5-8% [72], significantly different deterioration levels can occur in concrete specimens exposed to 30% CaCl₂ with air contents ranging from 5.0% to 6.5% [64]. Based on this information, [72] recommended it may be advisable to prescribe that required air contents meet the minimum ACI 201.2R-16 [140] specification recommendation for severe exposure conditions (6.0%) when potential for CAOXY formation exists.

Due to significant variations in aggregates, it is difficult to provide specific gradations for general use. However, utilizing local materials to develop a concrete with a densely packed matrix is highly recommended. Further, a 0.40 w/cm may be used to ensure decreased permeability and reduced susceptibility to deterioration [72]. NaCl and non-chloride based deicing salts should also be utilized when traffic safety can adequately be assured and when durability concerns regarding their use have been addressed.

It is further suggested that concrete mixture designs be checked for potential CAOXY formation using LT-DSC [22]. Though this is a paste test and paste-concrete damage correlation is in preliminary stages [49], determining CAOXY quantities in the paste portion of concrete mixtures could provide industry professionals the option to select a mixture design with the lowest

CAOXY potential. Such testing could provide a “best choice” recommendation for CAOXY mitigation when developing concrete mixture designs [22].

2.5.2. Future Research Recommendations

As mentioned throughout this article, a number of research opportunities exist to further understand this potential plague to concrete pavements.

1. Determining the exact failure mechanism associated with CAOXY: It is known that CAOXY (3:1:12) is 303% larger than $\text{Ca}(\text{OH})_2$ in terms of volume [47]. This transformation undoubtedly results in internal pressure in the concrete. However, as shown in **Section 2.2.6**, the exact mechanism responsible for the damage is still unclear and may be linked to multiple failure mechanisms simultaneously.
2. Utilizing SCMs for mitigating CAOXY: SCM have been shown to be effective at reducing CAOXY in paste, mortar, and concrete; however, effective mitigation levels have not been thoroughly established. Further, there has been significant concern about the availability of quality SCMs, such as fly ash, due to a reduction in coal power generation [141]. Given that SCMs are one of the most viable mitigation options, other SCM sources must be considered in the event that traditional quality SCMs are no longer available. Research also needs to be conducted to determine the potential for classification of SCM types based on their effectiveness to prevent CAOXY [108].
3. Verifying the threshold limit to mitigate CAOXY deterioration in laboratory and field specimens: For paste samples, it is currently accepted that CAOXY levels at or below 15 g/100 g paste are sufficient for suppressing deterioration. However, this threshold level is based on the flexural strength reductions of paste specimens [46,47,72]. While useful, other mechanical property threshold levels, such as compressive strength, MOE,

expansion, or change in rapid chloride ion penetration values must be validated.

Determining a holistic threshold level based on mechanical performance of paste allows the use of LT-DSC [22] as a performance check prior to mixture design acceptance for pavement projects. However, no known CAOXY threshold level has been established for concrete specimens, where aggregates, air content, and transport properties may significantly influence any deterioration due to CAOXY. A framework for testing powdered concrete specimens with TGA and LT-DSC has been proposed [116]. This data, in conjunction with mechanical performance data and ingress changes from recommendation 4, could be used to develop CAOXY limits for mixture design acceptance.

4. Determining deicing salt solution ingress prior to, during and following CAOXY formation: During crystal formation, many of the pores are blocked potentially mitigating any further ingress of solutions carrying Ca^{2+} and Cl^- ions [58,59,72,109]. Following further dissolution and leaching of the $\text{Ca}(\text{OH})_2$ and other phases, ingress rates may return to previous levels. Microcracking, associated with the formation of CAOXY in these pores, may also significantly increase the rate of ionic penetration. Therefore, at least three significantly different scenarios may occur when quantifying the ingress rate of chloride ions associated with CAOXY, and each can affect deterioration of the sample.
5. Linking laboratory results to field specimens: Laboratory conditions greatly exacerbate deterioration in specimens in order to quickly achieve results. However, field studies are more complicated as environmental conditions, time and resources are often mitigating factors. Therefore, outdoor exposure sites in conjunction with DOT field studies are needed to more comprehensively understand this deterioration mechanism. This research

may even help recommendation 3 as it could validate threshold limits for concrete pavements.

6. Validating/developing new test methods: VCM is a newly developed test method to determine potential significant volume change in specimens [23]. This technique could be utilized in mixture design qualification for pavements; however, research is needed to validate the correlation between the deterioration in concrete specimens or pavements and VCM measurements. Further, new techniques/testing procedures are required to continue understanding CAOXY and aid in providing recommendations to industry professionals.
7. Developing valid models to predict service life of concrete affected by CAOXY formation: While models have been developed [126,138], the complexity of modeling a constantly evolving system, such as concrete, has proved very difficult to accurately predict. Further complicating this system is an ever-changing environment. CAOXY is only one deterioration mechanism; however, the rapidity at which it occurs can cause severe deterioration warrants attention when developing lifecycle models. CAOXY is a potential factor that could significantly impact service life predictions [86], and further research is needed to accurately capture this deterioration mechanism in concrete service life models.

The need for future research exists, and will continue, most likely, for a number of years. To begin the process of building better concrete pavements, a complete understanding of this deterioration mechanism is required. Further, implementation of known mitigation techniques in conjunction with best mixture design and construction practices are needed to further refine mitigation strategies and best practice techniques.

Declaration of Interests

The authors have no declaration of interests to state.

Acknowledgements

The authors would like to thank the support of the Oklahoma/Arkansas Chapter of the American Concrete Pavement Association for their generous gift supporting this research. Without their support, this work would not be possible. Nima Hosseinzadeh (University of Miami) is thanked for taking **Fig. 2.3B**.

References

1. American Society of Civil Engineers, ASCE 2017 Infrastructure Report Card. <https://www.infrastructurereportcard.org/>, 2017 (accessed 18 April 2019).
2. T.C. Powers, A working hypothesis for further studies of frost resistance of concrete, *J. Am. Concr. Inst.* 16 (4) (1945) 245-272.
3. G.J. Verbeck, P. Klieger, Studies of "salt" scaling of concrete, *Highw. Res. Board Bull.* 150 (1957) 1-17.
4. J.J. Valenza II, G.W. Scherer, A review of salt scaling: I. Phenomenology, *Cem. Concr. Res.* 37 (7) (2007) 1007-1021. <https://doi.org/10.1016/j.cemconres.2007.03.005>.
5. J.J. Valenza II, G.W. Scherer, A review of salt scaling: II. Mechanisms, *Cem. Concr. Res.* 37 (7) (2007) 1022-1034. <https://doi.org/10.1016/j.cemconres.2007.03.003>.
6. Z. Sun, G.W. Scherer, Effect of air voids on salt scaling and internal freezing, *Cem. Concr. Res.* 40 (2) (2010) 260-270. <https://doi.org/10.1016/j.cemconres.2009.09.027>.
7. Z. Wu, C. Shi, P. Gao, D. Wang, Z. Cao, Effects of deicing salts on the scaling resistance of concrete, *J. Mater. Civ. Eng.* 27 (5) (2015) 04014160.
8. P. Van den Heede, J. Furniere, N. De Belie, Influence of air entraining agents on deicing salt scaling resistance and transport properties of high-volume fly ash concrete, *Cem. Concr. Comp.* 37 (2013) 293-303. <https://doi.org/10.1016/j.cemconcomp.2013.01.005>.
9. S. Ahmad, Reinforcement corrosion in concrete structures, its monitoring and service life prediction – a review, *Cem. Concr. Comp.* 25 (4-5) (2003) 459-471. [https://doi.org/10.1016/S0958-9465\(02\)00086-0](https://doi.org/10.1016/S0958-9465(02)00086-0).

10. U. Angst, B. Elsener, C.K. Larsen, Ø. Vennesland, Critical chloride content in reinforced concrete – a review, *Cem. Concr. Res.* 39 (12) (2009) 1122-1138. <https://doi.org/10.1016/j.cemconres.2009.08.006>.
11. K. Hornbostel, C.K. Larsen, M.R. Geiker, Relationship between concrete resistivity and corrosion rate – a literature review, *Cem. Concr. Comp.* 39 (2013) 60-72. <https://doi.org/10.1016/j.cemconcomp.2013.03.019>.
12. C.A. Apostolopoulos, V.G. Papadakis, Consequences of steel corrosion on the ductility properties of reinforcement bar, *Constr. Build. Mater.* 22 (12) (2008) 2316-2324. <https://doi.org/10.1016/j.conbuildmat.2007.10.006>.
13. Y. Zhou, B. Gencturk, K. William, A. Attar, Carbonation-induced and chloride-induced corrosion in reinforced concrete structures, *J. Mater. Civ. Eng.* 27 (9) (2014) 04014245.
14. ACI 222.3R-11, Guide to design and construction practices to mitigate corrosion of reinforcement in concrete structures. American Concrete Institute, Farmington Hills, Michigan, 2011.
15. Jansen DJ, Snyder MB. Resistance of concrete to freezing and thawing. Strategic Highway Research Program SHRP-C-391 (1994) 1-217. <http://onlinepubs.trb.org/onlinepubs/shrp/SHRP-C-391.pdf>.
16. H. Cai, X. Liu, Freeze-thaw durability of concrete: Ice formation process in pores, *Cem. Concr. Res.* 28 (9) (1998) 1281-1287. [https://doi.org/10.1016/S0008-8846\(98\)00103-3](https://doi.org/10.1016/S0008-8846(98)00103-3).
17. J. Tanesi, R. Meininger, Freeze-thaw resistance of concrete with marginal air content, *Transp. Res. Rec.* 2020 (2007) 61-66. <https://doi.org/10.3141/2020-08>.
18. E.K. Attiogbe, Predicting freeze-thaw durability of concrete – a new approach, *ACI Mater. J.* 93 (5) (1996) 457-464.
19. M. Pigeon, R. Pleau, Modern concrete technology 4: durability of concrete in cold climates, first ed., Taylor and Francis Group, Oxon, 1995.
20. S.H. Smith, C. Qiao, P. Suraneni, K.E. Kurtis, W.J. Weiss, Service-life of concrete in freeze-thaw environments: Critical degree of saturation and calcium oxychloride formation, *Cem. Concr. Res.* 122 (2019) 93-106. <https://doi.org/10.1016/j.cemconres.2019.04.014>.
21. J. Monical, C. Villani, Y. Farnam, E. Unal, J. Weiss, Using low-temperature differential scanning calorimetry to quantify calcium oxychloride formation for cementitious materials in the presence of calcium chloride, *Adv. Civ. Eng. Mater.* 5 (2) (2016) 142-156. <https://doi.org/10.1520/ACEM20150024>.
22. AASHTO T 365-17, Standard Method of Test for Quantifying Calcium Oxychloride Amounts in Cement Pastes Exposed to Deicing Salts, AASHTO, Washington D.C., 2017.

23. C. Qiao, P. Suraneni, J. Weiss, Measuring volume change caused by calcium oxychloride phase transformation in a $\text{Ca}(\text{OH})_2\text{-CaCl}_2\text{-H}_2\text{O}$ system, *Adv. Civ. Eng. Mater.* 6 (1) (2017) 157-169. <https://doi.org/10.1520/ACEM20160065>.
24. C. Qiao, P. Suraneni, J. Weiss, Phase diagram and volume change of the $\text{Ca}(\text{OH})_2\text{-CaCl}_2\text{-H}_2\text{O}$ system for varying $\text{Ca}(\text{OH})_2/\text{CaCl}_2$ molar ratios, *J. Mater. Civ. Eng.* 30 (2) (2018) 04017281. [https://doi.org/10.1061/\(ASCE\)MT.1943-5533.0002145](https://doi.org/10.1061/(ASCE)MT.1943-5533.0002145).
25. P. Rangaraju, Investigating premature deterioration of a concrete highway, *Transp. Res. Rec.* 1798 (2002) 1-7. <https://doi.org/10.3141/1798-01>.
26. J. Olek, M. Radlinski, M. del Mar Arribas, Premature deterioration of joints in selected Indiana portland cement concrete pavements. Proceedings of the 23rd Conference Awarie Budowlane, 2007, Szczecin, Poland, pp. 859–868.
27. P. Taylor, L. Sutter, J. Weiss, Investigation of deterioration of joints in concrete pavements, InTrans Project Reports 91, 2012. http://lib.dr.iastate.edu/intrans_reports/91.
28. P. Suraneni, V.J. Azad, O.B. Isgor, W.J. Weiss, Deicing salts and durability of concrete pavements and joints: mitigating calcium oxychloride formation, *Concr. Int.* 38 (4) (2016) 48-54.
29. A. Biolchini, What went wrong with M-6, the poster child for concrete failure. www.mlive.com/news/grand-rapids/index.ssf/2017/07/what_went_wrong_on_m-6_the_pos.html, 2017 (accessed 30 May 2019).
30. P. Suraneni, C. Qiao, V. Azad, Y. Farnam, J. Monical, E. Ural, C. Villani, B. Isgor, J. Weiss, A review of recent work on deicing salt damage to concrete pavements and its mitigation, International Conference on Advances in Construction Materials and Systems, 2017, Chennai, India, pp. 1-15.
31. C. Jones, W.M. Hale, The use of supplementary cementitious materials to reduce calcium oxychloride formation: a review of the literature, Proceedings of the 12th International PhD Symposium in Civil Engineering, 2018, Prague, Czech Republic, pp. 1121-1128.
32. ACI 201.3T-19, Joint deterioration and chloride-based deicing chemicals. American Concrete Institute, Farmington Hills, Michigan, 2019.
33. S. Sorel, On a new magnesium cement, *Compt. Rend.* 65 (1867) 102–104. (In French)
34. S.A. Walling, J.L. Provis, Magnesia based cements: a journey of 150 years, and cements for the future?, *Chem. Rev.* 116 (2016) 4170-4204. <https://doi.org/10.1021/acs.chemrev.5b00463>.
35. J.W.C. Davis, Composition of crystalline deposit from a solution of magnesium and ammonium chloride, *Chem. News J. Phys. Sci.* 25 (1872) 258-259.

36. W.O. Robinson, W.H. Waggaman, Basic magnesium chlorides, *J. Phys. Chem.* 13 (9) (1909) 673–678. <https://doi.org/10.1021/j150108a002>.
37. H.S. Lukens, The composition of magnesium oxychloride, *J. Am. Chem. Soc.* 54 (6) (1932) 2372–2380. <https://doi.org/10.1021/ja01345a026>.
38. T. Demediuk, W.F. Cole, H.V. Hueber, Studies on magnesium and calcium oxychlorides, *Aust. J. Chem.* 8 (2) (1955) 215-233.
39. W.J. Pitt, The effect of calcium chloride and calcium oxychloride on portland cement, *Chem. Eng. Min. Rev.* 21 (242) (1928) 65-70.
40. P. Rapp, Effect of calcium chloride on portland cements and concretes, *J. Res. Natl. Bur. Stand.* 14 (1935) 499-517.
41. M. Lawrence, H.E. Vivian, The action of calcium chloride on mortar and concrete, *Aust. J. Appl. Sci.* 11 (4) (1960) 490-498.
42. S. Monosi, A. Alvera, M. Collepardi, Chemical attack of calcium chloride on the portland cement paste, *Il Cemento* 86 (2) (1989) 97-104.
43. K. Wang, D.E. Nelson, W.A. Nixon, Damaging effects of deicing chemicals on concrete materials, *Cem. Concr. Comp.* 28 (2) (2006) 173-188. <https://doi.org/10.1016/j.cemconcomp.2005.07.006>.
44. H. Mori, R. Kuga, S. Ogawa, Y. Kubo, Chemical deterioration of hardened cement pastes immersed in calcium chloride solution, *Proceedings of the 3rd International Conference on Sustainable Construction Materials and Technologies*, 2013, Kyoto, Japan, Paper 329.
45. Y. Farnam, B. Zhang, J. Weiss, Evaluating the use of supplementary cementitious materials to mitigate damage in cementitious materials exposed to calcium chloride deicing salt, *Cem. Concr. Comp.* 81 (2017) 77-86. <https://doi.org/10.1016/j.cemconcomp.2017.05.003>.
46. C. Qiao, P. Suraneni, M.T. Chang, J. Weiss, The influence of calcium chloride on flexural strength of cement-based materials, *Proceedings of the 2017 fib Symposium*, 2017, Maastricht, Netherlands, pp. 2041-2048.
47. C. Qiao, P. Suraneni, J. Weiss, Flexural strength reduction of cement pastes exposed to CaCl₂ solutions, *Cem. Concr. Comp.* 86 (2018) 297-305. <https://doi.org/10.1016/j.cemconcomp.2017.11.021>.
48. P. Suraneni, V.J. Azad, O.B. Isgor, W.J. Weiss, Use of fly ash to minimize deicing salt damage in concrete pavements, *Transp. Res. Rec.* 2629 (2017) 24-32. <https://doi.org/10.3141/2629-05>.

49. X. Wang, S. Sadati, P. Taylor, C. Li, X. Wang, A. Sha, Material characterization to assess effectiveness of surface treatment to prevent joint deterioration from oxychloride formation mechanism, *Cem. Concr. Comp.* 104 (2019) 103394. <https://doi.org/10.1016/j.cemconcomp.2019.103394>.
50. S. Monosi, M. Collepardi, Research on $3\text{CaO}\cdot\text{CaCl}_2\cdot 15\text{H}_2\text{O}$ identified in concretes damaged by CaCl_2 attack, *Il Cemento* 87 (1990) 3-8.
51. H.G. Smolczyk, Chemical reactions of strong chloride-solutions with concrete, Proceedings of the 5th International Symposium on the Chemistry of Cement, 1968, Tokyo, Japan, pp. 274-280.
52. M. Collepardi, S. Monosi, Effect of the carbonation process on the concrete deterioration by CaCl_2 aggression, Proceedings of the 9th International Symposium on the Chemistry of Cement, 1992, New Delhi, India, pp. 389-395.
53. K. Torii, M. Kawamura, M. Yamada, S. Chatterji, Deterioration of cement mortars in NaCl and CaCl_2 solution, Proceedings of the JCA Cement and Concrete, 1992, No. 42 pp. 504-509. (In Japanese)
54. K. Torii, T. Sasatani, M. Kawamura, Effects of fly ash, blast furnace slag, and silica fume on resistance of mortar to calcium chloride attack, *ACI Spec. Publ.* 153 (1995) 931-950.
55. G.A. Julio-Betancourt, R.D. Hooton, Calcium and magnesium chloride attack on cement-based materials: formation, stability, and effects of oxychlorides, Proceedings of the 2nd RILEM International Workshop on Concrete Durability and Service Life Planning - ConcreteLife'09, 2009, Haifa, Israel, pp. 432-439.
56. G.A. Julio-Betancourt, Effect of de-icer and anti-icer chemicals on the durability, microstructure, and properties of cement based materials, University of Toronto, 2009, Ph.D. Thesis.
57. K. Peterson, G. Julio-Betancourt, L. Sutter, R.D. Hooton, D. Johnston, Observations of chloride ingress and calcium oxychloride formation in laboratory concrete and mortar at 5 °C, *Cem. Concr. Res.* 45 (2013) 79-90. <https://doi.org/10.1016/j.cemconres.2013.01.001>.
58. Y. Farnam, S. Dick, A. Wiese, J. Davis, D. Bentz, J. Weiss, The influence of calcium chloride deicing salt on phase changes and damage development in cementitious materials, *Cem. Concr. Comp.* 64 (2015) 1-15. <https://doi.org/10.1016/j.cemconcomp.2015.09.006>.
59. Y. Farnam, Damage development, phase changes, transport properties, and freeze-thaw performance of cementitious materials exposed to chloride based salts, Purdue University, 2015, Ph.D. Thesis.
60. S. Chatterji, A.D. Jensen, Studies of the mechanism calcium chloride attack on portland cement concrete, *Nordisk Beton* 19 (1975) 5-6.

61. L. Berntsson, S. Chandra, Damage of concrete sleepers by calcium chloride, *Cem. Concr. Res.* 12 (1982) 87-92.
62. O. Peterson, Chemical attack of strong chloride solutions on concrete. Does experience confirm that different chloride salts may influence concrete in different ways? Division of Building Materials, LTH, Lund University 3020 (1984) 1-30.
63. G. Moriconi, M. Pauri, I. Alvera, M. Collepari, Damage of concrete by exposure to calcium chloride, *Proceedings of the 2nd International Conference on Engineering Materials: From Research Applications to Design*, 1988, Bologna, Italy, pp. 20-23.
64. M. Collepari, L. Coppola, C. Pistolesi, Durability of concrete structures exposed to CaCl₂ based deicing salts, *Proceedings of the 3rd CANMET/ACI International Conference*, 1994, Nice, France, pp. 107-120.
65. H. Lee, R.D. Cody, A.M. Cody, P.G. Spry, Effects of various deicing chemicals on pavement concrete deterioration, *Proceedings of the Mid-Continent Transportation Symposium*, 2000, Ames, United States, pp. 151-155.
66. L. Sutter, T. Van Dam, K.R. Peterson, D.P. Johnston, Long-term effects of magnesium chloride and other concentrated salt solutions on pavement and structural portland cement concrete phase I results, *Transp. Res. Rec.* 1979 (2006) 60-68.
<http://dx.doi.org/10.3141/1979-10>.
67. L. Sutter, K. Peterson, G. Julio-Betancourt, D. Hooton, T. Van Dam, K. Smith, The deleterious chemical effects of concentrated deicing solutions on portland cement concrete, *Final Report for the South Dakota Department of Transportation*, SD2002-01, 2008.
68. D. Darwin, J. Browning, L. Gong, S.R. Hughes, Effects of deicers on concrete deterioration, *ACI Mater. J.* 105 (6) (2008) 622-627.
69. A.E. Janusz, Investigation of deicing chemicals and their interaction with concrete materials, Purdue University, 2010, M.S.C.E. Thesis.
70. J. Jain, A. Janusz, J. Olek, D. Jozwiak-Niedzwiedzka, Physico-chemical changes in plain and fly ash modified concretes exposed to different deicing chemicals, *Proceedings of the 13th International Congress on Chemistry of Cement*, 2011, Madrid, Spain.
71. J. Jain, J. Olek, A. Janusz, D. Jozwiak-Niedzwiedzka, Effects of deicing salt solutions on physical properties of pavement concretes, *Transp. Res. Rec.* 2290 (2012) 69-75.
<https://doi.org/10.3141/2290-09>.
72. J. Weiss, M.T. Ley, L. Sutter, D. Harrington, J. Gross, S.L. Tritsch, Guide to the prevention of and restoration of early joint deterioration in concrete pavements, *Final Report for the Iowa Department of Transportation*, TR-697, 2016.

73. A.A.M. Ghazy, Concrete pavements: deterioration due to de-icing salts and repair, University of Manitoba, 2017, Ph.D. Thesis.
74. A. Ghazy, M.T. Bassuoni, Resistance of concrete to different exposures with chloride-based salts, *Cem. Concr. Res.* 101 (2017) 144-158. <https://doi.org/10.1016/j.cemconres.2017.09.001>.
75. A.K.M. Rakinul Islam, Behaviour of concrete pavements exposed to de-icing salts: field and laboratory studies, University of Manitoba, 2017, M.S.C.E. Thesis.
76. J.K. Jang, H.G. Kim, J.H. Kim, J.S. Ryou, The evaluation of damage effects on MgO added concrete with slag cement exposed to calcium chloride deicing salt, *Mater.* 11 (5) (2018) 793. <https://dx.doi.org/10.3390%2Fma11050793>.
77. C.B. Van Niejenhuis, C.M. Hansson, Detrimental effects of anti-icing brines on concrete durability, *Concr. Int.* 41 (11) (2019) 30-34.
78. A.M. Neville, Behavior of concrete in saturated and weak solutions of magnesium sulfate or calcium chloride, *J. Mater.* 4 (4) (1969) 781-816.
79. R.H. Bogue, *The Chemistry of Portland Cement*, second ed., Reinhold Publishing Corporation, 1955.
80. S. Chatterji, Mechanism of the CaCl_2 attack on portland cement concrete, *Cem. Concr. Res.* 8 (1978) 461-468.
81. S. Monosi, M. Collepardi, Chemical attack of magnesium chloride on the portland cement paste, *Il Cemento* 90 (3) (1993) 169-173.
82. L. Sutter, K. Peterson, S. Touton, T. Van Dam, D. Johnston, Petrographic evidence of calcium oxychloride formation in mortars exposed to magnesium chloride solution, *Cem. Concr. Res.* 36 (2006) 1533-1541. <https://doi.org/10.1016/j.cemconres.2006.05.022>.
83. C. Qiao, P. Suraneni, M.T. Chang, J. Weiss, Damage in cement pastes exposed to MgCl_2 solutions, *Mater. Struct.* 51 (2018) 74. <https://doi.org/10.1617/s11527-018-1191-2>.
84. V.W. Rechenberg, H.-M. Sylla, The effect of magnesium on concrete, *ZKG Int.* 49 (1) (1996) 44-56.
85. P.J. Tumidajski, G.W. Chan, Durability of high performance concrete in magnesium brine, *Cem. Concr. Res.* 26 (4) (1996) 557-565. [https://doi.org/10.1016/0008-8846\(96\)00034-8](https://doi.org/10.1016/0008-8846(96)00034-8).
86. Y. Farnam, T. Washington, J. Weiss, The influence of calcium chloride salt solution on the transport properties of cementitious materials. *Adv. Civ. Eng.* (2015), 929864. <http://dx.doi.org/10.1155/2015/929864>.

87. U.A. Birnin-Yauri, Chloride in cement: Study of the system CaO-Al₂O₃-CaCl₂-H₂O, University of Aberdeen, 1993, Ph.D. Thesis.
88. I.M. Helmy, A.A. Amer, H. El-Didamony, Chemical attack on hardened pastes of blended cements-part 1: Attack of chloride solutions, *Zement-Kalk-Gips.*, 44 (1) (1991) 46-50.
89. C. Qiao, P. Suraneni, T.N.W. Ying, A. Choudhary, J. Weiss, Chloride binding of cement pastes with fly ash exposed to CaCl₂ solutions at 5 and 23 °C, *Cem. Concr. Comp.* 97 (2019) 43-53. <https://doi.org/10.1016/j.cemconcomp.2018.12.011>.
90. R. Obersted-Patdberg, Degradation of cements by magnesium brine, *Proceedings of the 7th International Conference on Cement Microscopy*, 1985, Duncanville, United States, pp. 24-36.
91. L.D. Wakeley, T.S. Poole, C.A. Weiss, J.P. Burkes, Geochemical stability of cement-based composites in magnesium brines, *Proceedings of the 14th International Conference on Cement Microscopy*, Costa Mesa, CA, 1992.
92. B.T. Mussato, O.K. Gepraegs, G. Farnden, Relative effects of sodium chloride and magnesium chloride on reinforced concrete: State of the art. *Transp. Res. Rec.* 1866 (2004) 59-66. <https://doi.org/10.3141/1866-08>.
93. R.L. Kozikowski, P.C. Taylor, W.A. Pyc, Evaluation of potential concrete deterioration related to magnesium chloride (MgCl₂) deicing salt, PCA R&D Serial No. 2770, Skokie, Illinois, 2007.
94. X. Shi, M. Akin, T. Pan, L. Fay, Y. Liu, Z. Yang, Deicer impacts on pavement materials: introduction and recent developments, *Open Civ. Eng. J.* 3 (2009) 16-27.
95. X. Shi, Y. Liu, M. Mooney, M. Berry, B. Hubbard, L. Fay, A.B. Leonard, Effect of chloride-based deicers on reinforced concrete structures, Final Report for the Washington State Department of Transportation, WA-RD 741.1, 2010.
96. X. Shi, N. Xie, Y. Dang, A. Muthumani, J. Huang, A. Hagel, S. Forsythe, E. Selig, D. Falk, E. McVey, A. Kessel, C. Martins, Y. Zhang, Y. Fang, Understanding and mitigating effects of chloride deicer exposure on concrete, Final Report for the Oregon Department of Transportation, SPR 742, 2014.
97. H.E. Álava, N. De Belie, G. De Schutter, Proposed mechanism for the formation of oxychloride crystals during sodium chloride application as a deicer salt in carbonated concrete, *Constr. Build. Mater.* 109 (2016) 188-197. <https://doi.org/10.1016/j.conbuildmat.2016.01.047>.
98. U.A. Birnin-Yauri, F. Glasser, Chlorides in cement: Phase studies of the Ca(OH)₂-CaCl₂-H₂O system, *Il Cemento* 88 (1991) 151-157.

99. C. Shi, Formation and stability of $3\text{CaO}\cdot\text{CaCl}_2\cdot 12\text{H}_2\text{O}$, *Cem. Concr. Res.* 31 (2001) 1373-1375. [https://doi.org/10.1016/S0008-8846\(01\)00576-2](https://doi.org/10.1016/S0008-8846(01)00576-2).
100. U.A. Birnin-Yauri, S. Garba, The effect and mechanism of chloride ion attack on portland cement concrete and the structural steel reinforcement, *IFE J. Sci.* 8 (2) (2006) 131-134. <http://dx.doi.org/10.4314/ijss.v8i2.32211>.
101. I. Galan, L. Perron, F.P. Glasser, Impact of chloride-rich environments on cement paste mineralogy, *Cem. Concr. Res.* 68 (2015) 174-183. <https://doi.org/10.1016/j.cemconres.2014.10.017>.
102. F. Häusler, H Schmidt, D. Freyer, Calcium hydroxide chlorides: The ternary system $\text{Ca}(\text{OH})_2\text{-CaCl}_2\text{-H}_2\text{O}$ at 25, 40, and 60 °C, phase stoichiometry and crystal structure, *J. Inorg. Gen. Chem.* 65 (10) (2019) 723-731. <https://doi.org/10.1002/zaac.201900051>.
103. R. Kuga, H. Mori, S. Ogawa, K. Komatsu, Synthesis and fundamental property of $3\text{CaO}\cdot\text{CaCl}_2\cdot 15\text{H}_2\text{O}$ related to CaCl_2 attack. *Cem. Sci. Concr. Tech.* 65 (2011) 420-426. <https://doi.org/10.14250/cement.65.420>. (In Japanese)
104. R. Kuga, H. Mori, S. Ogawa, Synthesis and fundamental properties of $3\text{CaO}\cdot\text{CaCl}_2\cdot 15\text{H}_2\text{O}$ causing CaCl_2 attack, and its formation in hardened cement paste exposed to CaCl_2 solution, *Proceedings of the 8th International Symposium on Cement and Concrete, 2013, Nanjing, China*, pp. 1-7.
105. T. Uchida, S. Hatanaka, N. Mishima, A. Maegawa, Study on deterioration mechanism of porous concrete by CaCl_2aq , *J. Struct. Constr. Eng.* 79 (706) (2014) 1709-1715. <https://doi.org/10.3130/aijs.79.1709>. (In Japanese)
106. P. Suraneni, V.J. Azad, O.B. Isgor, W.J. Weiss, Calcium oxychloride formation in pastes containing supplementary cementitious materials: thoughts on the role of role of cement and supplementary cementitious materials reactivity, *RILEM Tech. Lett.* 1 (2016) 24-30. <http://dx.doi.org/10.21809/rilemtechlett.v1.7>.
107. P. Suraneni, N. Salgado, H. Carolan, C. Li, V.J. Azad, O.B. Isgor, J.H. Ideker, W.J. Weiss, Mitigation of deicer damage in concrete pavements caused by calcium oxychloride salt formation – use of ground lightweight aggregates, *Proceedings of the International RILEM Conference on Materials, Systems and Structures in Civil Engineering, 2016, Lyngby, Denmark*, pp. 171-180.
108. P. Suraneni, V.J. Azad, O.B. Isgor, J. Weiss, Role of supplementary cementitious material type in the mitigation of calcium oxychloride formation in cementitious pastes, *J. Mater. Civ. Eng.* 30 (10) (2018) 04018248. [https://doi.org/10.1061/\(ASCE\)MT.1943-5533.0002425](https://doi.org/10.1061/(ASCE)MT.1943-5533.0002425).

109. Y. Farnam, A. Wiese, D. Bentz, J. Davis, J. Weiss, Damage development in cementitious materials exposed to magnesium chloride deicing salt, *Constr. Build. Mater.* 93 (2015) 384-392. <https://doi.org/10.1016/j.conbuildmat.2015.06.004>.
110. W. Jones, Y. Farnam, P. Imbrock, J. Sprio, C. Villani, M. Golias, J. Olek, W.J. Weiss, An overview of joint deterioration in concrete pavement: mechanisms, solution properties, and sealers, Purdue University (2013) pp. 1-69. <http://dx.doi.org/10.5703/1288284315339>.
111. R.M. Ghantous, Y. Farnam, E. Unal, J. Weiss, The influence of carbonation on the formation of calcium oxychloride, *Cem. Concr. Comp.* 73 (2016) 185-191. <https://doi.org/10.1016/j.cemconcomp.2016.07.016>.
112. J. Monical, E. Unal, T. Barrett, Y. Farnam, W.J. Weiss, Reducing joint damage in concrete pavements: quantifying calcium oxychloride formation, *Transp. Res. Rec.* 2577 (2016) 17-24. <https://doi.org/10.3141/2577-03>.
113. P. Suraneni, J. Monical, E. Unal, Y. Farnam, C. Vilani, T.J. Barrett, W.J. Weiss, Performance of concrete pavement in the presence of deicing salts and deicing salt cocktails, Joint Transportation Research Program Publication No. FHWA/IN/JTRP-2016/25 (2016) pp. 1-19. <http://dx.doi.org/10.5703/1288284316350>.
114. S.N. Whatley, P. Suraneni, V.J. Azad, O.B. Isgor, J. Weiss, Mitigation of calcium oxychloride formation in cement pastes using undensified silica fume, *J. Mater. Civ. Eng.* 29 (10) (2017) 04017198. [https://doi.org/10.1061/\(ASCE\)MT.1943-5533.0002052](https://doi.org/10.1061/(ASCE)MT.1943-5533.0002052).
115. P. Suraneni, J. Monical, E. Unal, Y. Farnam, J. Weiss, Calcium oxychloride formation potential in cementitious pastes exposed to blends of deicing salt, *ACI Mater. J.* 114 (4) (2017) 631-641. <http://dx.doi.org/10.14359/51689607>.
116. P. Suraneni, J. Weiss, Extending low-temperature differential scanning calorimetry from paste to mortar and concrete to quantify the potential for calcium oxychloride formation, *Adv. Civ. Eng. Mater.* 7 (1) (2018) 1-16. <https://doi.org/10.1520/ACEM20170113>.
117. C. Harvie, N. Moller, J. Weare, The prediction of mineral solubilities in natural waters: The Na-K-Mg-Ca-H-Cl-SO₄-OH-HCO₃-CO₂-H₂O system to high org ionic strengths at 25 °C, *Geochim. Cosmochim. Acta* 48 (4) (1984) 723-751. [https://doi.org/10.1016/0016-7037\(84\)90098-X](https://doi.org/10.1016/0016-7037(84)90098-X).
118. P. Brown, J. Bothe Jr., The system CaO-Al₂O₃-CaCl₂-H₂O at 23±2 °C and the mechanisms of chloride binding in concrete, *Cem. Concr. Res.* 34 (9) (2004) 1549-1553. <https://doi.org/10.1016/j.cemconres.2004.03.011>.
119. E.S. Sumsion, W.S. Guthrie, Physical and chemical effects of deicers on concrete pavement: literature review, Final Report for the Utah Department of Transportation, UT-13.09, 2013.

120. X. Shi, L. Fay, M.M. Peterson, M. Berry, M. Mooney, A FESEM/EDX investigation into how continuous deicer exposure affects the chemistry of Portland cement concrete, *Constr. Build. Mater.* 25 (2) (2011) 957-966. <https://doi.org/10.1016/j.conbuildmat.2010.06.086>.
121. C. Li, M. Wu, Q. Chen, Z. Jiang, Chemical and mineralogical alterations of concrete subjected to chemical attacks in complex underground tunnel environments during 20–36 years, *Cem. Concr. Comp.* 86 (2018) 139-159. <https://doi.org/10.1016/j.cemconcomp.2017.11.007>.
122. F.A. Schreinemakers, T. Figeer, The study of system: $\text{H}_2\text{O}-\text{CaCl}_2-\text{Ca}(\text{OH})_2$ at 25 °C, *Chemisch. Weekblad.* 8 (1989) 683-688. (In Dutch)
123. X. Shi, L. Fay, M.M. Peterson, Z. Yang, Freeze-thaw damage and chemical change of a portland cement concrete in the presence of diluted deicers, *Mater. Struct.* 43 (2010) 933-946. <https://doi.org/10.1617/s11527-009-9557-0>.
124. O.A. Markova, Physical chemistry of calcium hydroxide chlorides, *Russ. J. Phys. Chem.* 47 (1973) 608.
125. H. Justnes, K. De Weerd, M.R. Geiker, Chloride binding in concrete exposed to seawater and salt solutions, *Proceedings of the 7th International Conference on Concrete Under Severe Conditions – Environment and Loading (CONSEC13)*, 2013, Nanjing, China, pp. 647-659.
126. F.P. Glasser, J. Marchand, E. Samson, Durability of concrete – degradation phenomena involving detrimental chemical reactions, *Cem. Concr. Res.* 38 (2) (2008) 226-246. <https://doi.org/10.1016/j.cemconres.2007.09.015>.
127. N. Ewers, Effect of magnesium chloride brine on road concrete, *Baustoffindustrie*, 22 (1967) 281-283. (In German)
128. R.D. Cody, A.M. Cody, P.G. Spry, G.-L. Gan, Experimental deterioration of highway concrete by chloride deicing salts, *Environ. Eng. Geosci.* 2 (4) (1996) 575-588. <https://doi.org/10.2113/gsegeosci.II.4.575>.
129. I.I. Vol'nov, E.I. Latysheva, Separation of calcium chloride from solvay spent liquor through calcium hydroxide, *J. Appl. Chem. U.S.S.R.* 30 (1957) 1039-1046.
130. S.Z. Makarov, I.I. Vol'nov, Figure 2061-System $\text{Ca}(\text{OH})_2-\text{CaCl}_2-\text{H}_2\text{O}$, in: C. Robbins (Ed.), *Phase Diagrams Ceram*, Vol. 1, American Ceramic Society, Westerville, OH, 1964, p. 567.
131. R.P. Spragg, J. Castro, W. Li, M. Pour-Ghaz, P-T. Huang, J. Weiss, Wetting and drying of concrete using aqueous solutions containing deicing salts, *Cem. Concr. Comp.* 33 (5) (2011) 535-542. <https://doi.org/10.1016/j.cemconcomp.2011.02.009>.

132. E.M. Winkler, P.C. Singer, Crystallization pressure of salts in stone and concrete, *Geological Soc. Am. Bull.* 83 (1972) 3509-3514.
133. G.W. Scherer, Crystallization in pores, *Cem. Concr. Res.* 29 (8) (1999) 1347-1358. [https://doi.org/10.1016/S0008-8846\(99\)00002-2](https://doi.org/10.1016/S0008-8846(99)00002-2).
134. G.W. Scherer, Stress from crystallization of salt, *Cem. Concr. Res.* 34 (2003) 1613– 1624. <https://doi.org/10.1016/j.cemconres.2003.12.034>.
135. ICDD, Powder Diffraction File. <http://www.icdd.com/index.php/pdf-4/> (accessed 23 July 2019).
136. S.V. Borisov, N.V. Podberezkaya, X-ray diffraction analysis: A brief history and achievements of the first century, *J. Struct. Chem.* 53 (1) (2012) 1-3. <https://doi.org/10.1134/S0022476612070013>.
137. T. Kim, J. Olek, Effects of sample preparation and interpretation of thermogravimetric curves on calcium hydroxide in hydrated pastes and mortars, *Transp. Res. Rec.* 2290 (2012) 10-18. <https://doi.org/10.3141/2290-02>.
138. W.J. Weiss, Concrete pavement joint durability: a sorption-based model for saturation, the role of distributed cracking, and calcium oxychloride formation, *Proceedings of the 10th International Conference on Mechanics and Physics of Creep, Shrinkage, and Durability of Concrete and Concrete Structures, 2015, Vienna, Austria*, pp. 211-218. <https://doi.org/10.1061/9780784479346.025>.
139. Y. Farnam, Calcium-munching bacteria could be a secret weapon against road salt eating away at concrete roads and bridges. <https://theconversation.com/calcium-munching-bacteria-could-be-a-secret-weapon-against-road-salt-eating-away-at-concrete-roads-and-bridges-113970>, 2019 (accessed 12 April 2019).
140. ACI 201.2R-16, Guide to durable concrete. American Concrete Institute, Farmington Hills, Michigan, 2016.
141. Phys.Org, 50 US coal power plants shut under Trump. <https://phys.org/news/2019-05-coal-power-trump.html> (accessed 27 June 2019).

3. Mitigating Calcium Oxychloride Formation in Cementitious Paste Using Alternative Supplementary Cementitious Materials

Casey Jones^a, Sivakumar Ramanathan^b, Prannoy Suraneni^c, W. Micah Hale^d

^a Graduate Research Assistant, Department of Civil Engineering, University of Arkansas, 4190 Bell Engineering Center, Fayetteville, AR 72701, United States of America.

^b Graduate Research Assistant, Civil, Architectural, Environmental Engineering Department, University of Miami, 1251 Memorial Drive, Coral Gables, FL 33146, United States of America.

^c Assistant Professor, Civil, Architectural, Environmental Engineering Department, University of Miami, 1251 Memorial Drive, Coral Gables, FL 33146, United States of America.

^d Professor and Chair, Department of Civil Engineering, University of Arkansas, 4190 Bell Engineering Center, Fayetteville, AR 72701, United States of America. Email: micah@uark.edu.

Corresponding author: Casey Jones

Abstract

The use of supplementary cementitious materials (SCMs) has been shown to reduce calcium oxychloride (CAOXY) contents in cementitious pastes due to reductions in calcium hydroxide levels. However, when availability or cost precludes the use of traditional SCMs, such as fly ash, mitigation could be provided through alternative materials. In this study, fly ash (FA), rice husk ash (RHA), bottom ash (BA), limestone filler (LS), nepheline syenite filler (NS), sandstone filler (SS), and silica flour (SFL) were evaluated for CAOXY mitigation in cementitious paste. Each material was tested at 0, 15, 30, and 45% cement replacement by mass in cementitious

paste and CAOXY mitigation was quantified using low-temperature differential scanning calorimetry (LT-DSC). Reactivity testing, thermogravimetric analysis, and compressive strength testing were also investigated to determine their ability to predict CAOXY mitigation in comparison to LT-DSC. For the materials investigated, the order of efficiency to reduce CAOXY from least effective to most effective based on LT-DSC is SS, LS, SFL, NS, BA, FA, and RHA. Using test methods other than LT-DSC to predict CAOXY mitigation using SCMs is shown to be effective for pozzolanic materials (BA, FA, RHA). However, for the inert materials (i.e., mineral fillers), there is a slight discrepancy in the predicted effectiveness for CAOXY mitigation. Of the materials tested, only RHA, FA, and BA reduce CAOXY below the proposed threshold of 15 g/100 g paste at cement replacement levels of 18, 30, and 45%, respectively. The remaining SCM do not effectively reduce CAOXY amounts.

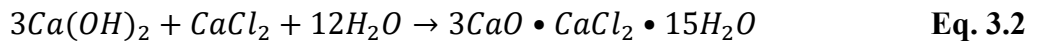
Keywords: Alternative Supplementary Cementitious Materials, Thermogravimetric Analysis, Low-Temperature Differential Scanning Calorimetry, Pozzolanic Reactivity

3.1. Introduction

3.1.1. Calcium Oxychloride Background

Regions prone to freezing conditions in winter must work to keep transportation infrastructure available for public use throughout these conditions. Chloride-based deicing and anti-icing agents are often employed to aid in the removal/prevention of gelid roadway conditions. However, the use of these materials can lead to significant durability concerns such as salt scaling [1-3], reinforcement corrosion [4,5] and chemical attack [6,7]. Calcium chloride (CaCl_2) and magnesium chloride (MgCl_2) deicing salts chemically interact with calcium hydroxide ($\text{Ca}(\text{OH})_2$) in the concrete leading to the formation of a deleterious phase known as calcium oxychloride (CAOXY) [8-12]. CAOXY is an expansive reaction product causing cracking in

concrete pavements, especially around the joints [8,11,12]. CAOXY formation is a major concern for pavement infrastructure, as it is premature, and the repair can be expensive and laborious [13]. The chemical composition of CAOXY may vary due to environmental factors [8,14]; however, the phase typically associated with damage in cementitious systems is shown in **Eq. 3.1** [8,10,12]. An alternative form of the calcium CAOXY phase is given in **Eq. 3.2** [6,7,11,14].



In order to mitigate damage due to CAOXY formation, several methodologies have been suggested. These include the use of supplementary cementitious materials (SCMs) [15-23], entrained air [7,23], preferential carbonation [24,25], sealants [11,26], and the use of non-chloride based deicing materials [14,26]. However, it should be noted that specimen type (i.e., cement paste, mortar, or concrete) may impact the effectiveness of mitigation techniques as aggregates modify transport properties and paste content [8]. While preferential carbonation and sealants can aid in damage mitigation, they are difficult to implement in traditional concrete pavements. The use of non-chloride deicers should be evaluated against public safety during winter weather and such materials could have other negative impacts associated with their use. Further research should be conducted prior to their use on concrete pavements. Therefore, the use of entrained air and SCM are the two most widely implementable mitigation techniques currently available [8].

3.1.2. Need for Research

SCMs, such as fly ash, have been shown to mitigate CAOXY in portland cement systems through pozzolanic reaction (reaction with calcium hydroxide ($Ca(OH)_2$)) to form calcium

silicate hydrate (C-S-H)) and dilution (reduction in the amount of cement available to form $\text{Ca}(\text{OH})_2$) [17-20,27]. However, quality and availability sometimes make certain SCMs unavailable for use in field concrete applications [19,28,29]. Further, coal power plants throughout the United States continue to be taken offline for cost and environmental reasons [30]. Though currently viable, the long-term availability of cost effective and quality SCMs, such as fly ash, may not be possible in all concrete mixtures. In conjunction with SCM availability is the need to significantly reduce greenhouse gas emissions associated with the production of cement [28]. The use of SCM provides an avenue to reduce cement consumption and in most cases increases concrete performance. In view of these factors taken together, this study focuses on alternative SCMs to determine their effectiveness to mitigate CAOXY formation in cementitious pastes. The alternative SCMs studied include rice husk ash (RHA), bottom ash (BA), limestone filler (LS), nepheline syenite filler (NS), sandstone filler (SS), and silica flour (SFL); fly ash (FA) is used as a conventional SCM for comparison purposes. As far as the authors are aware, five (RHA, BA, NS, SS, and SFL) of these materials have not been investigated for use as a CAOXY mitigation technique. Therefore, this research provides alternative SCM options for concrete professionals concerned with CAOXY deterioration.¹

3.2. Materials and Methods

3.2.1. Material Characterization

In order to study alternative SCM usage for CAOXY mitigation, cementitious paste samples were investigated. Though a need still exists to link deterioration observed in similarly designed

¹ Throughout this work, the designation of SCMs is used to collectively refer to the full group of materials investigated; however, some of these materials are shown to be inert mineral fillers. In the rest of the text, SCMs will refer to the full material list as given here, unless differentiated as SCMs and mineral fillers in a specific discussion.

paste and concrete specimens, the mitigation of CAOXY in the cementitious paste could provide a level of “expected” impact of the SCMs in concrete [11]. For this study, a Type I/II portland cement (PC) was used as the binder with the chemical composition and specific gravity provided in **Table 3.1**. The chemical composition and specific gravities for each alternative SCM are also listed in **Table 3.1**. Cement oxide compositions and specific gravity were determined using ASTM C114 [31]; SCM oxide compositions were determined using X-ray fluorescence (XRF) analysis and specific gravities were analyzed with a helium pycnometer per ASTM C604 [32]. The FA classifies as a Class C material based on ASTM C618 [33] and is used for comparison as a traditional SCM type. Suraneni et al. [18,19] investigated numerous fly ashes, including both Class C and Class F ashes, and determined that relatively minor differences exist between fly ash types for CAOXY mitigation in cementitious paste. Therefore, for this investigation only one fly ash was utilized for reference as a traditional SCM. The BA is from the same source as the FA; however, it should be noted that differences in chemical composition do exist between the BA and FA materials. The BA material was mechanically crushed and passed through a 75 μm sieve to obtain material for testing. The RHA is a commercially available material produced for the concrete industry. Similarly, SFL is a commercially available ground silica flour product. Local products were also selected as potential mineral fillers for this project. The LS and NS materials were collected as baghouse fines from the asphalt industry. As such, these materials may have some impurities given that asphalt plants often employ aggregates from multiple sources; however, LS is currently utilized in concrete mixtures in Arkansas. The SS material was collected by sieving crushed sandstone over a 75 μm sieve.

Table 3.1. Cement and alternative SCM chemical compositions (%) and specific gravities.

Oxide	PC	RHA	BA	LS	NS	SS	SFL	FA
SiO ₂	20.25	88.91	44.23	10.66	54.23	78.54	98.51	36.93
Al ₂ O ₃	4.54	0.52	16.93	5.10	20.22	9.65	0.24	20.12
Fe ₂ O ₃	4.20	0.53	5.75	1.69	4.63	3.16	0.82	5.56
CaO	63.73	0.68	22.92	47.81	2.34	0.65	0.03	22.71
MgO	0.91	0.54	4.39	1.47	1.87	0.80	0.03	5.64
SO ₃	3.09	0.23	0.37	0.49	0.20	0.14	0.04	1.89
Na ₂ O	0.16	0.12	1.16	0.44	6.43	0.86	0.06	2.49
K ₂ O	0.54	1.72	0.34	0.23	5.61	1.46	0.03	0.48
LOI	2.53	5.04	0.88	31.02	1.92	3.59	0.02	0.62
Specific gravity	3.15	1.94	2.70	2.59	2.53	2.54	2.49	2.56

While the bulk chemical composition of each material is important, only the amorphous portion of SCMs are typically reactive in concrete [28,34] and SCM reactivity strongly depends on amorphous content and amorphous phase composition [28]. A clear example of the importance of considering the amorphous phase composition can be seen when considering the SFL material. SFL and silica fume have similar bulk chemical compositions (mostly SiO₂).

However, SFL is very different from a conventional silica fume, as the former is highly crystalline while the latter is mostly amorphous [35-37]. Indeed, this research shows that SFL does not show any significant pozzolanic reaction (**Table 3.2**), similar to quartz [34].

Quantitative x-ray diffraction (QXRD) can be used to characterize amorphous content, amorphous phase composition, and crystalline phases in SCMs [28,34]. In this work, instead of QXRD, reactivity tests are used to determine SCM reactivity and to differentiate SCMs and inert materials.

The reactivity test, based on the R³ tests [38,39], is performed by mixing SCMs in a 1:3 mass ratio with Ca(OH)₂ in a 0.5 M KOH solution at 50 °C. The heat release of the SCM is monitored for 10-days using isothermal calorimetry and the Ca(OH)₂ consumption of the SCM at 10-days is measured using thermogravimetric analysis ((TGA) covered in **Section 3.2.3.2**) [40,41]. Further details of the experimental approach are presented elsewhere [40,41]. The reactivity test has

been used to group SCMs into different classifications based on reactivity and pozzolanic, hydraulic, or inert behavior [40,41]. This method was performed on each SCM and the results are reported in **Table 3.2**. These results are discussed further in **Section 3.3.4.4** to determine if reactivity testing can predict CAOXY mitigation prior to SCM usage in cementitious systems. The results suggest that SS, NS, LS, and SFL are not reactive and should be considered mineral fillers rather than SCM. This is in line with what is known about these materials from literature [34,37,40-42]. The BA, FA and RHA are pozzolanic and can be considered to be SCM, which is consistent with what is known about these materials (though BA can be a variable material) [35,40,41,43].

Table 3.2. Pozzolanic reactivity classification of alternative SCM (developed from [41]).

Classification	Reactivity	Ca(OH) ₂ Consumption (g/100 g SCM)	Heat Release (J/g SCM)	SCM
Inert	Not Reactive	0 – 50	0 – 120	SS, NS, LS, SF
Pozzolanic	Less Reactive	40 – 100	200 – 370	FA, BA
	More Reactive	100 – 180	400 – 750	RHA
Latent Hydraulic	Less Reactive	0 – 20	150 – 250	
	More Reactive	20 – 50	370 – 550	

Scanning electron microscopy (SEM) images of the cement and each SCM are provided in **Fig. 3.1** with all images at a similar magnification level. From the literature, similar SEM images of FA [43], BA [43], RHA [44], and SFL [45] are suggested. SS and NS have been less researched, and a deviation is noted in LS which typically consists of angular grains [45] similar to SFL. In this work, the LS has angular grains as well as some spherical particles. As previously discussed, this material is a by-product and could contain a small amount of “contamination” (i.e., potentially fly ash or other quarry material). From **Fig. 3.1**, significant differences in shape are apparent. FA has numerous spherical particles while the NS, SS, and SFL materials are comprised of angular particles. The BA has some spherical particles, but also contains rods that

could significantly impact workability. The BA is quite coarse when compared to FA. The RHA material also contains some small rod-shaped particles, possibly a portion of fibrous ligament associated with the plant structure. RHA has been shown to significantly reduce workability similar to silica fume [35]. These size and shape characteristics of each SCM should be considered when selecting a SCM for concrete mixture design as they can significantly impact workability, strength, and overall performance. While particle size distribution was not tested, **Fig. 3.1** suggests that all SCMs have roughly similar fineness, with median particle size between 10 and 20 μm .

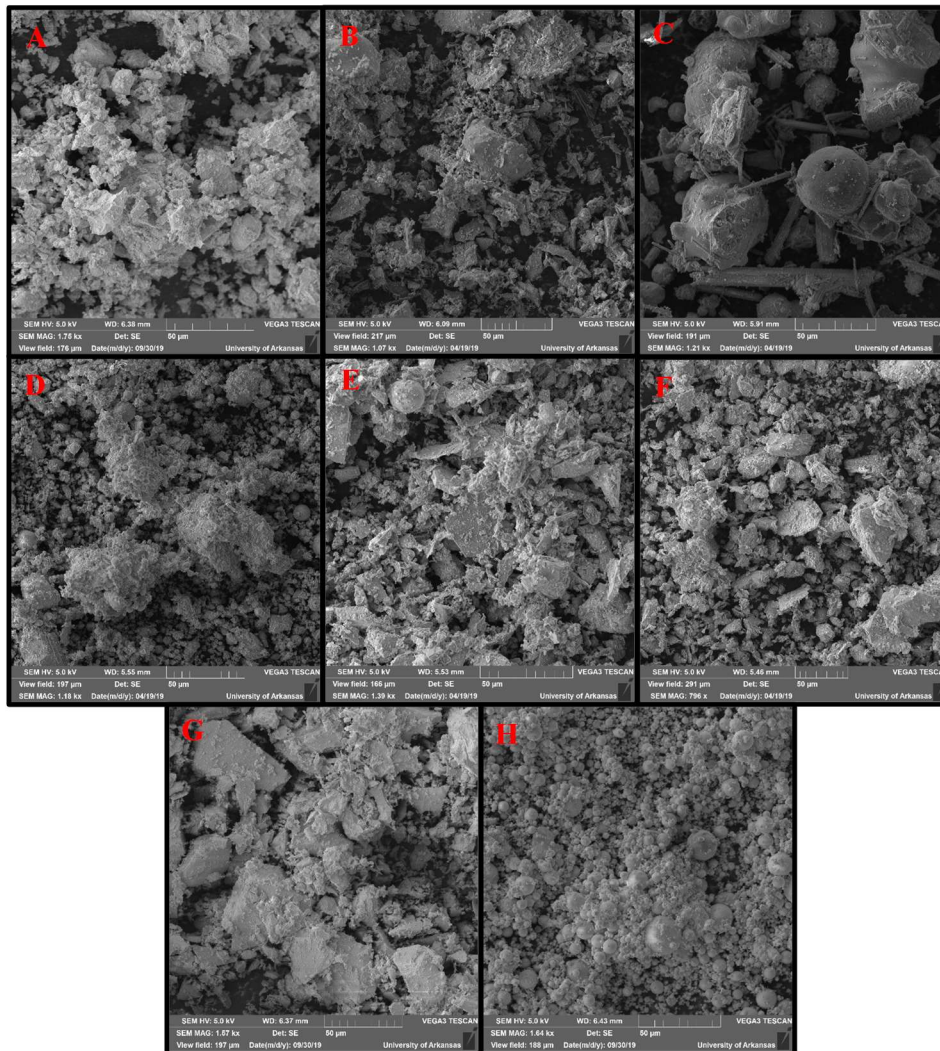


Figure 3.1. SEM images of cement and each alternative SCM: A) PC B) RHA C) BA D) LS E) NS F) SS G) SFL and H) FA.

3.2.2. Batching and Curing

All paste specimens were cast at an equivalent water to cementitious materials ratio (w/cm) of 0.45. Each SCM was incorporated at 0, 15, 30, and 45% cement replacement by mass and batch weights are provided in **Table 3.3**. It should be noted that some SCMs (the inert fillers and RHA) are used in higher quantities than typically reported as feasible cement replacement levels [29]; however, cement replacement levels were kept consistent for each SCM in order to compare results. Mass replacement was selected in order to mimic traditional field applications of cement replacement with SCM in concrete such as outlined in the Arkansas Department of Transportation (ARDOT) specifications [46]. A future portion of this research is to investigate CAOXY mitigation in concrete using SCM. Therefore, similar mixture design procedures were utilized in order to correlate the paste and concrete portion of the research. Prior to mixing, the dry cement and SCM were hand mixed to better distribute the SCM throughout the paste sample. Specimens were then mixed in general accordance with ASTM C305 [47]; however, a longer mixing duration (1-minute at low speed, 1-minute scrapping, 2-minute at high speed) was utilized to minimize paste clumping in the mixture. Following mixing, eighteen 50 mm cubes were cast, sealed with polyethylene sheeting, covered with wet towels, placed in a $23\text{ }^{\circ}\text{C} \pm 1.5\text{ }^{\circ}\text{C}$ environmental chamber at $50\% \pm 4\%$ humidity and allowed to cure for 1-day. At 24-hours, specimens were removed from the molds and stored for subsequent testing. Compressive strength specimens were cured in a limewater bath in accordance with ASTM C192 [48]. Specimens to be tested by TGA and low-temperature differential scanning calorimetry (LT-DSC) were removed from the cube molds at 24-hours and placed in sealed containers to cure for an additional 90-days. This curing method was adopted based on procedures established in

Monical et al. [49]; however, in Monical et al. [49], specimens were not demolded and placed in sealed containers, but rather, left in the molds for the duration of curing.

Table 3.3. Cementitious paste mixture design proportions.

Material (grams)	Mass cement replacement level with SCM			
	0%	15%	30%	45%
Cement	4254.7	3608.8	2972.0	2335.1
SCM	0.0	636.9	1273.7	1910.6
Water	1910.6	1910.6	1910.6	1910.6

3.2.3. Test Methodology

3.2.3.1. Compressive Strength Testing

Compressive strength testing was conducted on 50 mm cube cementitious paste specimens cast and cured in accordance with the procedures in **Section 3.2.2**. Specimens were removed from the curing tank at each designated test age and rinsed to remove free lime on the surface prior to testing. The specimens were kept moist and scraped to remove any protrusions or hard edges prior to testing. Specimens were then measured, placed in the compression machine and loaded at a rate of 75 psi/s in accordance with ASTM C109 [50]. Compressive strength testing was conducted on cube specimens at 1, 7, 28, 56, and 91-days of age.

3.2.3.2. Thermogravimetric Analysis

For this study, TGA is used to determine $\text{Ca}(\text{OH})_2$ content in cementitious paste (similar to ASTM C1872 [52]), as the CAOXY and $\text{Ca}(\text{OH})_2$ amounts in cementitious paste specimens are known to be linearly correlated [18-20,51]. One deviation from this standard is noted. In ASTM C1872 [52], the reported decomposition temperature range for $\text{Ca}(\text{OH})_2$ is 380 °C - 600 °C, however, in this study, mass loss in the temperature range of 380 °C - 460 °C was used, similar to other works in literature [12,16-20]. The $\text{Ca}(\text{OH})_2$ amount was determined using the tangent method as suggested by Kim and Olek [53]. The $\text{Ca}(\text{OH})_2$ available for CAOXY formation is lower than what is reported by TGA given that some $\text{Ca}(\text{OH})_2$ is encapsulated in other hydration

products [18,19]. Therefore, care should be taken when extending TGA results to quantify predicted CAOXY formation as discussed further in **Section 3.3.3**.

3.2.3.3. Low-Temperature Differential Scanning Calorimetry

LT-DSC is utilized to quantify CAOXY formation in cementitious systems [12,18-20,54-56].

Hydrated paste is ground and combined with a 20% CaCl₂ solution and run through a freezing/thawing cycle (-90 °C to 50 °C). During heating, at a temperature above freezing (the specific temperature varies based on the paste composition), a heat signature, associated with the formation of CAOXY, is observed. Using this heat signature, the amount of CAOXY in a cementitious paste mixture can be determined. It should be noted that by grinding the paste prior to mixing with the deicing solution, a higher CAOXY will be reported than might occur in hardened cementitious systems [56]. This test methodology was recently adopted by the American Association of State Highway and Transportation Officials as AASHTO T 365 [57]. For this investigation, AASHTO T 365 [57] was utilized to quantify CAOXY in the cementitious paste mixtures containing alternative SCMs. Further details about this test methodology can be found in Monical et al. [49].

3.3. Results and Discussion

3.3.1. Compressive Strength Results

Compressive strength testing was conducted on cementitious paste for each SCM type. Results from these tests (**Figs. 3.2 – 3.4**) indicate additions of LS, NS, and SS mineral fillers, along with BA and SFL generally reduce the compressive strength. A 15% cement replacement with FA and all cement replacements with RHA increased, or maintained compressive strength compared with a cement only mixture when specimens were allowed to cure 91-days prior to testing. Higher FA replacements reduced compressive strength, but less than at equivalent cement

replacements with LS, NS, SS, SFL, and BA. Though compressive strengths shown are for cementitious paste, a check is made to determine if the paste strength is adequate to meet the concrete mixture design minimum (27.6 MPa) per ARDOT [46] shown as a red-dashed line on **Figs. 3.2 – 3.4**. This check is to determine the potential impact/viability of using similar cementitious paste mixtures in the development of concrete mixture designs. All paste specimens in this research program attained a 27.6 MPa compressive strength or greater at 28-days. The coefficient of variation (CV) for compressive strength data averaged for all ages ranged from 2.3% (PC) to 5.0% (SFL); however, for a few individual ages, higher values up to 28% were observed. These deviations may have been caused by irregular or nonplanar specimens (although specimens were visually checked prior to testing) which led to irregular cracking patterns. When planar cracking was observed and the strength of one specimen generally deviated significantly from the other two, the errant data points were removed from the average shown in **Figs. 3.2 – 3.4**.

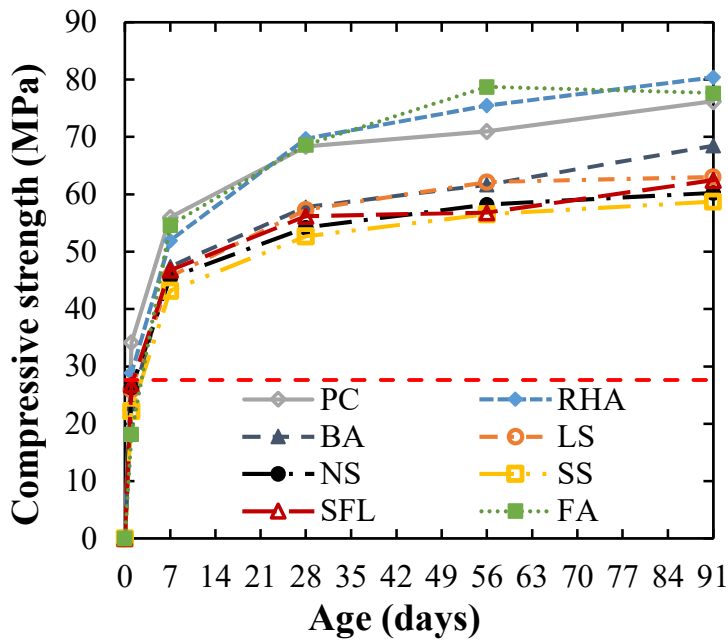


Figure 3.2. Compressive strength data for alternative SCM pastes (15% mass replacement).

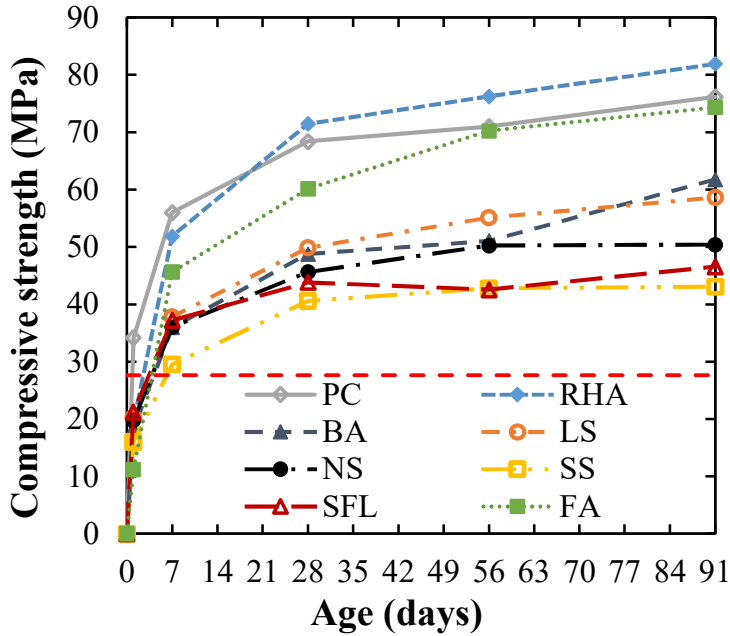


Figure 3.3. Compressive strength data for alternative SCM pastes (30% mass replacement).

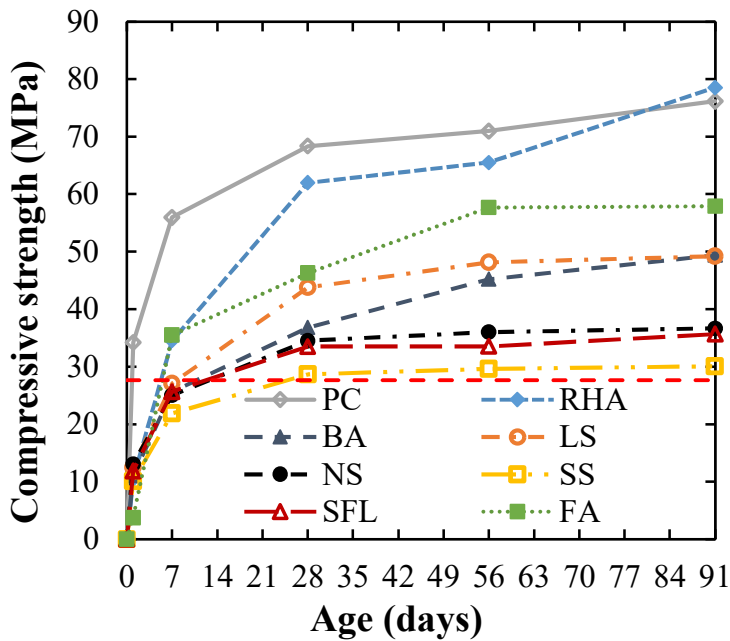


Figure 3.4. Compressive strength data for alternative SCM pastes (45% mass replacement).

From this data, it is clear that for most alternative SCMs tested (the exception being RHA), an increase in cement replacement with each alternative SCM reduces compressive strength. When cement is replaced by SCM, the cement hydration can be impacted through dilution and pozzolanic/hydraulic reaction [19,34]. By replacing a portion of the cement with SCM, a dilution effect occurs whereby reduced strength could be expected due to the reduction in the amount of hydration products due to lower cement contents [37]. For inert materials (**Table 3.2**), the major effect is dilution, leading to significantly lower strengths; however, as shown in **Figs. 3.2 – 3.4**, LS and BA appear to have some reactivity leading to less strength loss than SS, SFL, and NS. Inert materials may not be suitable for use at replacement levels above 15% due to decreased strength and other associated durability concerns [58].

Aluminosilicates in the SCM and $\text{Ca}(\text{OH})_2$ can react to form C-S-H [15-23,27] in what is known as the pozzolanic reaction. The additional C-S-H can provide increased long-term strength compared to a cement only system [27] (though strength depends on numerous other factors including the SCM replacement level, the SCM degree of reaction, and changes in porosity and pore sizes due to the SCM). In this investigation, when cement is replaced with 15% FA and at each RHA replacement, the strength remained constant or higher than in a cement only system. Given that $\text{Ca}(\text{OH})_2$ is consumed in the pozzolanic reaction, the increased compressive strength could be used to roughly predict the ability of alternative SCM to mitigate CAOXY. Further, SCMs classified as pozzolanic, more reactive per **Table 3.2** could possibly be used at higher replacement levels to provide increased protection against CAOXY formation without sacrificing durability concerns. However, durability factors other than compressive strength must also be considered prior to the use of high (> 30%) volume SCM cement replacements in cementitious systems.

Presented in **Fig. 3.5** are data showing the percentage strength loss at 91-days for each cement replacement with an alternative SCM. A larger reduction in strength due to cement replacement with SCM indicates a lack of pozzolanic reactivity; therefore, only a dilution effect is expected in mitigating CAOXY. For instance, in **Fig. 3.5** at a 45% cement replacement with SS, a reduction in compressive strength of 53.2% is observed when tested at an age of 91-days. Conversely, the compressive strength is increased by 3.1% in the RHA specimens at the same age and replacement level. These variations highlight the differences between materials that only provide dilution through cement replacements and those that provide both dilution and pozzolanic reaction.

For comparison, a line representing dilution is given as the black dash-dot line in **Fig. 3.5**. This line predicts the reduction in Ca(OH)_2 if cement is replaced by a completely inert material of equal size and density. However, often mineral fillers are not equivalent size or equivalent density to cement. This means that the incorporation of mineral fillers could change the hydration of the cementitious paste; however, for this work, only a pure dilution limit is shown for reference. It is observed that SS, NS, and SFL are near/above dilution while the other materials provide an increased benefit beyond dilution. Trend lines, based on percentage strength reduction, are presented in **Fig. 3.5** with corresponding equations given in **Table 3.4**.

Using the slope of each linear trend line, an order of potential CAOXY mitigation is established for each alternative SCM with a decreasing slope indicative of greater CAOXY mitigation potential. The order for the materials tested in this program from lowest mitigation potential to highest mitigation potential is SS, SFL, NS, BA, LS, FA, and RHA. It should be noted that for more pozzolanic materials, such as RHA and FA, a lower linear fit is observed. This is expected as the reduction in strength is a function of both dilution and pozzolanic reaction.

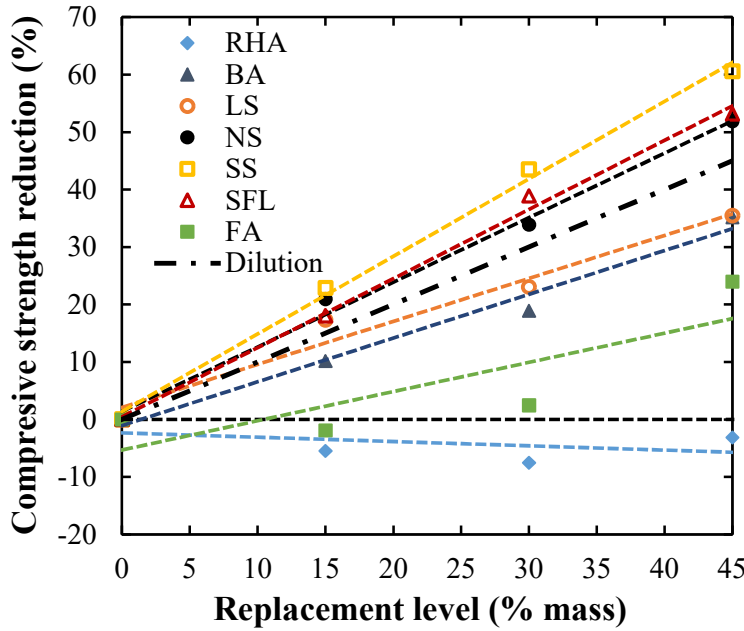


Figure 3.5. Strength loss percentage as a function of SCM replacement for each SCM.

Table 3.4. Linear trend line equations for percentage strength loss based for each alternative SCM.

Material	Trend Line	R ²
SS	$s = 1.345r + 0.014$	0.996
SFL	$s = 1.202r + 0.005$	0.995
NS	$s = 1.124r + 0.014$	0.993
BA	$s = 0.762r - 0.011$	0.980
LS	$s = 0.747r + 0.021$	0.966
FA	$s = 0.509r - 0.053$	0.669
RHA	$s = -0.076r - 0.023$	0.206

s = percentage strength loss; r = SCM replacement level.

3.3.2. Thermogravimetric Analysis Results

As discussed in **Section 3.2.3.2**, TGA is able to quantify the $\text{Ca}(\text{OH})_2$ in a cementitious system.

The $\text{Ca}(\text{OH})_2$ amount is a measure of the potential of a SCM to mitigate deleterious CAOXY formation through dilution and pozzolanic reaction. For SCMs that do not react with $\text{Ca}(\text{OH})_2$, the only potential benefit is the reduction of cement content in the system through dilution.

However, a measurable reduction in Ca(OH)_2 is still observed in these systems when compared to an equivalent cement only system. Suraneni et al. [18,19] have shown that Ca(OH)_2 reductions in a cementitious paste specimens are typically linearly correlated to the SCM replacement level. Results here, shown in **Fig. 3.6**, are in good accordance with literature as all materials tested reduced Ca(OH)_2 nearly linearly [18,19].

Also given in **Fig. 3.6** is a black, dash-dot line representing dilution of the cementitious paste due to the removal of cement, similar to **Fig. 3.5**. It can be observed in **Fig. 3.6** that RHA and FA reduce Ca(OH)_2 greater than expected through simple dilution while LS, SS and SFL increase Ca(OH)_2 especially at 15 and 30% cement replacements. Suraneni et al. [19] has suggested a 5% increase in the degree of hydration due to the physical presence of the mineral fillers increasing the hydration extent (known as the filler effect [34]). This means that even though inert mineral fillers decrease Ca(OH)_2 due to the removal of cement, a small increase in Ca(OH)_2 over what is expected from pure dilution can be observed in paste specimens containing mineral fillers compared to pure dilution as observed here. BA and NS follow the dilution line closely and the lack of increased Ca(OH)_2 could be influenced by the physical properties of the materials and some reactivity for BA. Given that LS and SFL classify as inert for pozzolanic reaction from **Table 3.2**, these materials act as mineral fillers leading to the increased Ca(OH)_2 above the dilution level. The replacement of cement with any of the tested materials does reduce the Ca(OH)_2 compared to an equivalent mass cement content as shown in **Fig. 3.6**.

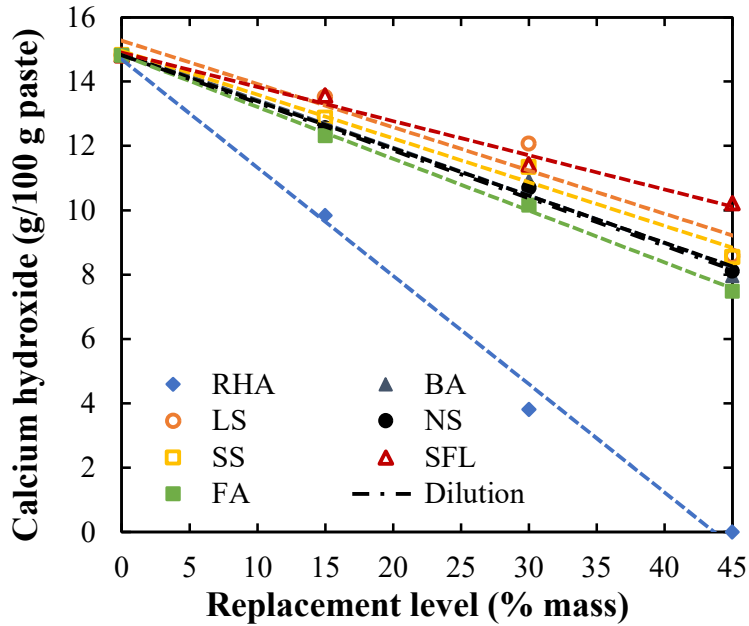


Figure 3.6. Calcium hydroxide mitigation at each cement replacement level with alternative SCM.

RHA reduces $\text{Ca}(\text{OH})_2$ more significantly than any other SCM type in this investigation. A 33.6% reduction in $\text{Ca}(\text{OH})_2$ was observed at a 15% mass cement replacement level with RHA and no measurable $\text{Ca}(\text{OH})_2$ was observed at a 45% replacement level. FA provided the second-best $\text{Ca}(\text{OH})_2$ reduction. At a 15% replacement level, $\text{Ca}(\text{OH})_2$ was reduced only 16.9% and the 45% replacement level with FA suppressed $\text{Ca}(\text{OH})_2$ by approximately 50%, respectively.

While these are significant reductions, they are much lower than the RHA. Presented in **Table 3.5** are the linear trend lines associated with the reduction of $\text{Ca}(\text{OH})_2$ for each SCM. The slope of each linear trend line represents the efficiency of that SCM to reduce $\text{Ca}(\text{OH})_2$ [19]. In order of increasing $\text{Ca}(\text{OH})_2$ reduction, SCMs are arranged as SFL, LS, SS, NS, BA, FA, and RHA.

Table 3.5. Linear trend line equations for Ca(OH)_2 reduction from **Fig. 3.6**.

Material	Trend line	R ²
SFL	$c = -0.106r + 14.90$	0.987
LS	$c = -0.135r + 15.28$	0.936
SS	$c = -0.136r + 14.95$	0.985
NS	$c = -0.147r + 14.85$	0.996
BA	$c = -0.148r + 14.91$	0.988
FA	$c = -0.161r + 14.82$	0.999
RHA	$c = -0.337r + 14.69$	0.993

$c = \text{Ca(OH)}_2$ content in g/100 g paste; $r = \text{SCM}$ replacement level

3.3.3. Low-Temperature Differential Scanning Calorimetry Results

Similar to TGA, mature (91-day age) specimens were tested in order to give the alternative SCMs time to react with available Ca(OH)_2 through pozzolanic reaction. Results from LT-DSC testing are compiled in **Fig. 3.7** which corroborates the TGA results and compressive strength data that RHA most effectively reduces CAOXY with FA as the second most effective SCM. In **Table 3.6**, linear trend lines are provided detailing the CAOXY reduction based on SCM replacement levels. In Suraneni et al. [18,19], it was noted that the Ca(OH)_2 observed in TGA did not develop an equivalent CAOXY content expected from reaction stoichiometry (**Eq. 1**) due to encapsulation effects. Best fit lines between CAOXY and Ca(OH)_2 were used by Suraneni et al. [19] to develop **Eq. 3.3** to predict CAOXY amounts using Ca(OH)_2 data. Similar to Ca(OH)_2 , by using the slope of each trend line, an order of efficiency can be established for CAOXY mitigation [19]. It should be noted that the RHA trend line was established using only the 0, 15, and 30% cement replacement levels. As shown in **Fig. 3.7**, at 30% cement replacement with RHA, there is little measurable CAOXY that forms and 0% recorded at the 45% replacement level. Therefore, the 45% cement replacement with RHA is not included in the trend line given the significant deviation. It should also be noted that the FA data presented here is part of the data used to develop research presented in Traore et al. [22]; and uses slightly

different cement replacement levels. A consistent, linear reduction in CAOXY levels is noted with an increasing fly ash content. In order of increasing CAOXY mitigation, SCM for this work are arranged as SS, LS, SFL, NS, BA, FA, and RHA.

$$y = 2.82x - 8.32 \quad \text{Eq. 3.3}$$

$$y = \text{CAOXY (g/100 g paste)}$$

$$x = \text{Ca(OH)}_2 \text{ (g/100 g paste)}$$

Table 3.6. Linear trend line equations for CAOXY mitigation in **Fig. 3.7** based on cement replacement with alternative SCM and predicted CAOXY mitigation based on [19].

Material	Measured trend line	R ²
SS	$c = -0.318r + 39.15$	0.900
LS	$c = -0.373r + 35.78$	0.685
SFL	$c = -0.397r + 38.50$	0.969
NS	$c = -0.456r + 37.71$	0.969
BA	$c = -0.542r + 38.99$	0.969
FA	$c = -0.700r + 35.75$	0.992
RHA	$c = -1.198r + 36.50$	0.995

c = CAOXY content in g/100 g paste; r = SCM replacement rate

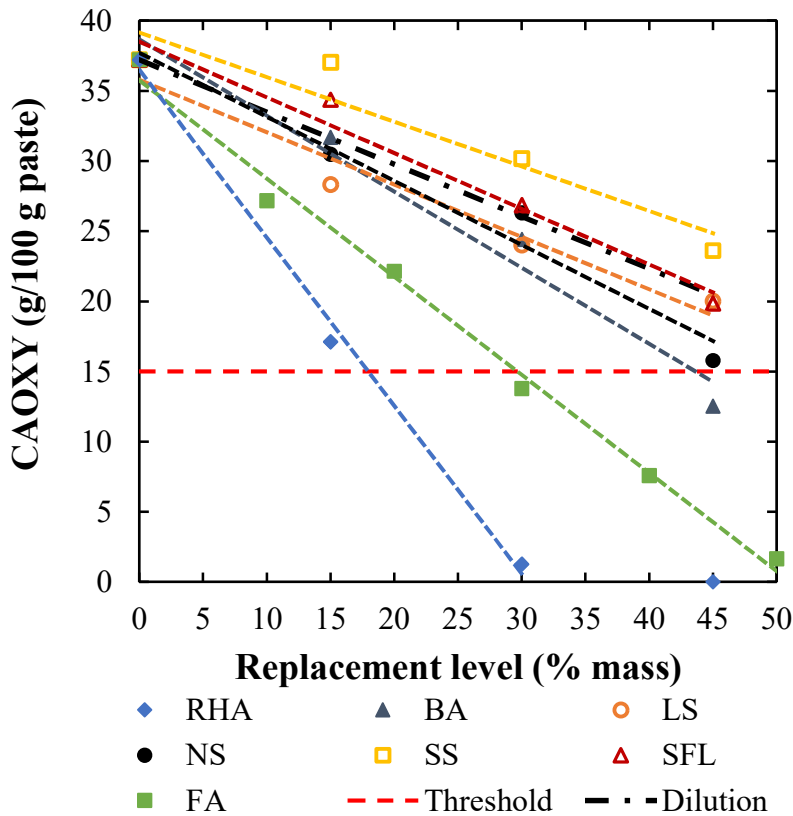


Figure 3.7. CAOXY mitigation with each alternative SCM and cement replacement level.

Further provided in **Fig. 3.7** is the dilution line (represented as a black dash-dot line) similar to that in **Fig. 3.6**. This dilution line represents the expected CAOXY reduction in a cementitious system where cement has been substituted with an equivalent inert material. From **Fig. 3.7**, the percentage reduction in CAOXY for all cement replacements with SS and the 15% cement replacement with SFL increased measurable CAOXY above dilution. This indicates the availability of large amounts of $\text{Ca}(\text{OH})_2$ to react with deicing solution when using these materials. LS filler was above the dilution line for TGA but not in **Fig. 3.7** for the LT-DSC data, while SS follows the dilution line closely in **Fig. 3.6** but is significantly above this limit in **Fig. 3.7**. These differences may be due to differences in the extent of filler effect and consequent encapsulation of $\text{Ca}(\text{OH})_2$ in LS and SS mixtures. As LS is a more effective filler [34], it is possible that the $\text{Ca}(\text{OH})_2$ with LS is more encapsulated than the $\text{Ca}(\text{OH})_2$ that is formed with SS. For the more pozzolanic reactive materials (RHA and FA), the reduction in CAOXY was greater than through simple dilution.

The current AASHTO PP 84 [59] recommendation is to mitigate CAOXY levels in cementitious paste below 15 g/100 g paste. A recent investigation found this limit may also correlate well with expansion in concrete specimens [11]. In **Fig. 3.7**, the threshold value of 15 g/100 g paste is plotted as a red dash-dot line. Only RHA, FA and BA mitigate CAOXY below the proposed threshold level at the cement replacement levels tested in this investigation. These findings correlate well with **Table 3.2** which indicates that these are the only three materials to classify as pozzolanic. Replacement levels of 17.9, 29.7, and 44.8% are needed to mitigate CAOXY below 15 g/100 g paste for RHA, FA, and BA, respectively. For BA, a replacement level above 40% may not be realistic as significant strength loss was observed in the companion compressive strength specimens shown in **Section 3.3.1**. Other durability factors should also be considered in

the concrete mixture design development stage to ensure long-term durability when using SCM. For RHA, a replacement level of 17.9% did not reduce the compressive strength of the cementitious paste. This material could have good potential for use as an SCM to significantly mitigate damage due to CAOXY; however, further investigations are needed to determine the impact of RHA on other factors such as workability. The use of FA at 29.7% is an acceptable cement replacement option for use in concrete mixture designs and is in good accordance with the AASHTP PP 84 [59] proposed minimum 30% SCM level for concretes exposed to CaCl_2 and MgCl_2 deicing solutions.

3.3.4. Discussion

In order to investigate the different testing methodologies, a cross comparison between each dataset is provided. Detailed discussions of these comparisons are given in the subsequent sections.

3.3.4.1. A Comparison of CAOXY and $\text{Ca}(\text{OH})_2$

Using the TGA and LT-DSC test results, a comparison is made of the measured $\text{Ca}(\text{OH})_2$ and measured CAOXY values. A linear correlation exists between the $\text{Ca}(\text{OH})_2$ and CAOXY values. The data are plotted in **Fig. 3.8** along with a trend line. The FA data are not plotted on **Fig. 3.8** given that the TGA and LT-DSC data are at different fly ash replacement levels; however, $\text{Ca}(\text{OH})_2$ and CAOXY levels have been shown to linearly correlate when fly ash is used to replace cement [18]. Further, one point is excluded from the fitting, which is the point at the origin (the point with 45% RHA replacement). This point is excluded because CAOXY does not form below a certain $\text{Ca}(\text{OH})_2$ threshold and including this point would cause an erroneous determination of the threshold. As expected from literature, the trend line has a positive X-axis intercept which represents the amount of $\text{Ca}(\text{OH})_2$ that is bound by cementitious hydration

products and is unavailable for CAOXY formation. This value is 2.79 g/100 g cement paste, which is similar to the value of 2.95 g/100 g cement paste from literature (Eq. 3) [19]. The equation of the best fit line here is very similar to the equation of the best fit line from [19]. The results of Fig. 3.8 verify that $\text{Ca}(\text{OH})_2$ can be used to predict CAOXY; however, it must be noted that not all $\text{Ca}(\text{OH})_2$ is available to form CAOXY. Care should be taken when extending TGA data to predict CAOXY formation.

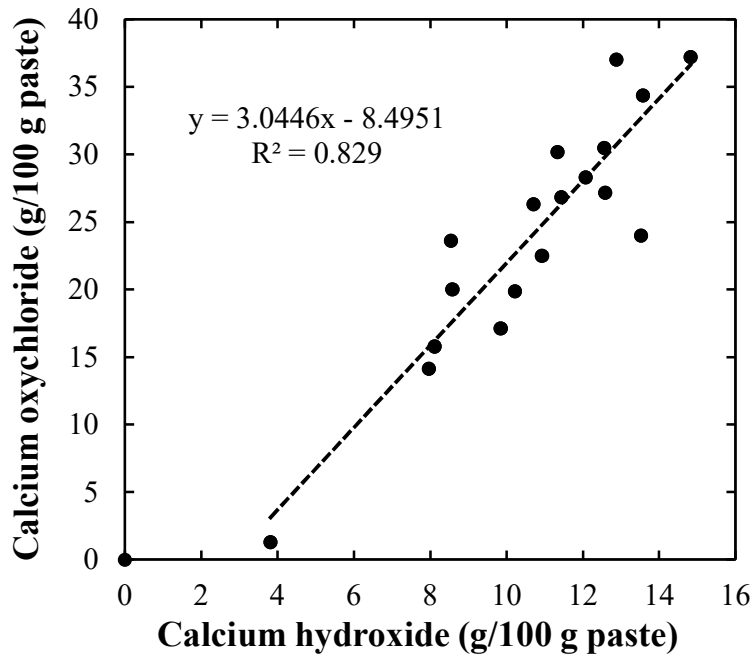


Figure 3.8. Comparison of calcium hydroxide and CAOXY contents with alternative SCMs and linear trend line.

3.3.4.2. A Comparison of $\text{Ca}(\text{OH})_2$ Reduction and Compressive Strength Reduction

A comparison of the $\text{Ca}(\text{OH})_2$ reduction and the compressive strength reduction is presented in Fig. 3.9. Strength and $\text{Ca}(\text{OH})_2$ reductions are nearly linearly correlated at a fixed replacement level; however, there is substantial scatter in the data points. The slope of each trend line for the 15, 30, and 45% cement replacement with SCM is -1.03, -0.74, and -0.84, respectively. It is expected that some deviation occurs between these slopes as dilution and pozzolanic reactions

impact $\text{Ca}(\text{OH})_2$ reduction and strength depends on other non-chemical factors. The slope of each trend line is negative. This indicates that at each fixed cement replacement level, there is a decrease in compressive strength reduction as the $\text{Ca}(\text{OH})_2$ is reduced by each SCM likely related to the pozzolanic reactivity of the material. This is highlighted by RHA and FA which show the lowest strength reductions and the highest $\text{Ca}(\text{OH})_2$ reductions compared to the other SCMs.

When comparing different cement replacement levels for an individual SCM, the effect of replacement level can be understood. For most materials, except the RHA, as replacement levels increase, the strength reductions and $\text{Ca}(\text{OH})_2$ reductions both increase. This suggests that the removal of cement (likely due to dilution) from the system reduces $\text{Ca}(\text{OH})_2$ and strength simultaneously; however, materials such as RHA, are able to overcome strength loss through pozzolanic reaction, increased hydration, and in-filling of available void space [35].

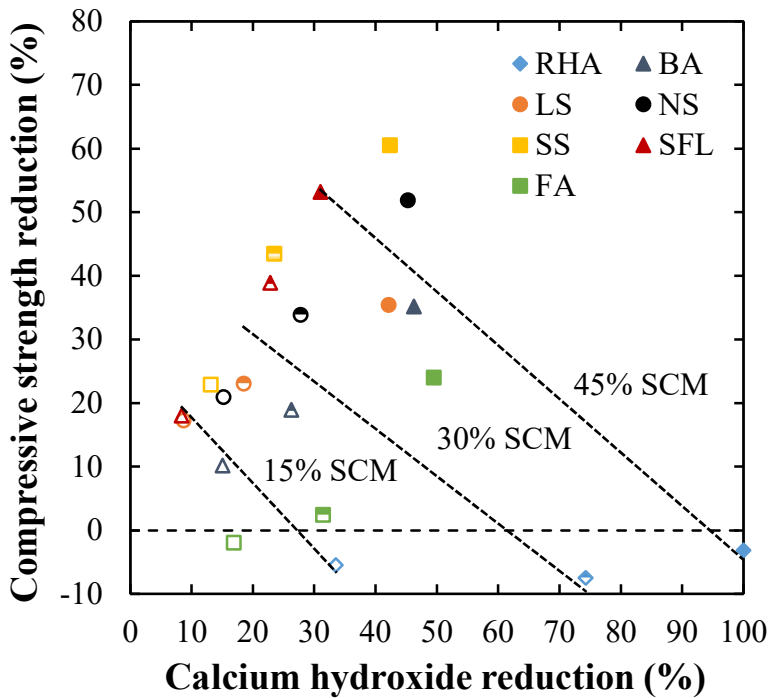


Figure 3.9. A comparison of the compressive strength reduction and $\text{Ca}(\text{OH})_2$ reduction for each SCM replacement type and level. Hollow markers denote a cement replacement level of 15%,

half-filled markers denote a cement replacement level of 30%, and filled markers denote a cement replacement level of 45%.

3.3.4.3. A Comparison of CAOXY Reduction and Compressive Strength Reduction

Presented in **Fig. 3.10** is a comparison of the compressive strength reduction and CAOXY mitigation. Similar to **Fig. 3.9**, each cement replacement level with SCM is grouped together and nearly congruent trend lines are observed. The slopes of each trend line corresponding to the 15, 30, and 45% cement replacement with SCM are -0.55, -0.64, and -0.95, respectively. The negative slope is expected as observed in **Fig. 3.9** given that CAOXY and Ca(OH)_2 are linearly related [18,19]. This indicates that for fixed cement replacement levels, SCMs which reduce CAOXY are also able to mitigate strength loss, and is likely an indication of the SCMs propensity for pozzolanic reactivity. Similar to **Fig. 3.9**, when comparing individual SCM types (i.e. the SS material represented by yellow squares), there is a propensity for reduced compressive strength as CAOXY is mitigated. Again, this is likely due to dilution of the system with SCM, as more pozzolanic materials, RHA and FA, have no or less compressive strength reduction than the more inert materials.

In order to compare the efficacy of the different mixtures, a highlighted area is shown indicating replacement levels of SCMs that are likely not suitable for CAOXY mitigation. This is based on the ability of the SCM at a given cement replacement level to mitigate CAOXY without sacrificing compressive strength. The region proposed (shown in white on **Fig. 3.10**) for acceptable specimens is quantified by a 30% or less compressive strength loss in conjunction with a 40% or more mitigation in CAOXY. This is done as a general example and obviously acceptable compressive strength reductions depend on the specific application. From this region, all RHA specimens could be used for CAOXY protection as well as the 30% and 45% FA

cement replacements. It should be noted that the specimens tested are paste and not concrete. These results should be also be investigated/verified in concrete samples prior to field use, especially because air content is also known to impact CAOXY deterioration [7,23]. Also, other durability factors must be investigated prior to use of high volume SCM in cementitious paste/concrete.

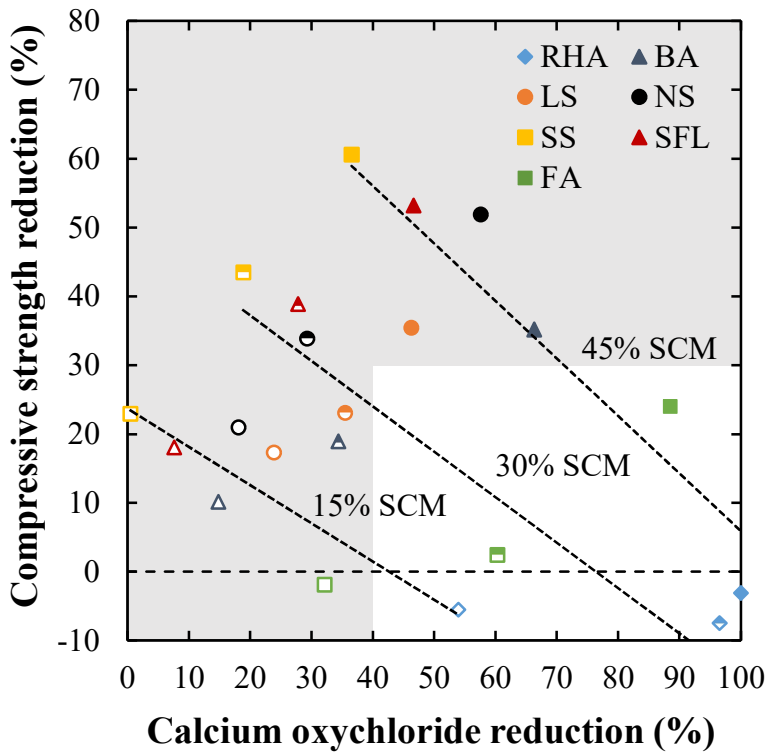


Figure 3.10. A comparison of the compressive strength reduction and CAOXY reduction for each SCM type and replacement level. Hollow markers denote a cement replacement level of 15%, half-filled markers denote a cement replacement level of 30%, and filled markers denote a cement replacement level of 45%.

3.3.4.4. A Comparison of Ca(OH)₂ Consumption: Reactivity Testing vs. Paste

As highlighted in Section 3.2.1, reactivity testing was conducted for each alternative SCM. In the reactivity test, consumption is directly measured on granulated Ca(OH)₂ powder; however, for cementitious paste, a calculation can be made to determine the level of consumption in each

specimen. Consumption for a paste specimen is calculated using **Eq. 3.4** and the average of each SCM replacement level (i.e., 15, 30, and 45%) are plotted in **Fig. 3.11**. The average is used given that only minor differences occur in the varying SCM levels in the paste specimens. In general, the data agrees with previous figures showing RHA as the most effective and FA as the second most effective material investigated in this study. However, it should be noted that reactivity testing shows greater Ca(OH)_2 consumption compared to corresponding values in the paste specimens. This could be due to the significant acceleration of the reactivity test (50 °C), compared to the 91-day paste specimens which were cured at 23 °C.

$$Ca(OH)_{2\text{ P.C.}} = ((Ca(OH)_{2D} - Ca(OH)_{2A}) / (SCM/100)) \quad \text{Eq. 3.4}$$

$\text{Ca(OH)}_{2\text{ P.C.}}$ = Ca(OH)_2 consumed by the cementitious paste (g/100 g paste)

Ca(OH)_{2D} = Ca(OH)_2 calculated from dilution (g/100 g paste)

Ca(OH)_{2A} = Actual Ca(OH)_2 measured by TGA (g/100 g paste)

SCM = Cement replacement level with SCM (%)

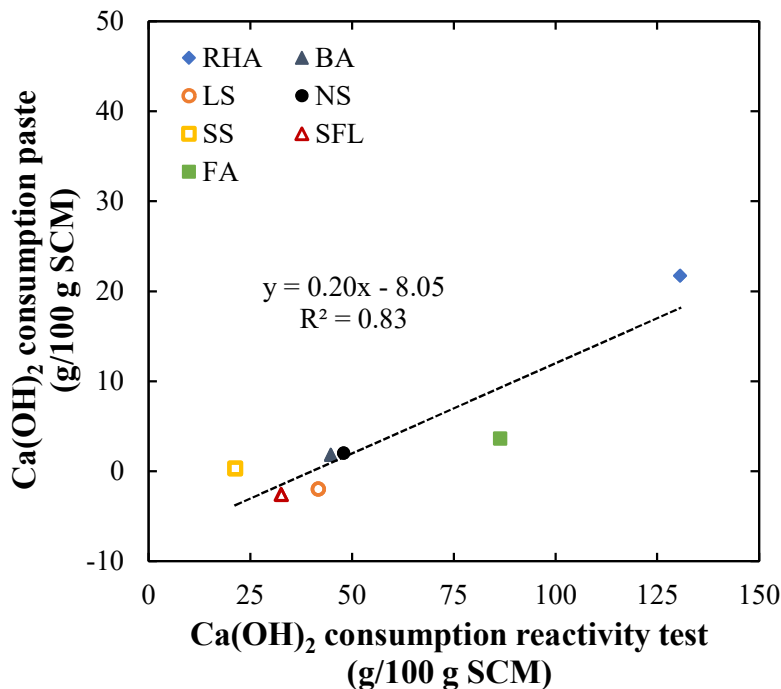


Figure 3.11. A comparison of Ca(OH)_2 consumption from the reactivity testing vs. Ca(OH)_2 consumption in the paste.

In **Section 3.2.1**, classifications were provided for the reactivity of each material tested. Provided in **Fig. 3.12** is the consumption of $\text{Ca}(\text{OH})_2$ by each SCM along with heat released from the pozzolanic reaction. It is shown that a correlation is established between $\text{Ca}(\text{OH})_2$ consumption of each SCM with that measured in the R^3 test; however, the overall trend of this correlation will change based on the type of SCM tested. Therefore, slope and fit are subject to change if compared to datasets with significantly different material types. Using data from **Fig. 3.12**, an order can be established from the reactivity testing of each material to predict its effectiveness at preventing CAOXY. In order of increasing effectiveness, alternative SCM types for this research program are established as SS, SFL, NS, LS, BA, FA, and RHA for reactivity testing.

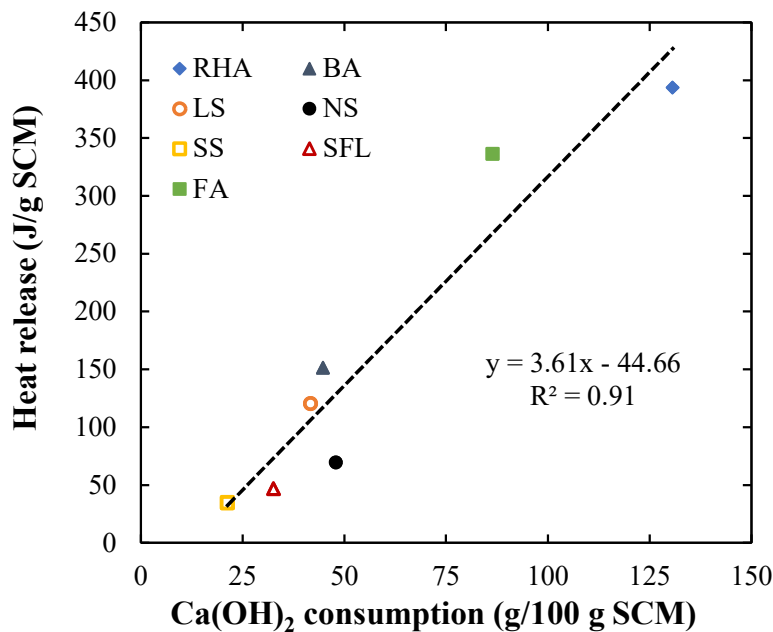


Figure 3.12. Reactivity testing of each alternative SCM type.

3.3.4.5. A Comparison of Predicted CAOXY Mitigation for Each Testing Methodology

For each test method (compressive strength, TGA, and LT-DSC), an order is established to determine the effectiveness for potential CAOXY mitigation. In **Table 3.7**, a comparison is

made of the predicted effectiveness of each alternative SCM to mitigate CAOXY based on the different tests. Given that LT-DSC is the only method directly quantifying CAOXY, the LT-DSC order is considered the baseline for comparison of the other three test methods. For each test program, RHA is predicted as the most effective material to mitigate CAOXY. Further, FA is predicted by each test method as the second most useful SCM from this material list. LT-DSC, TGA, and reactivity testing predict BA as the third most effective material to mitigate CAOXY; however compressive strength testing predicts LS as the third most effective material. It should be noted that the slope (used to predict CAOXY mitigation effectiveness) for BA is 0.747 and is 0.762 for LS in the compressive strength test results. These are very close and could be considered a negligible difference indicating that LS and BA are equivalent at CAOXY mitigation. Further, the difference in prediction could be caused by the particle size variation between the BA and LS materials. The smaller LS material (as shown in **Fig. 3.1**) possibly could have provided more preferential nucleation sites for the formation of C-S-H compared to BA [60,61]. After the third material, there is discrepancy between the methods as to the order of efficiency for CAOXY mitigation; however, given that these materials are inert, only minor differences are expected and could be influenced by physical properties of the SCMs. Given that only RHA, FA, and BA are able to mitigate CAOXY below the proposed threshold of 15 g/100 g paste for the replacement levels tested, these materials are considered the only potentially viable options for CAOXY mitigation. However, as shown throughout this work, these materials are not equivalent in their ability to mitigate CAOXY while maintaining strength. Therefore, a color-coding scheme is proposed to highlight the most potentially viable SCMs for CAOXY mitigation in conjunction with the potential for only minor strength/durability impact. SCMs classifying as pozzolanic reactive (**Table 3.2**) are colored green, blue, and yellow,

respectively in **Table 3.7**. Green coloring represents a highly effective SCM for CAOXY mitigation while blue is effective and yellow is minimally effective. The remaining alternative materials are considered mineral fillers and mitigate CAOXY mainly through dilution. In mineral fillers, variations based on particle size distribution could be more important than material type/chemical composition. These materials are shown in red as ineffective SCM types for significant CAOXY mitigation.

Table 3.7. Predicted effectiveness of each SCM for CAOXY mitigation for each test.

Test method	SCM order*						
LT-DSC	RHA	FA	BA	NS	SFL	LS	SS
TGA	RHA	FA	BA	NS	SS	LS	SFL
Compressive strength	RHA	FA	LS	BA	NS	SFL	SS
Reactivity testing	RHA	FA	BA	LS	NS	SFL	SS

*SCM order given in most effective to least effective for CAOXY mitigation

It is useful to establish methods other than LT-DSC to check CAOXY potential in order to verify the validity of the LT-DSC results. Also, if LT-DSC is not available for a given project, these tests could provide other checks to be made to determine the potential for CAOXY formation. It is therefore useful to utilize multiple testing strategies to elucidate the impact of each SCM type for CAOXY mitigation. Agreement among various test methods provides a more complete understanding into the impact of these SCM types. It should be noted that most LT-DSC testing has been conducted on paste specimens. While this is useful and provides a level of potential CAOXY in concrete, further research is needed to establish a correlation between cementitious paste and concrete testing. Currently, one investigation has attempted to correlate damage in concrete to the proposed LT-DSC threshold of 15 g/100 g paste [11].

3.4. Conclusion

In order to improve transportation infrastructure, an understanding of each durability concern is required. CAOXY formation is a deterioration mechanism primarily affecting joints in concrete pavements [8,11,12]. Though research has been conducted on this topic, a complete understanding of this failure mechanism is not established. It has been shown that the addition of SCM can reduce deterioration and CAOXY formation in cementitious paste specimens [17-22]. For this research, seven SCM types were investigated to determine the effectiveness of each material at reducing CAOXY formation. To the best knowledge of the authors, five of these materials have not been examined for CAOXY mitigation. From this research program, the following conclusions can be established:

- The use of each alternative cement replacement material does mitigate CAOXY formation through dilution; however, SCM may also reduce CAOXY through a combination of dilution and pozzolanic reactivity.
- From the materials tested, RHA is highly pozzolanic and FA and BA are less pozzolanic. LS, NS, SFL, and SS are mostly inert and can be considered mineral fillers.
- For this list of alternative SCM types, RHA is the most effective at mitigating CAOXY formation; further, RHA improved the compressive strength of paste at all cement replacement rates tested for this program.
- TGA, pozzolanic reactivity testing, and compressive strength testing provide effective means to predict the ability of SCM to mitigate CAOXY; however, slight variations in predictions may occur in similar materials (i.e., filler materials without a significant ability for pozzolanic reactivity). For filler materials, particle shape and size may govern the mitigation of CAOXY more than the chemical composition of the material.

- $\text{Ca}(\text{OH})_2$ can be used to predict CAOXY; however, it should be noted not all $\text{Ca}(\text{OH})_2$ is available for CAOXY formation. Approximately 3 g/100 g paste is bound in the hydration products of the paste [19]. The amount of $\text{Ca}(\text{OH})_2$ is linearly correlated to CAOXY formation.

The need continues in order to develop other alternative SCM options to mitigate CAOXY as the potential for traditional quality SCM is reduced. This research program has investigated the use of five new alternative SCM for CAOXY mitigation in cementitious paste. These materials have been found to reduce CAOXY either through dilution or dilution and pozzolanic reactivity. Materials that exhibit both dilution and pozzolanic reactivity are more effective than through dilution only. Further research is needed to determine the impact of these materials on other aspects of cementitious paste and concrete properties.

Declaration of Interests

The authors have no declaration of interests to state.

Acknowledgements

The authors would like to thank the support of the Oklahoma/Arkansas Chapter of the American Concrete Pavement Association for their generous gift supporting this research. Without their support this work would not be possible. The authors would also like to thank the Arkansas Department of Transportation and Ash Grove Cement Company for chemical analysis of the SCM and cement for this project. The authors would also like to thank Boral Resources for providing the fly ash and bottom ash utilized in this research project. Thanks are in order to Granite Mountain Quarries for providing the NS material and to Argos Cement and Ready Mix for providing the LS materials. Special thanks are also in order to David Gonzalez for helping acquire the SEM images and to Airam Marlee Morales Vega for collecting the SS material.

References

1. J.J. Valenza II, G.W. Scherer, A review of salt scaling: I. Phenomenology, *Cem. Concr. Res.* 37 (7) (2007) 1007-1021. <https://doi.org/10.1016/j.cemconres.2007.03.005>.
2. J.J. Valenza II, G.W. Scherer, A review of salt scaling: II. Mechanisms, *Cem. Concr. Res.* 37 (7) (2007) 1022-1034. <https://doi.org/10.1016/j.cemconres.2007.03.003>.
3. Z. Wu, C. Shi, P. Gao, D. Wang, Z. Cao, Effects of deicing salts on the scaling resistance of concrete, *J. Mater. Civ. Eng.* 27 (5) (2015) 04014160.
4. S. Ahmad, Reinforcement corrosion in concrete structures, its monitoring and service life prediction – a review, *Cem. Concr. Comp.* 25 (4-5) (2003) 459-471. [https://doi.org/10.1016/S0958-9465\(02\)00086-0](https://doi.org/10.1016/S0958-9465(02)00086-0).
5. K. Hornbostel, C.K. Larsen, M.R. Geiker, Relationship between concrete resistivity and corrosion rate – a literature review, *Cem. Concr. Comp.* 39 (2013) 60-72. <https://doi.org/10.1016/j.cemconcomp.2013.03.019>.
6. S. Monosi, A. Alvera, M. Collepardi, Chemical attack of calcium chloride on the portland cement paste, *Il Cemento* 86 (2) (1989) 97-104.
7. M. Collepardi, L. Coppola, C. Pistolesi, Durability of concrete structures exposed to CaCl₂ based deicing salts, *Proceedings of the 3rd CANMET/ACI International Conference, 1994, Nice, France*, pp. 107-120.
8. ACI 201.3T-19, Joint deterioration and chloride-based deicing chemicals. American Concrete Institute, Farmington Hills, Michigan, 2019.
9. C. Jones, S. Ramanathan, P. Suraneni, W.M. Hale, Calcium oxychloride: a critical review of the literature surrounding the formation, deterioration, testing procedures, and recommended mitigation techniques, *Cem. Concr. Comp.* 113 (2020) 103663. <https://doi.org/10.1016/j.cemconcomp.2020.103663>.
10. S.H. Smith, C. Qiao, P. Suraneni, K.E. Kurtis, W.J. Weiss, Service-life of concrete in freeze-thaw environments: Critical degree of saturation and calcium oxychloride formation, *Cem. Concr. Res.* 122 (2019) 93-106. <https://doi.org/10.1016/j.cemconres.2019.04.014>.
11. X. Wang, S. Sadati, P. Taylor, C. Li, X. Wang, A. Sha, Material characterization to assess effectiveness of surface treatment to prevent joint deterioration from oxychloride formation mechanism, *Cem. Concr. Comp.* 104 (2019) 103394. <https://doi.org/10.1016/j.cemconcomp.2019.103394>.
12. P. Suraneni, J. Monical, E. Unal, Y. Farnam, J. Weiss, Calcium oxychloride formation potential in cementitious pastes exposed to blends of deicing salt, *ACI Mater. J.* 114 (4) (2017) 631-641. <http://dx.doi.org/10.14359/51689607>.

13. W. Jones, Y. Farnam, P. Imbrock, J. Sprio, C. Villani, M. Golias, J. Olek, W.J. Weiss, An overview of joint deterioration in concrete pavement: mechanisms, solution properties, and sealers, Purdue University (2013) pp. 1-69. <http://dx.doi.org/10.5703/1288284315339>.
14. L. Sutter, K. Peterson, S. Touton, T. Van Dam, D. Johnston, Petrographic evidence of calcium oxychloride formation in mortars exposed to magnesium chloride solution, *Cem. Concr. Res.* 36 (2006) 1533-1541. <https://doi.org/10.1016/j.cemconres.2006.05.022>.
15. K. Torii, T. Sasatani, M. Kawamura, Effects of fly ash, blast furnace slag, and silica fume on resistance of mortar to calcium chloride attack, *ACI Spec. Publ.* 153 (1995) 931-950.
16. Y. Farnam, B. Zhang, J. Weiss, Evaluating the use of supplementary cementitious materials to mitigate damage in cementitious materials exposed to calcium chloride deicing salt, *Cem. Concr. Comp.* 81 (2017) 77-86. <https://doi.org/10.1016/j.cemconcomp.2017.05.003>.
17. C. Qiao, P. Suraneni, J. Weiss, Flexural strength reduction of cement pastes exposed to CaCl_2 solutions, *Cem. Concr. Comp.* 86 (2018) 297-305. <https://doi.org/10.1016/j.cemconcomp.2017.11.021>.
18. P. Suraneni, V.J. Azad, O.B. Isgor, W.J. Weiss, Use of fly ash to minimize deicing salt damage in concrete pavements, *Transp. Res. Rec.* 2629 (2017) 24-32. <https://doi.org/10.3141/2629-05>.
19. P. Suraneni, V.J. Azad, O.B. Isgor, J. Weiss, Role of supplementary cementitious material type in the mitigation of calcium oxychloride formation in cementitious pastes, *J. Mater. Civ. Eng.* 30 (10) (2018) 04018248. [https://doi.org/10.1061/\(ASCE\)MT.1943-5533.0002425](https://doi.org/10.1061/(ASCE)MT.1943-5533.0002425).
20. P. Suraneni, V.J. Azad, O.B. Isgor, W.J. Weiss, Calcium oxychloride formation in pastes containing supplementary cementitious materials: thoughts on the role of cement and supplementary cementitious materials reactivity, *RILEM Tech. Lett.* 1 (2016) 24-30. <http://dx.doi.org/10.21809/rilemtechlett.v1.7>.
21. C. Qiao, P. Suraneni, T.N.W. Ying, A. Choudhary, J. Weiss, Chloride binding of cement pastes with fly ash exposed to CaCl_2 solutions at 5 and 23 °C, *Cem. Concr. Comp.* 97 (2019) 43-53. <https://doi.org/10.1016/j.cemconcomp.2018.12.011>.
22. F. Traore, C. Jones, S. Ramanathan, P. Suraneni, W.M. Hale, Using compressive strength and mass change to verify the calcium oxychloride threshold in cementitious pastes with fly ash, *Constr. Build. Mater.* 296 (2021) 123640. <https://doi.org/10.1016/j.conbuildmat.2021.123640>.
23. C. Jones, P. Suraneni, W.M. Hale, Investigating concrete deterioration due to calcium oxychloride formation, *Cem. Concr. Comp.* 2021. (Submitted).

24. R.M. Ghantous, Y. Farnam, E. Unal, J. Weiss, The influence of carbonation on the formation of calcium oxychloride, *Cem. Concr. Comp.* 73 (2016) 185-191. <https://doi.org/10.1016/j.cemconcomp.2016.07.016>.
25. M. Collepardi, S. Monosi, Effect of the carbonation process on the concrete deterioration by CaCl_2 aggression, *Proceedings of the 9th International Symposium on the Chemistry of Cement*, 1992, New Delhi, India, pp. 389-395.
26. J. Weiss, M.T. Ley, L. Sutter, D. Harrington, J. Gross, S.L. Tritsch, Guide to the prevention of and restoration of early joint deterioration in concrete pavements, Final Report for the Iowa Department of Transportation, TR-697, 2016.
27. P.K. Mehta, P.J.M. Monteiro, *Concrete: Microstructure, Properties, and Materials*, third ed., McGraw Hill Education, New York, 2006.
28. R. Snellings, Assessing, understanding and unlocking supplementary cementitious materials, *RILEM Tech. Lett.* 10 (2016) 50-55. <https://doi.org/10.21809/rilemtechlett.2016.12>.
29. S. Ramanathan, A. Hajibabae, C. Jones, M. Kasaniya, E.A. Olivetti, M. Shakouri, M.D.A. Thomas, B. Traynor, Y. Wang, W.J. Weiss, P. Suraneni, Reactivity of alternative supplementary cementitious materials, *Cem. Concr. Res.* 2020. (Submitted).
30. Phys.Org, 50 US coal power plants shut under Trump. <https://phys.org/news/2019-05-coal-power-trump.html> (accessed 27 June 2019).
31. ASTM C114-18, Standard Test Method for Chemical Analysis of Hydraulic Cement, ASTM International, West Conshohocken, PA, 2018.
32. ASTM C604-18, Standard Test Method for True Specific Gravity of Refractory Materials by Gas-Comparison Pycnometer, ASTM International, West Conshohocken, PA, 2018.
33. ASTM C618-19, Standard Specification for Coal Fly Ash and Raw or Calcined Natural Pozzolan for Use in Concrete, ASTM International, West Conshohocken, PA, 2019.
34. E. Berodier, K. Scrivener, Understanding the filler effect on the nucleation and growth of C-S-H, *J. Am. Ceram. Soc.* 97 (12) (2014) 3764-3773. <https://doi.org/10.1111/jace.13177>.
35. W. Xu, T. Yiu Lo, W. Wang, D. Ouyang, P. Wang, F. Xing, Pozzolanic reactivity of silica fume and ground rice husk ash as reactive silica in cementitious system: a comparative study, *Mater.* 9 (3) (2016) 146. <https://doi.org/10.3390/ma9030146>.
36. Z. Li, H.K. Venkata, P.R. Rangaraju, Influence of silica flour-silica fume combination on the properties of high performance cementitious mixtures at ambient temperature curing, *Constr. Build. Mater.* 100 (2015) 225-233. <https://doi.org/10.1016/j.conbuildmat.2015.09.042>.

37. P. Lawrence, M. Cyr, E. Ringot, Mineral admixtures in mortars: effect of inert materials on short-term hydration, *Cem. Concr. Res.* 33 (12) (2003) 1939-1947. [https://doi.org/10.1016/S0008-8846\(03\)00183-2](https://doi.org/10.1016/S0008-8846(03)00183-2).
38. R. Snellings, K.L. Scrivener, Rapid screening tests for supplementary cementitious materials: past and future, *Mater. Struct.* 49 (2016) 3265-3279. <https://doi.org/10.1617/s11527-015-0718-z>.
39. F. Avet, R. Snellings, A.A. Diaz, M.B. Haha, K. Scrivener, Development of a new rapid, relevant and reliable (R^3) test method to evaluate the pozzolanic reactivity of calcined kaolinitic clays, *Cem. Concr. Res.* 85 (2016) 1-11. <https://doi.org/10.1016/j.cemconres.2016.02.015>.
40. P. Suraneni, W.J. Weiss, Examining the pozzolanicity of supplementary cementitious materials using isothermal calorimetry and thermogravimetric analysis, *Cem. Concr. Comp.* 83 (2017) 273-278. <https://doi.org/10.1016/j.cemconcomp.2017.07.009>.
41. P. Suraneni, A. Hajibabae, S. Ramanathan, Y. Wang, J. Weiss, New insights from reactivity testing of supplementary cementitious materials, *Cem. Concr. Comp.* 103 (2019) 331-338. <https://doi.org/10.1016/j.cemconcomp.2019.05.017>.
42. E. Bacarji, R.D. Toledo Filho, E.A.B. Koenders, E.P. Figueiredo, J.L.M.P. Lopes, Sustainability perspective of marble and granite residues as concrete fillers, *Constr. Build. Mater.* 45 (2013) 1-10. <https://doi.org/10.1016/j.conbuildmat.2013.03.032>.
43. C. Argiz, M.Á. Sanjuán, E. Menéndez, Coal bottom ash for portland cement production, *Adv. Mater. Sci. Eng.* 2017 (2017) 6068286. <https://doi.org/10.1155/2017/6068286>.
44. F. Ameri, P. Shoaie, N. Bahrami, M. Vaezi, T. Ozbakkaloglu, Optimum rice husk ash content and bacterial concentration in self-compacting concrete, *Constr. Build. Mater.* 222 (2019) 796-813. <https://doi.org/10.1016/j.conbuildmat.2019.06.190>.
45. B.L. Damineli, V.M. John, B. Lagerblad, R.G. Pileggi, Viscosity prediction of cement-filler suspensions using interference model: a route for binder efficiency enhancement, *Cem. Concr. Res.* 84 (2016) 8-19. <https://doi.org/10.1016/j.cemconres.2016.02.012>.
46. Arkansas Department of Transportation. Standard specifications for highway construction. 2014. http://www.arkansashighways.com/standard_spec/2014/2014SpecBook.pdf.
47. ASTM C305-14, Standard Practice for Mechanical Mixing of Hydraulic Cement Pastes and Mortars of Plastic Consistency, ASTM International, West Conshohocken, PA, 2014.
48. ASTM C192/C192M-18, Standard Practice for Making and Curing Concrete Test Specimens in the Laboratory, ASTM International, West Conshohocken, PA, 2018.

49. J. Monical, C. Villani, Y. Farnam, E. Unal, J. Weiss, Using low-temperature differential scanning calorimetry to quantify calcium oxychloride formation for cementitious materials in the presence of calcium chloride, *Adv. Civ. Eng. Mater.* 5 (2) (2016) 142-156. <https://doi.org/10.1520/ACEM20150024>.
50. ASTM C109/C109M-16a, Standard Test Method for Compressive Strength of Hydraulic Cement Mortars (Using 2-in. or [50mm] Cube Specimens), ASTM International, West Conshohocken, PA, 2016.
51. P. Suraneni, J. Monical, E. Unal, Y. Farnam, C. Vilani, T.J. Barrett, W.J. Weiss, Performance of concrete pavement in the presence of deicing salts and deicing salt cocktails, Joint Transportation Research Program Publication No. FHWA/IN/JTRP-2016/25 (2016) pp. 1-19. <http://dx.doi.org/10.5703/1288284316350>.
52. ASTM C1872-18e2, Standard Test Method for Thermogravimetric Analysis of Hydraulic Cement, ASTM International, West Conshohocken, PA, 2018.
53. T. Kim, J. Olek, Effects of sample preparation and interpretation of thermogravimetric curves on calcium hydroxide in hydrated pastes and mortars, *Transp. Res. Rec.* 2290 (2012) 10-18. <https://doi.org/10.3141/2290-02>.
54. Y. Farnam, S. Dick, A. Wiese, J. Davis, D. Bentz, J. Weiss, The influence of calcium chloride deicing salt on phase changes and damage development in cementitious materials, *Cem. Concr. Comp.* 64 (2015) 1-15. <https://doi.org/10.1016/j.cemconcomp.2015.09.006>.
55. J. Monical, E. Unal, T. Barrett, Y. Farnam, W.J. Weiss, Reducing joint damage in concrete pavements: quantifying calcium oxychloride formation, *Transp. Res. Rec.* 2577 (2016) 17-24. <https://doi.org/10.3141/2577-03>.
56. P. Suraneni, V.J. Azad, O.B. Isgor, W.J. Weiss, Deicing salts and durability of concrete pavements and joints: mitigating calcium oxychloride formation, *Concr. Int.* 38 (4) (2016) 48-54.
57. AASHTO T 365-17, Standard Method of Test for Quantifying Calcium Oxychloride Amounts in Cement Pastes Exposed to Deicing Salts, AASHTO, Washington D.C., 2017.
58. T. Celik, K. Marar, Effects of crushed stone dust on some properties of concrete, *Cem. Concr. Res.* 26 (7) (1996) 1121-1130. [https://doi.org/10.1016/0008-8846\(96\)00078-6](https://doi.org/10.1016/0008-8846(96)00078-6).
59. AASHTO PP 84-20, Developing Performance Engineered Concrete Pavement Mixtures, American Association of State Highway and Transportation Officials, Washington D.C., 2020.
60. T. Oey, A. Kumar, J.W. Bullard, N. Neithalath, G. Sant, The filler effect: The influence of filler content and surface area on cementitious reaction rates, *J. Amer. Ceram. Soc.* 96 (6) (2013) 1978-1990. <https://doi.org/10.1111/jace.12264>.

61. A. Schöler, B. Lothenbach, F. Winnefeld, M.B. Haha, M. Zajac, H.-M. Ludwig, Early hydration of SCM-blended Portland cements: A pore solution and isothermal calorimetry study, *Cem. Concr. Res.* 93 (2017) 71-82. <https://doi.org/10.1016/j.cemconres.2016.11.013>.

4. Investigating Concrete Deterioration Due to Calcium Oxychloride Formation

Casey Jones^a, Prannoy Suraneni^b, W. Micah Hale^c

^a Graduate Research Assistant, Department of Civil Engineering, University of Arkansas, 4190 Bell Engineering Center, Fayetteville, AR 72701, United States of America.

^b Assistant Professor, Civil, Architectural, Environmental Engineering Department, University of Miami, 1251 Memorial Drive, Coral Gables, FL 33146, United States of America.

^c Professor and Chair, Department of Civil Engineering, University of Arkansas, 4190 Bell Engineering Center, Fayetteville, AR 72701, United States of America.

Corresponding author: Casey Jones

Abstract

Calcium oxychloride is a serious deterioration mechanism affecting concrete pavements. In order to mitigate calcium oxychloride deterioration in concrete, fly ash is used as partial cement replacement in conjunction with entrained air. Concrete specimens were stored in a 30% calcium chloride solution at 5 °C for 202 days. Following storage, specimens were evaluated through compressive and flexural strength loss along with mass change, length change, and chloride penetration. Results indicate that a partial cement replacement with 15% fly ash mitigates deterioration in concrete specimens when tested for flexural strength loss; however, 30% or more fly ash is needed for similar mitigation based on compressive strength. Further, results indicate that specimens cast with 6% entrained air outperform those without air entrainment. Class C fly ash generally mitigated strength loss to a greater extent than Class F fly ash.

Keywords: Calcium oxychloride; Compressive strength; Flexural strength; Mass change; Length change; Silver nitrate

4.1. Introduction

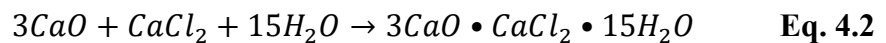
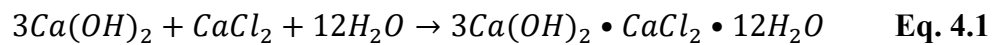
4.1.1. Background

In North America, the choice of freight transportation is most commonly done through the use of truck transit with approximately 63% of goods moved by this method [1]. In addition to truck transit, pavements are also heavily used by commuters – in October of 2020, in the US, nearly 260 billion vehicle miles were recorded [2]. With such a high percentage of freight and commuters relying upon roadways, it is critical that engineers develop pavements designed to withstand continual use. Further, it is now imperative that highways and interstates be available even in the most extreme weather conditions, including snow and ice. More than 70% of the roadways in the U.S. are built in regions receiving more than 13 cm of snow annually [3]; however, these thoroughfares are often needed during winter weather. Therefore, engineers are tasked with developing durable pavement solutions able to withstand changing traffic counts as well as survive harsh winter weather.

To mitigate snow and ice accumulation on pavement surfaces during winter weather, chloride-based deicing salts are often employed [4]. Sodium chloride (NaCl) is the most commonly used and traditionally cheapest material to mitigate winter weather accumulation on pavement surfaces; however, it is less effective as the temperature drops below $-12\text{ }^{\circ}\text{C}$ [5]. For adverse weather, where NaCl is rendered ineffective to preserve safe driving conditions, materials such as calcium chloride (CaCl_2) and magnesium chloride (MgCl_2) may be required to maintain safe passage. However, these materials have been shown to react with portions of the cementitious

paste in concrete causing the formation of a deleterious phase known as calcium oxychloride (CAOXY) [6,7].

CAOXY occurs when CaCl_2 [6,7,8] or MgCl_2 [9,10] reacts with calcium hydroxide (Ca(OH)_2) in the cementitious paste [11,12]. The phase believed responsible for damage in concrete joints is given in **Eq. 4.1** [13] but is sometimes reported as shown in **Eq. 4.2** [6,8]. It should be noted that minor phase variations (due to water content) have also been reported [9,10,14]. This reaction has been shown to deteriorate cementitious paste [15,16,18,19,19], mortar [8], and concrete [7,9,10,12,20,21]; however, as discussed in Jones et al. [22], specimen type (i.e. paste, mortar, and concrete), may influence observed deterioration. For instance, Suraneni et al. [19] found that an increase in the water to cementitious materials ratio (w/cm) increases CAOXY levels in paste, while Collepari et al. [7] found reduced CAOXY damage in concrete specimens with a w/cm of 0.60 compared to similar specimens cast with w/cm values of 0.40 and 0.50. Though it is still unclear exactly why these differences occur, it has been suggested that variations in transport properties, air content, and the introduction of aggregates could cause different levels of deterioration between various specimen types [22].



The use of supplementary cementitious materials (SCM) [7,15,18,19,23,24,25] and entrained air/quality air void system [26,27] have shown promise for mitigating CAOXY deterioration in concrete. Therefore, this study seeks to prevent/mitigate CAOXY deterioration in portland cement concrete pavement (PCCP) specimens using SCMs in conjunction with entrained air.

4.1.2. Need for Research

CAOXY deterioration is typically observed in the jointing regions where localized deposition of deicing materials may occur [13,21]. In order to prolong the life of concrete pavements, each deterioration mechanism that attacks PCCP must be clearly understood. While research has investigated CAOXY [7,8,15], continued examination is required in order to mitigate its destructive presence in concrete. This research investigates PCCP with and without fly ash in conjunction with air entrained (AE) and non-air entrained (NAE) specimens. Very limited work exists where effects of both fly ash and air entrainment on CAOXY formation and damage have been investigated. Previous research [7] focused on compressive strength reduction due to CAOXY formation; however, in this investigation compressive strength and flexural strength specimens are both investigated. To the authors knowledge, this is the first work to investigate flexural strength loss in concrete deteriorated by CAOXY formation. This is a significant advancement as pavements are subjected to significant flexural loading. A correlation between deteriorated compressive strength and flexural strength specimens is provided which is expected to help in prediction of strength loss in field concrete impacted by CAOXY. Further, mass change, length change, and chloride penetration are collected in order to corroborate the strength measurements and to better explain damage mechanisms.

4.2. Materials and Methods

4.2.1. Materials and Mixture Design Development

To investigate CAOXY deterioration in concrete pavements, specimens were designed in accordance with the Arkansas Department of Transportation (ARDOT) PCCP specification [28]. Design requirements for these mixtures are provided in **Table 4.1**. It should be noted that the use of SCMs in a PCCP mixture is at the discretion of the state and that SCMs are not always

employed for PCCP placement. Therefore, mixture designs were developed with and without the use of SCM (specifically fly ash).

Table 4.1. PCCP prescriptive requirements developed from [28].

Design standards	Prescriptive requirements
Minimum compressive strength, MPa	28
Minimum cementitious content, kg/m ³	335
Maximum Class C or F fly ash level, % (mass)	20
Maximum slag level, % (mass)	25
Maximum w/cm	0.45
Slump range, mm	25 - 50
Air content, %	6 ± 2

For this research, a Type I/II portland cement was utilized in conjunction with a Class C and Class F fly ash (ASTM C618 [29]). A chemical analysis utilizing ASTM C114 [30] was conducted on the cement while ASTM C311 [31] was used to determine the chemical composition of each fly ash. Results from these analyses are provided in **Table 4.2**. Cement was replaced with fly ash on a mass basis at 0, 15, 30, and 45% levels. It should be noted that a mass replacement was chosen in order to represent typical field incorporation of fly ash in concrete mixture designs in accordance with ARDOT specifications [28]. While the **Table 4.1** requirement limits cement replacement with fly ash to 20% (mass), AASHTO PP 84 [32] specifies a minimum of 30% (mass) fly ash for protection against CAOXY in concrete. Therefore, this research investigated PCCP mixtures with up to 45% (mass) cement replacement with fly ash to determine the impact of relatively high volumes of fly ash on CAOXY mitigation in PCCP mixtures. The maximum PCCP water to cementitious materials ratio (w/cm) of 0.45 was held constant for specimen development. It has been shown by Suraneni et al. [19] that a higher w/cm leads to increased CAOXY levels in cementitious paste. Therefore, the maximum w/cm per **Table 4.1** is used for this investigation in order to simulate a worst-case scenario for pavement deterioration.

Table 4.2. Chemical analysis of the cement and each fly ash (Bulk oxides given as % mass).

Oxide	Cement	Class C fly ash	Class F fly ash
SiO ₂	20.25	34.57	56.25
Al ₂ O ₃	4.54	20.26	18.91
Fe ₂ O ₃	4.20	5.69	9.59
CaO	63.73	26.47	7.61
MgO	0.91	4.85	1.88
SO ₃	3.09	1.73	1.47
Na ₂ O	0.16	1.60	1.27
K ₂ O	0.54	0.50	2.61
LOI	2.53	0.58	0.50
Specific gravity	3.15	2.58	2.40

The coarse aggregate was a 25 mm crushed limestone material with a specific gravity of 2.57 and an absorption of 2.40%. While this absorption content is higher than typically reported for limestone, it should be noted that intermixed at the quarry in the limestone aggregate is a portion of hard, quality chert and soft, weathered chert. The weathered chert by itself can be considered to be a lightweight aggregate, as it has high absorption values (> 7%). To account for this material in the air content measurements, an aggregate correction factor of 1.2%, as established in Schrader [33] is applied to determine the final air content. The fine aggregate was a 9.5 mm Arkansas River sand with a specific gravity of 2.63 and an absorption content of 0.55%. Using these values and the **Table 4.1** requirements, volumetric concrete mixture designs were developed and are provided in **Table 4.3**.

Table 4.3. Concrete mixture designs (Materials given in kg/m³).

Batch ID	Name	Cement	Fly ash	Rock	Sand	Water	Air*	AEA†	w/cm
1	PC-AE	335	0	949	822	151	6.0%	31	0.45
2	FACC-15AE	284	50	949	813	151	6.0%	67	0.45
3	FACC-30AE	234	100	949	804	151	6.0%	113	0.45
4	FACC-45AE	184	151	949	795	151	6.0%	187	0.45
5	FACF-15AE	284	50	949	809	151	6.0%	35	0.45
6	FACF-30AE	234	100	949	796	151	6.0%	42	0.45
7	FACF-45AE	184	151	949	783	151	6.0%	35	0.45
8	PC-NAE	335	0.0	949	928	151	2.0%	0	0.45
9	FACC-15NAE	284	50	949	918	151	2.0%	0	0.45
10	FACC-30NAE	234	100	949	909	151	2.0%	0	0.45
11	FACC-45NAE	184	151	949	900	151	2.0%	0	0.45
12	FACF-15NAE	284	50	949	915	151	2.0%	0	0.45
13	FACF-30NAE	234	100	949	901	151	2.0%	0	0.45
14	FACF-45NAE	184	151	949	888	151	2.0%	0	0.45

*Design air contents are 6% air volume for each AE mixture and 2% air content for NAE mixtures; actual measured values are shown in **Table 4.4**.

†AEA given in ml/cwt. Given the minor AEA levels utilized, the volume of admixture was not accounted for in mixture design development.

4.2.2. Mixing and Casting Specimens

Aggregate was sampled a minimum of 1-day prior to batching to determine moisture content.

Free moisture on the aggregate surface was accounted for in the mixing water based on saturated surface dry (SSD) aggregate. In general, at the time of batching, most measured aggregate moisture contents were above SSD. Concrete was mixed in accordance with ASTM C192 [34] and then discharged from the mixer for appropriate testing and molding of specimens.

Testing of the fresh concrete properties commenced by taking the unit weight of each sample in accordance with ASTM C138 [35]. Immediately following the unit weight measurement, the air content was determined in general accordance with ASTM C231 [36]. These tests were conducted first in order to determine if the concrete for batch IDs 1 - 7 met the **Table 4.1** air requirement prior to use for testing, and samples were discarded if the requirement was violated.

For this research, a super air meter (SAM) rather than a traditional Type A or B air meter as

specified in ASTM C231 [36] was used; however, an analysis of the SAM data is not made in this work as the effects of lightweight aggregates on SAM data are not completely clear. Further investigations using the SAM meter are in progress. While the prescribed **Table 4.1** air content requirement was 4 - 8%, recorded values were maintained within a much closer grouping (4.8 – 5.2%) in order to minimize strength and permeability differences between mixtures. This close range of air content also means that in the air entrained mixtures, the effect of varying fly ash replacement dominates the effects of variations in air content when considering CAOXY damage. Using ASTM C143 [37], the slump of each mixture was tested. It should be noted that with higher cement replacements with fly ash, slump values above the **Table 4.1** requirements were measured; however, samples were used “as is” in order not to lower/change the w/cm. Temperature was measured in accordance with ASTM C1064 [38]. Fresh concrete property data are given in **Table 4.4**.

Table 4.4. Plastic property data for each concrete mixture. Air contents are corrected for aggregate effects.

Batch ID	Name	Temperature (°C)	Slump (mm)	Air (%)	Unit weight (kg/m³)
1	PC-AE	23.5	45	4.9	2255
2	FACC-15AE	16.5	50	4.8	2243
3	FACC-30AE	21.5	55	4.7	2244
4	FACC-45AE	23.5	50	4.9	2235
5	FACF-15AE	25.0	30	4.7	2262
6	FACF-30AE	22.0	45	5.1	2227
7	FACF-45AE	15.0	75	5.1	2231
8	PC-NAE	30.0	40	2.0	2307
9	FACC-15NAE	19.5	30	1.7	2326
10	FACC-30NAE	22.0	40	1.3	2321
11	FACC-45NAE	23.0	70	1.1	2321
12	FACF-15NAE	20.0	30	2.3	2302
13	FACF-30NAE	19.0	45	2.0	2293
14	FACF-45NAE	23.0	75	1.4	2294

Following testing of the fresh concrete, nine 100 mm x 200 mm cylinders, six 100 mm x 100 mm x 405 mm beams, and three 100 mm x 100 mm x 285 mm length change prisms were cast. The cylindrical specimens were capped to prevent moisture loss immediately following molding,

while the beams and prisms were covered with polyethylene sheeting and wet towels. Specimens were stored in an environmental chamber at 23 ± 2 °C with a relative humidity of $50 \pm 4\%$ for approximately 24-hours. Specimens were subsequently demolded and stored in a limewater bath in accordance with ASTM C511 [39].

4.2.3. Specimen Storage and Testing

Specimens were continuously stored in the limewater bath for 90 days. Work by Collepari et al. [7] investigated CAOXY deterioration in concrete at a similar age. By curing the specimens longer than 28 days, an increased resistance to CAOXY deterioration is expected as $\text{Ca}(\text{OH})_2$ reacts with fly ash in a pozzolanic reaction [7,18]. At 91 days of age, specimens were removed from the limewater bath, and the surfaces were scrapped/brushed with a wire brush, and rinsed to remove free lime. Compressive strength (ASTM C39 [40]) and flexural strength (ASTM C78 [41]) were recorded at 91 days. Three specimens were tested for each measurement with the average reported. These values are the basis from which deterioration is determined for specimens stored in a CaCl_2 solution. Following removal of free lime, the remaining specimens were placed in a 30% mass CaCl_2 solution. The liquid-to-solid ratio (L/S) somewhat varied for the different specimens due to the nature of the large specimens and substantial differences in their sizes. Flexural strength beams were stored in solution with a L/S of 0.7 while compressive strength specimens and length change prisms were stored in solution with a L/S of 1.0 and 1.2, respectively. Once in solution, the specimens were stored at “room temperature” (approximately 20 °C) for 2-weeks. This allows for diffusion of chloride ions into the concrete prior to storage in a cold solution in order to accelerate deterioration. A similar procedure was established by Collepari et al. [7] except that a 2-week storage temperature of 40 °C was used; however, more recently, Mori et al. [42] utilized a “room “temperature” environment for paste specimens. It has

been shown that CAOXY is stable in a 30% CaCl₂ solution up to nearly 50 °C [15,25] and CAOXY crystals were observed on PC-AE and PC-NAE specimens prior to storage in a 5 °C environment. It is the authors opinion that a “warm” storage solution prior to a cold storage is likely not needed for “accelerated” CAOXY deterioration and this step could be omitted in future research. When sufficient solution volume is present, a 30% CaCl₂ solution is typically sufficiently aggressive to ensure rapid damage in a 5 °C storage environment unless the mixture has relatively large contents of SCMs and entrained air.

At the end of the 2-week storage at approximately 20 °C, specimens were placed in a 5 °C environment for 24-hours. At this time, initial mass and length change (ASTM C157 [43]) measurements were collected. Storage in solution prior to initial measurements mitigated error caused by temperature differentials. Subsequent data were compared to these values in order to determine deterioration. For mass measurements, specimens were dried with paper towels to a surface dry condition similar to SSD for aggregates. It should be noted that consistent “surface dry” measurements were difficult to obtain due to the deicing salt solution and seepage of solution was noted in heavily deteriorated samples. A similar methodology was applied by Traore et al. [19] for cementitious pastes. It should be noted that the test methodology originally called for mass and length change measurements every two weeks; however, due to COVID-19 restrictions, consistent measurements over time were unable to be acquired. Therefore, data are shown as ultimate mass and length change in **Section 4.3**.

After approximately 202 days in cold storage, severe deterioration of several specimens containing no fly ash was noted. Therefore, the test was ended and subsequent specimens tested for compressive strength, flexural strength, mass change, and length change. It should be noted that some studies have replaced the storage solution during testing [42] while others have left the

solution “as is” for the duration of storage [7]. This investigation followed the precedent of Collepardi et al. [7] leaving the solution “as is” during specimen storage. A potential exists for the observation of greater damage with consistent solution replacement; however, in this study, consistent solution replacement would have needed thousands of liters of solution, and is therefore impractical. No current procedures are established for storing concrete specimens in CaCl_2 solutions and solution replacement to observe CAOXY deterioration.

Following testing of the flexural strength samples, the cross section of each specimen was sprayed with a 0.1 N silver nitrate (AgNO_3) solution. The AgNO_3 reacts with chloride in the concrete causing a white precipitant. This precipitant provides a visual analysis of the depth of chloride penetration within each specimen. A penetration depth measurement was taken on each side of the cross section using a Starrett caliper. The measurements were averaged in order to compute the average chloride penetration depth for each sample. A similar methodology was employed in Mori et al. [42] to determine chloride depth. Also, following the final mass change measurement, specimens were rinsed with water to remove unsound concrete from the external surface of each sample. No wire brushing or mechanical action was applied during this process. Specimens were then dried to a similar external dry surface and reweighed in order to determine the net mass of sound concrete. This provided a pre- and post-wash mass measurement for data analysis.

4.3. Results and Discussion

4.3.1. Visual Observations

Though visual observations offer somewhat limited value when discussing deterioration in concrete specimens, a few important points were noted during testing. First, needlelike diaphanous CAOXY crystals were present on the exterior surface of nearly every concrete

specimen tested regardless of fly ash or air content level. Similar exterior diaphanous CAOXY crystals were reported by Sutter et al. [10] and Ghazy and Bassuoni [14] on concrete specimens exposed to CaCl_2 solutions. Though CAOXY crystals were observed on the exterior surface of the 45% fly ash specimens, little damage was recorded (see **Sections 4.3.2 – 4.3.5**). This could indicate that the combination of fly ash and entrained air mitigated damage even though some crystal formation was present. The second observation was that some of these needlelike prismatic crystals were near 20 mm in length as observed in **Fig. 4.1**. Others have reported diaphanous shaped crystals of “several” millimeters in length [14] on the exterior surface of specimens stored in solution for 2 weeks. Given that the current experiment stored specimens for 202 days, longer storage could account for potential increase in the crystal size on the surface of the specimens.

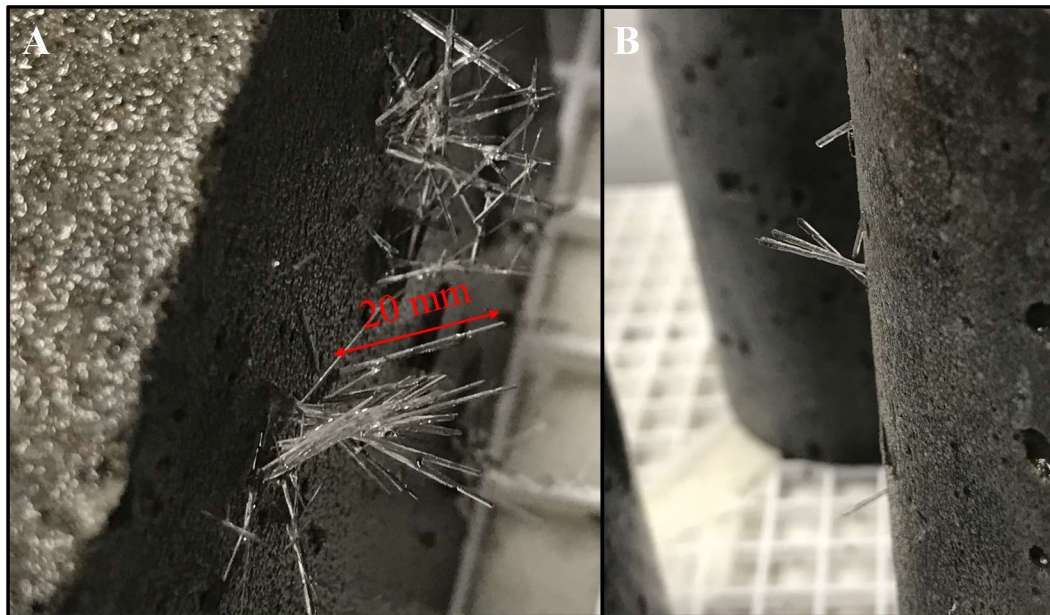


Figure. 4.1. Exterior CAOXY crystal formation in concrete cast with 45% Class C fly ash: A) flexural strength beam (100 mm x 100 mm x 405 mm), B) cylindrical specimen (100 mm x 200 mm).

4.3.2. Concrete Strength

4.3.2.1. Compressive Strength

While compressive strength deterioration in concrete due to deicing salt deterioration has been documented by Collepardi et al. [7], less research has focused on determining the impact of entrained air in aiding strength deterioration. It is known that the addition of SCMs such as fly ash can increase concrete resistance to deicing salt deterioration [7,13,14]. Therefore, in this work, critically, the impacts of entrained air and varying amounts of fly ash are investigated. Presented in **Fig. 4.2** are the 91-day compressive strength data for each concrete mixture based on fly ash level following curing. Error bars above and below each datum represent one standard deviation in the set of three specimens. It is shown from **Fig. 4.2** that NAE specimens provide higher compressive strength than AE concrete prior to submersion in a CaCl_2 solution which is in good accordance with the literature [44]. The Class C fly ash performs better than the Class F fly ash. Various factors affect strength development with fly ashes and the reasons behind the strength differences seen are not totally clear [45]; however, the fly ashes used for this work were also apart of another investigation [33]. In Schrader [33], numerous fly ashes were tested for their specific surface area using Brunauer-Emmett-Teller (BET) testing. Though BET analysis is outside the scope of this present work, the specific surface area of the Class C fly ash is $2.866 \text{ m}^2/\text{g}$ while the specific surface area of the Class F fly ash is $0.907 \text{ m}^2/\text{g}$. The Class C fly ash has more than 3 times the specific surface area of the Class F fly ash; therefore, the increased strength in the Class C results could be due to the increased specific surface area available for reaction with the cement hydrates.

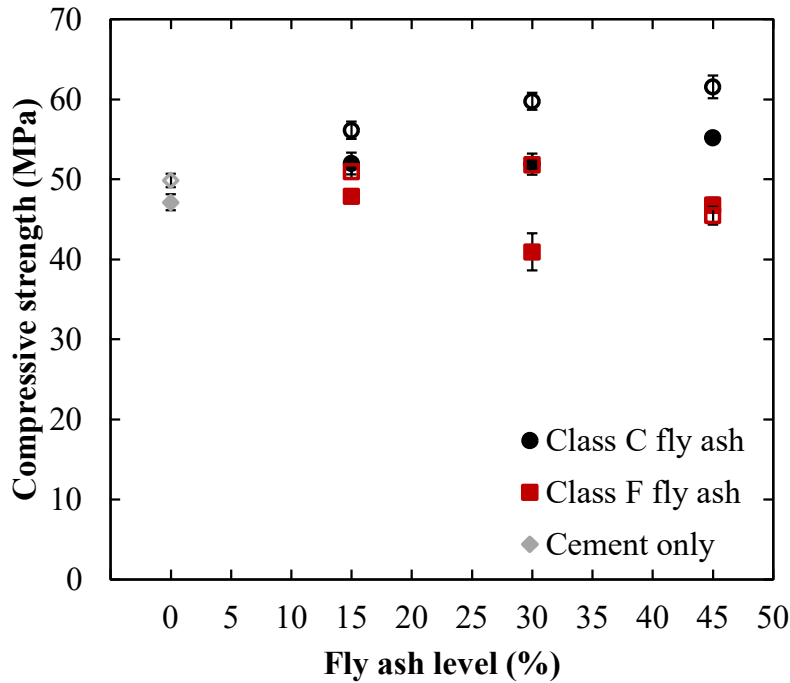


Figure 4.2. Compressive strength data for each concrete mixture following 90 days of curing in a limewater bath. Hollow markers represent NAE specimens while filled markers represent AE specimens.

In order to quantify deterioration, data from **Fig. 4.2** were compared with similar specimens tested for strength after storage in a 30% CaCl_2 solution stored in a 5 °C environment. Data showing the difference in strength for both NAE and AE concrete specimens stored in a 30% CaCl_2 solution are presented in **Fig. 4.3**. It should be noted that the cement only specimens were unable to be tested due to heavy external deterioration rendering the specimens unusable as shown in **Fig. 4.4**; however, a “core” of solid concrete was present in some of these specimens. Therefore, both NAE and AE cement only specimens are shown as having 100% strength loss due to exposure to a 30% CaCl_2 solution. Following storage in a 30% CaCl_2 solution, the standard deviation between sets of specimens increased compared to sets cured in limewater. The largest coefficient of variation (COV) was 23% (Batch ID 12); however, the remaining concrete specimens recorded a COV less than 7.2%.

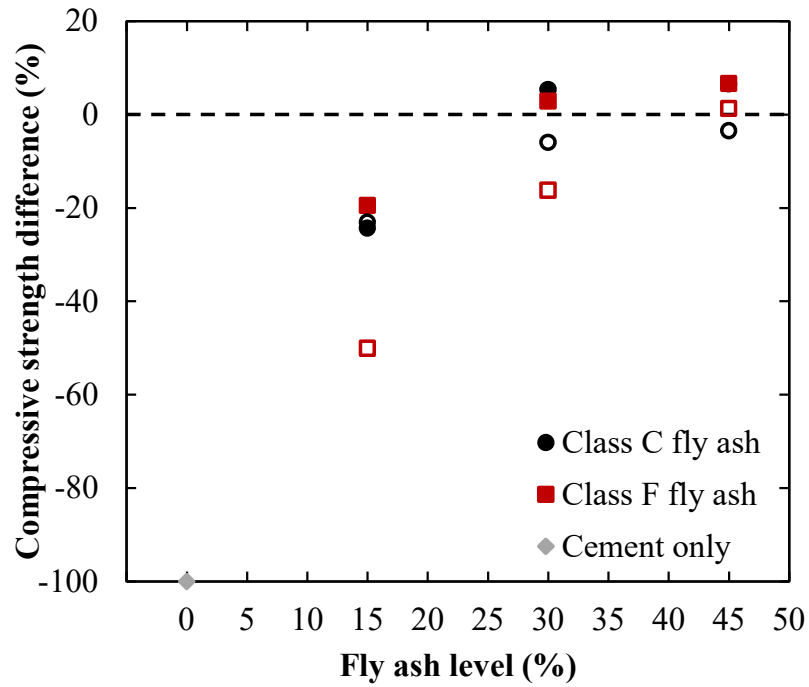


Figure. 4.3. Compressive strength difference based on fly ash level in NAE (hollow markers) and AE (filled markers) concrete specimens.

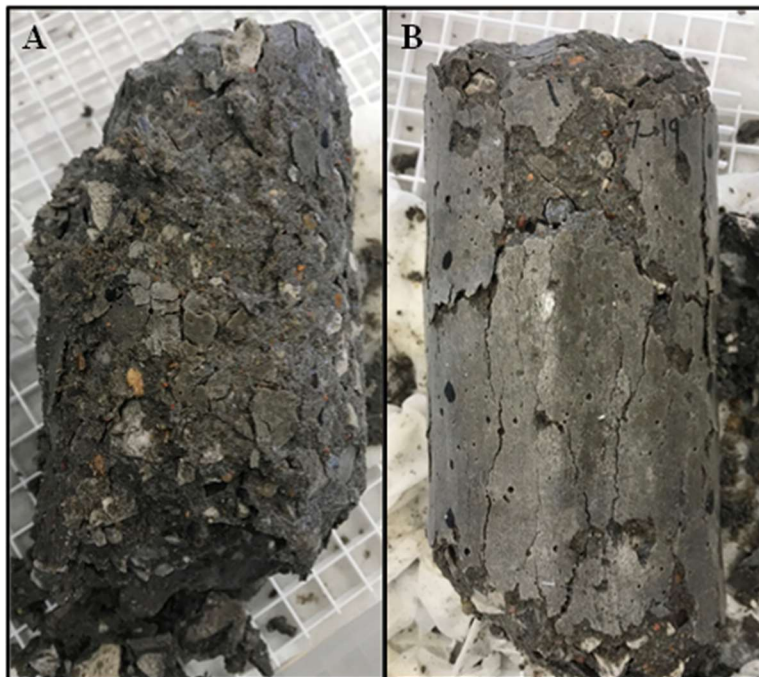


Figure. 4.4. Deteriorated cylindrical compressive strength specimen following storage in a 30% mass CaCl_2 solution at 5 °C: A) cement only NAE concrete, B) cement only 4.9% AE concrete.

From **Fig. 4.3**, it is shown that a 50% compressive strength loss occurred in the 15% NAE Class F fly ash specimens while only a 23% strength loss occurred in similar Class C specimens. For similar AE concrete, a 19 and 24% strength loss occurred, respectively. At 30% cement replacement with fly ash, a 16% compressive strength loss occurred in the NAE Class F fly ash specimens while a 6% strength loss occurred in similar Class C specimens. Though these changes in compressive strength are “relatively” small compared to the cement only and 15% fly ash specimens, this is a larger decrease in compressive strength when compared to similar AE specimens. The AE specimens cast with 30% fly ash (both Class C and F) had improved strength following storage in a 30% CaCl_2 solution along with most of the specimens cast with 45% fly ash. These findings suggest that the presence of air and fly ash clearly aid in mitigating CAOXY deterioration. The results from this work are in good agreement with data from Collepari et al. [7] who found limited impact on compressive strength of concrete specimens cast with 6% entrained air and 30% fly ash when stored in a 30% mass CaCl_2 solution for 300 days. These results also suggest that there was limited impact on CAOXY damage mitigation based on fly ash type (i.e., Class C or F) in AE concrete.

In this dataset, the 45% fly ash specimens did not exhibit noticeable damage. This finding suggests that 45% (mass) cement replacement with fly ash is sufficient to mitigate CAOXY irrespective of air content following these storage conditions; however, 30% fly ash with 6% air content was sufficient to mitigate damage. Further research is needed to correlate laboratory storage conditions with field exposed concrete in order to establish laboratory procedures able to predict field performance. It is also interesting to note that for both the 15 and 30% fly ash specimens, the Class C fly ash concrete outperformed the Class F fly ash concrete. It is unclear why the Class C fly ash performed better in this case, and further testing is needed to evaluate

whether this finding is generally true for other fly ashes. There is a possibility that if the storage duration was prolonged similar deterioration levels between the Class C and F fly ash specimens may be observed.

When entrained air is not present in concrete (i.e., entrapped air only), the level of CAOXY protection is significantly reduced. It should be noted that an increase in storage time or consistent replacement of the CaCl_2 solution during could impact these results, specifically, increased damage could be observed in NAE and/or low fly ash specimens. In the absence of consistent solution replacement, damage rates may slow as equilibrium is approached. While visual assessments of equilibrium are non-trivial, excessive precipitation was not observed in the solutions in this study. However, since solubility information for CAOXY is not available, consistent solution replacement regimens cannot be formulated at this time. The lack of solution replacement could explain the rather limited damage seen in the 15% and 30% fly ash NAE specimens – considering that a significant amount of CAOXY can form under such conditions [14], substantial damage would be expected when there is no air entrainment. Alternatively, the limited damage could be because the lightweight chert aggregates (which comprise a portion of the coarse aggregates) provide space which can accommodate the expansion caused by CAOXY formation. While the effect of lightweight aggregates on CAOXY mitigation is unknown, similar effects are known to occur in alkali-silica reaction damage mitigation [46].

4.3.2.2. Flexural Strength

Given the numerous properties correlated with concrete compressive strength, there is value in determining the impact of deicing materials on compressive strength; however, the majority of deicing salt/CAOXY damage is relevant to concrete pavements where flexural strength is of greater importance. Therefore, an investigation into the impact of CAOXY on concrete flexural

strength has been conducted. To the authors' knowledge this is the first investigation into flexural strength loss of concrete specimens due to CAOXY deterioration. Similar to compressive strength, the flexural strength data is divided into NAE and AE concrete. Presented in **Fig. 4.5** are data showing the strength of both the NAE and AE concrete flexural strength specimens following curing in limewater for 90 days. Similar to compressive strength, it is observed that NAE specimens are slightly stronger than AE specimens. On average, a 6.1% strength increase is observed in the NAE specimens compared to the AE specimens. This provides an average decrease in flexural strength of 1.9% for each percent of additional air in the mixtures.

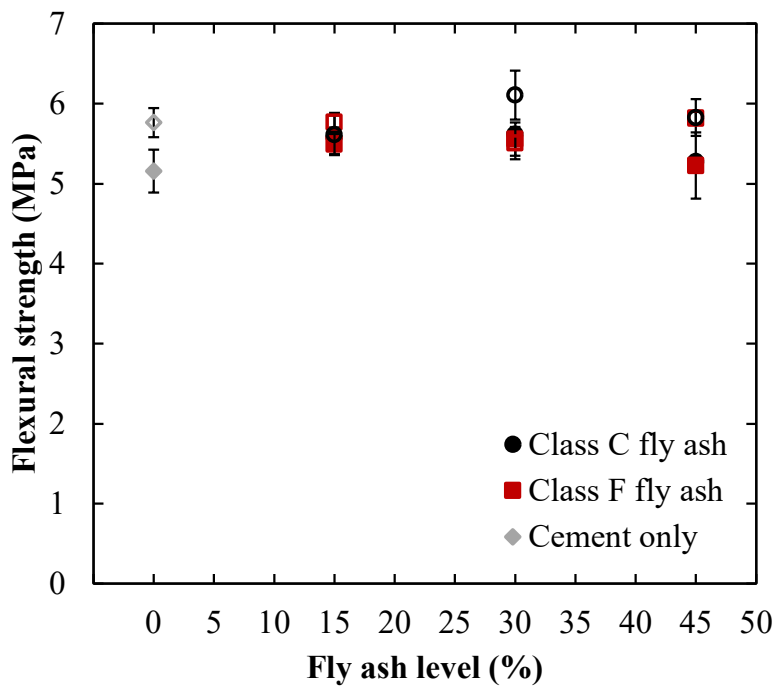


Figure. 4.5. Flexural strength data for each concrete mixture following 90 days of curing in a limewater bath. Hollow markers represent NAE specimens while filled markers represent AE specimens.

Data presented in **Fig. 4.6** shows the flexural strength difference after testing specimens stored in a 30% CaCl_2 solution for 202 days. Similar to the compressive strength specimens, the cement

only concrete was heavily deteriorated regardless of air content. Several of the NAE and AE cement only specimens fractured into two pieces approximately 130 mm from the outer edge along the length of the sample. For NAE specimens cast with 15% Class C fly ash, almost no deterioration is observed; however, those cast with 15% Class F fly ash had flexural strength loss of 47%. It is interesting that similar strength loss was observed in the NAE 15% Class F fly ash specimens tested in compressive strength. For NAE specimens cast with 30 and 45% fly ash, little impact is observed in the Class F specimens while flexural strength increases of 11 and 26% were observed in the Class C specimens. The largest recorded COV for flexural strength specimens tested following storage in 30% CaCl₂ solution was 12.2%; however, most specimens had a COV of less than 10%.

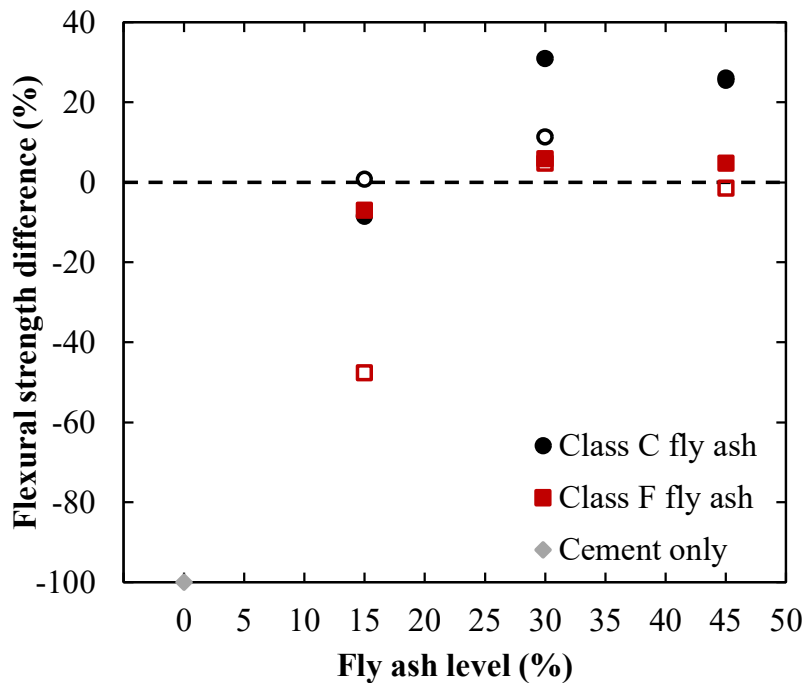


Figure 4.6. Flexural strength difference based on fly ash level in NAE (hollow markers) and AE (filled markers) concrete specimens.

In general, for the flexural strength specimens, strength loss is reduced compared to the compressive strength results in **Section 4.3.2.1**. For instance, the AE compressive strength

specimens had approximately 20% compressive strength loss at a 15% fly ash level while similar flexural strength specimens had minimal strength loss at 7%. It should be noted that specimen size may impact these results. The volume of a compressive strength cylinder is 1600 cm³ while a flexural strength specimen is 4000 cm³. This gives a compressive to flexural strength specimen size ratio of 0.4. When comparing similar strength loss as noted above for the 15% fly ash level specimens, a compressive to flexural strength loss ratio of 0.35 is determined. This is evidence that specimen size may impact/govern observed deterioration during testing. Given that flexural specimens are more than double the size of the compressive strength specimens, there is an opportunity that less damage occurs due to the larger specimen size, when tested at the same duration of exposure. Similar to the compressive strength results, the Class C specimens outperformed the Class F fly ash specimens at 30 and 45% cement replacement. Previous work on cement paste has suggested that damage in cement pastes is seen even at 50% fly ash replacement [19]; however, this work suggests that with the combination of aggregates and entrained air, SCMs, such as fly ash, can be used in reduced quantities (15-30%) with effective protection from CAOXY deterioration for concrete pavements. However, the large number of variables associated with concrete testing implies that further testing is needed before exact replacement levels can be identified for a range of exposure scenarios.

4.3.2.3. Correlation of Compressive and Flexural Strength

The correlated compressive and flexural strength relationship (for SI units) provided in ACI 318 [47] for normal weight concrete is given in Eq. 4.3. Data shown in Fig. 4.7 indicates that the current correlation is not adequate to estimate correlated strength loss due to CAOXY deterioration; however, it should also be noted that specimens tested for strength prior to deicing salt exposure also did not follow the ACI prediction. On average, flexural strength was measured

to be more than 26% greater than predicted based on compressive strength at 91-days. For the deteriorated specimens, a linear relationship better details the correlation and is given in **Eq. 4.4**. To develop **Fig. 4.7**, the NAE and AE specimens were first plotted separately; however, the correlations of both sets were similar. The AE concrete had a slope of 0.119 with a R^2 of 0.95 while the NAE concrete had a slope of 0.125 with a R^2 of 0.99. Given the close similarities, **Fig. 4.7** was developed using all specimens in the investigation with a trendline characterized as a black dashed line. The combined fit has a slope of 0.122 with a R^2 of 0.97. The ACI 318 [47] normal weight concrete correlation overestimates flexural strength at lower compressive strength levels, but underestimates flexural strength once the compressive strength is above approximately 30 MPa. This important correlation could be used to help better understand the impact of concrete pavements subjected CAOXY deterioration.

$$f'_{ct} = 0.62\sqrt{f'_c} \quad \text{Eq. 4.3.}$$

f'_{ct} = Estimated flexural strength (MPa)

f'_c = Measured compressive strength (MPa)

$$y = 0.122x + 0.1328 \quad \text{Eq. 4.4.}$$

y = Flexural strength (MPa)

x = Compressive strength (MPa)

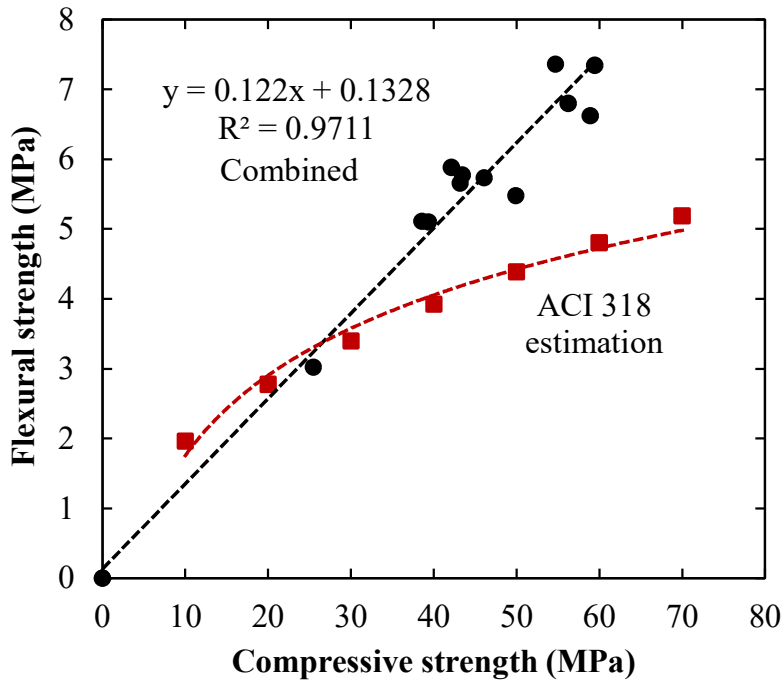


Figure. 4.7. Correlation of compressive and flexural strength in CAOXY deteriorated samples.

4.3.3. Mass Change

Another method to determine the impact of CAOXY on concrete pavements is to measure the mass change of the specimens. Mass change aids in determining the overall infiltration of the deicing solution into the concrete. In paste specimens, it has been shown that up to 40% strength loss may occur without changes in the specimen mass [19]. For concrete, the influence of aggregates and air may impact these results. Presented in **Fig. 4.8** are the mass change results for the NAE and AE concrete specimens. It should be noted that data are not delineated based on Class C or Class F fly ash as in the strength specimens, but are separated based on pre- and post-wash measurements. Also, along the Y-axis of **Fig. 4.8**, mass change in the positive direction is considered mass loss while negative is mass gain. It is shown that the cement only specimens are most impacted when measuring mass change for both NAE and AE concrete. This correlates well with the strength results. It is also interesting to note that even though heavy deterioration

occurs in the cement only specimens (as observed in **Fig. 4.4**), the pre-wash mass change is 33% for the NAE concrete while only 3% for the AE specimens. While crumbling of the specimen due to the heavy deterioration is observed, absorption of solution into the specimen offsets some of the corresponding mass loss. However, when washed, this unsound exterior is easily removed. Therefore, the washed results are the better proxy for use to determine the impact of CAOXY deterioration.

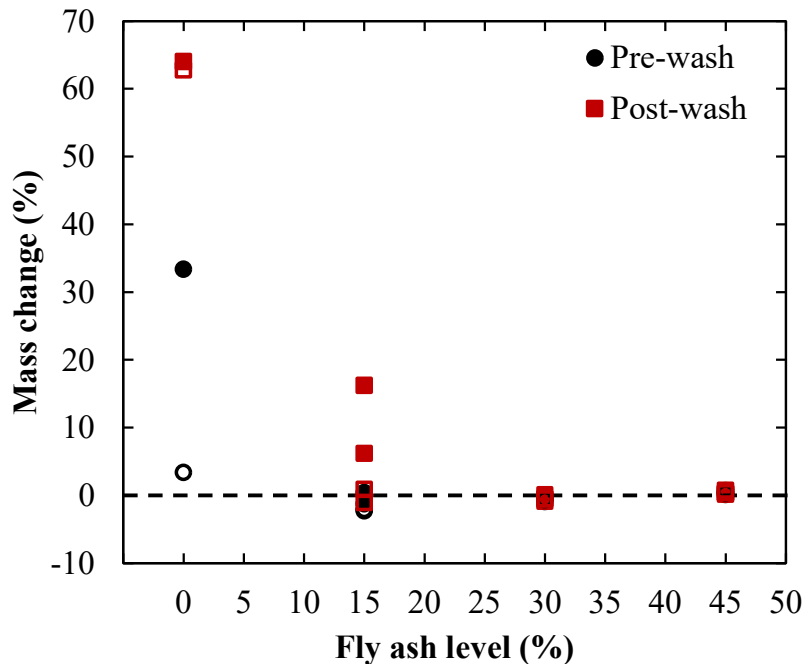


Figure. 4.8. Mass change data based on fly ash level for NAE (filled markers) and AE (hollow markers) concrete specimens.

For concrete cast with 15% fly ash (mass), NAE specimens do exhibit some mass loss at 6 and 16% for the Class C and Class F fly ash, respectively; however, when combined with 6% air no mass change in recorded. While the pre-wash 15% fly ash (mass) specimens show minor change in mass, the post-wash specimens indicate that material was removed during the rinsing process. As shown in the compressive (**Fig. 4.3**) and flexural strength (**Fig. 4.6**) NAE specimen data, deterioration is more prevalent than in AE concrete. This is likely due to a reduction of

deposition locations for the expanding CAOXY phase. Though the material does not flake as heavily as the cement only specimens, the unsoundness of the outer layer in the 15% fly ash (mass) NAE specimens is characterized by mass loss following washing. The 30 and 45% fly ash (mass) specimens exhibit minimal change in mass for either condition. Presented in **Fig. 4.9** are the compressive and flexural strength difference compared to the percentage of mass change in the post-wash specimens when grouped by fly ash level. While it is expected that little mass change would be observed when strength is increased, it is also revealed that mass change is not impacted up to a 24% compressive strength loss and an 8% flexural strength loss for both NAE and AE specimens; however, above this deterioration level, the NAE specimens had 16% mass loss at 50% compressive strength loss with similar results recorded for the flexural specimens. It appears that flexural strength difference correlates closer with the mass change data than compressive strength; however, given the differences, mass change is likely not the best proxy to determine damage (based on strength) in CAOXY deteriorated specimens. While the strength loss prior to mass change is lower in these concrete specimens, work by Traore et al. [19] observed a 40% loss in compressive strength prior to measurable mass changes in cementitious paste specimens.

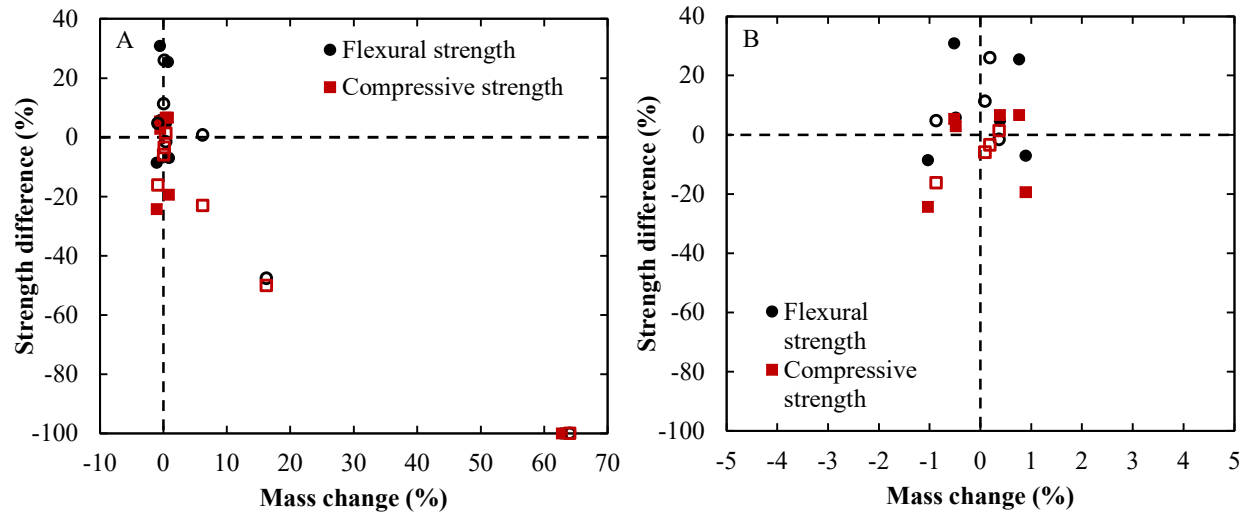


Figure. 4.9. Comparison of mass change percentage and strength difference in CAOXY deteriorated concrete specimens with hollow markers indicating NAE specimens while filled markers are AE specimens: A) all specimens, B) specimens near 0% mass change.

4.3.4. Silver Nitrate

While chloride penetration is a not proxy for determining CAOXY deterioration, it can be used to determine the infiltration depth of the chloride solution in concrete. This could provide an estimate of the depth at which CAOXY may form inside the concrete prism. Following testing of the flexural strength specimens, a 0.1 N AgNO_3 solution was applied to the rupture face of each specimen to determine chloride depth. Presented in **Fig. 4.10** are average chloride depths for both NAE and AE concrete specimens based on fly ash level. It is observed that as the fly ash level increases there is a reduction in chloride penetration; however, the impact of fly ash is reduced above a 30% cement replacement level. This could be caused by a reduction in the extent of hydration products due to the reduction of portland cement content. Though the fly ash will offset some hydration product loss (through a pozzolanic reaction), the reduced cement content could result in the 45% fly ash specimens may have higher paste porosity than specimens cast with 30% fly ash or lower. It is shown that at a 45% mass cement replacement with fly ash

chloride penetration depth can be reduced in NAE concrete up to 50% and approximately 60% when combined with 6% air.

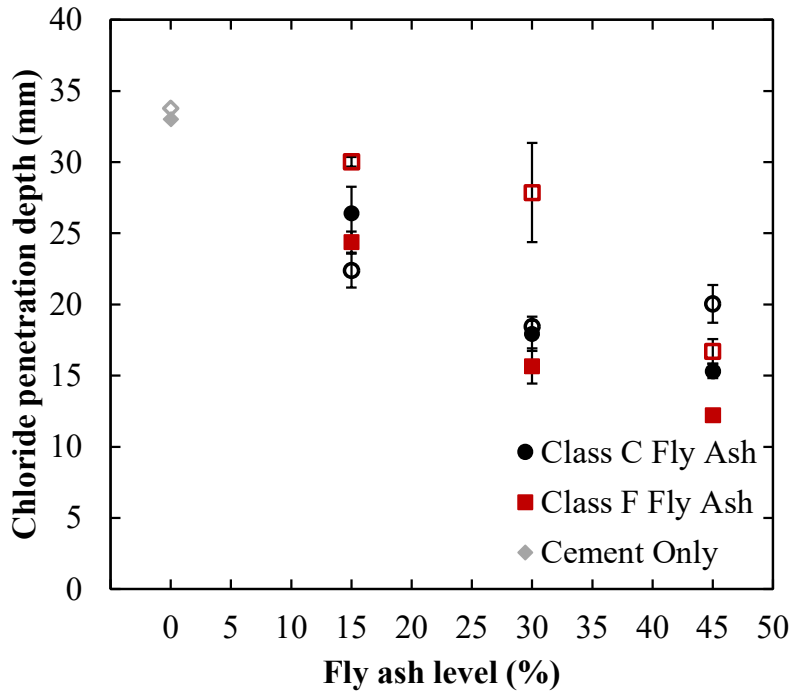


Figure. 4.10. Chloride penetration depth based on fly ash level for concrete specimens exposed to a 30% CaCl_2 solution. Hollow markers represent NAE concrete while filled markers represent AE concrete.

Interestingly, chloride penetration was mitigated better in the AE concrete specimens than the NAE specimens. This could be caused by two factors. First, in the NAE concrete there is a lack of deposition locations for CAOXY formation which possibly leads to cracking of the concrete. These cracks then allow more solution to further penetrate the specimen leading to further deterioration. Though no noticeable deterioration was observed through strength testing, mass change, or visual observation, in the 30 and 45% fly ash (mass) specimens, a potential may exist for microcracking to occur allowing solution to infiltrate to a greater depth than the air entrained specimens. The second potential mechanism to mitigate solution infiltration is the deposition of CAOXY crystals in the air voids. Given that CAOXY infiltrates from the exterior surface of the

concrete towards the interior, precipitating CAOXY may fill air voids blocking solution ingress in AE concrete. Filled air voids with CAOXY remnants inside concrete have been reported by Sutter et al. [9] and Ghazy and Bassuoni [14]. Cross sections of deteriorated flexural strength specimens presented in **Fig. 4.11** show the variation in chloride penetration depth in NAE concrete specimens.

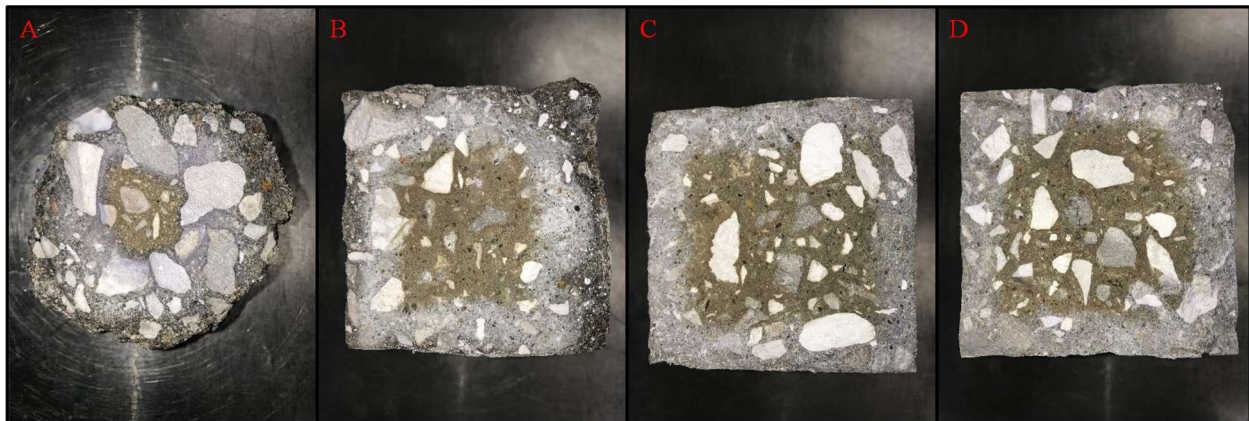


Figure. 4.11. Chloride penetration depth in NAE concrete specimens when sprayed with a 0.1 N AgNO_3 solution: A) cement only, B) 15% mass Class C fly ash, C) 30% mass Class C fly ash, and D) 45% mass Class C fly ash.

4.3.5. Length Change

A further method to determine degradation in concrete is to measure the length change that occurs in the specimen during exposure to a potential deterioration mechanism. In cementitious paste specimens, CAOXY has been shown to expand paste to the point of complete failure [12]; however, in concrete, less research has been conducted on length change of CAOXY deteriorated specimens. Presented in **Fig. 4.12** are ultimate length change data for the NAE and AE concrete specimens. Ideally, this data would be shown as strain over time; however, due to restrictions regarding the current pandemic, measurements were unable to be acquired consistently. Therefore, data are presented as total strain rather than strain throughout the

duration of testing. Upper and lower error bars represent one standard deviation for each set of specimens for the strain reading. For **Fig. 4.12**, cement only specimens are not provided. These specimens were heavily deteriorated (similar to **Fig. 4.4**) and the gage studs became dislodged from the specimens while attempting to take measurements following storage for 202 days in a 30% CaCl_2 solution. It is known that the specimens expanded, but the extent was unable to be ascertained. Further, the non-air entrained 30% fly ash and the 15% fly ash (mass) air entrained specimens are not presented. The data collected for these specimens gave strain readings above 2900 and 1300 μm , respectively. It is believed that these measurements are errant and therefore, not presented. These discrepancies along with the large standard deviation for the AE 15% Class C fly ash specimens could indicate damage in the concrete causing the gage stud to become dislodged leading to error. However, for specimens with gage studs not compromised, 15% fly ash NAE concrete expanded to almost 500 μm while expansion at 30 and 45% fly ash was abated to approximately 140 and 75 μm , respectively. For the AE specimens, expansion was much smaller at 162, 62, and 60 μm for the 15, 30, and 45% fly ash specimens, respectively. This is continued evidence that when air (6%) is used in combination with a partial cement replacement with fly ash (30% or greater), CAOXY deterioration is mitigated when compared with only fly ash or only air as a mitigation technique. Continued research is needed to verify these results; however, given that deterioration progressively moves from external to internal within the specimens, length change may not be the best measurement to determine deterioration as the gage studs can become compromised.

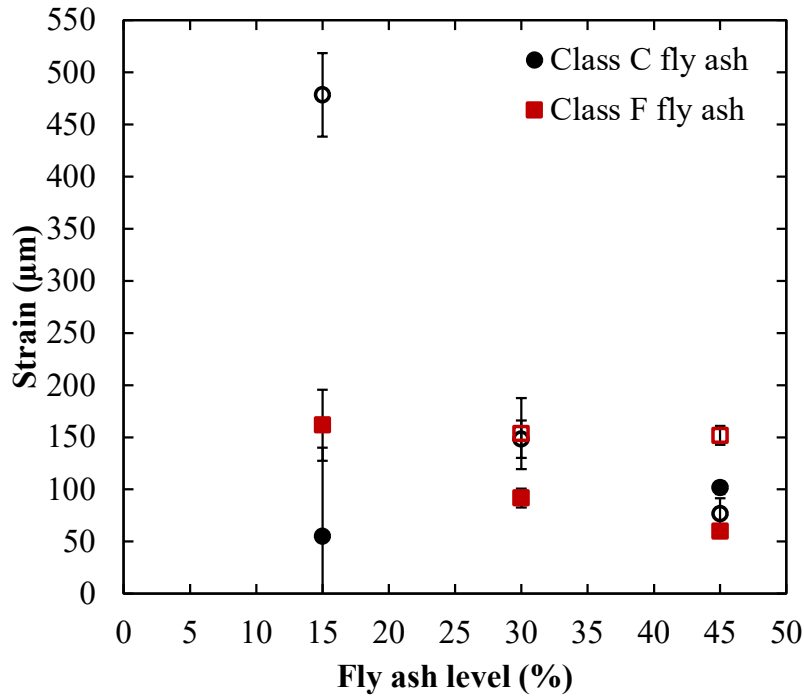


Figure. 4.12. Ultimate strain measurements in CAOXY deteriorated concrete specimens. Hollow markers represent NAE concrete while filled markers represent AE concrete.

4.4. Conclusions

A set of experiments is carried out where CAOXY deterioration in concrete specimens exposed to a 5 °C, 30% CaCl₂ solution for 202 days is studied. Deterioration is quantified by compressive and flexural strength changes, mass change, chloride penetration, and length change. The following are the most important conclusions from these test methods:

- Compressive strength loss is reduced as fly ash levels and air content increases (up to 5%) in concrete specimens. For NAE specimens, 45% fly ash is needed to mitigate CAOXY deterioration while 30% fly ash is required for AE specimens.
- Flexural strength loss is reduced as fly ash levels and air content increases (up to 5%) in concrete specimens. For both NAE and AE specimens, 15% fly ash significantly mitigates CAOXY deterioration; however, deterioration was noted in the 15% Class F fly ash specimens.

- Mass change results for CAOXY deteriorated specimens should be conducted following the removal of unsound concrete from the external surface. Mass gain (due to the infiltration of deicing solution in deteriorated specimens) is mitigated when fly ash is used as a partial cement replacement up to 45% (mass) in concrete. In NAE specimens, fly ash levels at 30% or greater mitigated mass change. In AE concrete, fly ash levels need to be 15% or greater.
- While chloride depth is not a proxy for CAOXY deterioration, chloride penetration depth is significantly mitigated in concrete specimens cast with cement replaced with fly ash up to 30%. At levels above 30% fly ash, no further changes in chloride penetration were recorded.
- Due to heavy external deterioration prior to internal deterioration, length change may not be the best method to quantify CAOXY deterioration in concrete. Results do indicate that as fly ash levels increase up to 45% of the cementitious content there is a decrease in the expansion of the specimens. AE concrete specimens had less expansion than NAE specimens.

While continued efforts are needed to elucidate the complex role of CAOXY deterioration in concrete, this current work provides new insights into the strength reduction in CAOXY deteriorated samples. Work investigating CAOXY deterioration in conjunction with other destructive mechanisms such as cyclic freeze/thaw deterioration is needed to develop durable, long lasting concrete pavements. In addition, the effects of solution change, specimen size/shape, and air void parameters on the ensuing damage must also be investigated.

Declaration of Interests

The authors have no declaration of interests to state.

Acknowledgements

The authors would like to thank the support of the Oklahoma/Arkansas Chapter of the American Concrete Pavement Association for their generous gift supporting this research. Without their

support this work would not be possible. The authors would also like to thank the Arkansas Department of Transportation for the chemical analysis of the cement and fly ash. The authors would also like to thank the team at the Engineering Research Center at the University of Arkansas for helping setup cold storage for this work.

References

1. Bureau of Transportation Statistics, 2017 North American freight numbers. <https://www.bts.gov/newsroom/2017-north-american-freight-numbers> (accessed 19 January 2021).
2. Bureau of Transportation Statistics, Monthly transportation statistics. <https://data.bts.gov/stories/s/m9eb-yevh#highway-travel> (accessed 19 January 2021).
3. U.S. Department of Transportation Federal Highway Administration, Snow and ice. https://ops.fhwa.dot.gov/weather/weather_events/snow_ice.htm (accessed 19 January 2021).
4. National Academies of Sciences, Engineering, and Medicine 2004. Snow and Ice Control: Guidelines for Materials and Methods, Washington, DC: The National Academies Press. <https://doi.org/10.17226/13776>.
5. X. Shi, L. Fay, C. Gallaway, K. Volkening, M.M. Peterson, T. Pan, A. Creighton, C. Lawlor, S. Mumma, Y. Liu, T.A. Nguyen, Evaluation of alternative anti-icing and deicing compounds using sodium chloride and magnesium chloride as baseline deicers – Phase I, Final Report for the Colorado Department of Transportation, CDOT-2009-1.
6. S. Monosi, M. Collepari, Research on $3\text{CaO}\cdot\text{CaCl}_2\cdot 15\text{H}_2\text{O}$ identified in concretes damaged by CaCl_2 attack, *Il Cemento* 87 (1990) 3-8.
7. M. Collepari, L. Coppola, C. Pistolesi, Durability of concrete structures exposed to CaCl_2 based deicing salts, Proceedings of the 3rd CANMET/ACI International Conference, 1994, Nice, France, pp. 107-120.
8. K. Torii, T. Sasatani, M. Kawamura, Effects of fly ash, blast furnace slag, and silica fume on resistance of mortar to calcium chloride attack, *ACI Spec. Publ.* 153 (1995) 931-950.
9. L. Sutter, K. Peterson, S. Touton, T. Van Dam, D. Johnston, Petrographic evidence of calcium oxychloride formation in mortars exposed to magnesium chloride solution, *Cem. Concr. Res.* 36 (2006) 1533-1541. <https://doi.org/10.1016/j.cemconres.2006.05.022>.
10. L. Sutter, T. Van Dam, K.R. Peterson, D.P. Johnston, Long-term effects of magnesium chloride and other concentrated salt solutions on pavement and structural portland cement

concrete phase I results, *Transp. Res. Rec.* 1979 (2006) 60-68.
<http://dx.doi.org/10.3141/1979-10>.

11. G.A. Julio-Betancourt, R.D. Hooton, Calcium and magnesium chloride attack on cement-based materials: formation, stability, and effects of oxychlorides, *Proceedings of the 2nd RILEM International Workshop on Concrete Durability and Service Life Planning - ConcreteLife'09*, 2009, Haifa, Israel, pp. 432-439.
12. G.A. Julio-Betancourt, Effect of de-icer and anti-icer chemicals on the durability, microstructure, and properties of cement based materials, University of Toronto, 2009, Ph.D. Thesis.
13. ACI 201.3T-19, Joint deterioration and chloride-based deicing chemicals. American Concrete Institute, Farmington Hills, Michigan, 2019.
14. A. Ghazy, M.T. Bassuoni, Resistance of concrete to different exposures with chloride-based salts, *Cem. Concr. Res.* 101 (2017) 144-158.
<https://doi.org/10.1016/j.cemconres.2017.09.001>.
15. C. Qiao, P. Suraneni, J. Weiss, Flexural strength reduction of cement pastes exposed to CaCl₂ solutions, *Cem. Concr. Comp.* 86 (2018) 297-305.
<https://doi.org/10.1016/j.cemconcomp.2017.11.021>.
16. P. Suraneni, J. Monical, E. Unal, Y. Farnam, J. Weiss, Calcium oxychloride formation potential in cementitious pastes exposed to blends of deicing salt, *ACI Mater. J.* 114 (4) (2017) 631-641. <http://dx.doi.org/10.14359/51689607>.
17. P. Suraneni, V.J. Azad, O.B. Isgor, W.J. Weiss, Use of fly ash to minimize deicing salt damage in concrete pavements, *Transp. Res. Rec.* 2629 (2017) 24-32.
<https://doi.org/10.3141/2629-05>.
18. P. Suraneni, V.J. Azad, O.B. Isgor, J. Weiss, Role of supplementary cementitious material type in the mitigation of calcium oxychloride formation in cementitious pastes, *J. Mater. Civ. Eng.* 30 (10) (2018) 04018248. [https://doi.org/10.1061/\(ASCE\)MT.1943-5533.0002425](https://doi.org/10.1061/(ASCE)MT.1943-5533.0002425).
19. F. Traore, C. Jones, S. Ramanathan, P. Suraneni, W.M. Hale, Using compressive strength and mass change to verify the calcium oxychloride threshold in cementitious pastes with fly ash, *Constr. Build. Mater.* 296 (2021) 123640.
<https://doi.org/10.1016/j.conbuildmat.2021.123640>.
20. K. Peterson, G. Julio-Betancourt, L. Sutter, R.D. Hooton, D. Johnston, Observations of chloride ingress and calcium oxychloride formation in laboratory concrete and mortar at 5 °C, *Cem. Concr. Res.* 45 (2013) 79-90. <https://doi.org/10.1016/j.cemconres.2013.01.001>.

21. X. Wang, S. Sadati, P. Taylor, C. Li, X. Wang, A. Sha, Material characterization to assess effectiveness of surface treatment to prevent joint deterioration from oxychloride formation mechanism, *Cem. Concr. Comp.* 104 (2019) 103394. <https://doi.org/10.1016/j.cemconcomp.2019.103394>.
22. C. Jones, S. Ramanathan, P. Suraneni, W.M. Hale, Calcium oxychloride: a critical review of the literature surrounding the formation, deterioration, testing procedures, and recommended mitigation techniques, *Cem. Concr. Comp.* 113 (2020) 103663. <https://doi.org/10.1016/j.cemconcomp.2020.103663>.
23. P. Suraneni, V.J. Azad, O.B. Isgor, W.J. Weiss, Calcium oxychloride formation in pastes containing supplementary cementitious materials: thoughts on the role of cement and supplementary cementitious materials reactivity, *RILEM Tech. Lett.* 1 (2016) 24-30. <http://dx.doi.org/10.21809/rilemtechlett.v1.7>.
24. P. Suraneni, V.J. Azad, O.B. Isgor, W.J. Weiss, Deicing salts and durability of concrete pavements and joints: mitigating calcium oxychloride formation, *Concr. Int.* 38 (4) (2016) 48-54.
25. C. Qiao, P. Suraneni, T.N.W. Ying, A. Choudhary, J. Weiss, Chloride binding of cement pastes with fly ash exposed to CaCl₂ solutions at 5 and 23 °C, *Cem. Concr. Comp.* 97 (2019) 43-53. <https://doi.org/10.1016/j.cemconcomp.2018.12.011>.
26. J. Weiss, M.T. Ley, L. Sutter, D. Harrington, J. Gross, S.L. Tritsch, Guide to the prevention of and restoration of early joint deterioration in concrete pavements, Final Report for the Iowa Department of Transportation, TR-697, 2016.
27. S.H. Smith, C. Qiao, P. Suraneni, K.E. Kurtis, W.J. Weiss, Service-life of concrete in freeze-thaw environments: Critical degree of saturation and calcium oxychloride formation, *Cem. Concr. Res.* 122 (2019) 93-106. <https://doi.org/10.1016/j.cemconres.2019.04.014>.
28. Arkansas Department of Transportation. Standard specifications for highway construction. 2014. http://www.arkansashighways.com/standard_spec/2014/2014SpecBook.pdf.
29. ASTM C618-19, Standard Specification for Coal Fly Ash and Raw or Calcined Natural Pozzolan for Use in Concrete, ASTM International, West Conshohocken, PA, 2019.
30. ASTM C114-18, Standard Test Method for Chemical Analysis of Hydraulic Cement, ASTM International, West Conshohocken, PA, 2018.
31. ASTM C311/C311M-18, Standard Test Methods for Sampling and Testing Fly Ash or Natural Pozzolans for Use in Portland-Cement Concrete, ASTM International, West Conshohocken, PA, 2018.

32. AASHTO PP 84-20, Developing Performance Engineered Concrete Pavement Mixtures, American Association of State Highway and Transportation Officials, Washington D.C., 2020.
33. Y. Schrader, An investigation into the effects of fly ash on freeze-thaw durability prediction, University of Arkansas, 2020, M.S.C.E. Thesis.
34. ASTM C192/C192M-18, Standard Practice for Making and Curing Concrete Test Specimens in the Laboratory, ASTM International, West Conshohocken, PA, 2018.
35. ASTM C138/C138M-17a, Standard Test Method for Density (Unit Weight), Yield, and Air Content (Gravimetric) of Concrete, ASTM International, West Conshohocken, PA, 2017.
36. ASTM C231/C231M-17a, Standard Test Method for Air Content of Freshly Mixed Concrete by the Pressure Method, ASTM International, West Conshohocken, PA, 2017.
37. ASTM C143/C143M-20, Standard Test Method for Slump of Hydraulic-Cement Concrete, ASTM International, West Conshohocken, PA, 2020.
38. ASTM C1064/C1064M-17, Standard Test Method for Temperature of Freshly Mixed Hydraulic-Cement Concrete, ASTM International, West Conshohocken, PA, 2017.
39. ASTM C511-19, Standard Specification for Mixing Rooms, Moist Cabinets, Moist Rooms, and Water Storage Tanks Used in the Testing of Hydraulic Cements and Concretes, ASTM International, West Conshohocken, PA, 2019.
40. ASTM C39/C39M-20, Standard Test Method for Compressive Strength of Cylindrical Concrete Specimens, ASTM International, West Conshohocken, PA, 2020.
41. ASTM C78/C78M-18, Standard Test Method for Flexural Strength of Concrete (Using Simple Beam with Third-Point Loading), ASTM International, West Conshohocken, PA, 2018.
42. H. Mori, R. Kuga, S. Ogawa, Y. Kubo, Chemical deterioration of hardened cement pastes immersed in calcium chloride solution, Proceedings of the 3rd International Conference on Sustainable Construction Materials and Technologies, 2013, Kyoto, Japan, Paper 329.
43. ASTM C157/C157M-17, Standard Test Method for Length Change of Hardened Hydraulic-Cement Mortar and Concrete, ASTM International, West Conshohocken, PA, 2017.
44. E. Yurdakul, P.C. Taylor, H. Ceylan, F. Bektas, Effect of water-to-binder ratio, air content, and type of cementitious materials on fresh and hardened properties of binary and ternary blended concrete, *J. Mater. Civ. Eng.* 26 (6) (2014) 04014002.
[https://doi.org/10.1061/\(ASCE\)MT.1943-5533.0000900](https://doi.org/10.1061/(ASCE)MT.1943-5533.0000900).

45. M.D.A. Thomas, Optimizing the use of fly ash in concrete, *Port. Cem. Assoc.* (2007) 24.
https://www.cement.org/docs/default-source/fc_concrete_technology/is548-optimizing-the-use-of-fly-ash-concrete.pdf (accessed 2 February 2021).
46. C. Li, M.D.A. Thomas, J.H. Ideker, A mechanistic study on mitigation of alkali-silica reaction by fine lightweight aggregates, *Cem. Concr. Res.* 104 (2018) 13-24.
<https://doi.org/10.1016/j.cemconres.2017.10.006>.
47. ACI 318R-19, *Building Code Requirements for Structural Concrete and Commentary*. American Concrete Institute, Farmington Hills, Michigan, 2019.

5. Correlating Calcium Hydroxide and Calcium Oxychloride Formation with Resulting Deterioration in Cementitious Paste and Concrete Mixtures

Casey Jones^a, Sivakumar Ramanathan^b, Prannoy Suraneni^c, W. Micah Hale^d

^aGraduate Research Assistant, Department of Civil Engineering, University of Arkansas, 4190 Bell Engineering Center, Fayetteville, AR 72701, United States of America.

^bGraduate Research Assistant, Civil, Architectural, Environmental Engineering Department, University of Miami, 1251 Memorial Drive, Coral Gables, FL 33146, United States of America.

^cAssistant Professor, Civil, Architectural, Environmental Engineering Department, University of Miami, 1251 Memorial Drive, Coral Gables, FL 33146, United States of America.

^dProfessor and Chair, Department of Civil Engineering, University of Arkansas, 4190 Bell Engineering Center, Fayetteville, AR 72701, United States of America.

Corresponding author: Casey Jones

Abstract

Presented in this work are results from an investigation correlating calcium oxychloride (CAOXY) formation and damage in cementitious paste and concrete. CAOXY is believed to cause significant damage in concrete pavements; however, quantifying its presence in concrete is challenging due to its transient nature in varying environments. The use of thermogravimetric analysis and low-temperature differential scanning calorimetry to quantify calcium hydroxide and CAOXY levels in concrete is described. Calcium hydroxide and CAOXY levels in cementitious paste and concrete are linearly correlated; however, significant deviation is reported between measured and stoichiometrically predicted CAOXY levels in concrete. Compressive

strength change in concrete due to exposure to a 30% calcium chloride solution is correlated with calcium hydroxide and stoichiometric CAOXY in concrete. Fly ash successfully mitigates strength loss caused by CAOXY formation. From this study, for non-air entrained concrete specimens, calcium hydroxide and stoichiometric CAOXY should be less than 0.85 g/100 g powder and 2 g/100 g powder, respectively, to mitigate strength loss. Corresponding calcium hydroxide and stoichiometric CAOXY values for air entrained concrete should be below 1.5 g/100 g powder and 3.5 g/100 g powder, respectively.

Keywords: Calcium Oxychloride; Low-Temperature Differential Scanning Calorimetry; Thermogravimetric Analysis; Concrete-Paste Correlation; Stoichiometric Calcium Oxychloride

5.1. Introduction

Chloride-based deicing solutions have been extensively investigated and are known to cause deterioration in concrete pavements [1-4]. While some deterioration mechanisms such as surface scaling [5,6] and reinforcement corrosion [7] are easily identifiable, other deterioration mechanisms are more difficult to establish. For instance, calcium hydroxide ($\text{Ca}(\text{OH})_2$) found in the cementitious paste portion of portland cement concrete is known to interact with calcium chloride (CaCl_2) and magnesium chloride (MgCl_2) to form calcium oxychloride (CAOXY) [2,8-10]. This expansive phase is believed to be responsible for joint damage in concrete pavements [8,11]; however, to the authors knowledge, the phase has not been comprehensively identified in deteriorated concrete pavements. This is due in part to the instability of the CAOXY phase when significant moisture or temperature changes occur or under conditions of carbonation [12]. Therefore, when coring deteriorated jointing regions, a high potential exists for the phase to be damaged/destroyed prior to investigation. Though the CAOXY phase is difficult to establish in

the field, it appears to be easily observed in the laboratory as shown in **Fig. 5.1** with similar exterior phases reported in Jones et al. [10] and Peterson et al. [13].

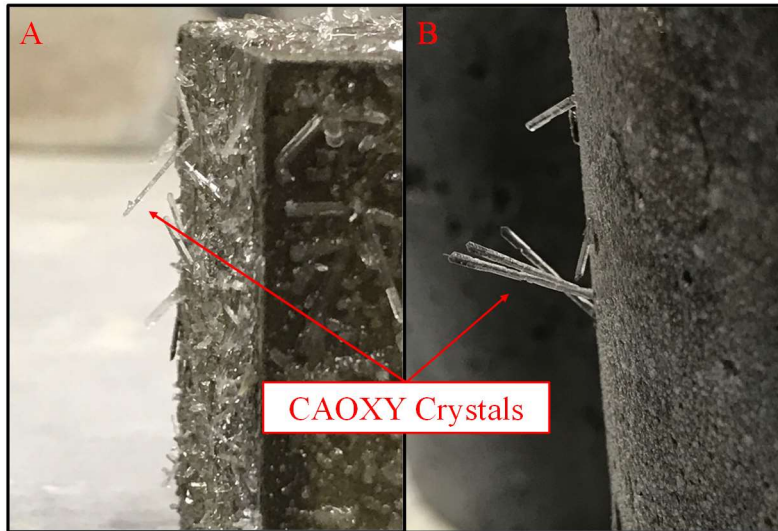


Figure 5.1. Diaphanous CAOXY crystals on the surface of specimens exposed to a 30% (mass) CaCl_2 solution stored at 5 °C; A) cementitious paste and B) concrete.

Both, portland cement-based cementitious paste and concrete specimens are known to deteriorate under laboratory conditions due to CAOXY formation [2,14-17]. To prevent/mitigate this deterioration, the use of supplementary cementitious materials (SCMs) in conjunction with an air content of 5 – 6% have been shown to be highly effective in concrete [16,17]. While the use of SCMs is known to mitigate CAOXY, quantifying the amount of CAOXY in concrete has proved difficult. The use of thermogravimetric analysis (TGA) (covered in **Section 5.2.2**) and low-temperature differential scanning calorimetry (LT-DSC) (covered in **Section 5.2.3**) have been shown to be effective methods for CAOXY estimation and quantification in cementitious paste. Therefore, a number of investigations have focused on using these techniques for cementitious paste [18-21]. However, less research has focused on these techniques for concrete specimens due to lower $\text{Ca}(\text{OH})_2$ levels in concrete (compared to paste) and the interference caused by aggregates [22].

Currently, the AASHTO PP 84 [23] recommendation for concrete exposed to a CaCl_2 or MgCl_2 deicer is to limit the CAOXY content in paste below 15 g/100 g paste based on AASHTO T 365 [24]. However, this recommendation has not been definitively linked to concrete deterioration. It is believed that aggregates and air content will impact CAOXY deterioration in concrete [10,17,22]. Therefore, linking CAOXY levels in cementitious paste and concrete to deterioration is vital to begin closing the gap between cementitious paste research and field concrete deterioration. Presented in this work is an investigation to begin closing this gap. Research in this article focuses on obtaining TGA and LT-DSC data for concrete specimens cast with various levels of fly ash. Given that this work is part of a larger investigation into CAOXY deterioration in concrete pavements, cementitious paste and concrete deterioration are correlated to investigate the current 15 g/100 g paste limit. Also, a recommendation is made for a similar limit when testing concrete samples. While further research is still required, this work lays a foundation for continued research to refine the CAOXY limit in concrete. Once established, this threshold could potentially be added to the AASHTO PP 84 [23] recommendation for concrete mixtures instead of using only cementitious paste.

5.2. Materials and Methods

5.2.1. Materials

For this research, a Type I/II portland cement was utilized in conjunction with an ASTM C618 Class C fly ash and Class F fly ash [25]. The chemical composition of the cement was tested in accordance with ASTM C114 [26] while each fly ash was tested in accordance with ASTM C311 [27]. The results of these analyses are provided in **Table 5.1**. Further, fly ash is used to reduce $\text{Ca}(\text{OH})_2$ in the cementitious paste and concrete in order to mitigate CAOXY damage. For the cementitious paste specimens, cement was replaced with fly ash at 10, 20, 30, 40, and

50% by mass; however, in concrete, cement was replaced with fly ash at 15, 30, and 45% on a mass basis. Given that triplicate testing is required for the concrete samples (see **Sections 5.2.2** and **5.2.3**), the cost associated with this testing is greater. Further, Suraneni et al. [22] have shown that CAOXY is mitigated in cementitious paste and mortar on a linear basis which is correlated to the amount of $\text{Ca}(\text{OH})_2$ in the system. Therefore, given the extra cost associated with the concrete samples and the potential linearity of the correlation, it is proposed to investigate nearly equivalent cement replacement levels with fly ash in concrete compared to the paste. A water to cementitious materials ratio (w/cm) of 0.45 was utilized for both the paste and concrete which is the maximum allowable per the Arkansas Department of Transportation (ARDOT) specifications for portland cement concrete pavement (PCCP) [28]. It should be noted that a mass cement replacement was chosen in order to represent typical field incorporation of fly ash in concrete mixture designs in accordance with ARDOT [28]. Aggregates used for the concrete mixture designs are a 9.5 mm Arkansas River sand and a 25 mm crushed limestone material. Aggregate properties are located at the bottom of **Table 5.1**. The coarse aggregate was approximately 43% of the total material in each mixture by mass while the fine aggregate represented more than 35% of the material present. The cementitious paste portion of the mixtures represented approximately 21.5% of each mixture by mass.

Table 5.1. Cement, fly ash and aggregate properties. Developed from Jones et al. [16]. (Bulk oxide given in percent mass.)

Oxide	Cement	Fly ash Class C	Fly ash Class F	Coarse aggregate	Fine aggregate
SiO ₂	20.25	34.57	56.25	-	-
Al ₂ O ₃	4.54	20.26	18.91	-	-
Fe ₂ O ₃	4.20	5.69	9.59	-	-
CaO	63.73	26.47	7.61	-	-
MgO	0.91	4.85	1.88	-	-
SO ₃	3.09	1.73	1.47	-	-
Na ₂ O	0.16	1.60	1.27	-	-
K ₂ O	0.54	0.50	2.61	-	-
LOI*	2.53	0.58	0.50	-	-
Specific gravity	3.15	2.58	2.40	2.57	2.63
Absorption (%)	-	-	-	2.40	0.55

5.2.2. Previous Work

This work is part of a larger investigation into CAOXY deterioration in both cementitious paste and concrete. Several papers have been produced from this project and a portion of the data that is shown in this paper has been published in prior works [10,15,16]. However, the objective of prior work was to separately analyze cementitious pastes and concrete. In order to correlate Ca(OH)₂ and CAOXY levels in concrete (covered in this work) with deterioration in cementitious paste and concrete, similar paste and concrete mixture designs are required. The Ca(OH)₂, CAOXY and damage in the cementitious pastes is published in Traore et al. [15] while concrete damage is from Jones et al. [16]. The calcium hydroxide and CAOXY measurements in concrete, and a detailed comparison of paste and concrete responses, which are not published elsewhere, are the novel contributions of this paper. Summaries of the two previous works are covered in **Sections 5.2.2.1** and **5.2.2.2**.

5.2.2.1. Summary of Cementitious Paste Investigation

In Traore et al. [15], cementitious paste mixtures were cast with varying amounts and types of fly ash. Three Class C fly ashes and one Class F fly ash (ASTM C618 [25]) were utilized with

cement replacement levels ranging from 0 to 50% (mass) at 10% increments. The specimens were tested using thermogravimetric analysis (ASTM C1872 [29]), low-temperature differential scanning calorimetry (AASHTO T 365 [24]), compressive strength (ASTM C109 [30]), and mass change. Specimens for TGA and LT-DSC testing were stored in the molds for 24 hours and then placed in sealed containers for an additional 90 days. Following this curing period, the specimens were tested using TGA and LT-DSC. For strength, specimens were cured in a limewater bath for 90 days after which they were placed in a 30% CaCl₂ solution at 5 °C for 91 days. Strength data was collected throughout storage in both the limewater and CaCl₂ solution. For the current investigation, Ca(OH)₂, CAOXY, and strength differences (compared to the strength values before CaCl₂ exposure) in the paste samples from Traore et al. [15] are used to compare with concrete samples batched with the same fly ash types as summarized in **Table 5.2**.

Table 5.2. Cementitious paste data summarized from Traore et al. [15].

	Mixture	w/cm	Ca(OH) ₂ (g/100 g paste)	CAOXY (g/100 g paste)	*Strength difference (%)
	Cement only	0.45	14.82	32.25	-73
Class C	10% Fly ash	0.45	12.88	27.16	-57
	20% Fly ash		11.60	22.14	-28
	30% Fly ash		9.01	13.80	-52
	40% Fly ash		7.77	7.59	-57
	50% Fly ash		5.40	1.65	-14
Class F	10% Fly ash	0.45	12.82	27.97	-72
	20% Fly ash		11.45	20.55	-54
	30% Fly ash		9.51	13.71	-50
	40% Fly ash		7.37	4.91	-10
	50% Fly ash		5.86	2.13	-21

*Positive strength difference indicates strength gain while negative indicates strength loss after 91 days of exposure to 30% CaCl₂ solution.

5.2.2.2. Summary of Concrete Deterioration Investigation

In Jones et al. [16], an investigation into concrete deterioration was conducted. The investigation focused on examining deterioration in concrete specimens following exposure to a 30% CaCl₂ solution. Concrete specimens were cast with and without fly ash following requirements set forth in the ARDOT construction procedures [28]. Both a Class C and Class F fly ash (ASTM

C618 [25] and two of the same fly ashes from Traore et al. [15]) were used to replace cement in the mixtures at 15, 30 and 45% (mass) replacement levels. Fly ash replacement levels deviated slightly from Traore et al. [15] due to testing cost and the linear correlation of Ca(OH)_2 and CAOXY in the samples. Once cast, specimens were removed from the forms and cured in a limewater bath for 90 days. Specimens were then tested for compressive (ASTM C39 [31]) and flexural strength (ASTM C78 [32]), initial mass measurements, and initial length measurements (ASTM C157 [33]). Samples were collected from the failed compressive strength specimens and finely ground to a powder ($-75 \mu\text{m}$) in order to facilitate TGA and LT-DSC testing. The remaining specimens were then rinsed with water and scraped with wire brushes to remove adhered lime from storage. The specimens were placed in a 30% CaCl_2 solution for 2-weeks at room temperature ($\sim 20 \text{ }^\circ\text{C}$). Following the room temperature storage, specimens were placed in a $5 \text{ }^\circ\text{C}$ environment for the remainder of the 202-day solution storage time. At the end of storage, specimens were tested for compressive and flexural strength difference (compared to the 91-day strengths), mass change, length change, and chloride penetration. The current work focuses on correlating strength loss (both compressive and flexural) with Ca(OH)_2 and CAOXY levels determined using TGA and LT-DSC, respectively. Data utilized from Jones et al. [16] are summarized in **Table 5.3**.

Table 5.3. Concrete data summarized from Jones et al. [16].

	Mixture	w/cm	Air content (%)	*Compressive strength difference (%)	*Flexural strength difference (%)
Class C	Cement only	0.45	4.9	-100	-100
	15% Fly ash		4.8	-24	-9
	30% Fly ash		4.7	5	31
	45% Fly ash		4.9	7	25
Class F	15% Fly ash	0.45	4.7	-19	-7
	30% Fly ash		5.1	3	6
	45% Fly ash		5.1	7	5
Class C	Cement only	0.45	2.0	-100	-100
	15% Fly ash		1.7	-50	-48
	30% Fly ash		1.3	-16	5
	45% Fly ash		1.1	1	-2
Class F	15% Fly ash	0.45	2.3	-23	1
	30% Fly ash		2.0	-6	11
	45% Fly ash		1.4	-3	26

*Positive strength difference indicates strength gain while negative indicates strength loss after 91 days of exposure to 30% CaCl₂ solution.

5.2.3. Thermogravimetric Analysis

In order to correlate CAOXY levels in cementitious paste and concrete, TGA and LT-DSC are employed. For this investigation, 91-day aged samples (before exposure) were tested using both TGA and LT-DSC. For the paste specimens, a 50 mm cube was taken from storage and the outer, potentially carbonated layers were removed by a chisel. With the inner layer exposed, a representative portion of the interior paste was ground to a fine powder (-75 μm) and placed in the TGA apparatus. The 30-50 mg powder sample was heated in a nitrogen atmosphere to 500 °C in accordance with ASTM C1872 [29]. The level of Ca(OH)₂ in the paste was determined using the tangential method in accordance with Kim and Olek [34]. The typical temperature range used to quantify Ca(OH)₂ was 380 °C - 460 °C; however, it should be noted this is a lower temperature range than in ASTM C1872 [29], which specifies 380 °C - 600 °C. The smaller range utilized here helps mitigate the influence of mass loss due to other cementitious hydration products. The TGA results for the paste samples are discussed in Traore et al. [15].

For the concrete, specimens were removed from the water bath (before exposure) and tested for compressive strength. Following failure of the cylinder in compressive strength, pieces of the specimen were collected from the load frame for TGA. The outer, potentially carbonated layers of the collected pieces of concrete were removed with a chisel. Once the outer layers were removed, the sample was fractured into smaller pieces and a minimum of 750 grams was collected for each specimen. These pieces were placed in front of a fan for 1-2 hours to remove moisture from each piece prior to grinding. After drying, the pieces were mechanically ground and a minimum of 40 grams was collected for TGA testing. On average, 45-50 mg of powder was utilized for TGA analysis of these samples. Suraneni and Weiss [22] have shown that the inclusion of aggregate in the powder content can dilute the sample and the subsequently measured $\text{Ca}(\text{OH})_2$. Therefore, Suraneni and Weiss [22] suggest conducting triplicate testing of each sample and reporting the average of the three tests as the $\text{Ca}(\text{OH})_2$ content for each concrete sample. Similar to the paste, the tangential baseline method approach proposed by Kim and Olek [34] is used to quantify $\text{Ca}(\text{OH})_2$ with a typical mass loss range of 380 - 460 °C. Results of the TGA testing are covered in **Section 5.3.1**.

5.2.4. Low-Temperature Differential Scanning Calorimetry

LT-DSC has been used to quantify CAOXY levels in cementitious paste by measuring the latent heat development associated with the CAOXY phase transformation [18]. For this investigation, for cement pastes, similar to TGA, mature samples (91-day) were investigated. The specimens were ground to a fine powder (-75 μm) and a sample of 10 mg was selected for testing. The 10 mg sample was mixed with a 20% CaCl_2 deicing solution on a 1:1 mass basis in a sealed container. The container was placed in the LT-DSC, cooled to -90 °C at 1 °C/minute, and subsequently heated to 50 °C at 0.25 °C/minute. At temperatures above freezing, a heat

signature is registered signaling the formation of CAOXY (typically between 30 – 40 °C). The heat signature provides a means to quantify CAOXY formation. Research has shown this to be a reliable test method to directly measure CAOXY in paste specimens [18] and the American Association of State Highway Transportation Officials recently adopted this test method as AASHTO T 365 [24]. Results for the LT-DSC paste samples are discussed in Traore et al. [15]. For the concrete samples, similar to TGA, the influence of the aggregates complicates the quantification of CAOXY by LT-DSC [22]. In order to collect the powdered portion (-75 μm) required for LT-DSC, the same method of sample preparation and collection from the concrete specimens was utilized as for TGA. Following procedures established in Suraneni and Weiss [22], the powdered portion was mixed with a 20% CaCl₂ solution in a 4:1 mass mixture (4 parts powder:1 part CaCl₂ solution). The increase in powder proportion, compared to paste specimens, helps alleviate the lower Ca(OH)₂ content due to ground aggregates in the mixture. Mixtures are placed in sealed containers inside the LT-DSC and run through the same cooling and heating cycle as the paste. Further, while singular LT-DSC tests are shown to have a low coefficient of variation in paste specimens, a larger coefficient of variation is typically observed in the concrete specimens [22]. Therefore, triplicate testing was conducted on each sample in this investigation. Further details establishing a consistent test methodology to acquire LT-DSC results from concrete can be found in Suraneni and Weiss [22]. Data from this analysis are presented in **Section 5.3.2**.

5.3. Results and Discussion

5.3.1. Thermogravimetric Test Data

5.3.1.1. Paste and Concrete TGA Data

From **Table 5.2**, the TGA data for pastes with the two specific fly ashes utilized in this work are presented in **Fig. 5.2**. As the fly ash level increases in cementitious paste, the corresponding Ca(OH)_2 level decreases. When using SCMs such as fly ash, for CAOXY mitigation, the reduction in CAOXY is due to both dilution and pozzolanic reactivity of the SCM [20,21]. Dilution occurs due to the decrease in amounts of hydration products caused by the removal of the cement. The dilution line is represented by the black line on **Fig. 5.2**. If “simple” dilution were to be assumed, then reduction in hydration products would be equal to the amount of cement replaced. However, most SCMs are not equivalent in size and density to cement, alter water content in the paste and also provide increased nucleation sites for hydration products [35,36]. This filler effect causes the amounts of hydrates, such as calcium hydroxide, to be different from the values expected by pure dilution, even for inert SCMs. Pozzolanic reactivity is the reaction between Ca(OH)_2 in the cement paste and reactive aluminosilicate phases in the SCM [36]. This reaction forms calcium (alumino) silicate hydrate (C-A-S-H) and further reduces the Ca(OH)_2 amount [18,20], as seen from the values in **Fig. 5.2** being lower than expected from dilution. It is well established in the literature that fly ash is pozzolanic [37,38]. Therefore, it is expected that fly ash mitigates CAOXY through a combination of both dilution and pozzolanic reaction. Also, at higher replacement levels, SCM degree of reaction decreases, but this reduction appears to be more than compensated for by the greater amount of material [39]. Therefore, increased deviations from dilution are observed at higher fly ash levels. A red dashed line is shown in **Fig. 5.2** which corresponds to the theoretical threshold at which CAOXY

is mitigated in cementitious paste. This threshold is developed based on the relationship between Ca(OH)_2 and CAOXY established in Suraneni et al. [21].

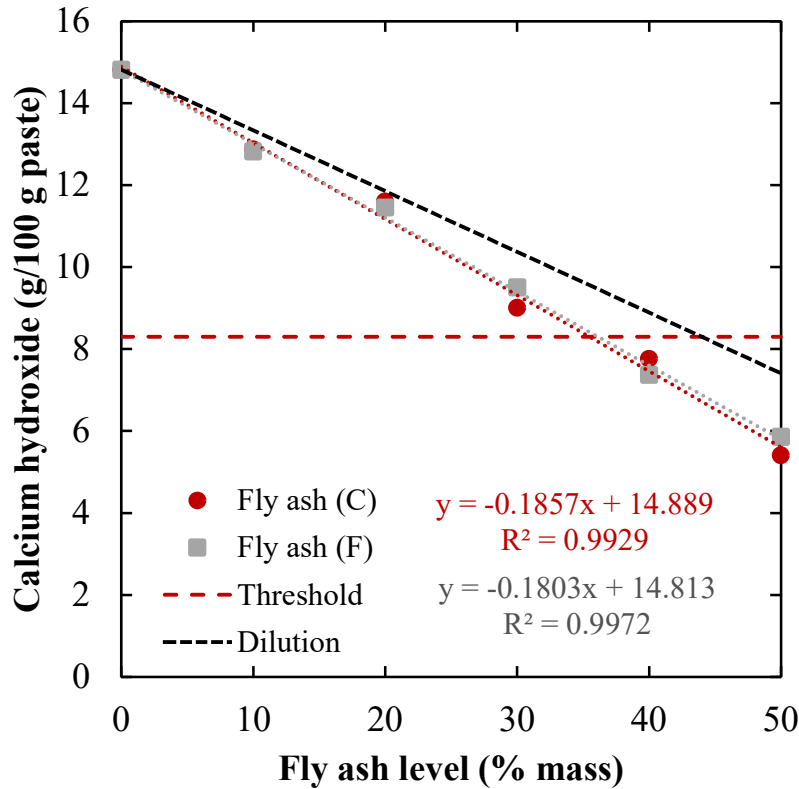


Figure 5.2. Calcium hydroxide levels in cementitious paste specimens.

For concrete, TGA is a valid test method; however, due to reduced Ca(OH)_2 levels, testing is more difficult and can lead to larger coefficient of variations when compared with paste samples [22]. Aggregate, used in concrete, causes dilution reducing the quantifiable amount of Ca(OH)_2 in concrete samples. This dilution is observed in **Fig. 5.3** as the concrete samples cast with cement only have a Ca(OH)_2 content of 2.37 g/100 g powder compared to the corresponding paste specimens at 14.82 g/100 g paste. This is in good accordance with Suraneni and Weiss [22], who measured Ca(OH)_2 levels of 2.66 g/100 g powder for cement only concrete samples. However, despite the reduced Ca(OH)_2 content in concrete, significant damage by CAOXY has been linked to its presence in the paste portion of concrete [9,16,17,40]. From **Fig. 5.3**, it is also

observed that the reduction in $\text{Ca}(\text{OH})_2$ in concrete is linear, similar to the paste specimens. Also, similar to the paste, fly ash is shown to be more efficient than expected from simple dilution of the cement through pozzolanic reaction. There is larger variability in testing concrete compared to paste specimens as the coefficient of variations ranged from 0.8% to 15.0% for the different sets of specimens but this finding is consistent with the literature [22]. However, as shown by the trend lines, a good fit is still observed for both fly ash types.

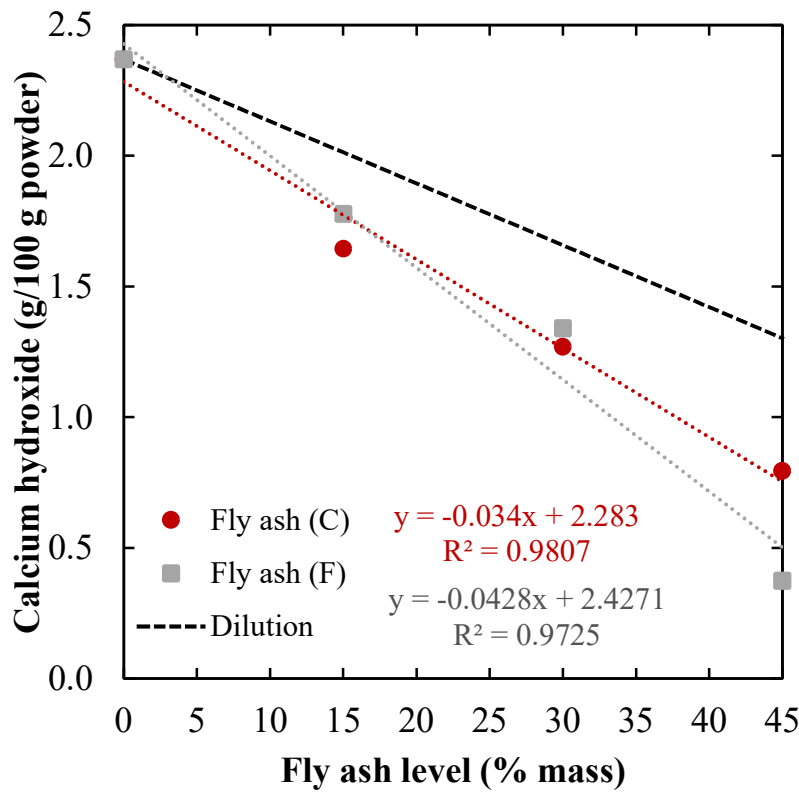


Figure 5.3. Calcium hydroxide levels in concrete specimens.

When reviewing data from **Fig. 5.3**, it should be noted that minor carbonation prior to testing may be present. The effects of carbonation can be accounted for in mortar/concrete mixtures that do not contain limestone aggregates [34]; however, in specimens cast with limestone aggregates, there is no method to separate the aggregate CaCO_3 and the CaCO_3 due to carbonation of the ground powder. Therefore, any potential carbonation is unable to be accounted for in the

concrete specimens. Even though the quantifiable Ca(OH)_2 in the concrete samples is small, it is shown that when cement is replaced with fly ash by mass at 15, 30, and 45%, it reduces Ca(OH)_2 by 27.8, 44.9, and 75.3% on average, respectively.

5.3.1.2. Correlating Paste-Concrete TGA Results

To correlate these two datasets, data for similar fly ash levels are needed. Therefore, using the average Ca(OH)_2 level for the cementitious paste at 91 days from **Fig. 5.2**, **Eq. 5.1** is developed to predict Ca(OH)_2 in cementitious paste based on fly ash level. Using **Eq. 5.1**, Ca(OH)_2 levels in paste at 15, 30, and 45% fly ash are calculated and plotted against the average Ca(OH)_2 measured in the concrete specimens. This plot is presented in **Fig. 5.4** and the TGA paste-concrete correlation is presented in **Eq. 5.2**. The reason why the relationship between the two amounts is not a simple ratio with the line passing through the origin is unclear. While **Eq. 5.2** is useful in order to understand the correlation of these datasets, caution should be exercised when extending this correlation to other work. Suraneni and Weiss [22] showed that coarse aggregate content impacts Ca(OH)_2 amounts in concrete. Other factors that may impact comparative analysis include filler effects due to the fine and coarse aggregates, differences in mixing techniques, and the congregation of Ca(OH)_2 around the interfacial transition zone. Further, when using limestone aggregates, such as in this study, no carbonation influence can be accounted for when determining Ca(OH)_2 [34].

$$y = -0.183x + 14.851 \qquad \text{Eq. 5.1}$$

$$y = \text{Ca(OH)}_2 \text{ in paste (g/100 g paste)}$$

$$x = \text{Fly ash level in paste (\% mass)}$$

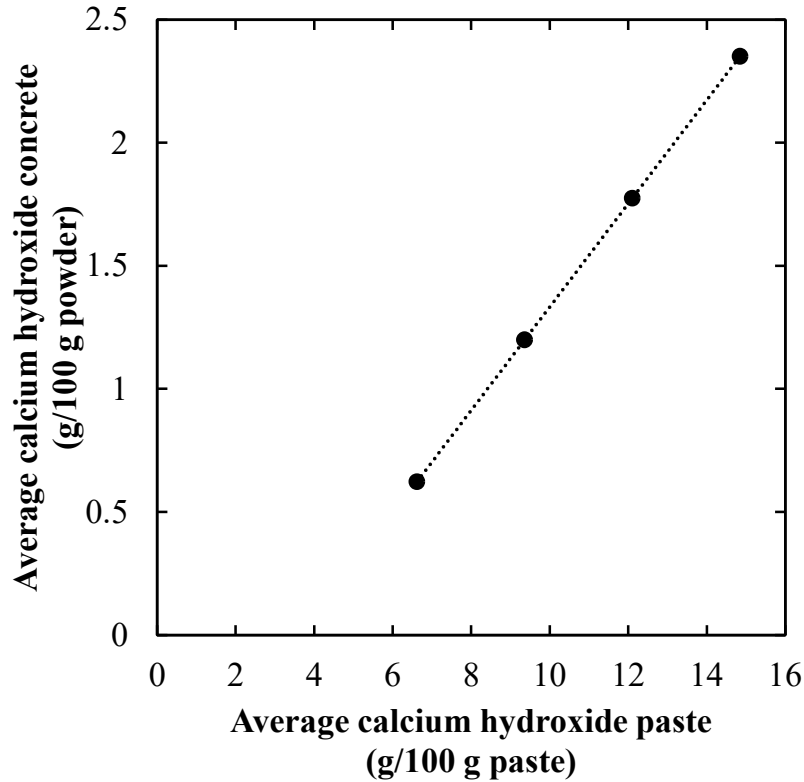


Figure 5.4. Correlated average $\text{Ca}(\text{OH})_2$ concrete and paste data.

$$y = 0.21x - 0.765$$

Eq. 5.2

$$y = \text{Ca}(\text{OH})_2 \text{ in concrete (g/100 g powder)}$$

$$x = \text{Ca}(\text{OH})_2 \text{ in paste (g/100 g paste)}$$

Presented in **Fig. 5.5** is the influence of the fly ash when comparing $\text{Ca}(\text{OH})_2$ levels in the paste and concrete samples at 91 days. The c/p is a ratio of $\text{Ca}(\text{OH})_2$ in the concrete (c) and $\text{Ca}(\text{OH})_2$ in the paste (p). A corresponding theoretical c/p value is also provided on **Fig. 5.5** as a solid black line. This line represents the reduction in expected $\text{Ca}(\text{OH})_2$ due to the reduced portions of cementitious products in concrete when compared with cementitious paste. For this investigation, the paste portion of the concrete samples (i.e., cement, fly ash, and water) ranged from 21.5% paste (mass) to 21.8% based on the varying fly ash levels. As the fly ash

replacement in the samples increases, there is a greater reduction in the measurable Ca(OH)_2 in the concrete specimens compared to the paste specimens. While it is expected that this ratio of Ca(OH)_2 in cement paste and concrete would be consistent at each fly ash level, the concrete calcium hydroxide values are extremely small, especially at high fly ash levels. These small values could lead to variability and errors, which combined with potential carbonation and a slight increase in paste volume (given that cement was replaced based on mass with fly ash) at increased fly ash levels could explain the deviation from the theoretical c/p. Further work is needed to validate differences in paste and concrete calcium hydroxide and how these differences are affected by fly ash.

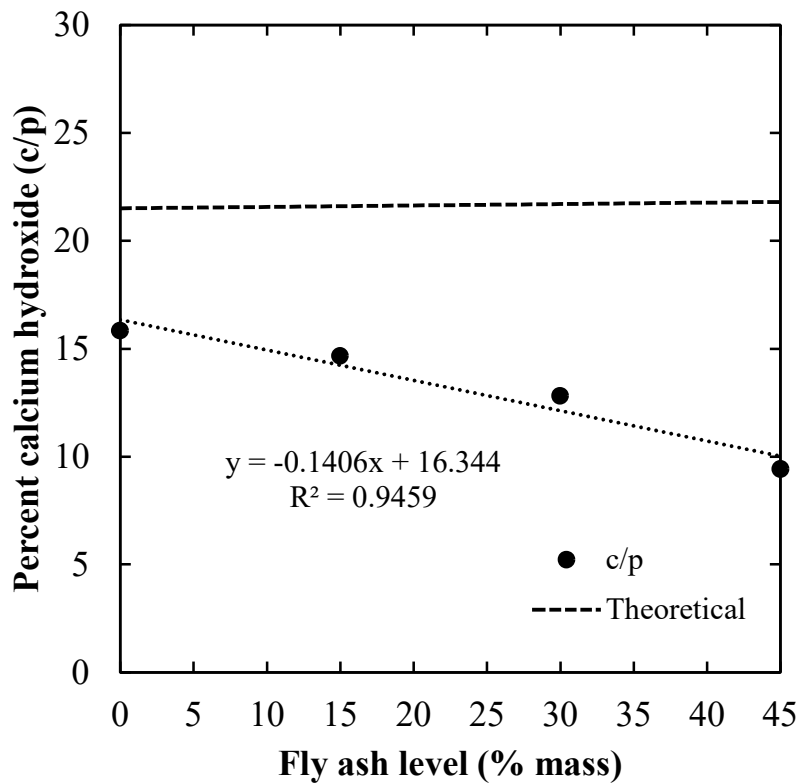


Figure 5.5. Percentage of Ca(OH)_2 measured in concrete (c) compared to Ca(OH)_2 measured in paste (p) at each cement replacement level with fly ash (0, 15, 30, and 45%).

5.3.2. Low-Temperature Differential Scanning Calorimetry Test Data

5.3.2.1. Paste and Concrete LT-DSC Data

Using data from **Table 5.2**, CAOXY levels in the cementitious paste are presented in **Fig. 5.6**.

From this data, it is observed that as cement is replaced with fly ash, a decrease in measured CAOXY is observed. This is in good accordance with the literature [14,20,21]. As discussed in **Section 5.3.1.1**, SCMs mitigate CAOXY through dilution and pozzolanic reaction. A black line representing dilution and red dashed line representing the current CAOXY threshold in cementitious paste shown in **Fig. 5.6**. The threshold is 15 g/100 g paste as given in AASHTO PP 84 [23].

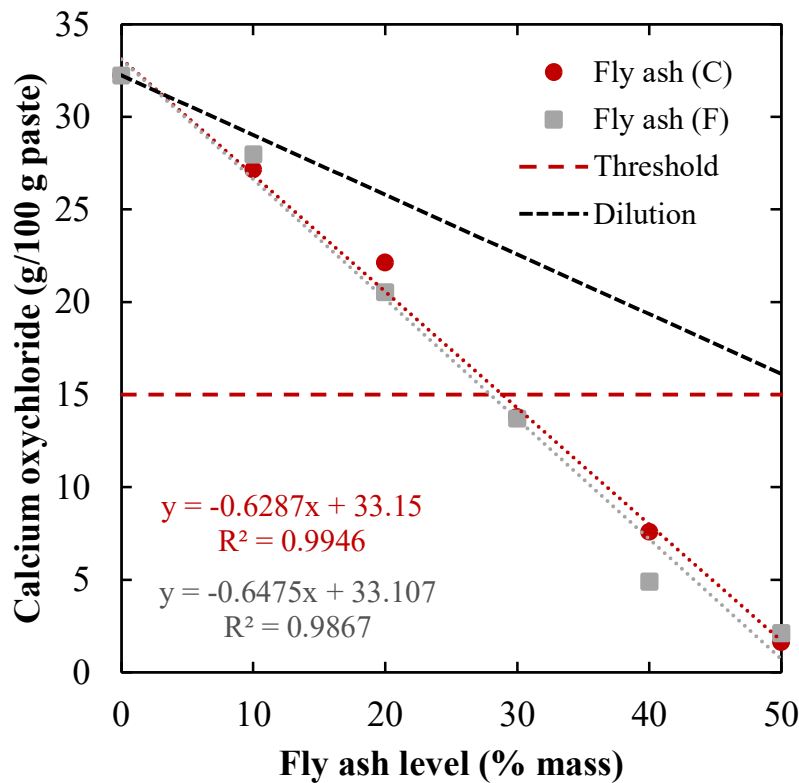
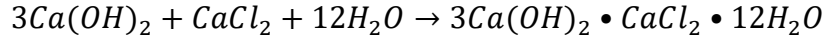


Figure 5.6. Calcium oxychloride levels in the cementitious paste samples cast with varying levels of fly ash.

The concrete LT-DSC data are presented in **Fig. 5.7**. As expected, based on the Ca(OH)_2 data, there is a decrease in CAOXY content in the concrete as cement is replaced with increasing levels of fly ash. Data are divided into Class C and Class F fly ash for comparison with linear trends provided. It is observed that a difference of approximately 7% exists between the slopes of these trend lines. The greater slope, found for the Class F fly ash, indicates a greater potential for Class F to suppress CAOXY than Class C fly ash; however, at 15 and 30% cement replacement levels, the Class C fly ash is more effective at reducing CAOXY levels. While there is some difference between the different fly ash types, possibly dependent upon CaO content, the impact of varying fly ash types compared to changing replacement level or using an inert filler (characterized by dilution in **Fig. 5.3**) is low. The impact of additional materials in the mixtures (i.e., fine and coarse aggregates) compared to paste may also cause some of the differences observed between the different fly ash types.

The data presented in **Fig. 5.7** do not follow the theoretical stoichiometric predictions for CAOXY based on the concrete Ca(OH)_2 levels from **Fig. 5.3**. The reaction governing the formation of the most common form of CAOXY is given in **Eq. 5.3**. From stoichiometry, for every 1 g $\text{Ca(OH)}_2/100$ g powder measured, 2.47 g CAOXY/100 g powder is expected. Using this relationship, a “predicted” or theoretical line is provided in **Fig. 5.7** indicating the expected CAOXY based on the average measured Ca(OH)_2 data. The measured CAOXY levels are much higher than the predicted CAOXY. Given that the powder used for the TGA and LT-DSC analysis is from the same sample, this discrepancy was not expected; however, the data are reported as measured. At this time, the authors are not aware of any potential error that could have caused these differences. As noted in **Section 5.3.1.1**, a correction could not be made in the Ca(OH)_2 data for potential carbonation since limestone aggregate was used; however, if

carbonation did significantly reduce the measured Ca(OH)_2 levels in the TGA data, then a reduction in CAOXY levels would also be expected given that they are from the same powder sample. The TGA data is in good accordance with similar work in Suraneni and Weiss [26], but the measured concrete LT-DSC data appear to be higher than those in Suraneni and Weiss. However, Suraneni and Weiss [22] only carried out very limited testing using LT-DSC to test concrete specimens. They reported a CAOXY level of 2.79 g/100 g powder for cement only concrete specimens; however, this value is lower than expected based on stoichiometric analysis as the equivalent Ca(OH)_2 level was reported to be 2.56 g/100 g powder. The expected CAOXY level (assuming all Ca(OH)_2 reacted to form CAOXY) would be 6.32 g/100 g powder. The authors hypothesized a potential for aggregates to influence/entrap Ca(OH)_2 rendering it unavailable for reaction, however evidence for the same was not presented [22]. However, in this present study, the CAOXY quantities were measured to be higher than expected rather than lower. Wang et al. [9] also used LT-DSC to measure CAOXY levels in concrete. From Wang et al. [9], CAOXY levels in concrete were reported to be as high as 58.6 g/100 g paste; however, it should be noted that CAOXY is reported in g/100 g paste instead of g/100 g powder as shown in this work. The powder collected for analysis in Wang et al. [9] intentionally excluded coarse aggregate from the powder sample and adjusted the CAOXY levels for the paste portion based on the w/cm, unit weight and paste content. In removing coarse aggregate from the test powder, higher CAOXY levels are expected when compared with the work of Suraneni and Weiss [22] and this present work. Though reported data differ significantly across the literature, the extent of data is limited, and it is clear that the introduction of aggregates along with test methodology complicates concrete CAOXY measurement and measured CAOXY values are significantly impacted.



Eq. 5.3

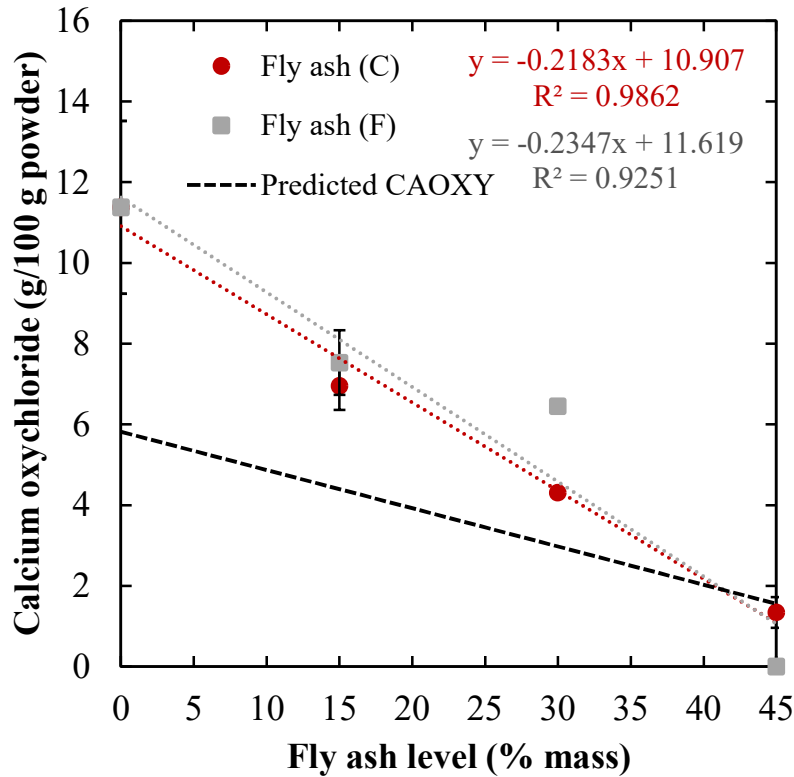


Figure 5.7. Calcium oxychloride levels in concrete specimens cast with varying levels of fly ash.

5.3.2.2. Correlating Paste-Concrete LT-DSC Results

Similar to the $Ca(OH)_2$ data, equivalent cement replacement with fly ash levels are needed to correlate CAOXY between the cementitious paste and concrete. Therefore, average CAOXY levels in paste are used to develop Eq. 5.4 in order to predict CAOXY based on fly ash use in paste. Using Eq. 5.4, CAOXY levels in paste at 15, 30, and 45% fly ash are calculated and plotted against the average CAOXY measured in the concrete specimens. This plot is presented on Fig. 5.8; however, as noted in Section 5.3.2.1 there is a significant difference between measured and predicted CAOXY levels. Therefore, the stoichiometric predictions (using data from Fig. 5.3) are also plotted on Fig. 5.8.

Using the stoichiometric predictions, the LT-DSC paste-concrete correlation is presented in **Eq. 5.5**. This correlation could be used to estimate CAOXY in concrete using the simpler paste analysis; however, this relationship should be refined using updated experimental results. Currently, the proposed limit to mitigate CAOXY based on LT-DSC of paste specimens is 15 g/100 g paste [23]. However, this threshold has only tentatively been linked to damage in concrete [9]. With a correlation equation to estimate CAOXY in concrete based on paste data, CAOXY deterioration in concrete specimens can be investigated to refine the current paste limit while also providing a proposed concrete CAOXY limit. This equation would be a powerful tool for designers and the concrete industry to develop concrete pavements protected against CAOXY deterioration. It should be noted that the same impact of aggregates, paste content in the concrete, and testing methodology are applicable as discussed in **Section 5.3.1.1**. Further, in paste, CAOXY levels determined by LT-DSC could represent a “worse-case” scenario as the sample is finely ground maximizing the potential for CAOXY formation [21]. In hardened concrete specimens, the ability of Ca(OH)₂ to react with deicing solutions may be lower as the reactants are not as readily available as in the finely ground LT-DSC samples.

$$y = -0.663x + 31.97 \qquad \text{Eq. 5.4}$$

y = CAOXY in paste (g/100 g paste)

x = Fly ash level in paste (% mass)

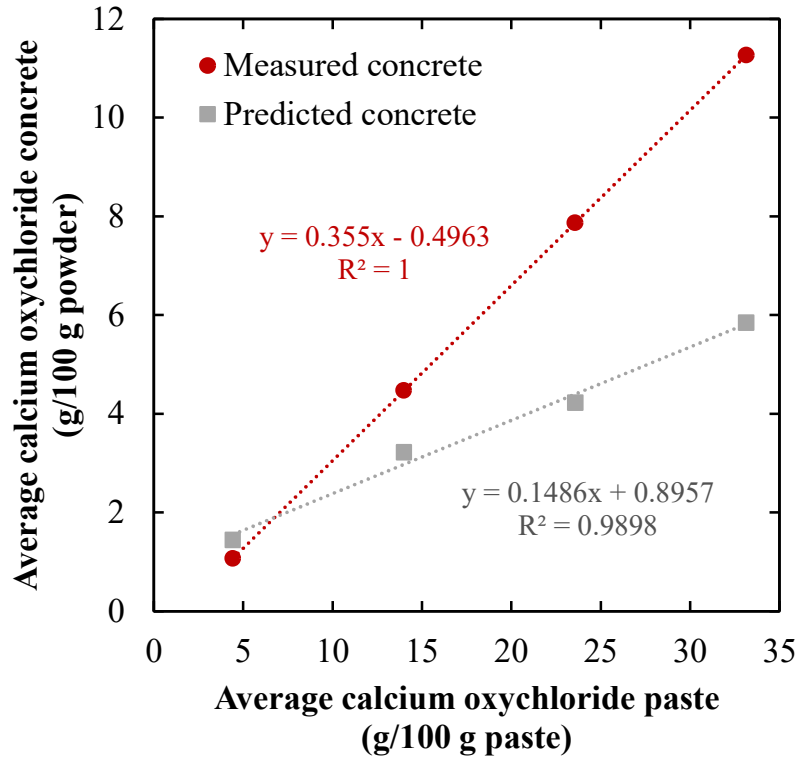


Figure 5.8. Correlated calcium oxychloride levels in cementitious paste and concrete.

$$y = 0.1486x + 0.8957 \quad \text{Eq. 5.5}$$

$$y = \text{CAOXY in concrete (g/100 g powder)}$$

$$x = \text{CAOXY in paste (g/100 g paste)}$$

Presented in **Fig. 5.9** is the influence of fly ash on CAOXY levels in concrete and paste samples.

The impact of fly ash is roughly linear and the percent CAOXY when comparing paste and concrete decreases as the fly ash level increases. The ratio of c/p is given for the measured data as red dots with a red dashed trendline. Further, a theoretical solid black line is given to show the anticipated adjustment in the CAOXY levels when comparing paste and concrete due to the impact of aggregates. Measured CAOXY levels in this work are higher than anticipated for the concrete samples. This is in good accordance with data from **Fig. 5.8** which shows that the measured CAOXY levels are above the stoichiometrically predicted levels using Ca(OH)_2 as the

limiting reactant. Therefore, a predicted c/p is also provided. In order to develop the predicted ratio, Ca(OH)_2 levels in the cementitious paste were converted to CAOXY using 2.47 g CAOXY/100 g paste for every 1 g Ca(OH)_2 /100 g paste. The measured Ca(OH)_2 in the concrete was converted to CAOXY and the c/p was calculated with these two correlated CAOXY levels. The predicted c/p is plotted as grey blocks in **Fig. 5.9** with a grey trendline. The predicted c/p shows lower levels of CAOXY in the concrete than just based on dilution of aggregate. This could support the theory that aggregates may bind/render Ca(OH)_2 inert from producing CAOXY in concrete [22]. The fit lines for the predicted and measured values of CAOXY are roughly parallel and vertically offset.

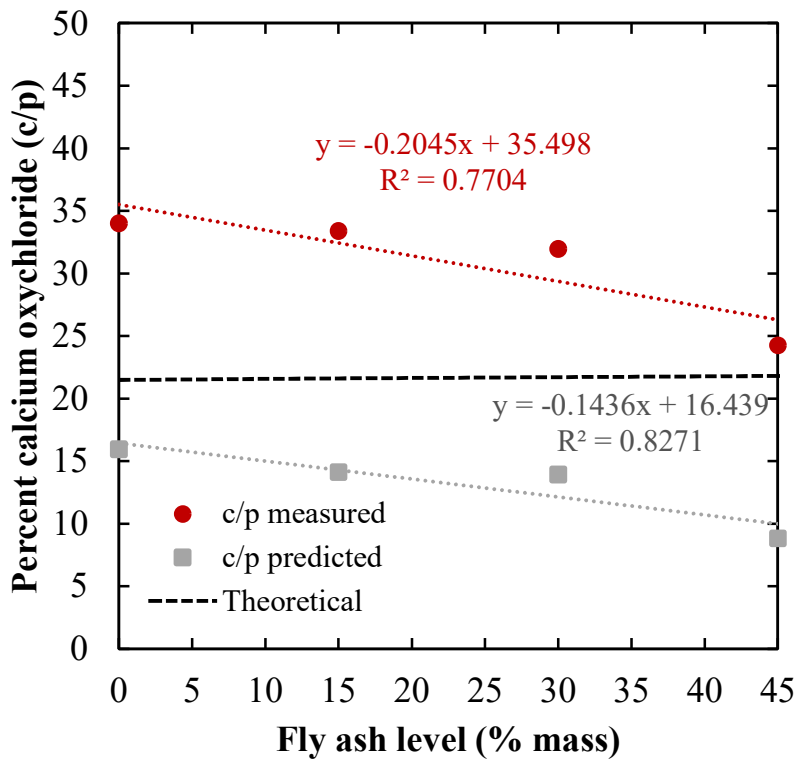


Figure 5.9. Percentage of CAOXY measured in concrete (c) compared to CAOXY measured in paste (p) at each cement replacement level with fly ash (0, 15, 30, and 45%).

5.3.3. Correlated Ca(OH)₂ Levels and Damage in Concrete

While developing correlations between the LT-DSC results of cementitious paste and concrete samples are important, using these data to determine expected deterioration in concrete is critical and has never been attempted before. In Jones et al. [16], results were divided into non-air entrained (NAE) concrete and air entrained (AE) concrete. Therefore, a correlation of compressive strength loss in conjunction with Ca(OH)₂ is presented with correlations based on NAE and AE concrete data. Given that there is a discrepancy between measured CAOXY levels using LT-DSC and predicted CAOXY levels based on stoichiometric calculations, the measured CAOXY levels were not correlated with damage in the specimens. However, a correlation is provided based on predicted CAOXY levels. It should be noted these correlations need to be further refined through continued experimental analysis, but do provide a basis for potential expected deterioration based on CAOXY levels in concrete.

5.3.3.1. Non-Air Entrained Concrete

A correlation is made between strength loss in NAE concrete specimens and Ca(OH)₂ levels in the concrete specimens. These results are presented in **Fig. 5.10**. It is observed that when Ca(OH)₂ is greater than 0.85 g/100 g powder, deterioration is observed in the concrete. While some minor (< 5%) strength loss is observed at Ca(OH)₂ levels below 0.85 g/100 g powder, this strength loss can be considered negligible and within normal deviations for compressive strength testing. Data within the shaded region indicates acceptable performance of concrete mixtures exposed to CaCl₂ deterioration. From **Fig. 5.3**, approximately 39% fly ash is needed to reduce Ca(OH)₂ levels below 0.85 g/100 g powder. Currently, AASHTO PP 84 [23] recommends cement be replaced by SCM at a replacement level of 30% or greater when CAOXY deterioration is possible; however, this recommendation is typically in conjunction with an air

content of 5 – 8 %. Therefore, these results seem in good accordance with this recommendation given that these are NAE specimens. It should be noted, however, that currently, no laboratory procedures have been established to determine the impact of CAOXY on concrete pavements. Therefore, differences in testing methodology may determine the findings presented here ineffective if a more aggressive/significantly different test method is utilized.

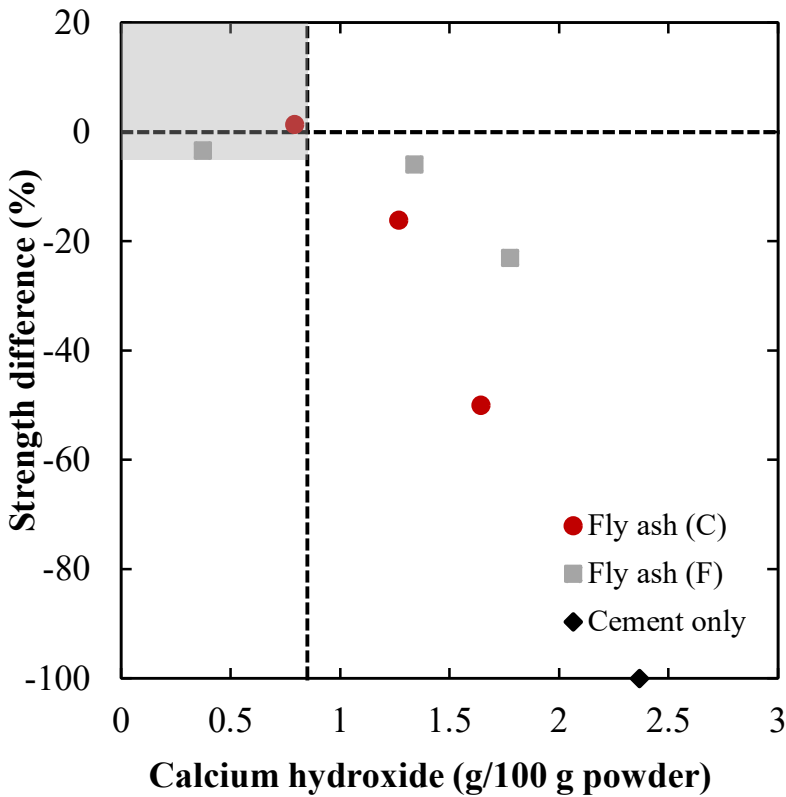


Figure 5.10. Correlated compressive strength difference and Ca(OH)_2 levels in NAE concrete specimens. Data are grouped at similar fly ash levels.

For comparison, paste and concrete Ca(OH)_2 and strength difference levels are presented in **Fig. 5.11**. Using the current CAOXY threshold of 15 g/100 g paste, an equivalent Ca(OH)_2 content of 8.3 g/100 g paste is the maximum limit to ensure protection against CAOXY deterioration [21]. However, as shown in **Fig. 5.11** some deterioration (~30% strength loss) is still observed in paste samples at this level while no strength loss is observed in the concrete specimens at 0.85

g/100 powder. Using **Eq. 5.2** and setting the concrete Ca(OH)_2 level to 0.85 g/100 g powder, the maximum paste Ca(OH)_2 at which no correlated damage is observed in concrete is 7.7 g/100 g powder. Using the current limit of 8.3 Ca(OH)_2 g/100 g paste, an equivalent expected Ca(OH)_2 level in concrete is 0.98 g/100 g powder which is more than 0.85 g/100 g powder. This shows that the current paste limit is unconservative when correlated with damage from NAE concrete specimens.

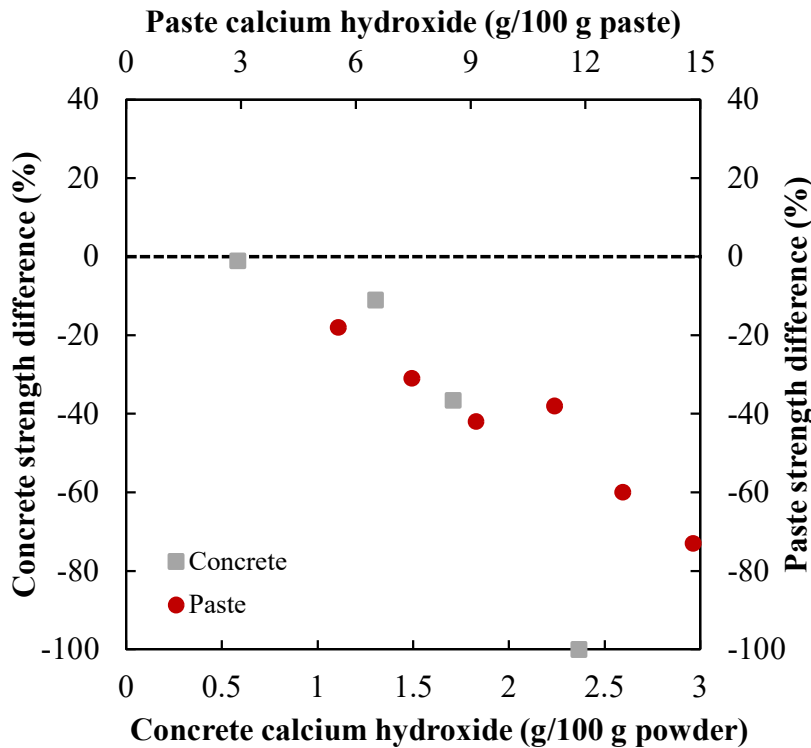


Figure 5.11. Comparison of paste and concrete compressive strength difference based on Ca(OH)_2 in NAE concrete specimens. Concrete data are plotted on the primary X-Y axis while paste data are plotted on the secondary X-Y axis.

As mentioned in **Section 5.3.3**, no correlation is given for the measured CAOXY levels.

However, the stoichiometrically predicted CAOXY levels are plotted against deterioration as provided in **Fig. 5.12**. In NAE concrete specimens, damage occurs at CAOXY levels above 2 g/100 g powder. Therefore, a proposed theoretical maximum CAOXY level in concrete could be

2 g/100 g powder. The shaded region indicates good performance of concrete mixtures with minor strength loss being less than 5%. When used in Eq. 5.5, the correlated CAOXY level in paste is 7.4 g/100 g paste. This is much lower than the AASHTO PP 84 [23] of 15 g/100 g paste; however, this value needs refinement based on experimental analysis. Suraneni and Weiss [22] found that actual CAOXY levels in concrete and mortar are lower than stoichiometric predictions due to potential aggregate interactions in the experimental analysis; therefore, this current proposed maximum theoretical limit should be used with caution until further refinement is available from experimental research.

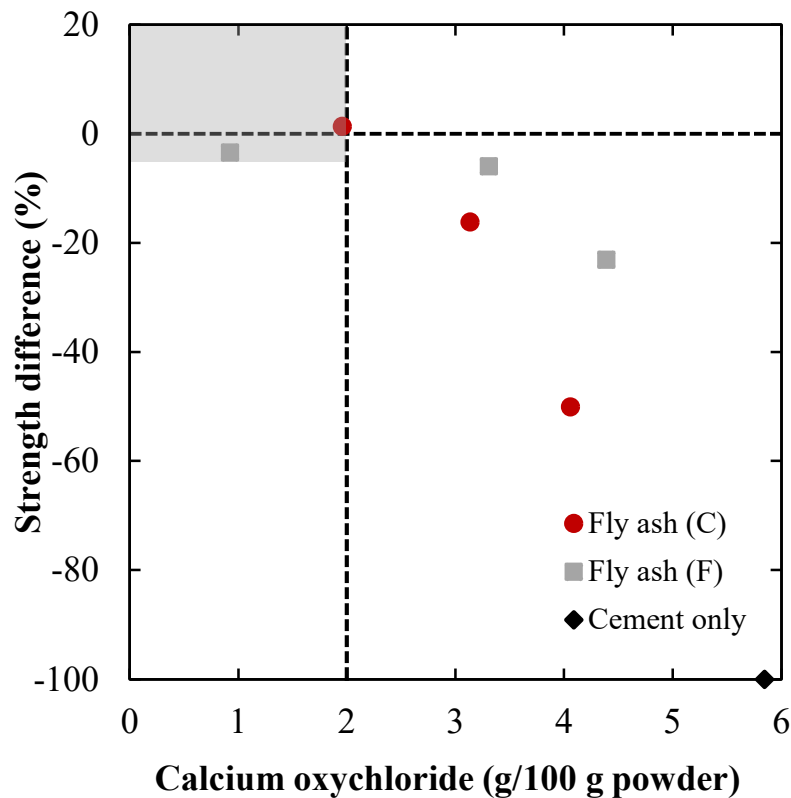


Figure 5.12. Stoichiometric CAOXY levels correlated with compressive strength loss in NAE concrete.

5.3.3.2. Air Entrained Concrete

For the AE concrete specimens, correlated $\text{Ca}(\text{OH})_2$ and compressive strength differences are presented in **Fig. 5.13**. Adequate concrete performance is highlighted by the shaded region. It is observed that when $\text{Ca}(\text{OH})_2$ values are below 1.5 g/100 g powder, deterioration due to CAOXY is mitigated. This is a 50% increase in $\text{Ca}(\text{OH})_2$ content for similar CAOXY mitigation when compared to the NAE specimens which shows the influence of air in preventing CAOXY deterioration. Using **Fig. 5.3**, a cement replacement of approximately 25% is adequate to mitigate $\text{Ca}(\text{OH})_2$ below 1.5 g/100 g powder. This is lower than the AASHTO PP 84 [23] recommendation minimum of 30% SCM indicating that the current recommendation is conservative; however, as discussed in **Section 5.3.3.1**, differences in test methodologies could impact these results.

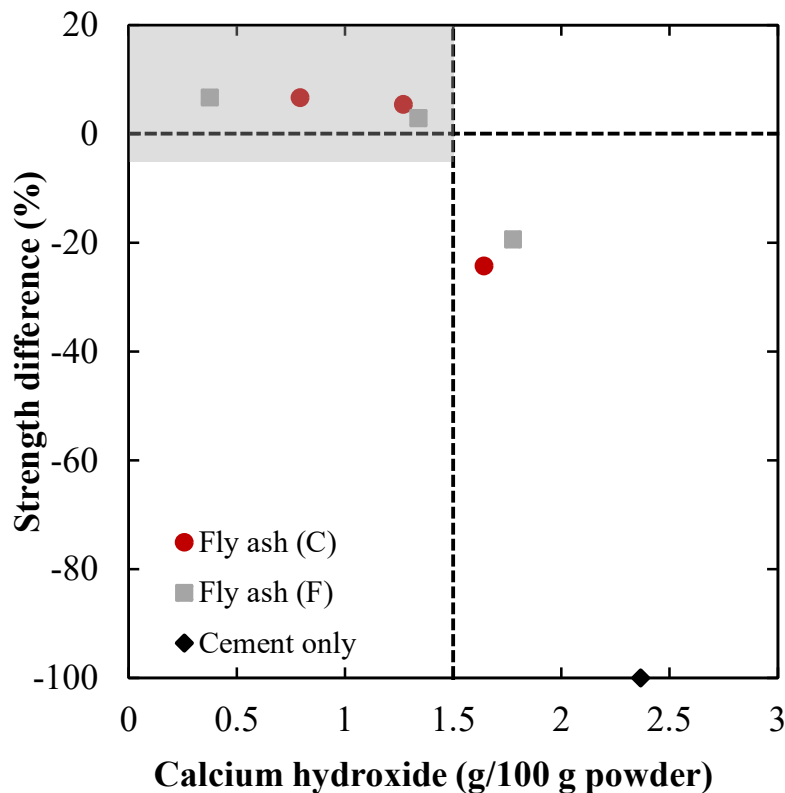


Figure 5.13. Correlated $\text{Ca}(\text{OH})_2$ levels and compressive strength difference in AE concrete specimens. Data are grouped at similar fly ash levels.

Presented in **Fig. 5.14** are data comparing compressive strength loss of paste and AE concrete with corresponding Ca(OH)_2 levels. It should be noted that the paste was cast without air; however, since TGA uses ground specimen samples, the use of air should not impact Ca(OH)_2 levels significantly. Using **Eq. 5.2** and setting the concrete CAOXY level to 1.5 g/100 g powder, the predicted paste level is 10.7 g/100 g paste at which concrete is protected against CAOXY. As discussed in **Section 5.3.3.1**, the Ca(OH)_2 threshold is 8.3 g/100 g paste for cementitious paste samples. This indicates that the current paste Ca(OH)_2 threshold is conservative based on deterioration in concrete specimens.

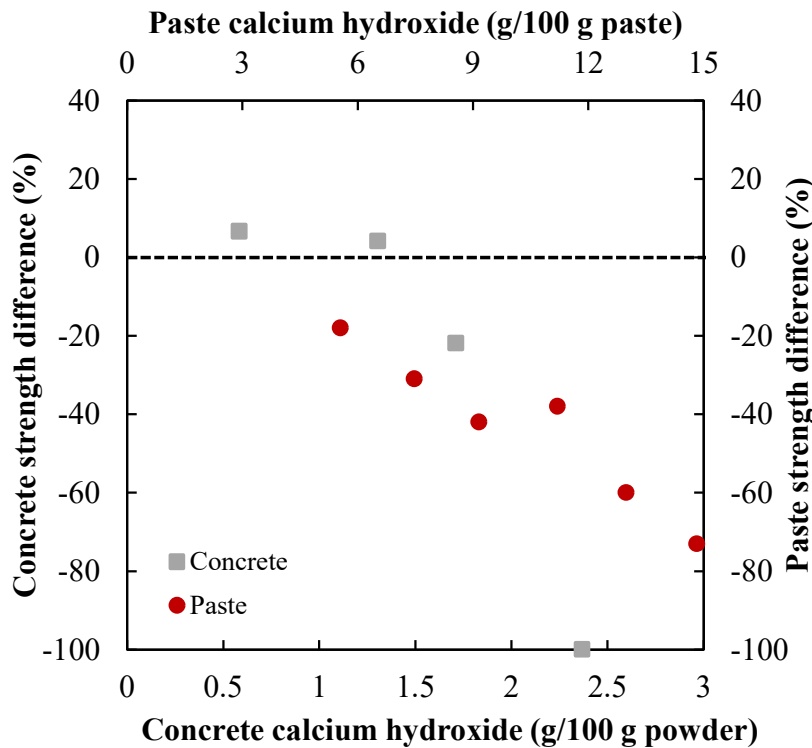


Figure 5.14. Comparison of paste and concrete compressive strength difference based on Ca(OH)_2 in AE concrete specimens. Concrete data are plotted on the primary X-Y axis while paste data are plotted on the secondary X-Y axis.

Similar to the NAE concrete, the stoichiometrically predicted CAOXY levels for the AE concrete are plotted against deterioration and provided in **Fig. 5.15**. Adequate concrete

performance is highlighted by the shaded region. It is shown that a potential maximum theoretical upper limit to mitigate CAOXY deterioration in concrete is 3.5 g/100 g powder. This is a 1.5 g/100 g powder increase in CAOXY when compared with the NAE concrete. Using the proposed maximum threshold and comparing it with Eq. 5.5, a predicted paste CAOXY level of 17.5 g/100 g paste is calculated. This shows that the maximum theoretical upper limit is conservative when correlated with the current proposed 15 g CAOXY/100 g paste limit proposed in AASHTO PP 84 [23]. As shown in Collepari et al. [17] and Jones et al. [16], the air content can significantly mitigate CAOXY deterioration. This 3.5 g/100 g powder accounts for the impact of air in the concrete and could be a powerful tool to predict the impact of CAOXY deterioration in AE concrete. Again, further refinement of this limit is needed based on experimental data to determine the impact of aggregate on the predicted level.

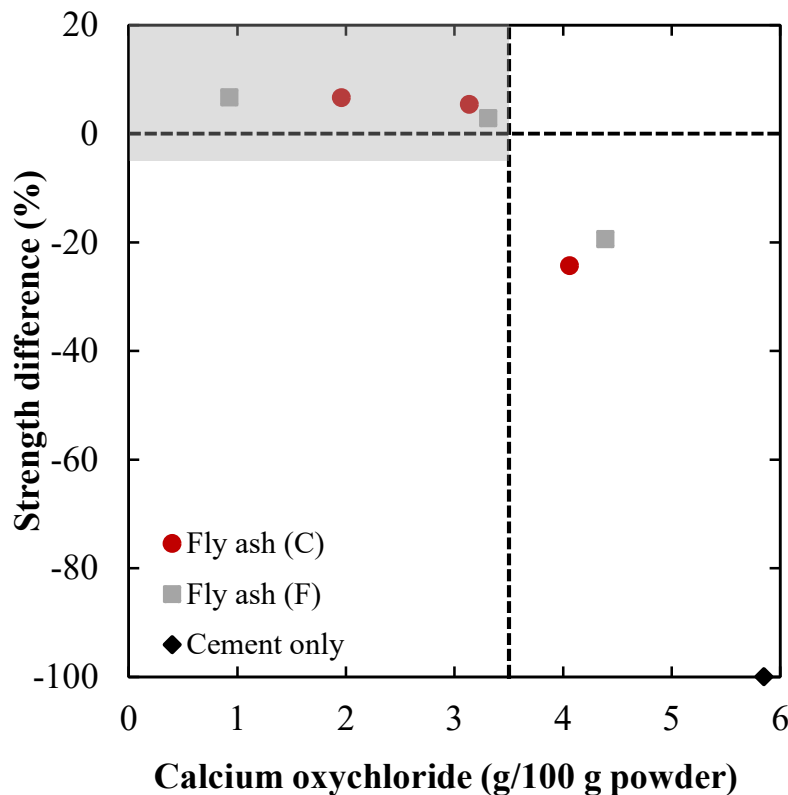


Figure 5.15. Stoichiometric CAOXY levels correlated with compressive strength loss in AE concrete.

5.4. Conclusions

In conclusion, an investigation has been presented correlating CAOXY levels/deterioration in cementitious paste and concrete samples. Currently, paste specimens have been investigated using analyses such as TGA and LT-DSC due to the ease of testing when compared with concrete. It is recommended in AASHTO PP 84 [23] that the CAOXY level be less than 15 g/100 g paste when testing cementitious paste; however, no threshold has been established for concrete. Further, the paste threshold has only tentatively been linked to deterioration in concrete [9]. Therefore, this work sought to correlate CAOXY levels in concrete using TGA and LT-DSC to levels in paste. Further, an analysis of concrete deterioration correlated with Ca(OH)_2 and stoichiometric CAOXY levels concrete is made. Findings for this investigation are summarized by the following:

- Ca(OH)_2 levels in concrete are reduced linearly as cement is replaced with fly ash. Further, Ca(OH)_2 values in paste and concrete are linearly correlated and captured by **Eq. 5.2**.
- CAOXY levels in concrete are reduced linearly as cement is replaced with fly ash. CAOXY levels in paste are linearly correlated with stoichiometric CAOXY levels in **Eq. 5.5**.
- In NAE concrete, Ca(OH)_2 levels should be less than 0.85 g/100 g powder (as measured by TGA) in order to mitigate damage due to CAOXY while AE concrete levels should be less than 1.5 g/100 g powder.
- In NAE concrete, a maximum theoretical upper CAOXY level is 2 g/100 g powder (based on stoichiometry) in order to mitigate damage due to CAOXY while a maximum theoretical upper CAOXY level for AE concrete is 3.5 g/100 g powder.

- For AE concrete specimens, it was shown that the AASHTO PP 84 [23] paste maximum CAOXY level of 15 g/100 g paste is conservative; however, for NAE specimens it is found to be unconservative.

This work provides insight into concrete deterioration due to CAOXY. The intent is to begin closing the gap between paste and concrete analyses in order to more fully understand the impact of this deterioration mechanism in concrete pavements. As noted, significant deviations from the testing methodology presented here could impact the results. Standard laboratory procedures for consistently testing CAOXY are needed to effectively establish CAOXY limits in concrete.

Declaration of Interests

The authors have no declaration of interests to state.

Acknowledgements

The authors would like to thank the support of the Oklahoma/Arkansas Chapter of the American Concrete Pavement Association for their generous gift supporting this research. Without their support this work would not be possible. The authors would also like to thank the Arkansas Department of Transportation for chemical analysis of the fly ash and cement for this project. The authors would also like to thank Boral Resources for providing the fly ash utilized in this research project. Many thanks are in order to the team at Iowa State University for their support in obtaining the TGA and LT-DSC data for the concrete samples.

References

1. H. Lee, R.D. Cody, A.M. Cody, P.G. Spry, Effects of various deicing chemicals on pavement concrete deterioration, Proceedings of the Mid-Continent Transportation Symposium, 2000, Ames, United States, pp. 151-155.
2. J. Jain, J. Olek, A. Janusz, D. Jozwiak-Niedzwiedzka, Effects of deicing salt solutions on physical properties of pavement concretes, Transp. Res. Rec. 2290 (2012) 69-75. <https://doi.org/10.3141/2290-09>.

3. A. Ghazy, M.T. Bassuoni, Resistance of concrete to different exposures with chloride-based salts, *Cem. Concr. Res.* 101 (2017) 144-158.
<https://doi.org/10.1016/j.cemconres.2017.09.001>.
4. C.B. Van Niejenhuis, C.M. Hansson, Detrimental effects of anti-icing brines on concrete durability, *Concr. Int.* 41 (11) (2019) 30-34.
5. J.J. Valenza II, G.W. Scherer, A review of salt scaling: I. Phenomenology, *Cem. Concr. Res.* 37 (7) (2007) 1007-1021. <https://doi.org/10.1016/j.cemconres.2007.03.005>.
6. J.J. Valenza II, G.W. Scherer, A review of salt scaling: II. Mechanisms, *Cem. Concr. Res.* 37 (7) (2007) 1022-1034. <https://doi.org/10.1016/j.cemconres.2007.03.003>.
7. S. Ahmad, Reinforcement corrosion in concrete structures, its monitoring and service life prediction – a review, *Cem. Concr. Comp.* 25 (4-5) (2003) 459-471.
[https://doi.org/10.1016/S0958-9465\(02\)00086-0](https://doi.org/10.1016/S0958-9465(02)00086-0).
8. ACI 201.3T-19, Joint deterioration and chloride-based deicing chemicals. American Concrete Institute, Farmington Hills, Michigan, 2019.
9. X. Wang, S. Sadati, P. Taylor, C. Li, X. Wang, A. Sha, Material characterization to assess effectiveness of surface treatment to prevent joint deterioration from oxychloride formation mechanism, *Cem. Concr. Comp.* 104 (2019) 103394.
<https://doi.org/10.1016/j.cemconcomp.2019.103394>.
10. C. Jones, S. Ramanathan, P. Suraneni, W.M. Hale, Calcium oxychloride: a critical review of the literature surrounding the formation, deterioration, testing procedures, and recommended mitigation techniques, *Cem. Concr. Comp.* 113 (2020) 103663.
<https://doi.org/10.1016/j.cemconcomp.2020.103663>.
11. J. Weiss, M.T. Ley, L. Sutter, D. Harrington, J. Gross, S.L. Tritsch, Guide to the prevention of and restoration of early joint deterioration in concrete pavements, Final Report for the Iowa Department of Transportation, TR-697, 2016.
12. G.A. Julio-Betancourt, Effect of de-icer and anti-icer chemicals on the durability, microstructure, and properties of cement based materials, University of Toronto, 2009, Ph.D. Thesis.
13. K. Peterson, G. Julio-Betancourt, L. Sutter, R.D. Hooton, D. Johnston, Observations of chloride ingress and calcium oxychloride formation in laboratory concrete and mortar at 5 °C, *Cem. Concr. Res.* 45 (2013) 79-90. <https://doi.org/10.1016/j.cemconres.2013.01.001>.
14. C. Qiao, P. Suraneni, J. Weiss, Flexural strength reduction of cement pastes exposed to CaCl₂ solutions, *Cem. Concr. Comp.* 86 (2018) 297-305.
<https://doi.org/10.1016/j.cemconcomp.2017.11.021>.

15. F. Traore, C. Jones, S. Ramanathan, P. Suraneni, W.M. Hale, Using compressive strength and mass change to verify the calcium oxychloride threshold in cementitious pastes with fly ash, *Constr. Build. Mater.* 296 (2021) 123640.
<https://doi.org/10.1016/j.conbuildmat.2021.123640>.
16. C. Jones, P. Suraneni, W.M. Hale, Investigating concrete deterioration due to calcium oxychloride formation, *Cem. Concr. Comp.* 2021. (Submitted).
17. M. Collepardi, L. Coppola, C. Pistolesi, Durability of concrete structures exposed to CaCl₂ based deicing salts, *Proceedings of the 3rd CANMET/ACI International Conference, 1994, Nice, France*, pp. 107-120.
18. J. Monical, C. Villani, Y. Farnam, E. Unal, J. Weiss, Using low-temperature differential scanning calorimetry to quantify calcium oxychloride formation for cementitious materials in the presence of calcium chloride, *Adv. Civ. Eng. Mater.* 5 (2) (2016) 142-156.
<https://doi.org/10.1520/ACEM20150024>.
19. P. Suraneni, J. Monical, E. Unal, Y. Farnam, J. Weiss, Calcium oxychloride formation potential in cementitious pastes exposed to blends of deicing salt, *ACI Mater. J.* 114 (4) (2017) 631-641. <http://dx.doi.org/10.14359/51689607>.
20. P. Suraneni, V.J. Azad, O.B. Isgor, W.J. Weiss, Use of fly ash to minimize deicing salt damage in concrete pavements, *Transp. Res. Rec.* 2629 (2017) 24-32.
<https://doi.org/10.3141/2629-05>.
21. P. Suraneni, V.J. Azad, O.B. Isgor, J. Weiss, Role of supplementary cementitious material type in the mitigation of calcium oxychloride formation in cementitious pastes, *J. Mater. Civ. Eng.* 30 (10) (2018) 04018248. [https://doi.org/10.1061/\(ASCE\)MT.1943-5533.0002425](https://doi.org/10.1061/(ASCE)MT.1943-5533.0002425).
22. P. Suraneni, J. Weiss, Extending low-temperature differential scanning calorimetry from paste to mortar and concrete to quantify the potential for calcium oxychloride formation, *Adv. Civ. Eng. Mater.* 7 (1) (2018) 1-16. <https://doi.org/10.1520/ACEM20170113>.
23. AASHTO PP 84-20, *Developing Performance Engineered Concrete Pavement Mixtures*, American Association of State Highway and Transportation Officials, Washington D.C., 2020.
24. AASHTO T 365-20, *Standard Method of Test for Quantifying Calcium Oxychloride Amounts in Cement Pastes Exposed to Deicing Salts*, AASHTO, Washington D.C., 2020.
25. ASTM C618-19, *Standard Specification for Coal Fly Ash and Raw or Calcined Natural Pozzolan for Use in Concrete*, ASTM International, West Conshohocken, PA, 2019.
26. ASTM C114-18, *Standard Test Method for Chemical Analysis of Hydraulic Cement*, ASTM International, West Conshohocken, PA, 2018.

27. ASTM C311/C311M-18, Standard Test Methods for Sampling and Testing Fly Ash or Natural Pozzolans for Use in Portland-Cement Concrete, ASTM International, West Conshohocken, PA, 2018.
28. Arkansas Department of Transportation. Standard specifications for highway construction. 2014. http://www.arkansashighways.com/standard_spec/2014/2014SpecBook.pdf.
29. ASTM C1872-18e2, Standard Test Method for Thermogravimetric Analysis of Hydraulic Cement, ASTM International, West Conshohocken, PA, 2018.
30. ASTM C109/C109M-20a, Standard Test Method for Compressive Strength of Hydraulic Cement Mortars (Using 2-in. or [50-mm] Cube Specimens), ASTM International, West Conshohocken, PA, 2020.
31. ASTM C39/C39M-20, Standard Test Method for Compressive Strength of Cylindrical Concrete Specimens, ASTM International, West Conshohocken, PA, 2020.
32. ASTM C78/C78M-18, Standard Test Method for Flexural Strength of Concrete (Using Simple Beam with Third-Point Loading), ASTM International, West Conshohocken, PA, 2018.
33. ASTM C157/C157M-17, Standard Test Method for Length Change of Hardened Hydraulic-Cement Mortar and Concrete, ASTM International, West Conshohocken, PA, 2017.
34. T. Kim, J. Olek, Effects of sample preparation and interpretation of thermogravimetric curves on calcium hydroxide in hydrated pastes and mortars, *Transp. Res. Rec.* 2290 (2012) 10-18. <https://doi.org/10.3141/2290-02>.
35. R. Snellings, Assessing, understanding and unlocking supplementary cementitious materials, *RILEM Tech. Lett.* 10 (2016) 50-55. <https://doi.org/10.21809/rilemtechlett.2016.12>.
36. E. Berodier, K. Scrivener, Understanding the filler effect on the nucleation and growth of C-S-H, *J. Am. Ceram. Soc.* 97 (12) (2014) 3764-3773. <https://doi.org/10.1111/jace.13177>.
37. P. Suraneni, W.J. Weiss, Examining the pozzolanicity of supplementary cementitious materials using isothermal calorimetry and thermogravimetric analysis, *Cem. Concr. Comp.* 83 (2017) 273-278. <https://doi.org/10.1016/j.cemconcomp.2017.07.009>.
38. P. Suraneni, A. Hajibabae, S. Ramanathan, Y. Wang, J. Weiss, New insights from reactivity testing of supplementary cementitious materials, *Cem. Concr. Comp.* 103 (2019) 331-338. <https://doi.org/10.1016/j.cemconcomp.2019.05.017>.
39. S. Ramanathan, M. Croly, P. Suraneni, Comparison of the effects that supplementary cementitious materials replacement levels have on cementitious properties, *Cem. Concr. Comp.* 112 (2020) 103678. <https://doi.org/10.1016/j.cemconcomp.2020.103678>.

40. L. Sutter, T. Van Dam, K.R. Peterson, D.P. Johnston, Long-term effects of magnesium chloride and other concentrated salt solutions on pavement and structural portland cement concrete phase I results, *Transp. Res. Rec.* 1979 (2006) 60-68.
<http://dx.doi.org/10.3141/1979-10>.

6. Conclusions and Additions to the Field of Knowledge

In conclusion, this work detailed an investigation into the current knowledge of CAOXY, mitigation strategies for both cementitious paste and concrete, deterioration due to CAOXY in both cementitious paste and concrete, and a correlation of CAOXY in both cementitious paste and concrete. This work is designed to begin closing the gap between laboratory paste research and field concrete deterioration. While this work does not fully accomplish this goal (as no field study was conducted), it does expand the current understanding of CAOXY deterioration in cementitious paste and concrete. Each chapter/individual work is summarized below.

6.1. Summary of Each Publication

6.1.1. Paper 1: Review of the Literature

- In **Chapter 2**, a review of the current state of knowledge surrounding CAOXY is presented. To the author's knowledge, this is the first review of the literature focusing on CAOXY formation in portland cement-based concrete.
- Testing techniques such as XRD, EDXS, ESEM, TGA, LT-DSC, and VCM are identified as novel methods to examine/quantify CAOXY formation.
- Mitigation techniques to prevent CAOXY formation/deterioration include the use of SCMs, proper air entrainment (5 – 8 %), alternative deicing materials, sealers, preferential carbonation, and bacteria known as *Sporosarcina pasteurii*. For concrete, the two most viable options identified are the use of SCMs in conjunction with an adequate air void system.
- Recommendations from this work include using 20-25% Class F fly ash replacement, 30-35% Class C fly ash replacement, or a 20% slag and 20% Class C fly ash

combination replacement of the cement content in conjunction with an air content of 6% or greater.

- Future research recommendations include determining the exact failure mechanism associated with CAOXY, validating the current paste threshold, developing new testing techniques, correlating the current paste threshold to concrete specimens, and determining changes in the absorption rate of chloride ions into paste specimens during the formation of CAOXY.

6.1.2. Paper 2: Alternative SCM Investigation

- In **Chapter 3**, an investigation into alternative SCMs for CAOXY mitigation is presented. To the author's knowledge this is the first investigation to use rice husk ash, bottom ash, limestone filler, sandstone filler, nepheline syenite filler, and silica flour as CAOXY mitigation. For comparison a traditional SCM, fly ash, is also investigated.
- It is shown that each material does mitigate CAOXY through dilution (i.e. reduced cement content), but only rice husk ash, bottom ash, and fly ash mitigate CAOXY by dilution and pozzolanic reaction. Further, rice husk ash is shown to be the most effective SCM for CAOXY mitigation from the alternative list tested.
- Compressive strength, TGA, and pozzolanic reactivity testing are compared to LT-DSC results to determine if alternative test methods can predict mitigation of CAOXY for each alternative SCM. It is shown that TGA is the most effective test method investigated to predict CAOXY mitigation based on SCM type.
- Ca(OH)_2 is shown to linearly correlated with CAOXY and can be used to predict CAOXY; however, not all Ca(OH)_2 is converted to CAOXY. Approximately 3 g/100 g

paste are unavailable for reaction with the deicing solution as it is bound in the hydration products of the cementitious paste.

6.1.3. Paper 3: Calcium Oxychloride Deterioration in Concrete

- Presented in **Chapter 4** is an investigation detailing concrete deterioration due to CAOXY formation. Specimens were investigated on strength change (compressive and flexural), mass change, length change, and chloride penetration. To the author's knowledge this is the first investigation into flexural strength change of concrete exposed to CAOXY deterioration.
- For both NAE specimens and AE specimens, compressive strength loss is reduced in concrete when exposed to a 30% CaCl_2 at 5 °C as cement is replaced with increasing levels of fly ash. For the NAE specimens up to 45% cement replacement with fly ash is needed to mitigate strength loss while 30% is required for the AE specimens.
- For the flexural strength specimens, strength loss is mitigated in both the NAE and AE concrete specimens at 15% cement replacement with fly ash; however, it should be noted some strength loss was still observed in the Class F fly ash samples at this level.
- A recommendation is made that when measuring mass change in deteriorated concrete samples, the unsound material should be removed prior to the measurement. It was shown that mass change was minimal when the unsound material remained attached to the "core" sound material, but increased greatly with its removal. For NAE specimens, 30% fly ash or greater was needed to mitigate damage while 15% fly ash or greater was needed for the AE specimens.
- Length change was not recommended for use to investigate CAOXY deterioration as the concrete surrounding the embedded gage stud can become loose causing errant

measurements or even complete removal of the gage stud. Length change measurements did tentatively show mitigation in expansion caused by CAOXY with increasing levels of cement replaced with fly ash; however, scatter in the data was larger than typically observed for length change measurements.

- Results of silver nitrate testing indicate that up to a 30% cement replacement fly ash mitigated chloride penetration, but that at levels beyond 30% reduced efficacy was observed.

6.1.4. Paper 4: Correlated Calcium Oxychloride Levels in Paste and Concrete

- In **Chapter 5**, a summation of previous work in conjunction with new concrete TGA and LT-DSC data are presented in order to correlate CAOXY levels in paste and concrete.
- Ca(OH)_2 levels in concrete are reduced linearly as cement is replaced with fly ash. Further, Ca(OH)_2 values in paste and concrete are linearly correlated as described by **Eq. 5.2**.
- CAOXY levels in concrete are reduced linearly as cement is replaced with fly ash. CAOXY levels in paste are linearly correlated with stoichiometric CAOXY levels in **Eq. 5.5**.
- In NAE concrete, Ca(OH)_2 levels should be less than 0.85 g/100 g powder (as measured by TGA) in order to mitigate damage due to CAOXY while AE concrete levels should be less than 1.5 g/100 g powder.
- In NAE concrete, a maximum theoretical upper CAOXY level is 2 g/100 g powder (based on stoichiometry) in order to mitigate damage due to CAOXY while a maximum theoretical upper CAOXY level for AE concrete is 3.5 g/100 g powder.

- For AE concrete specimens, it was shown that the AASHTO PP 84 paste maximum CAOXY level of 15 g/100 g paste is conservative; however, for NAE specimens it is found to be unconservative.

6.2. Additions to the Field of Knowledge

The additions to the field of knowledge regarding CAOXY in cementitious paste and concrete specimens are as follows:

- A succinct review of the literature is the first of its kind to holistically state what is known about CAOXY while also exposing gaps in the knowledge of this concrete pavement deterioration mechanism.
- Alternative SCMs (RHA, BA, LS, SS, NS, and SFL) were shown to aid in CAOXY mitigation. This is the first work to investigate these materials for CAOXY mitigation.
- This is the first work to investigate flexural strength loss in concrete exposed to CAOXY deterioration. This is of significance given that CAOXY predominantly impacts concrete pavements where flexural strength may be the governing design criteria as opposed to compressive strength. It was shown that less SCM is needed to mitigate flexural strength loss than in the compressive strength specimens.
- CAOXY mitigation is linearly correlated in concrete specimens as cement is replaced with fly ash. Previously, testing of concrete samples using LT-DSC to quantify CAOXY in concrete had focused on cement only samples. Now it is known that similar trends as observed in paste are observed in concrete as well regarding the use of fly ash.
- A correlation equation is developed for CAOXY in paste and concrete based on LT-DSC testing.

- This is the first work to analyze flexural strength change in concrete specimens exposed to CAOXY deterioration.
- This is the first work to recommend concrete CAOXY levels for potential inclusion in codes such as AASHTO PP 84. For NAE specimens, CAOXY should be less than 2 g/100 g powder while for AE specimens, CAOXY should be less than 3.5 g/100 g powder.

This work is designed to begin closing the gap between paste research and concrete deterioration. Though much work is still needed, this research provides data to reduce the work needed for this endeavor while also providing steps to continue closing this gap. The next major step forward is to begin linking laboratory deterioration with field deterioration in concrete pavements. This is the item needed to allow designers to confidently predict field deterioration based on laboratory analysis.

7. Complete Reference List

1. AASHTO PP 84-20, Developing Performance Engineered Concrete Pavement Mixtures, American Association of State Highway and Transportation Officials, Washington D.C., 2020.
2. AASHTO T 365-20, Standard Method of Test for Quantifying Calcium Oxychloride Amounts in Cement Pastes Exposed to Deicing Salts, AASHTO, Washington D.C., 2020.
3. ACI 201.2R-16, Guide to durable concrete. American Concrete Institute, Farmington Hills, Michigan, 2016.
4. ACI 201.3T-19, Joint deterioration and chloride-based deicing chemicals. American Concrete Institute, Farmington Hills, Michigan, 2019.
5. ACI 222.3R-11, Guide to design and construction practices to mitigate corrosion of reinforcement in concrete structures. American Concrete Institute, Farmington Hills, Michigan, 2011.
6. ACI 318R-19, Building Code Requirements for Structural Concrete and Commentary. American Concrete Institute, Farmington Hills, Michigan, 2019.
7. ASTM C39/C39M-20, Standard Test Method for Compressive Strength of Cylindrical Concrete Specimens, ASTM International, West Conshohocken, PA, 2020.
8. ASTM C78/C78M-18, Standard Test Method for Flexural Strength of Concrete (Using Simple Beam with Third-Point Loading), ASTM International, West Conshohocken, PA, 2018.
9. ASTM C109/C109M-16a, Standard Test Method for Compressive Strength of Hydraulic Cement Mortars (Using 2-in. or [50mm] Cube Specimens), ASTM International, West Conshohocken, PA, 2016.
10. ASTM C114-18, Standard Test Method for Chemical Analysis of Hydraulic Cement, ASTM International, West Conshohocken, PA, 2018.
11. ASTM C138/C138M-17a, Standard Test Method for Density (Unit Weight), Yield, and Air Content (Gravimetric) of Concrete, ASTM International, West Conshohocken, PA, 2017.
12. ASTM C143/C143M-20, Standard Test Method for Slump of Hydraulic-Cement Concrete, ASTM International, West Conshohocken, PA, 2020.
13. ASTM C157/C157M-17, Standard Test Method for Length Change of Hardened Hydraulic-Cement Mortar and Concrete, ASTM International, West Conshohocken, PA, 2017.

14. ASTM C192/C192M-18, Standard Practice for Making and Curing Concrete Test Specimens in the Laboratory, ASTM International, West Conshohocken, PA, 2018.
15. ASTM C231/C231M-17a, Standard Test Method for Air Content of Freshly Mixed Concrete by the Pressure Method, ASTM International, West Conshohocken, PA, 2017.
16. ASTM C305-14, Standard Practice for Mechanical Mixing of Hydraulic Cement Pastes and Mortars of Plastic Consistency, ASTM International, West Conshohocken, PA, 2014.
17. ASTM C311/C311M-18, Standard Test Methods for Sampling and Testing Fly Ash or Natural Pozzolans for Use in Portland-Cement Concrete, ASTM International, West Conshohocken, PA, 2018.
18. ASTM C511-19, Standard Specification for Mixing Rooms, Moist Cabinets, Moist Rooms, and Water Storage Tanks Used in the Testing of Hydraulic Cements and Concretes, ASTM International, West Conshohocken, PA, 2019.
19. ASTM C604-18, Standard Test Method for True Specific Gravity of Refractory Materials by Gas-Comparison Pycnometer, ASTM International, West Conshohocken, PA, 2018.
20. ASTM C618-19, Standard Specification for Coal Fly Ash and Raw or Calcined Natural Pozzolan for Use in Concrete, ASTM International, West Conshohocken, PA, 2019.
21. ASTM C1064/C1064M-17, Standard Test Method for Temperature of Freshly Mixed Hydraulic-Cement Concrete, ASTM International, West Conshohocken, PA, 2017.
22. ASTM C1872-18e2, Standard Test Method for Thermogravimetric Analysis of Hydraulic Cement, ASTM International, West Conshohocken, PA, 2018.
23. S. Ahmad, Reinforcement corrosion in concrete structures, its monitoring and service life prediction – a review, *Cem. Concr. Comp.* 25 (4-5) (2003) 459-471.
[https://doi.org/10.1016/S0958-9465\(02\)00086-0](https://doi.org/10.1016/S0958-9465(02)00086-0).
24. H.E. Álava, N. De Belie, G. De Schutter, Proposed mechanism for the formation of oxychloride crystals during sodium chloride application as a deicer salt in carbonated concrete, *Constr. Build. Mater.* 109 (2016) 188-197.
<https://doi.org/10.1016/j.conbuildmat.2016.01.047>.
25. F. Ameri, P. Shoaie, N. Bahrami, M. Vaezi, T. Ozbakkaloglu, Optimum rice husk ash content and bacterial concentration in self-compacting concrete, *Constr. Build. Mater.* 222 (2019) 796-813. <https://doi.org/10.1016/j.conbuildmat.2019.06.190>.
26. American Society of Civil Engineers, ASCE 2017 Infrastructure Report Card.
<https://www.infrastructurereportcard.org/>, 2017 (accessed 18 April 2019).

27. U. Angst, B. Elsener, C.K. Larsen, Ø. Vennesland, Critical chloride content in reinforced concrete – a review, *Cem. Concr. Res.* 39 (12) (2009) 1122-1138.
<https://doi.org/10.1016/j.cemconres.2009.08.006>.
28. C.A. Apostolopoulos, V.G. Papadakis, Consequences of steel corrosion on the ductility properties of reinforcement bar, *Constr. Build. Mater.* 22 (12) (2008) 2316-2324.
<https://doi.org/10.1016/j.conbuildmat.2007.10.006>.
29. C. Argiz, M.Á. Sanjuán, E. Menéndez, Coal bottom ash for portland cement production, *Adv. Mater. Sci. Eng.* 2017 (2017) 6068286. <https://doi.org/10.1155/2017/6068286>.
30. Arkansas Department of Transportation. Standard specifications for highway construction. 2014. http://www.arkansashighways.com/standard_spec/2014/2014SpecBook.pdf.
31. E.K. Attiogbe, Predicting freeze-thaw durability of concrete – a new approach, *ACI Mater. J.* 93 (5) (1996) 457-464.
32. F. Avet, R. Snellings, A.A. Diaz, M.B. Haha, K. Scrivener, Development of a new rapid, relevant and reliable (R^3) test method to evaluate the pozzolanic reactivity of calcined kaolinitic clays, *Cem. Concr. Res.* 85 (2016) 1-11.
<https://doi.org/10.1016/j.cemconres.2016.02.015>.
33. E. Bacarji, R.D. Toledo Filho, E.A.B. Koenders, E.P. Figueiredo, J.L.M.P. Lopes, Sustainability perspective of marble and granite residues as concrete fillers, *Constr. Build. Mater.* 45 (2013) 1-10. <https://doi.org/10.1016/j.conbuildmat.2013.03.032>.
34. L. Berntsson, S. Chandra, Damage of concrete sleepers by calcium chloride, *Cem. Concr. Res.* 12 (1982) 87-92.
35. E. Berodier, K. Scrivener, Understanding the filler effect on the nucleation and growth of C-S-H, *J. Am. Ceram. Soc.* 97 (12) (2014) 3764-3773. <https://doi.org/10.1111/jace.13177>.
36. A. Biolchini, What went wrong with M-6, the poster child for concrete failure. www.mlive.com/news/grand-rapids/index.ssf/2017/07/what_went_wrong_on_m-6_the_pos.html, 2017 (accessed 30 May 2019).
37. U.A. Birnin-Yauri, Chloride in cement: Study of the system $\text{CaO-Al}_2\text{O}_3\text{-CaCl}_2\text{-H}_2\text{O}$, University of Aberdeen, 1993, Ph.D. Thesis.
38. U.A. Birnin-Yauri, S. Garba, The effect and mechanism of chloride ion attack on portland cement concrete and the structural steel reinforcement, *IFE J. Sci.* 8 (2) (2006) 131-134.
<http://dx.doi.org/10.4314/ijs.v8i2.32211>.
39. U.A. Birnin-Yauri, F. Glasser, Chlorides in cement: Phase studies of the $\text{Ca(OH)}_2\text{-CaCl}_2\text{-H}_2\text{O}$ system, *Il Cemento* 88 (1991) 151-157.

40. R.H. Bogue, *The Chemistry of Portland Cement*, second ed., Reinhold Publishing Corporation, 1955.
41. S.V. Borisov, N.V. Podberezskaya, X-ray diffraction analysis: A brief history and achievements of the first century, *J. Struct. Chem.* 53 (1) (2012) 1-3.
<https://doi.org/10.1134/S0022476612070013>.
42. P. Brown, J. Bothe Jr., The system $\text{CaO-Al}_2\text{O}_3\text{-CaCl}_2\text{-H}_2\text{O}$ at 23 ± 2 °C and the mechanisms of chloride binding in concrete, *Cem. Concr. Res.* 34 (9) (2004) 1549-1553.
<https://doi.org/10.1016/j.cemconres.2004.03.011>.
43. Bureau of Transportation Statistics, 2017 North American Freight Numbers.
<https://www.bts.gov/newsroom/2017-north-american-freight-numbers>, 2017, (accessed 23 March 2020).
44. Bureau of Transportation Statistics, National Household Travel Survey Daily Travel Quick Facts. <https://www.bts.gov/statistical-products/surveys/national-household-travel-survey-daily-travel-quick-facts>, 2017, (accessed 23 March 2020).
45. Bureau of Transportation Statistics, Monthly transportation statistics.
<https://data.bts.gov/stories/s/m9eb-yevh#highway-travel> (accessed 19 January 2021).
46. H. Cai, X. Liu, Freeze-thaw durability of concrete: Ice formation process in pores, *Cem. Concr. Res.* 28 (9) (1998) 1281-1287. [https://doi.org/10.1016/S0008-8846\(98\)00103-3](https://doi.org/10.1016/S0008-8846(98)00103-3).
47. T. Celik, K. Marar, Effects of crushed stone dust on some properties of concrete, *Cem. Concr. Res.* 26 (7) (1996) 1121-1130. [https://doi.org/10.1016/0008-8846\(96\)00078-6](https://doi.org/10.1016/0008-8846(96)00078-6).
48. S. Chatterji, Mechanism of the CaCl_2 attack on portland cement concrete, *Cem. Concr. Res.* 8 (1978) 461-468.
49. S. Chatterji, A.D. Jensen, Studies of the mechanism calcium chloride attack on portland cement concrete, *Nordisk Beton* 19 (1975) 5-6.
50. R.D. Cody, A.M. Cody, P.G. Spry, G.-L. Gan, Experimental deterioration of highway concrete by chloride deicing salts, *Environ. Eng. Geosci.* 2 (4) (1996) 575-588.
<https://doi.org/10.2113/gseegeosci.II.4.575>.
51. M. Collepardi, L. Coppola, C. Pistolesi, Durability of concrete structures exposed to CaCl_2 based deicing salts, *Proceedings of the 3rd CANMET/ACI International Conference, 1994, Nice, France*, pp. 107-120.
52. M. Collepardi, S. Monosi, Effect of the carbonation process on the concrete deterioration by CaCl_2 aggression, *Proceedings of the 9th International Symposium on the Chemistry of Cement, 1992, New Delhi, India*, pp. 389-395.

53. B.L. Damineli, V.M. John, B. Lagerblad, R.G. Pileggi, Viscosity prediction of cement-filler suspensions using interference model: a route for binder efficiency enhancement, *Cem. Concr. Res.* 84 (2016) 8-19. <https://doi.org/10.1016/j.cemconres.2016.02.012>.
54. D. Darwin, J. Browning, L. Gong, S.R. Hughes, Effects of deicers on concrete deterioration, *ACI Mater. J.* 105 (6) (2008) 622-627.
55. J.W.C. Davis, Composition of crystalline deposit from a solution of magnesium and ammonium chloride, *Chem. News J. Phys. Sci.* 25 (1872) 258-259.
56. T. Demediuk, W.F. Cole, H.V. Hueber, Studies on magnesium and calcium oxychlorides, *Aust. J. Chem.* 8 (2) (1955) 215-233.
57. N. Ewers, Effect of magnesium chloride brine on road concrete, *Baustoffindustrie*, 22 (1967) 281-283. (In German)
58. Y. Farnam, Damage development, phase changes, transport properties, and freeze-thaw performance of cementitious materials exposed to chloride based salts, Purdue University, 2015, Ph.D. Thesis.
59. Y. Farnam, Calcium-munching bacteria could be a secret weapon against road salt eating away at concrete roads and bridges. <https://theconversation.com/calcium-munching-bacteria-could-be-a-secret-weapon-against-road-salt-eating-away-at-concrete-roads-and-bridges-113970>, 2019 (accessed 12 April 2019).
60. Y. Farnam, S. Dick, A. Wiese, J. Davis, D. Bentz, J. Weiss, The influence of calcium chloride deicing salt on phase changes and damage development in cementitious materials, *Cem. Concr. Comp.* 64 (2015) 1-15. <https://doi.org/10.1016/j.cemconcomp.2015.09.006>.
61. Y. Farnam, T. Washington, J. Weiss, The influence of calcium chloride salt solution on the transport properties of cementitious materials. *Adv. Civ. Eng.* (2015), 929864. <http://dx.doi.org/10.1155/2015/929864>.
62. Y. Farnam, A. Wiese, D. Bentz, J. Davis, J. Weiss, Damage development in cementitious materials exposed to magnesium chloride deicing salt, *Constr. Build. Mater.* 93 (2015) 384-392. <https://doi.org/10.1016/j.conbuildmat.2015.06.004>.
63. Y. Farnam, B. Zhang, J. Weiss, Evaluating the use of supplementary cementitious materials to mitigate damage in cementitious materials exposed to calcium chloride deicing salt, *Cem. Concr. Comp.* 81 (2017) 77-86. <https://doi.org/10.1016/j.cemconcomp.2017.05.003>.
64. I. Galan, L. Perron, F.P. Glasser, Impact of chloride-rich environments on cement paste mineralogy, *Cem. Concr. Res.* 68 (2015) 174-183. <https://doi.org/10.1016/j.cemconres.2014.10.017>.

65. R.M. Ghantous, Y. Farnam, E. Unal, J. Weiss, The influence of carbonation on the formation of calcium oxychloride, *Cem. Concr. Comp.* 73 (2016) 185-191. <https://doi.org/10.1016/j.cemconcomp.2016.07.016>.
66. A.A.M. Ghazy, *Concrete pavements: deterioration due to de-icing salts and repair*, University of Manitoba, 2017, Ph.D. Thesis.
67. A. Ghazy, M.T. Bassuoni, Resistance of concrete to different exposures with chloride-based salts, *Cem. Concr. Res.* 101 (2017) 144-158. <https://doi.org/10.1016/j.cemconres.2017.09.001>.
68. F.P. Glasser, J. Marchand, E. Samson, Durability of concrete – degradation phenomena involving detrimental chemical reactions, *Cem. Concr. Res.* 38 (2) (2008) 226-246. <https://doi.org/10.1016/j.cemconres.2007.09.015>.
69. C. Harvie, N. Moller, J. Weare, The prediction of mineral solubilities in natural waters: The Na-K-Mg-Ca-H-Cl-SO₄-OH-HCO₃-CO₂-H₂O system to high org ionic strengths at 25 °C, *Geochim. Cosmochim. Acta* 48 (4) (1984) 723-751. [https://doi.org/10.1016/0016-7037\(84\)90098-X](https://doi.org/10.1016/0016-7037(84)90098-X).
70. F. Häusler, H Schmidt, D. Freyer, Calcium hydroxide chlorides: The ternary system Ca(OH)₂-CaCl₂-H₂O at 25, 40, and 60 °C, phase stoichiometry and crystal structure, *J. Inorg. Gen. Chem.* 65 (10) (2019) 723-731. <https://doi.org/10.1002/zaac.201900051>.
71. I.M. Helmy, A.A. Amer, H. El-Didamony, Chemical attack on hardened pastes of blended cements-part 1: Attack of chloride solutions, *Zement-Kalk-Gips.*, 44 (1) (1991) 46-50.
72. K. Hornbostel, C.K. Larsen, M.R. Geiker, Relationship between concrete resistivity and corrosion rate – a literature review, *Cem. Concr. Comp.* 39 (2013) 60-72. <https://doi.org/10.1016/j.cemconcomp.2013.03.019>.
73. ICDD, Powder Diffraction File. <http://www.icdd.com/index.php/pdf-4/> (accessed 23 July 2019).
74. J. Jain, A. Janusz, J. Olek, D. Jozwiak-Niedzwiedzka, Physico-chemical changes in plain and fly ash modified concretes exposed to different deicing chemicals, *Proceedings of the 13th International Congress on Chemistry of Cement*, 2011, Madrid, Spain.
75. J. Jain, J. Olek, A. Janusz, D. Jozwiak-Niedzwiedzka, Effects of deicing salt solutions on physical properties of pavement concretes, *Transp. Res. Rec.* 2290 (2012) 69-75. <https://doi.org/10.3141/2290-09>.
76. J.K. Jang, H.G. Kim, J.H. Kim, J.S. Ryou, The evaluation of damage effects on MgO added concrete with slag cement exposed to calcium chloride deicing salt, *Mater.* 11 (5) (2018) 793. <https://dx.doi.org/10.3390%2Fma11050793>.

77. Jansen DJ, Snyder MB. Resistance of concrete to freezing and thawing. Strategic Highway Research Program SHRP-C-391 (1994) 1-217.
<http://onlinepubs.trb.org/onlinepubs/shrp/SHRP-C-391.pdf>.
78. A.E. Janusz, Investigation of deicing chemicals and their interaction with concrete materials, Purdue University, 2010, M.S.C.E. Thesis.
79. W. Jones, Y. Farnam, P. Imbrock, J. Sprio, C. Villani, M. Golias, J. Olek, W.J. Weiss, An overview of joint deterioration in concrete pavement: mechanisms, solution properties, and sealers, Purdue University (2013) pp. 1-69. <http://dx.doi.org/10.5703/1288284315339>.
80. C. Jones, W.M. Hale, The use of supplementary cementitious materials to reduce calcium oxychloride formation: a review of the literature, Proceedings of the 12th International PhD Symposium in Civil Engineering, 2018, Prague, Czech Republic, pp. 1121-1128.
81. C. Jones, S. Ramanathan, P. Suraneni, W.M. Hale, Calcium oxychloride: a critical review of the literature surrounding the formation, deterioration, testing procedures, and recommended mitigation techniques, *Cem. Concr. Comp.* 113 (2020) 103663.
<https://doi.org/10.1016/j.cemconcomp.2020.103663>.
82. C. Jones, P. Suraneni, W.M. Hale, Investigating concrete deterioration due to calcium oxychloride formation, *Cem. Concr. Comp.* 2021. (Submitted).
83. G.A. Julio-Betancourt, Effect of de-icer and anti-icer chemicals on the durability, microstructure, and properties of cement based materials, University of Toronto, 2009, Ph.D. Thesis.
84. G.A. Julio-Betancourt, R.D. Hooton, Calcium and magnesium chloride attack on cement-based materials: formation, stability, and effects of oxychlorides, Proceedings of the 2nd RILEM International Workshop on Concrete Durability and Service Life Planning - ConcreteLife'09, 2009, Haifa, Israel, pp. 432-439.
85. H. Justnes, K. De Weerd, M.R. Geiker, Chloride binding in concrete exposed to seawater and salt solutions, Proceedings of the 7th International Conference on Concrete Under Severe Conditions – Environment and Loading (CONSEC13), 2013, Nanjing, China, pp. 647-659.
86. T. Kim, J. Olek, Effects of sample preparation and interpretation of thermogravimetric curves on calcium hydroxide in hydrated pastes and mortars, *Transp. Res. Rec.* 2290 (2012) 10-18.
<https://doi.org/10.3141/2290-02>.
87. R.L. Kozikowski, P.C. Taylor, W.A. Pyc, Evaluation of potential concrete deterioration related to magnesium chloride (MgCl₂) deicing salt, PCA R&D Serial No. 2770, Skokie, Illinois, 2007.
88. R. Kuga, H. Mori, S. Ogawa, Synthesis and fundamental properties of 3CaO·CaCl₂·15H₂O causing CaCl₂ attack, and its formation in hardened cement paste exposed to CaCl₂ solution,

Proceedings of the 8th International Symposium on Cement and Concrete, 2013, Nanjing, China, pp. 1-7.

89. R. Kuga, H. Mori, S. Ogawa, K. Komatsu, Synthesis and fundamental property of $3\text{CaO}\cdot\text{CaCl}_2\cdot 15\text{H}_2\text{O}$ related to CaCl_2 attack. *Cem. Sci. Concr. Tech.* 65 (2011) 420-426. <https://doi.org/10.14250/cement.65.420>. (In Japanese)
90. P. Lawrence, M. Cyr, E. Ringot, Mineral admixtures in mortars: effect of inert materials on short-term hydration, *Cem. Concr. Res.* 33 (12) (2003) 1939-1947. [https://doi.org/10.1016/S0008-8846\(03\)00183-2](https://doi.org/10.1016/S0008-8846(03)00183-2).
91. M. Lawrence, H.E. Vivian, The action of calcium chloride on mortar and concrete, *Aust. J. Appl. Sci.* 11 (4) (1960) 490-498.
92. H. Lee, R.D. Cody, A.M. Cody, P.G. Spry, Effects of various deicing chemicals on pavement concrete deterioration, Proceedings of the Mid-Continent Transportation Symposium, 2000, Ames, United States, pp. 151-155.
93. C. Li, M.D.A. Thomas, J.H. Ideker, A mechanistic study on mitigation of alkali-silica reaction by fine lightweight aggregates, *Cem. Concr. Res.* 104 (2018) 13-24. <https://doi.org/10.1016/j.cemconres.2017.10.006>.
94. Z. Li, H.K. Venkata, P.R. Rangaraju, Influence of silica flour-silica fume combination on the properties of high performance cementitious mixtures at ambient temperature curing, *Constr. Build. Mater.* 100 (2015) 225-233. <https://doi.org/10.1016/j.conbuildmat.2015.09.042>.
95. C. Li, M. Wu, Q. Chen, Z. Jiang, Chemical and mineralogical alterations of concrete subjected to chemical attacks in complex underground tunnel environments during 20–36 years, *Cem. Concr. Comp.* 86 (2018) 139-159. <https://doi.org/10.1016/j.cemconcomp.2017.11.007>.
96. H.S. Lukens, The composition of magnesium oxychloride, *J. Am. Chem. Soc.* 54 (6) (1932) 2372–2380. <https://doi.org/10.1021/ja01345a026>.
97. S.Z. Makarov, I.I. Vol'nov, Figure 2061-System $\text{Ca}(\text{OH})_2\text{-CaCl}_2\text{-H}_2\text{O}$, in: C. Robbins (Ed.), *Phase Diagrams Ceram*, Vol. 1, American Ceramic Society, Westerville, OH, 1964, p. 567.
98. O.A. Markova, Physical chemistry of calcium hydroxide chlorides, *Russ. J. Phys. Chem.* 47 (1973) 608.
99. P.K. Mehta, P.J.M. Monteiro, *Concrete: Microstructure, Properties, and Materials*, third ed., McGraw Hill Education, New York, 2006.
100. J. Monical, E. Unal, T. Barrett, Y. Farnam, W.J. Weiss, Reducing joint damage in concrete pavements: quantifying calcium oxychloride formation, *Transp. Res. Rec.* 2577 (2016) 17-24. <https://doi.org/10.3141/2577-03>.

101. J. Monical, C. Villani, Y. Farnam, E. Unal, J. Weiss, Using low-temperature differential scanning calorimetry to quantify calcium oxychloride formation for cementitious materials in the presence of calcium chloride, *Adv. Civ. Eng. Mater.* 5 (2) (2016) 142-156. <https://doi.org/10.1520/ACEM20150024>.
102. S. Monosi, A. Alvera, M. Collepardi, Chemical attack of calcium chloride on the portland cement paste, *Il Cemento* 86 (2) (1989) 97-104.
103. S. Monosi, M. Collepardi, Research on $3\text{CaO}\cdot\text{CaCl}_2\cdot 15\text{H}_2\text{O}$ identified in concretes damaged by CaCl_2 attack, *Il Cemento* 87 (1990) 3-8.
104. S. Monosi, M. Collepardi, Chemical attack of magnesium chloride on the portland cement paste, *Il Cemento* 90 (3) (1993) 169-173.
105. H. Mori, R. Kuga, S. Ogawa, Y. Kubo, Chemical deterioration of hardened cement pastes immersed in calcium chloride solution, *Proceedings of the 3rd International Conference on Sustainable Construction Materials and Technologies*, 2013, Kyoto, Japan, Paper 329.
106. G. Moriconi, M. Pauri, I. Alvera, M. Collepardi, Damage of concrete by exposure to calcium chloride, *Proceedings of the 2nd International Conference on Engineering Materials: From Research Applications to Design*, 1988, Bologna, Italy, pp. 20-23.
107. B.T. Mussato, O.K. Gepraegs, G. Farnden, Relative effects of sodium chloride and magnesium chloride on reinforced concrete: State of the art. *Transp. Res. Rec.* 1866 (2004) 59-66. <https://doi.org/10.3141/1866-08>.
108. National Academies of Sciences, Engineering, and Medicine 2004. *Snow and Ice Control: Guidelines for Materials and Methods*, Washington, DC: The National Academies Press. <https://doi.org/10.17226/13776>.
109. A.M. Neville, Behavior of concrete in saturated and weak solutions of magnesium sulfate or calcium chloride, *J. Mater.* 4 (4) (1969) 781-816.
110. R. Obersted-Patdberg, Degradation of cements by magnesium brine, *Proceedings of the 7th International Conference on Cement Microscopy*, 1985, Duncanville, United States, pp. 24-36.
111. T. Oey, A. Kumar, J.W. Bullard, N. Neithalath, G. Sant, The filler effect: The influence of filler content and surface area on cementitious reaction rates, *J. Amer. Ceram. Soc.* 96 (6) (2013) 1978-1990. <https://doi.org/10.1111/jace.12264>.
112. J. Olek, M. Radlinski, M. del Mar Arribas, Premature deterioration of joints in selected Indiana portland cement concrete pavements. *Proceedings of the 23rd Conference Awarie Budowlane*, 2007, Szczecin, Poland, pp. 859-868.

113. Personal Communication with Chad Davis and Alan Meadors. 8 August 2018.
114. O. Peterson, Chemical attack of strong chloride solutions on concrete. Does experience confirm that different chloride salts may influence concrete in different ways? Division of Building Materials, LTH, Lund University 3020 (1984) 1-30.
115. K. Peterson, G. Julio-Betancourt, L. Sutter, R.D. Hooton, D. Johnston, Observations of chloride ingress and calcium oxychloride formation in laboratory concrete and mortar at 5 °C, *Cem. Concr. Res.* 45 (2013) 79-90. <https://doi.org/10.1016/j.cemconres.2013.01.001>.
116. M. Pigeon, R. Pleau, *Modern concrete technology 4: durability of concrete in cold climates*, first ed., Taylor and Francis Group, Oxon, 1995.
117. W.J. Pitt, The effect of calcium chloride and calcium oxychloride on portland cement, *Chem. Eng. Min. Rev.* 21 (242) (1928) 65-70.
118. Phys.Org, 50 US coal power plants shut under Trump. <https://phys.org/news/2019-05-coal-power-trump.html> (accessed 27 June 2019).
119. T.C. Powers, A working hypothesis for further studies of frost resistance of concrete, *J. Am. Concr. Inst.* 16 (4) (1945) 245-272.
120. C. Qiao, P. Suraneni, M.T. Chang, J. Weiss, The influence of calcium chloride on flexural strength of cement-based materials, *Proceedings of the 2017 fib Symposium*, 2017, Maastricht, Netherlands, pp. 2041-2048.
121. C. Qiao, P. Suraneni, M.T. Chang, J. Weiss, Damage in cement pastes exposed to MgCl₂ solutions, *Mater. Struct.* 51 (2018) 74. <https://doi.org/10.1617/s11527-018-1191-2>.
122. C. Qiao, P. Suraneni, J. Weiss, Measuring volume change caused by calcium oxychloride phase transformation in a Ca(OH)₂-CaCl₂-H₂O system, *Adv. Civ. Eng. Mater.* 6 (1) (2017) 157-169. <https://doi.org/10.1520/ACEM20160065>.
123. C. Qiao, P. Suraneni, J. Weiss, Phase diagram and volume change of the Ca(OH)₂-CaCl₂-H₂O system for varying Ca(OH)₂/CaCl₂ molar ratios, *J. Mater. Civ. Eng.* 30 (2) (2018) 04017281. [https://doi.org/10.1061/\(ASCE\)MT.1943-5533.0002145](https://doi.org/10.1061/(ASCE)MT.1943-5533.0002145).
124. C. Qiao, P. Suraneni, J. Weiss, Flexural strength reduction of cement pastes exposed to CaCl₂ solutions, *Cem. Concr. Comp.* 86 (2018) 297-305. <https://doi.org/10.1016/j.cemconcomp.2017.11.021>.
125. C. Qiao, P. Suraneni, T.N.W. Ying, A. Choudhary, J. Weiss, Chloride binding of cement pastes with fly ash exposed to CaCl₂ solutions at 5 and 23 °C, *Cem. Concr. Comp.* 97 (2019) 43-53. <https://doi.org/10.1016/j.cemconcomp.2018.12.011>.

126. A.K.M. Rakinul Islam, Behaviour of concrete pavements exposed to de-icing salts: field and laboratory studies, University of Manitoba, 2017, M.S.C.E. Thesis.
127. S. Ramanathan, M. Croly, P. Suraneni, Comparison of the effects that supplementary cementitious materials replacement levels have on cementitious properties, *Cem. Concr. Comp.* 112 (2020) 103678. <https://doi.org/10.1016/j.cemconcomp.2020.103678>.
128. S. Ramanathan, A. Hajibabae, C. Jones, M. Kasaniya, E.A. Olivetti, M. Shakouri, M.D.A. Thomas, B. Traynor, Y. Wang, W.J. Weiss, P. Suraneni, Reactivity of alternative supplementary cementitious materials, *Cem. Concr. Res.* 2020. (Submitted).
129. P. Rangaraju, Investigating premature deterioration of a concrete highway, *Transp. Res. Rec.* 1798 (2002) 1-7. <https://doi.org/10.3141/1798-01>.
130. P. Rapp, Effect of calcium chloride on portland cements and concretes, *J. Res. Natl. Bur. Stand.* 14 (1935) 499-517.
131. V.W. Rechenberg, H.-M. Sylla, The effect of magnesium on concrete, *ZKG Int.* 49 (1) (1996) 44-56.
132. W.O. Robinson, W.H. Waggaman, Basic magnesium chlorides, *J. Phys. Chem.* 13 (9) (1909) 673–678. <https://doi:10.1021/j150108a002>.
133. G.W. Scherer, Crystallization in pores, *Cem. Concr. Res.* 29 (8) (1999) 1347-1358. [https://doi.org/10.1016/S0008-8846\(99\)00002-2](https://doi.org/10.1016/S0008-8846(99)00002-2).
134. G.W. Scherer, Stress from crystallization of salt, *Cem. Concr. Res.* 34 (2003) 1613– 1624. <https://doi.org/10.1016/j.cemconres.2003.12.034>.
135. A. Schöler, B. Lothenbach, F. Winnefeld, M.B. Haha, M. Zajac, H.-M. Ludwig, Early hydration of SCM-blended Portland cements: A pore solution and isothermal calorimetry study, *Cem. Concr. Res.* 93 (2017) 71-82. <https://doi.org/10.1016/j.cemconres.2016.11.013>.
136. Y. Schrader, An investigation into the effects of fly ash on freeze-thaw durability prediction, University of Arkansas, 2020, M.S.C.E. Thesis.
137. F.A. Schreinemakers, T. Figee, The study of system: $\text{H}_2\text{O}-\text{CaCl}_2-\text{Ca}(\text{OH})_2$ at 25 °C, *Chemisch. Weekblad.* 8 (1989) 683-688. (In Dutch)
138. C. Shi, Formation and stability of $3\text{CaO}\cdot\text{CaCl}_2\cdot 12\text{H}_2\text{O}$, *Cem. Concr. Res.* 31 (2001) 1373-1375. [https://doi.org/10.1016/S0008-8846\(01\)00576-2](https://doi.org/10.1016/S0008-8846(01)00576-2).
139. X. Shi, M. Akin, T. Pan, L. Fay, Y. Liu, Z. Yang, Deicer impacts on pavement materials: introduction and recent developments, *Open Civ. Eng. J.* 3 (2009) 16-27.

140. X. Shi, L. Fay, C. Gallaway, K. Volkening, M.M. Peterson, T. Pan, A. Creighton, C. Lawlor, S. Mumma, Y. Liu, T.A. Nguyen, Evaluation of alternative anti-icing and deicing compounds using sodium chloride and magnesium chloride as baseline deicers – Phase I, Final Report for the Colorado Department of Transportation, CDOT-2009-1.
141. X. Shi, L. Fay, M.M. Peterson, M. Berry, M. Mooney, A FESEM/EDX investigation into how continuous deicer exposure affects the chemistry of Portland cement concrete, *Constr. Build. Mater.* 25 (2) (2011) 957-966. <https://doi.org/10.1016/j.conbuildmat.2010.06.086>.
142. X. Shi, L. Fay, M.M. Peterson, Z. Yang, Freeze-thaw damage and chemical change of a portland cement concrete in the presence of diluted deicers, *Mater. Struct.* 43 (2010) 933-946. <https://doi.org/10.1617/s11527-009-9557-0>.
143. X. Shi, Y. Liu, M. Mooney, M. Berry, B. Hubbard, L. Fay, A.B. Leonard, Effect of chloride-based deicers on reinforced concrete structures, Final Report for the Washington State Department of Transportation, WA-RD 741.1, 2010.
144. X. Shi, N. Xie, Y. Dang, A. Muthumani, J. Huang, A. Hagel, S. Forsythe, E. Selig, D. Falk, E. McVey, A. Kessel, C. Martins, Y. Zhang, Y. Fang, Understanding and mitigating effects of chloride deicer exposure on concrete, Final Report for the Oregon Department of Transportation, SPR 742, 2014.
145. S.H. Smith, C. Qiao, P. Suraneni, K.E. Kurtis, W.J. Weiss, Service-life of concrete in freeze-thaw environments: Critical degree of saturation and calcium oxychloride formation, *Cem. Concr. Res.* 122 (2019) 93-106. <https://doi.org/10.1016/j.cemconres.2019.04.014>.
146. H.G. Smolczyk, Chemical reactions of strong chloride-solutions with concrete, *Proceedings of the 5th International Symposium on the Chemistry of Cement*, 1968, Tokyo, Japan, pp. 274-280.
147. R. Snellings, Assessing, understanding and unlocking supplementary cementitious materials, *RILEM Tech. Lett.* 10 (2016) 50-55. <https://doi.org/10.21809/rilemtechlett.2016.12>.
148. R. Snellings, K.L. Scrivener, Rapid screening tests for supplementary cementitious materials: past and future, *Mater. Struct.* 49 (2016) 3265-3279. <https://doi.org/10.1617/s11527-015-0718-z>.
149. S. Sorel, On a new magnesium cement, *Compt. Rend.* 65 (1867) 102–104. (In French)
150. R.P. Spragg, J. Castro, W. Li, M. Pour-Ghaz, P-T. Huang, J. Weiss, Wetting and drying of concrete using aqueous solutions containing deicing salts, *Cem. Concr. Comp.* 33 (5) (2011) 535-542. <https://doi.org/10.1016/j.cemconcomp.2011.02.009>.
151. E.S. Sumsion, W.S. Guthrie, Physical and chemical effects of deicers on concrete pavement: literature review, Final Report for the Utah Department of Transportation, UT-13.09, 2013.

152. Z. Sun, G.W. Scherer, Effect of air voids on salt scaling and internal freezing, *Cem. Concr. Res.* 40 (2) (2010) 260-270. <https://doi.org/10.1016/j.cemconres.2009.09.027>.
153. P. Suraneni, V.J. Azad, O.B. Isgor, W.J. Weiss, Deicing salts and durability of concrete pavements and joints: mitigating calcium oxychloride formation, *Concr. Int.* 38 (4) (2016) 48-54.
154. P. Suraneni, V.J. Azad, O.B. Isgor, W.J. Weiss, Calcium oxychloride formation in pastes containing supplementary cementitious materials: thoughts on the role of cement and supplementary cementitious materials reactivity, *RILEM Tech. Lett.* 1 (2016) 24-30. <http://dx.doi.org/10.21809/rilemtechlett.v1.7>.
155. P. Suraneni, V.J. Azad, O.B. Isgor, W.J. Weiss, Use of fly ash to minimize deicing salt damage in concrete pavements, *Transp. Res. Rec.* 2629 (2017) 24-32. <https://doi.org/10.3141/2629-05>.
156. P. Suraneni, V.J. Azad, O.B. Isgor, J. Weiss, Role of supplementary cementitious material type in the mitigation of calcium oxychloride formation in cementitious pastes, *J. Mater. Civ. Eng.* 30 (10) (2018) 04018248. [https://doi.org/10.1061/\(ASCE\)MT.1943-5533.0002425](https://doi.org/10.1061/(ASCE)MT.1943-5533.0002425).
157. P. Suraneni, A. Hajibabae, S. Ramanathan, Y. Wang, J. Weiss, New insights from reactivity testing of supplementary cementitious materials, *Cem. Concr. Comp.* 103 (2019) 331-338. <https://doi.org/10.1016/j.cemconcomp.2019.05.017>.
158. P. Suraneni, J. Monical, E. Unal, Y. Farnam, C. Vilani, T.J. Barrett, W.J. Weiss, Performance of concrete pavement in the presence of deicing salts and deicing salt cocktails, Joint Transportation Research Program Publication No. FHWA/IN/JTRP-2016/25 (2016) pp. 1-19. <http://dx.doi.org/10.5703/1288284316350>.
159. P. Suraneni, J. Monical, E. Unal, Y. Farnam, J. Weiss, Calcium oxychloride formation potential in cementitious pastes exposed to blends of deicing salt, *ACI Mater. J.* 114 (4) (2017) 631-641. <http://dx.doi.org/10.14359/51689607>.
160. P. Suraneni, C. Qiao, V. Azad, Y. Farnam, J. Monical, E. Unal, C. Villani, B. Isgor, J. Weiss, A review of recent work on deicing salt damage to concrete pavements and its mitigation, International Conference on Advances in Construction Materials and Systems, 2017, Chennai, India, pp. 1-15.
161. P. Suraneni, N. Salgado, H. Carolan, C. Li, V.J. Azad, O.B. Isgor, J.H. Ideker, W.J. Weiss, Mitigation of deicer damage in concrete pavements caused by calcium oxychloride salt formation – use of ground lightweight aggregates, Proceedings of the International RILEM Conference on Materials, Systems and Structures in Civil Engineering, 2016, Lyngby, Denmark, pp. 171-180.

162. P. Suraneni, W.J. Weiss, Examining the pozzolanicity of supplementary cementitious materials using isothermal calorimetry and thermogravimetric analysis, *Cem. Concr. Comp.* 83 (2017) 273-278. <https://doi.org/10.1016/j.cemconcomp.2017.07.009>.
163. P. Suraneni, J. Weiss, Extending low-temperature differential scanning calorimetry from paste to mortar and concrete to quantify the potential for calcium oxychloride formation, *Adv. Civ. Eng. Mater.* 7 (1) (2018) 1-16. <https://doi.org/10.1520/ACEM20170113>.
164. L. Sutter, K. Peterson, G. Julio-Betancourt, D. Hooton, T. Van Dam, K. Smith, The deleterious chemical effects of concentrated deicing solutions on portland cement concrete, Final Report for the South Dakota Department of Transportation, SD2002-01, 2008.
165. L. Sutter, K. Peterson, S. Touton, T. Van Dam, D. Johnston, Petrographic evidence of calcium oxychloride formation in mortars exposed to magnesium chloride solution, *Cem. Concr. Res.* 36 (2006) 1533-1541. <https://doi.org/10.1016/j.cemconres.2006.05.022>.
166. L. Sutter, T. Van Dam, K.R. Peterson, D.P. Johnston, Long-term effects of magnesium chloride and other concentrated salt solutions on pavement and structural portland cement concrete phase I results, *Transp. Res. Rec.* 1979 (2006) 60-68. <http://dx.doi.org/10.3141/1979-10>.
167. J. Tanesi, R. Meininger, Freeze-thaw resistance of concrete with marginal air content, *Transp. Res. Rec.* 2020 (2007) 61-66. <https://doi.org/10.3141/2020-08>.
168. P. Taylor, L. Sutter, J. Weiss, Investigation of deterioration of joints in concrete pavements, InTrans Project Reports 91, 2012. http://lib.dr.iastate.edu/intrans_reports/91.
169. M.D.A. Thomas, Optimizing the use of fly ash in concrete, *Port. Cem. Assoc.* (2007) 24. https://www.cement.org/docs/default-source/fc_concrete_technology/is548-optimizing-the-use-of-fly-ash-concrete.pdf (accessed 2 February 2021).
170. K. Torii, M. Kawamura, M. Yamada, S. Chatterji, Deterioration of cement mortars in NaCl and CaCl₂ solution, *Proceedings of the JCA Cement and Concrete*, 1992, No. 42 pp. 504-509. (In Japanese)
171. K. Torii, T. Sasatani, M. Kawamura, Effects of fly ash, blast furnace slag, and silica fume on resistance of mortar to calcium chloride attack, *ACI Spec. Publ.* 153 (1995) 931-950.
172. F. Traore, C. Jones, S. Ramanathan, P. Suraneni, W.M. Hale, Using compressive strength and mass change to verify the calcium oxychloride threshold in cementitious pastes with fly ash, *Constr. Build. Mater.* 296 (2021) 123640. <https://doi.org/10.1016/j.conbuildmat.2021.123640>.
173. P.J. Tumidajski, G.W. Chan, Durability of high performance concrete in magnesium brine, *Cem. Concr. Res.* 26 (4) (1996) 557-565. [https://doi.org/10.1016/0008-8846\(96\)00034-8](https://doi.org/10.1016/0008-8846(96)00034-8).

174. T. Uchida, S. Hatanaka, N. Mishima, A. Maegawa, Study on deterioration mechanism of porous concrete by CaCl₂aq, *J. Struct. Constr. Eng.* 79 (706) (2014) 1709-1715. <https://doi.org/10.3130/aajs.79.1709>. (In Japanese)
175. U.S. Department of Transportation Federal Highway Administration, Road Weather Management Program, Snow and Ice. https://ops.fhwa.dot.gov/weather/weather_events/snow_ice.htm, (accessed November 18, 2019).
176. J.J. Valenza II, G.W. Scherer, A review of salt scaling: I. Phenomenology, *Cem. Concr. Res.* 37 (7) (2007) 1007-1021. <https://doi.org/10.1016/j.cemconres.2007.03.005>.
177. J.J. Valenza II, G.W. Scherer, A review of salt scaling: II. Mechanisms, *Cem. Concr. Res.* 37 (7) (2007) 1022-1034. <https://doi.org/10.1016/j.cemconres.2007.03.003>.
178. P. Van den Heede, J. Furniere, N. De Belie, Influence of air entraining agents on deicing salt scaling resistance and transport properties of high-volume fly ash concrete, *Cem. Concr. Comp.* 37 (2013) 293-303. <https://doi.org/10.1016/j.cemconcomp.2013.01.005>.
179. C.B. Van Niejenhuis, C.M. Hansson, Detrimental effects of anti-icing brines on concrete durability, *Concr. Int.* 41 (11) (2019) 30-34.
180. G.J. Verbeck, P. Klieger, Studies of "salt" scaling of concrete, *Highw. Res. Board Bull.* 150 (1957) 1-17.
181. I.I. Vol'nov, E.I. Latysheva, Separation of calcium chloride from solvay spent liquor through calcium hydroxichloride, *J. Appl. Chem. U.S.S.R.* 30 (1957) 1039-1046.
182. L.D. Wakeley, T.S. Poole, C.A. Weiss, J.P. Burkes, Geochemical stability of cement-based composites in magnesium brines, *Proceedings of the 14th International Conference on Cement Microscopy*, Costa Mesa, CA, 1992.
183. S.A. Walling, J.L. Provis, Magnesia based cements: a journey of 150 years, and cements for the future?, *Chem. Rev.* 116 (2016) 4170-4204. <https://doi.org/10.1021/acs.chemrev.5b00463>.
184. K. Wang, D.E. Nelson, W.A. Nixon, Damaging effects of deicing chemicals on concrete materials, *Cem. Concr. Comp.* 28 (2) (2006) 173-188. <https://doi.org/10.1016/j.cemconcomp.2005.07.006>.
185. X. Wang, S. Sadati, P. Taylor, C. Li, X. Wang, A. Sha, Material characterization to assess effectiveness of surface treatment to prevent joint deterioration from oxychloride formation mechanism, *Cem. Concr. Comp.* 104 (2019) 103394. <https://doi.org/10.1016/j.cemconcomp.2019.103394>.

186. W.J. Weiss, Concrete pavement joint durability: a sorption-based model for saturation, the role of distributed cracking, and calcium oxychloride formation, Proceedings of the 10th International Conference on Mechanics and Physics of Creep, Shrinkage, and Durability of Concrete and Concrete Structures, 2015, Vienna, Austria, pp. 211-218.
<https://doi.org/10.1061/9780784479346.025>.
187. J. Weiss, M.T. Ley, L. Sutter, D. Harrington, J. Gross, S.L. Tritsch, Guide to the prevention of and restoration of early joint deterioration in concrete pavements, Final Report for the Iowa Department of Transportation, TR-697, 2016.
188. E.M. Winkler, P.C. Singer, Crystallization pressure of salts in stone and concrete, Geological Soc. Am. Bull. 83 (1972) 3509-3514.
189. S.N. Whatley, P. Suraneni, V.J. Azad, O.B. Isgor, J. Weiss, Mitigation of calcium oxychloride formation in cement pastes using undensified silica fume, J. Mater. Civ. Eng. 29 (10) (2017) 04017198. [https://doi.org/10.1061/\(ASCE\)MT.1943-5533.0002052](https://doi.org/10.1061/(ASCE)MT.1943-5533.0002052).
190. Z. Wu, C. Shi, P. Gao, D. Wang, Z. Cao, Effects of deicing salts on the scaling resistance of concrete, J. Mater. Civ. Eng. 27 (5) (2015) 04014160.
191. W. Xu, T. Yiu Lo, W. Wang, D. Ouyang, P. Wang, F. Xing, Pozzolanic reactivity of silica fume and ground rice husk ash as reactive silica in cementitious system: a comparative study, Mater. 9 (3) (2016) 146. <https://doi.org/10.3390/ma9030146>.
192. E. Yurdakul, P.C. Taylor, H. Ceylan, F. Bektas, Effect of water-to-binder ratio, air content, and type of cementitious materials on fresh and hardened properties of binary and ternary blended concrete, J. Mater. Civ. Eng. 26 (6) (2014) 04014002.
[https://doi.org/10.1061/\(ASCE\)MT.1943-5533.0000900](https://doi.org/10.1061/(ASCE)MT.1943-5533.0000900).
193. Y. Zhou, B. Gencturk, K. William, A. Attar, Carbonation-induced and chloride-induced corrosion in reinforced concrete structures, J. Mater. Civ. Eng. 27 (9) (2014) 04014245.